THE HUMAN MICROBIOME AND CANCER

EDITED BY: Gary Moran and Nezar Al-Hebshi
PUBLISHED IN: Frontiers in Microbiology

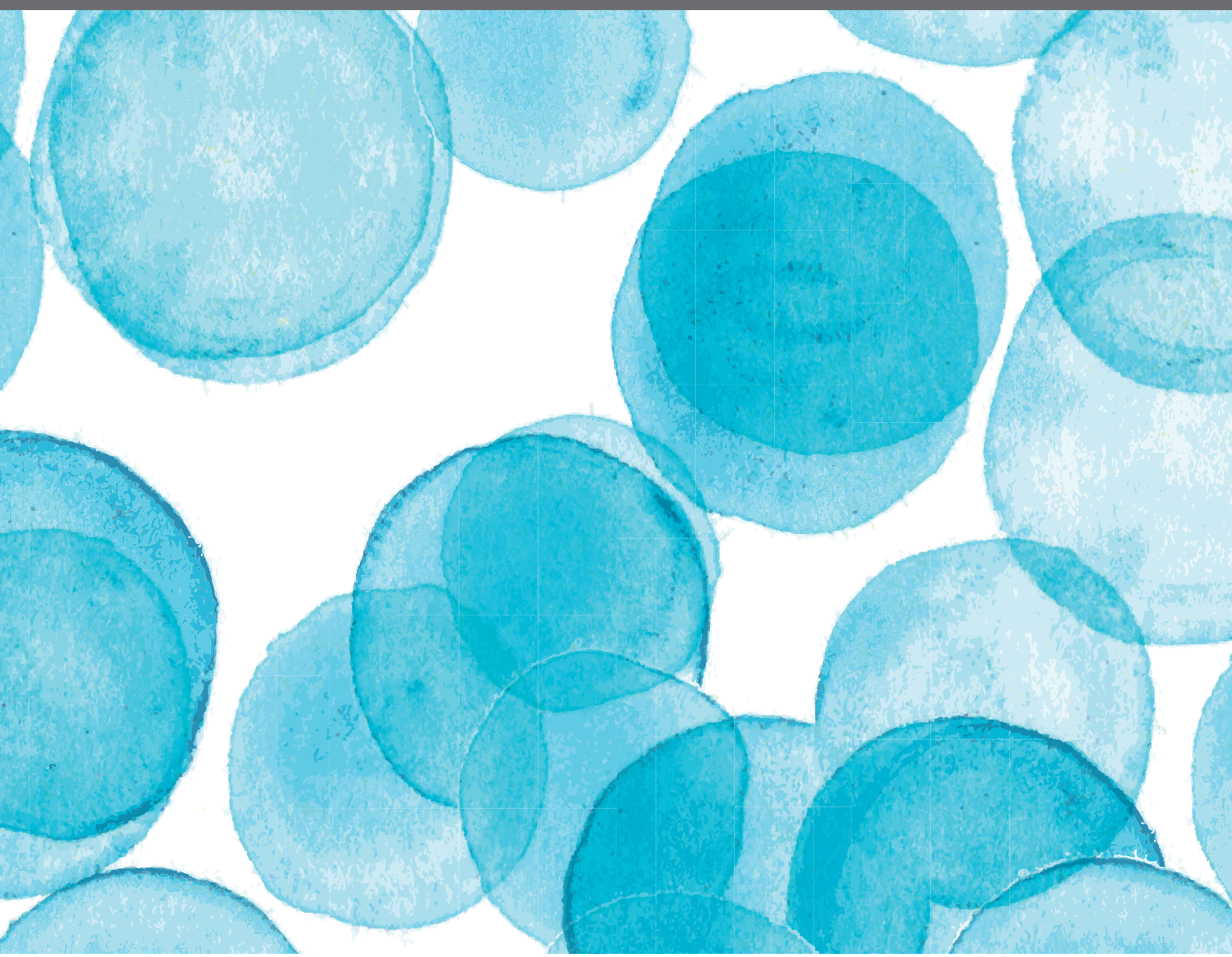

frontiers Research Topics

frontiers

ISSN 1664-8714
ISBN 978-2-88963-989-2
DOI 10.3389/978-2-88963-989-2

About Frontiers

Frontiers is more than just an open-access publisher of scholarly articles: it is a pioneering approach to the world of academia, radically improving the way scholarly research is managed. The grand vision of Frontiers is a world where all people have an equal opportunity to seek, share and generate knowledge. Frontiers provides immediate and permanent online open access to all its publications, but this alone is not enough to realize our grand goals.

Frontiers Journal Series

The Frontiers Journal Series is a multi-tier and interdisciplinary set of open-access, online journals, promising a paradigm shift from the current review, selection and dissemination processes in academic publishing. All Frontiers journals are driven by researchers for researchers; therefore, they constitute a service to the scholarly community. At the same time, the Frontiers Journal Series operates on a revolutionary invention, the tiered publishing system, initially addressing specific communities of scholars, and gradually climbing up to broader public understanding, thus serving the interests of the lay society, too.

Dedication to Quality

Each Frontiers article is a landmark of the highest quality, thanks to genuinely collaborative interactions between authors and review editors, who include some of the world's best academicians. Research must be certified by peers before entering a stream of knowledge that may eventually reach the public - and shape society; therefore, Frontiers only applies the most rigorous and unbiased reviews.
Frontiers revolutionizes research publishing by freely delivering the most outstanding research, evaluated with no bias from both the academic and social point of view. By applying the most advanced information technologies, Frontiers is catapulting scholarly publishing into a new generation.

What are Frontiers Research Topics?

Frontiers Research Topics are very popular trademarks of the Frontiers Journals Series: they are collections of at least ten articles, all centered on a particular subject. With their unique mix of varied contributions from Original Research to Review Articles, Frontiers Research Topics unify the most influential researchers, the latest key findings and historical advances in a hot research area! Find out more on how to host your own Frontiers Research Topic or contribute to one as an author by contacting the Frontiers Editorial Office: researchtopics@frontiersin.org

THE HUMAN MICROBIOME AND CANCER

Topic Editors:
Gary Moran, Trinity College Dublin, Ireland
Nezar Al-Hebshi, Temple University, United States

Citation: Moran, G., Al-Hebshi, N., eds. (2020). The Human Microbiome and Cancer. Lausanne: Frontiers Media SA. doi: 10.3389/978-2-88963-989-2

Table of Contents

frontiers in Microbiology

EDITORIAL
published: 21 July 2020
doi: 10.3389/fmicb.2020.01514

Editorial: The Human Microbiome and Cancer

Gary P. Moran[1]* *and Nezar Al-Hebshi*[2]

[1] School of Dental Science, Dublin Dental University Hospital and Trinity College Dublin, Dublin, Ireland, [2] Kornberg School of Dentistry, Temple University, Philadelphia, PA, United States

Keywords: cancer, microbiome, bacteria, virus, fungus

Editorial on the Research Topic

The Human Microbiome and Cancer

The role of microorganisms in carcinogenesis has been a hotly contested area of research for over a century. Early pioneers such as Peyton Rous were the first to demonstrate that viral pathogens could initiate transformation of avian cells (Rous, 1910). Since then, the roles of viral pathogens such as Epstein-Barr virus and human papilloma virus in carcinogenesis have been well-established (Sarid and Gao, 2011). More recently, the role of the bacterium *Helicobacter pylori* in the etiology of gastric cancer has been elucidated (Alfarouk et al., 2019) and compelling evidence for a fungal etiology in pancreatic cancer has been proposed (Aykut et al., 2019). A role of the endogenous microbiota in the etiology and progression of human cancers is now under intense investigation (Al-Hebshi et al., 2019; Elinav et al., 2019; Healy and Moran, 2019). Advances in DNA sequencing have opened up a new frontier in microbiome analysis leading to an explosion in studies to analyse changes in human bacterial, fungal, and viral communities during the development of human cancers. Metabolomics also allows us to study the impact of microbial metabolites (e.g., acetaldehyde) on human physiology (Amer et al., 2020). These studies aim not only to identify novel etiologic agents, but to determine if microbiome changes could have diagnostic potential or whether the microbiome has a direct role in malignant progression, metastatic spread, or the success of chemotherapeutic regimens. Most studies focusing on the human microbiome and cancer have investigated the role of the bacteriome on mucosal surfaces in the gastrointestinal tract. The role of the microbiome in non-mucosal cancers such as breast and prostate cancers is also under investigation (Sfanos et al., 2017; Chen et al., 2019). This Research Topic brings together a collection of studies investigating the microbiome of the oral and gastrointestinal (GIT) microbiomes, combining original research and up to date reviews.

One of the most important aspects of a microbiome study is DNA extraction and in the first chapter of this collection, Zhang C. et al. explore whether homogenization or enzymatic lysis of microbiome samples affects microbiome profiles in endoscopic biopsy samples. The authors conclude that although both methods produce similar profiles, homogenization provides higher microbial DNA content.

One area where microbiome profiling could potentially improve patient outcomes is as a diagnostic tool to identify those at high risk of malignant transformation or to identify the stage of cancer development. The diagnostic potential of the gut microbiome is highlighted by Ni et al. who develop a measurement of microbial disturbance, termed dysbiosis index (D_{dys}), based on changes to the fecal microbiota in hepatocellular carcinoma patients. This dysbiosis index may have the potential to diagnose those with the disease and may in the future determine prognosis at different stages of hepatocellular carcinoma (Ni et al.).

OPEN ACCESS

Edited by:
George Tsiamis, University of Patras, Greece

Reviewed by:
Soumaya Kouidhi, University of Manouba, Tunisia

***Correspondence:**
Gary P. Moran
gpmoran@dental.tcd.ie

Specialty section:
This article was submitted to Systems Microbiology, a section of the journal Frontiers in Microbiology

Received: *03 March 2020*
Accepted: *10 June 2020*
Published: *21 July 2020*

Citation:
Moran GP and Al-Hebshi N (2020) Editorial: The Human Microbiome and Cancer. Front. Microbiol. 11:1514. doi: 10.3389/fmicb.2020.01514

The collection continues with several studies of the oral microbiome. The oral cavity is one of the most diverse areas of the human GIT and an increasing number of studies are demonstrating the increased abundance of *Fusobacterium* spp. in the development of OSCC (Al-hebshi et al., 2017; Amer et al., 2017). Zhang Z. et al. show that enrichments for *Fusobacterium* spp. are specific to tumor sites in OSCC patients, with reduced levels observed in saliva and oral rinse specimens from the same patients. Kageyama et al. extend the analysis of the salivary microbiome to include patients with diverse cancers throughout the GIT. This study also demonstrates elevated levels of *F. nucleatum* in patients with oropharyngeal cancers and identifies a general enrichment of *P. gingivalis* in all patients with cancers of the digestive tract (Kageyama et al.). The influence of the oral microbiome may also extend beyond the oral cavity, as shown by Chen X-H. et al., who demonstrate that gastric cancers exhibit increased abundance of taxa normally associated with the oral microbiome. The presence of *H. pylori* in these gastric samples also impacts upon the composition of these communities, suggesting that *H. pylori* may have a central role in the development of dysbiosis. The involvement of *H. pylori* the development of gastric biofilms is further explored by Rizatto et al., who discuss the potential role and mechanisms of biofilm formation in the gastric mucosa and identify future directions for this research area.

The intestinal microbiota is under intense investigation for its roles in regulating metabolism, immunity, and the interaction with cancer cells. In addition, specific pathogens have been implicated in carcinogenesis including *F. nucleatum* and *Streptococcus gallolyticus* subsp. *Gallolyticus*. Ma et al. present a timely and comprehensive review of the impact of the gut microbiome on cancer chemotherapy. Continuing this topic, Cong, Zhu, Zhang et al. present novel data showing the impact of chemotherapy on microbial networks in the intestinal microbiota, opening up the possibility to explore how these changes impact upon chemotherapeutic outcomes. The same authors also investigate the effect of surgical interventions on the gut microbiome of patients with CRC (Cong, Zhu, Liu et al.). These data show that surgical interventions have a strong impact on the microbiome resulting in increased levels of *Klebsiella* spp., which was significantly linked with lymphatic invasion.

Targeted interventions to restore healthy or beneficial microbiomes are still in their infancy. Here, Wu et al. present exciting data showing that chitooligosaccharides protect mice from colorectal carcinomas by reducing the levels of *Escherichia-Shigella*, *Enterococcus*, and *Turicibacter* and by promoting the growth of butyrate producing bacteria.

In summary, this collection offers an insight into the developing area of microbiome research in oncology, and highlights the growing potential of these scientific tools for improving diagnosis and treatment of these devastating diseases.

AUTHOR CONTRIBUTIONS

The manuscript was written and prepared by GM and NA-H. All authors contributed to the article and approved the submitted version.

FUNDING

GM was supported by the Irish Health Research Board (Grant No. ILP-POR-2019-030).

REFERENCES

Alfarouk, K. O., Bashir, A. H. H., Aljarbou, A. N., Ramadan, A. M., Muddathir, A. K., AlHoufie, S. T. S., et al. (2019). The possible role of *Helicobacter pylori* in gastric cancer and its management. *Front. Oncol.* 9:75. doi: 10.3389/fonc.2019.00075

Al-Hebshi, N. N., Borgnakke, W. S., and Johnson, N. W. (2019). The microbiome of oral squamous cell carcinomas: a functional perspective. *Curr. Oral Heal. Rep.* 6, 145–160. doi: 10.1007/s40496-019-0215-5

Al-hebshi, N. N., Nasher, A. T., Maryoud, M. Y., Homeida, H. E., Chen, T., Idris, A. M., et al. (2017). Inflammatory bacteriome featuring *Fusobacterium nucleatum* and *Pseudomonas aeruginosa* identified in association with oral squamous cell carcinoma. *Sci. Rep.* 7:1–10. doi: 10.1038/s41598-017-02079-3

Amer, A., Galvin, S., Healy, C. M., and Moran, G. P. (2017). The microbiome of potentially malignant oral leukoplakia exhibits enrichment for *Fusobacterium*, *Leptotrichia*, *Campylobacter*, and *Rothia* Species. *Front. Microbiol.* 8:2391. doi: 10.3389/fmicb.2017.02391

Amer, A., Whelan, A., Al-Hebshi, N. N., Healy, C. M., and Moran, G. P. (2020). Acetaldehyde production by *Rothia mucilaginosa* isolates from patients with oral leukoplakia. *J. Oral Microbiol.* 12:1743066. doi: 10.1080/20002297.2020.1743066

Aykut, B., Pushalkar, S., Chen, R., Li, Q., Abengozar, R., Kim, J. I., et al. (2019). The fungal mycobiome promotes pancreatic oncogenesis via activation of MBL. *Nature* 574, 264–267. doi: 10.1038/s41586-019-1608-2

Chen, J., Douglass, J., Prasath, V., Neace, M., Atrchian, S., Manjili, M. H., et al. (2019). The microbiome and breast cancer: a review. *Breast Cancer Res. Treat.* 178, 493–496. doi: 10.1007/s10549-019-05407-5

Elinav, E., Garrett, W. S., Trinchieri, G., and Wargo, J. (2019). The cancer microbiome. *Nat. Rev. Cancer* 19, 371–376. doi: 10.1038/s41568-019-0155-3

Healy, C. M., and Moran, G. P. (2019). The microbiome and oral cancer: more questions than answers. *Oral Oncol.* 89, 30–33. doi: 10.1016/j.oraloncology.2018.12.003

Rous, P. (1910). A transmissible avian neoplasm (sarcoma of the common fowl). *J. Exp. Med.* 12, 696–705. doi: 10.1084/jem.12.5.696

Sarid, R., and Gao, S.-J. (2011). Viruses and human cancer: from detection to causality. *Cancer Lett.* 305, 218–227. doi: 10.1016/j.canlet.2010.09.011

Sfanos, K. S., Yegnasubramanian, S., Nelson, W. G., and Marzo, A. M. D. (2017). The inflammatory microenvironment and microbiome in prostate cancer development. *Nat. Rev. Urol.* 15, 11–24. doi: 10.1038/nrurol.2017.167

Conflict of Interest: The authors declare that the research was conducted in the absence of any commercial or financial relationships that could be construed as a potential conflict of interest.

frontiers in Microbiology

ORIGINAL RESEARCH
published: 20 November 2018
doi: 10.3389/fmicb.2018.02777

A Pilot Study: Changes of Gut Microbiota in Post-surgery Colorectal Cancer Patients

*Jing Cong[1,2], Hua Zhu[1], Dong Liu[1,2], Tianjun Li[1], Chuantao Zhang[1], Jingjuan Zhu[1], Hongying Lv[1], Kewei Liu[1], Chenxing Hao[1], Zibin Tian[3], Jianli Zhang[4] and Xiaochun Zhang[1,2]**

[1] Department of Medical Oncology, The Affiliated Hospital of Qingdao University, Qingdao University, Qingdao, China, [2] Qingdao Cancer Institute, Qingdao, China, [3] Department of Gastroenterology, The Affiliated Hospital of Qingdao University, Qingdao University, Qingdao, China, [4] Department of General Surgery, The Affiliated Hospital of Qingdao University, Qingdao University, Qingdao, China

OPEN ACCESS

Edited by:
Nezar Al-hebshi,
Temple University, United States

Reviewed by:
Stéphanie Olivier-Van Stichelen,
National Institutes of Health (NIH), United States
Elizabeth P. Ryan,
Colorado State University, United States

***Correspondence:**
Xiaochun Zhang
zhangxiaochun9670@126.com

Specialty section:
This article was submitted to Systems Microbiology, a section of the journal Frontiers in Microbiology

Received: 08 May 2018
Accepted: 30 October 2018
Published: 20 November 2018

Citation:
Cong J, Zhu H, Liu D, Li T, Zhang C, Zhu J, Lv H, Liu K, Hao C, Tian Z, Zhang J and Zhang X (2018) A Pilot Study: Changes of Gut Microbiota in Post-surgery Colorectal Cancer Patients. Front. Microbiol. 9:2777. doi: 10.3389/fmicb.2018.02777

Colorectal cancer (CRC) is a growing health problem throughout the world. Strong evidences have supported that gut microbiota can influence tumorigenesis; however, little is known about what happens to gut microbiota following surgical resection. Here, we examined the changes of gut microbiota in CRC patients after the surgical resection. Using the PCoA analysis and dissimilarity tests, the microbial taxonomic compositions and diversities of gut microbiota in post-surgery CRC patients (A1) were significantly different from those in pre-surgery CRC patients (A0) and healthy individuals (H). Compared with A0 and H, the Shannon diversity and Simpson diversity were significantly decreased in A1 ($P < 0.05$). Based on the LEfSe analysis, the relative abundance of phylum *Proteobacteria* in A1 was significantly increased than that in A0 and H. The genus *Klebsiella* in A1 had higher proportions than that in A0 ($P < 0.05$). Individual variation was distinct; however, 90% of CRC patients in A1 had more abundances of *Klebsiella* than A0. The *Klebsiella* in A1 was significantly associated with infectious diseases ($P < 0.05$), revealed by the correlation analysis between differentiated genera and metabolic pathway. The *Klebsiella* (*Proteobacteria*, *Gammaproteobacteria*, *Enterobacteriales*, *Enterobacteriaceae*) in A1 was significantly linked with lymphatic invasion ($P < 0.05$). Furthermore, the PCA of KEGG pathways indicated that gut microbiota with a more scattered distribution in A1 was noticeably different from that in A0 and H. The nodes, the links, and the kinds of phylum in each module in A1 were less than those in A0 and H, indicating that gut microbiota in A1 had a relatively looser ecologcial interaction network. To sum up, this pilot study identified the changes of gut microbiota in post-surgery CRC patients, and highlights future avenues in which the gut microbiota is likely to be of increasing importance in the care of surgical patients.

Keywords: gut microbiota, colorectal cancer, surgery, high-throughput sequencing, real-time quantitative PCR

INTRODUCTION

Colorectal cancer (CRC) is the third leading cause of cancer mortality in the world (Jemal et al., 2011), and is influenced by heredity, diet, lifestyle, gut microbiota, and other factors (Berstad et al., 2015; Sun and Kato, 2016). The human intestinal tract is a nutrient-rich environment housing the largest microbial communities (Zheng et al., 2016). The gut microbiota has garnered great attentions because of its important role in influencing CRC risk by metabolites and immunity in the host (Saleh and Trinchieri, 2011). For example, some bacteria producing hydrogen sulfide, acetaldehyde and secondary bile acids can contribute to the risk of CRC (Huycke and Gaskins, 2004; Bernstein et al., 2009). Simultaneously, some bacteria, including the orders *Clostridiales*, *Lactobacillales*, *Bifidobacteriales*, and *Actinomycetales* (Devillard et al., 2007), may reduce CRC risk by producing butyrate and conjugated linoleic acids (Scharlau et al., 2009). Therefore, understanding the role of gut microbiota contributes to improving CRC patients' care.

Human gut microbiota is considered as an essential "organ," which plays a key role in providing nourishment, regulating epithelial development, and modulating immunity (Eckburg et al., 2005). In recent years, many researchers have attempted to understand the differences in gut microbiota by comparing the microbial community structures of CRC patients and healthy individuals and identify reliable microbial markers for CRC precursors (Zeller et al., 2014). Previously, it has been reported that the abundances of *Enterococcus faecalis* (Balamurugan et al., 2008) and *Desulfovibrio* sp. (Scanlan et al., 2009) were observably higher in CRC patients than that in healthy individuals, whereas *Bacteroides/Prevotella* levels were significantly lower (Sobhani et al., 2011). Differences were also observed in the overall structure of gut microbiota between CRC patients and healthy individuals (Sobhani et al., 2011). Despite of advances in understanding the connections between gut microbiota and CRC, little is known about how surgery resection influences the gut microbiota. Current studies have indicated that many patients who undergo treatment may experience recurrence and even die within several years (Ryuk et al., 2014). Therefore, identifying valid methods to evaluate post-surgery patients' condition is vital in reducing mortality and healthcare costs.

Gut microbiota is strongly influenced by the surgical removal of lesions, and influences the intestinal healing, particularly with respect to anastomotic tissues in colorectal surgery (Bachmann et al., 2017). In this pilot study, we analyzed fecal samples of CRC patients and healthy individuals by 16S rRNA gene sequencing and real-time quantitative PCR. First, we used the classical community analysis and statistical tests to compare the gut microbial community structure and composition between CRC patients and healthy individuals. Next, we generated functional discrepancy prediction and molecular ecological network to further examine the differences among them. Finally, we discussed the correlates of gut microbiota and clinical variables for the probabilities to assess whether gut microbiota played a key role in identifying the condition for post-surgery CRC patients.

MATERIALS AND METHODS

Study Design

Our pilot study subjects comprised 10 CRC patients and 11 healthy individuals (**Supplementary Figure S1**). The CRC patients, aged 34–63 years, were from the affiliated hospital of Qingdao University (Qingdao, China, **Table 1** and **Supplementary Tables S1**, **S2**). The pilot study selected from untreated CRC patients and excluded those (N = 6) who had previously undergone surgery, chemotherapy, radiation, or targeted therapies before samples collection. Fecal samples from these pre-surgery CRC patients were collected prior to a colonoscopy (O'Brien et al., 2013). The lesion location of all the selected CRC patients was in rectum. These CRC patients were treated with palliative surgery or radical surgery, such as Dixon, Miles and Hartmann (**Supplementary Table S2**). Following up samples were obtained in approximately 1 month after the surgery. The healthy individuals, aged 49–64 years, were selected as controls (**Table 1** and **Supplementary Table S2**). During a routine physical examination, none had any recorded antibiotics usage or gastrointestinal tract disorders within 3 months preceding the sample collection. All of the participants have been local residents of Qingdao city. This pilot study was approved by the Affiliated Hospital of Qingdao University Institutional Review Board, and all pilot study participants signed the informed consent before participation. All fecal samples were collected within 3 h after defecation in the morning. The collected samples from the healthy individuals, pre-surgery CRC patients and post-surgery CRC patients were named by H, A0, and A1, respectively. Fresh fecal samples were put into 5 ml tubes and immediately stored at −80°C until the day of analysis.

DNA Extraction, Purification, Sequencing and Data Processing

Extraction of bacterial DNA was performed from fecal samples using a QIAamp Fast DNA Stool Mini Kit as previously reported (Wu et al., 2016). The freshly extracted DNA was purified by 0.5% melting point agarose gel followed by phenolchloroform-butanol extraction. The V3-V4 region of the bacterial 16S rRNA gene from each DNA sample was amplified using the bacterial universal primers (forward primer: 5′-ACTCCTACGGGRSGCAGCAG-3′; reverse primer: 5′-GGACTACVVGGGTATCTAATC-3′). PCR amplification was

TABLE 1 | Baseline characteristics in healthy individuals and colorectal cancer patients.

Variable	Healthy individuals	Colorectal cancer patients	*P*-value
Number	11	10	/
Age, year, median (IQR)	60 (49–64)	59 (34–63)	0.386
Sex (Female/Male), n	9/2	4/6	0.051
BMI, median (IQR)	24.1 (21.4–28.2)	25.5 (19.5–31.8)	0.211
Tumor location	/	Rectum	/

performed in a 30 μl reaction, containing 15 μl of 2 × KAPA HiFi Hotstart ReadyMix, 1 μl of each primer (forward and reverse primer), 10 ng of template DNA, and the remaining volume of ddH_2O. The reaction mixtures were denatured at 95°C for 1 min; followed by 12 cycles of 98°C for 15 s, 72°C for 10 s, 94°C for 20 s, 65°C for 10 s and 72°C for 10 s; then 11 cycles of 94°C for 20 s, 58℃ for 30 s, 72°C for 30 s; and a final extension at 72°C for 150 s. The PCR amplification products were purified with an AxyPrep DNA Gel Extraction Kit (Axygen, United States), eluted in 30 μl water, and aliquoted into three PCR tubes. DNA quality and quantity were assessed by the ratios of 260/280 nm and 260/230 nm, and final DNA contents were quantified with a Qubit® dsDNA HS Assay Kit (Invitrogen, United States). Finally, we used bacterial DNA amplicons from each fecal sample for 2 × 250 bp paired-end sequencing based on the Illumina Hiseq 2500.

Raw sequences were separated into samples by barcodes using the Galaxy Illumina sequencing pipeline[1]. Adapters, ambiguous and low-quality reads ("N") were trimmed by Btrim (Kong, 2011). Forward and reverse reads were incorporated into a whole sequence by FLASH (Magoč and Salzberg, 2011). After quality control of the raw data, the clean reads were clustered into operational taxonomic units (OTUs) at 97% similarity level by using UCLUST (Edgar, 2010). Each OTU was considered to represent a species (Deng et al., 2012). Rarefaction analysis was performed using the original detected OTUs (**Supplementary Figure S2**). The ribosomal database project (RDP) classifier was used to determine the taxonomic assignment (Wang et al., 2007). Random resampling was conducted on 48,360 sequences per fecal sample.

Real-Time Quantitative PCR

Three specific primers were used for real-time quantitative PCR (qPCR), including 16S rRNA universal primer for bacteria, primer for *Fusobacterium nucleatum* (Castellarin et al., 2012), primer for *Klebsiella pneumonia* (Sun et al., 2010) (**Supplementary Table S3**). The primers were synthesized at Shanghai Sangon Company (China). The PCR program was as follows: 95°C for 3 min; 35 cycles of 94°C for 30 s, 57°C for 30 s, and 72°C for 30 s; 72°C for 8 min. The PCR products were purified with gel extraction kit (Sangon SK8131), quantified using Micro-spectrophotometer SMA4000 (Merinton), and used to construct standard curves. The copy number of PCR products was calculated based on the formula: Copy number/μL = $6.02 \times 10^{14} \times C/(M \times W)$. The C (unit, ng/μL) represents the concentration of PCR products, *M* (unit, bp) represents the length of PCR products, and *W* (660 Da/bp) represents the constant. The PCR products were diluted from 10^7 to 10^{10} copies/μL and amplified to construct standard curves. The real-time qPCR was run with LightCycler480 II (Roche, German). The reaction mixture contained 5 μL SybrGreen qPCR Master Mix (Roche, German), 1 μL of template DNA, and 0.2 μL forward/reverse primer (10 μM), and ddH2O was added to reach a total volume of 10 μL. The real-time qPCR program was as follows: 95°C for 3 min; 45 cycles of 95°C for 15 s, 57°C for 20 s, and 72°C for 30 s. The melting curves for the amplicons were measured while monitoring fluorescence. The amplification efficiencies of three primers were between 80 and 110%, and the melting curves all showed a single peak (**Supplementary Figure S3**), indicating that the results were credible. The copies of each sample based on 16S rRNA universal primer were considered as the bacterial biomass per gram. The following formula was used to calculate the relative abundance: Relative abundance = Ci/C0 × 100%, where Ci represents the copies of the species and C0 represents the bacterial biomass (Xiao et al., 2018).

Network Analysis

Gut microbial ecological networks were constructed and analyzed by random matrix theory (RMT) methods by the online MENA pipeline[2]. OTUs detected in less than 70% from each group were removed to ensure reliable correlations. For comparisons with different networks, the same cutoff of 0.77 was applied to construct ecological networks for gut microbial communities. Each ecological network was separated into modules by the fast greedy modularity optimization to characterize the modularity property. Furthermore, a network developed from OTU abundance data represented the ecological co-occurrence (links) of different OTU markers (nodes) in a microbial community, and different nodes played distinct roles (Guimerà et al., 2007).

Statistical Analysis

The common OTUs mean that the OTUs present in three groups (A1, A0 and H). Principal coordinate analysis (PCoA) was used to identify overall gut microbial composition between CRC patients and healthy individuals based on Bray-Curtis dissimilarity index. Principal components analysis (PCA) was used to determine the changes of KEGG pathways between CRC patients and healthy individuals. Alpha diversity was calculated using the observed species (richness), phylogenetic diversity, Shannon index and Simpson index. The significant differences referred to the multiple response permutation procedure (MRPP) algorithms and analysis of similarity (Anosim). Significant *P*-values associated with microbial clades and functions were identified by Linear Discriminant Analysis with Effect Size (LEfSe). Characteristics with an LDA score cut-off of 2.0 were considered as being different. Community analysis and differential abundance of OTUs were performed using the STAMP 2.0.8 (Parks et al., 2014). According to the Kyoto Encyclopedia of Genes and Genomes (KEGG) orthology, functional profiling of microbial communities was predicted using Phylogenetic Investigation of Communities by Reconstruction of Unobserved States (PICRUSt) (Langille et al., 2013). Gut microbial metabolic and other pathway differences were predicted by the correlations between the PICRUSt-generated functional profiles and STAMP-generated genus level bacterial abundance. Mantel test was used to evaluate the linkages between gut microbial structure and environmental attributes. The R software package (v3.4.1) was used for all statistical

[1] http://zhoulab5.rccc.ou.edu:8080/

[2] http://ieg2.ou.edu/MENA/

analysis, except for two-tailed unpaired *t*-tests by Microsoft Excel 2010, and Analysis of variance (ANOVA) and Pearson correlation by IBM SPSS statistic 19.0 to determine the significance of the differences and the clinical correlates.

RESULTS

Taxonomic Composition and Diversity of Gut Microbiota

A total of 1,819,210 quality-filtered 16S rRNA gene sequences were acquired from 31 samples, with an average of 58,684 ± 2602 reads per sample (**Supplementary Table S4**). A total of 648 OTUs were generated at the 97% similarity level, with an average of 189 ± 60 OTUs per sample (**Supplementary Table S4**). We compared the microbial alpha diversity (richness, phylogenetic diversity, Shannon diversity and Simpson diversity) between CRC patients and healthy individuals (**Table 2**). The results demonstrated that the Shannon diversity and Simpson diversity were significantly decreased in A1 compared with the A0 and H ($P < 0.05$, **Table 2**). However, no statistically significant differences were identified in the richness and phylogenetic diversity for CRC patients and healthy individuals ($P > 0.05$, **Table 2**). The dissimilarity tests showed that A1 was significantly different from A0 and H based on the multiple response permutation procedure (MRPP) algorithms and analysis of similarity (ANOSIM) ($P < 0.05$, **Supplementary Table S5**). PCoA based on Bray-Curtis dissimilarity index revealed overall gut microbial composition in CRC patients was well separated from each other, but partly overlapping with healthy individuals (**Figure 1**). Furthermore, A1 presented a more scattered distribution and had a distance from the A0 and H (**Figure 1**). Therefore, A1 had significantly different community structure with A0 and H.

Taxonomy-Based Comparisons of the Gut Microbiota

The gut microbial taxa and their relative abundance were significantly different among H, A0, and A1. At the phylum level, H was mainly characterized by *Firmicutes* and *Bacteroidetes*, whereas A0 and A1 had a very complicated community composition, especially for A1 (**Supplementary Figure S4**). Compared with H, the relative abundance of *Proteobacteria* was significantly increased by 12.90%, and *Bacteroidetes* was significantly decreased by 23.06% in A1 ($P < 0.05$, **Supplementary Table S6**). At the genus level, the members of *Faecalibacterium*, *Roseburia*, *Ruminococcus*, and *Lachnospiracea_incertae_sedis* were significantly lower in A1 than those in H ($P < 0.05$, **Supplementary Figure S5** and **Supplementary Table S7**). To identify gut microbial responses associated with surgery at the taxonomical level, we determined microbial clade differences using LEfSe analysis (**Figure 2**). At the phylum level, higher proportions of *Proteobacteria* were observed in A1 than that in A0 and H (**Figure 2A**). At the genus level, greater proportions of *Klebsiella* were detected in A1 than that in A0 (**Supplementary Figure S6**). The genus *Fusobacteria* was significantly enriched in A0 than that in A1 and H (**Figure 2B**). The members of *Clostridium XlVa*, *Fusobacterium*, *Parvimonas*, and *Peptostreptococcus* were more abundant on A0 than that on A1 and H (**Figure 2A**).

Sequencing data suggested that gut microbiota made changes in response to surgery, and we further used real-time qPCR to help validate changes observed and detected with 16S sequencing data. We selected *Fusobacterium nucleatum* and *Klebsiella pneumoniae* to examine the variations, which frequently present in CRC patients (**Supplementary Figure S7**). The results showed that the relative abundance of *Fusobacterium nucleatum* in A0 was significantly higher than that in H ($P < 0.05$). However, the relative abundance of *Klebsiella pneumoniae* was not significantly changed. In addition, individual differences were evident showed in **Supplementary Figure S8**. Notably, the relative abundance of *Fusobacterium* increased markedly in 8/10 patients of A0 compared with A1. The members of *Klebsiella* were distinctly higher in 9/10 patients of A1 than that in A0.

TABLE 2 | Comparison of alpha diversity indices of gut microbiota between the healthy volunteers (H) and CRC patients before and after surgery (A0 and A1).

Group	Richness	Phylogenetic diversity	Shannon diversity	Simpson diversity
A0	(199 ± 56)a	(15.10 ± 4.00)a	(4.63 ± 0.91)a	(0.90 ± 0.08)a
A1	(166 ± 77)a	(14.14 ± 5.25)a	(3.40 ± 1.27)b	(0.76 ± 0.23)b
H	(187 ± 41)a	(14.31 ± 2.44)a	(4.34 ± 0.91)a	(0.88 ± 0.08)a

Values are shown as mean ± standard deviation. Richness means the detected gene/sequence numbers. Significant differences among different groups are indicated by alphabetic letters, P < 0.05. The 'a' means there are no significance differences among groups. The 'b' means the group is significantly different from other two groups.

Functional and Metabolic Discrepancy of the Gut Microbiota

Further studies were required to understand the dynamics of gut microbiota following surgical treatment to evaluate the role of microbiota. The PCA of KEGG pathways indicated that A1 was notably different from A0 and H, which had a more scattered distribution based on the STAMP analysis (**Figure 3A**). In terms of KEGG pathways (L2, **Figure 3B**), the functions of 'replication and repair,' 'folding, sorting and degradation,' and 'cell growth and death,' which belong to the first level 'Genetic information processing' and 'Cellular processes,' respectively, were significantly enriched in A0 ($P < 0.05$) compared with H and A1 based on the LEfSe analysis. The results indicated that gut microbiota in pre-surgery patients was enriched in more conservative housekeeping functions. The 'infectious diseases,' 'xenobiotics biodegradation and metabolism,' 'metabolism of other amino acids,' 'neurodegenerative diseases,' and 'metabolism' were significant function hallmarks of gut microbiota in A1. Furthermore, we found that the genus *Klebsiella* in A1 was significantly and closely associated with infectious diseases, such as bacterial invasion of epithelial cells and *Staphylococcus aureus* infection ($P < 0.05$, **Figure 4**).

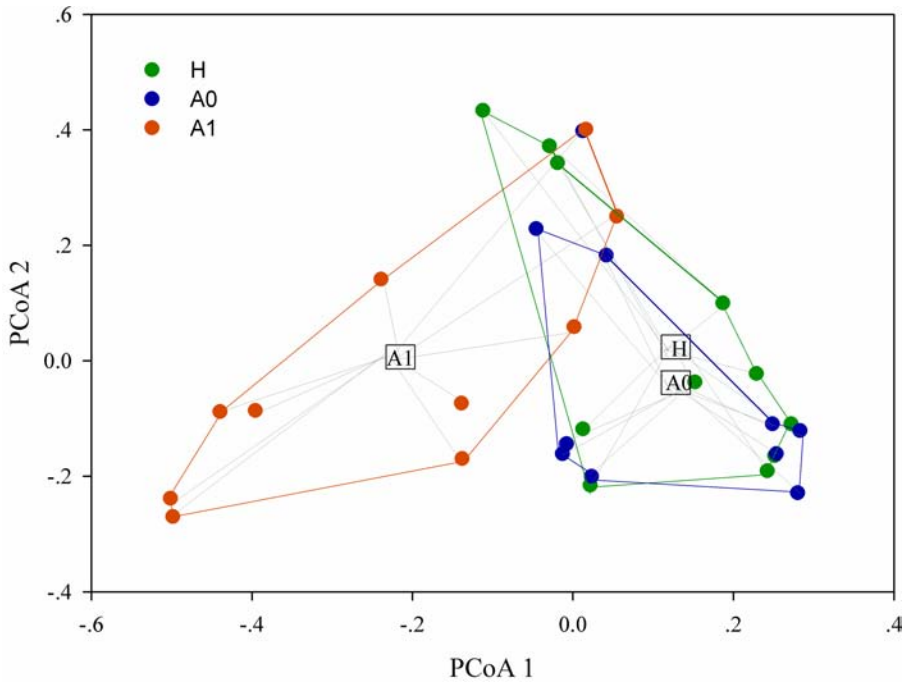

FIGURE 1 | Principal coordinates analysis (PCoA) ordination (operational taxonomic units = 97% 16S rRNA sequence similarity) showing distinctly different microbial composition between CRC patients and healthy individuals based on the Bray-Curtis dissimilarity matrix.

Modularity Analysis in Gut Microbiota

Microbes rarely live in isolation, but instead interact in complex ecological networks. To identify the assemblages that potentially interact within the intestinal tract, we focused on representative networks from CRC patients and healthy individuals. We selected more than five nodes to construct the modules and visualized the phylogeny for modules with at least two kinds of phyla (**Figure 5**). Overall, OTU tended to co-occur (positive correlations, gray lines) rather than co-exclude (negative correlations, pink lines). However, there were more negative correlations between gut microbes in A0 than that in A1 and H (**Figure 5**). The modules in A1 became smaller and less connected, which had fewer nodes and links (35, 37) than that in A0 (60, 113) and in H (91, 231). Furthermore, the kinds of phylum in each module were only two in A1, which were less than that in A0 and H.

Correlates of Gut Microbiota and Clinical Variables

Based on the mantel test, we explored the clinical correlates of gut microbiota and patients age, sex, BMI, and bowel treatment. The results showed that the whole gut microbiota and key phyla had no significant correlations with these clinical variables (**Supplementary Table S8**). Then, we analyzed the histopathological correlates of gut microbiota and tumor stage, grade of tumor differentiation, lymphatic invasion, perineural invasion, number of metastasis lymph nodes and tumor markers (CEA and CA199) (**Supplementary Table S9**). We found that the *Fusobacterium* (*Fusobacteria*, *Fusobacteriia*, *Fusobacteriales*, *Fusobacteriaceae*) in A0 and *Klebsiella* (*Proteobacteria*, *Gammaproteobacteria*, *Enterobacteriales*, *Enterobacteriaceae*) in A1 were significantly correlated with lymphatic invasion ($P < 0.05$). The *Fusobacterium* (*Fusobacteria*, *Fusobacteriia*, *Fusobacteriales*, *Fusobacteriaceae*) in A0 was significantly correlated with CA199 ($P < 0.05$).

DISCUSSION

The gut microbiota interacts extensively with the host by the co-metabolism of substrates and metabolic exchanges to maintain a healthy status and normal functions of the body (Nicholson et al., 2005). Previous studies have highlighted the significance of gut microbiota in the progression of intestinal diseases such as Crohn's disease, ulcerative colitis (Willing et al., 2010), celiac disease in children (Nadal et al., 2007), allergic inflammation in infants (Kalliomäki and Isolauri, 2003), and CRC (Bachmann et al., 2017). In this pilot study, we focused on exploring the feedback of gut microbiota of CRC patients in response to the surgical removal of lesions.

The gut microbial community composition and diversity in post-surgery CRC patients significantly differ from that in pre-surgery CRC patients and healthy individuals ($P < 0.05$, **Figure 1**, **Table 2**, and **Supplementary Table S5**). However, the gut microbial alpha diversity in A0 was not significantly different from that in H (**Table 2**). The findings may be explained by previous report that the fecal microbiota only partially reflected mucosal microbiota in CRC (Flemer et al., 2017a). The alpha diversity in A1 was significantly lower than that in

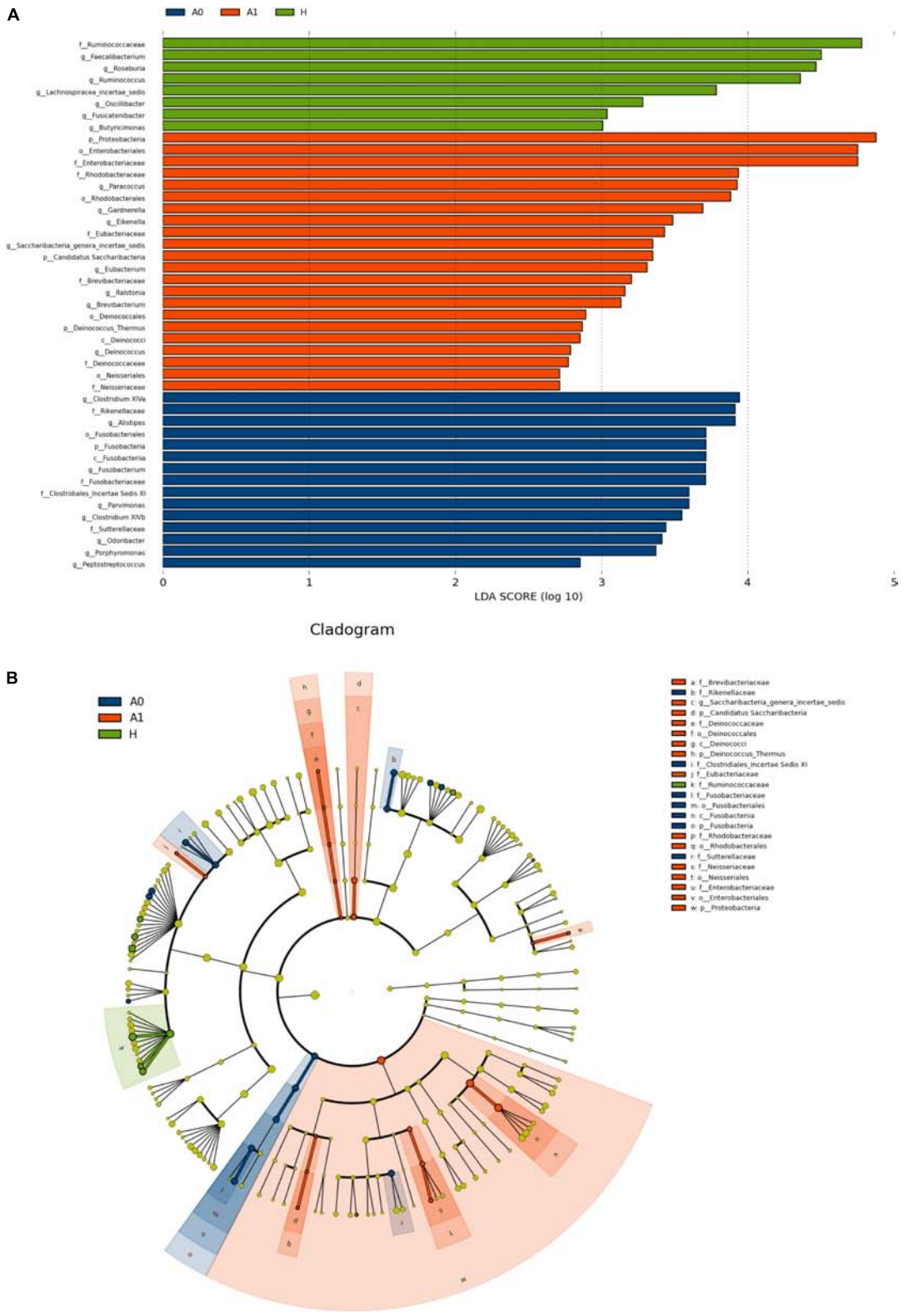

FIGURE 2 | Microbial biomarkers among healthy volunteers (H) and CRC patients (A0 and A1). **(A)** LEfSe analysis shows differentially abundant taxa as biomarkers using Kruskal–Wallis test ($P < 0.05$) with LDA score > 2.0. **(B)** Cladogram representation of the differentially abundant taxa. The root of the cladogram represents the domain bacteria. The size of each node represents their relative abundance. No significantly different taxa are labeled by yellow. Significant different taxa are labeled by following the color of each group.

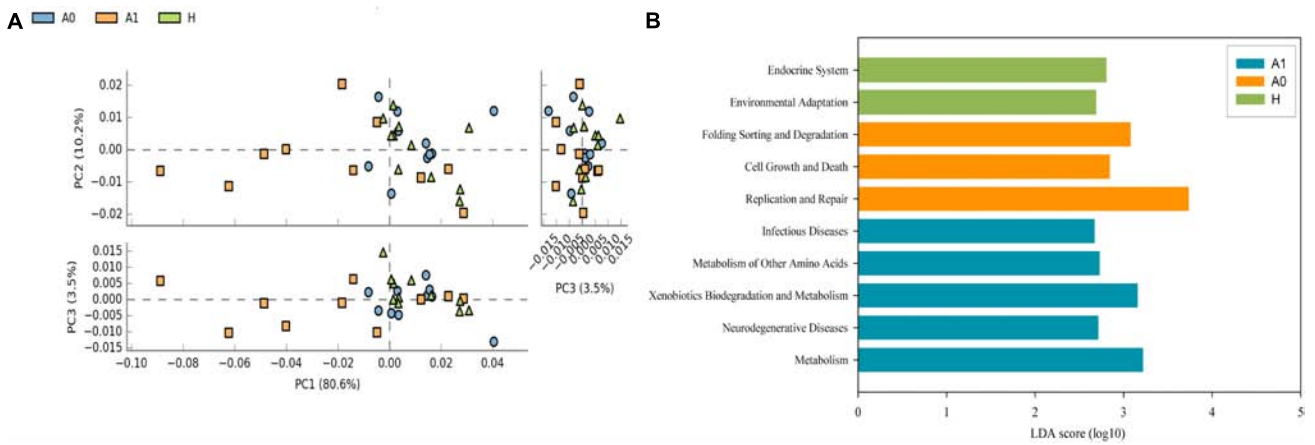

FIGURE 3 | Functional and metabolic discrepancy of the gut microbiota between CRC patients and healthy individuals. **(A)** Principal component analysis (PCA) plot of the KEGG pathway (L2) shows that the post-surgery CRC patients were noticeably different from the pre-surgery CRC patients and healthy individuals based on the STAMP analysis. Characteristics with an LDA score cut-off of 2.0 were considered as being different. The LDA scores (log10) > 2 are listed; **(B)** Discriminatory functional pathways (KEGG L2) shows the significantly different between CRC patients and healthy individuals based on the LDA score using the LEfSe analysis.

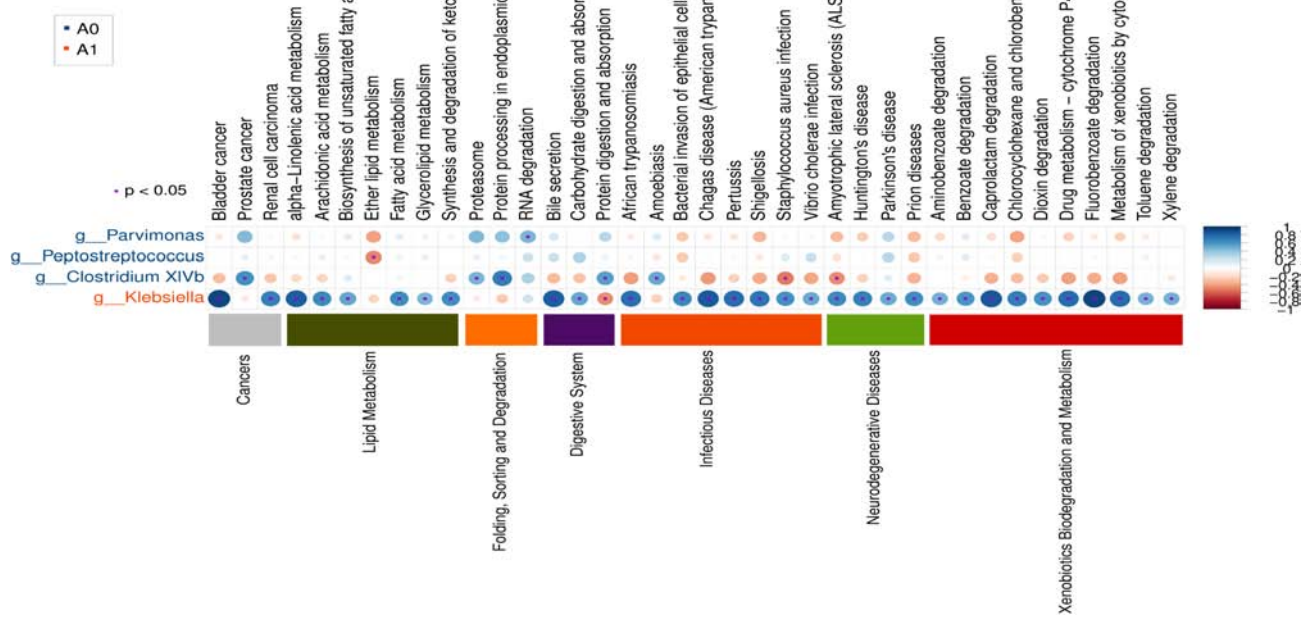

FIGURE 4 | Gut microbial metabolic and other pathway differences in pre-surgery CRC patients (A0) and post-surgery CRC patients (A1). Correlations between the PICRUSt-generated functional profiles and STAMP-generated genus level bacterial abundance are calculated and plotted.

H ($P < 0.05$). High diversity is always linked to health and temporal stability (Flores et al., 2014). Conversely, a relative lack of diversity is often observed in the gut microbiota of CRC patients (Gao et al., 2015). Antibiotics use causes a dramatic reduction in the diversity of gut microbiota (Dethlefsen and Relman, 2011), which was similar to our results that the gut microbial diversity was significantly decreased in post-surgery CRC patients, potentially weakening the community's ability to resist pathogens.

Flemer et al. (2017b) had previously confirmed that the microbiota of CRC patients differed from that of controls (Flemer et al., 2017b), and similar results had been found in our study that gut microbial taxa and their relative abundance of CRC patients, especially for post-surgery CRC patients, significantly

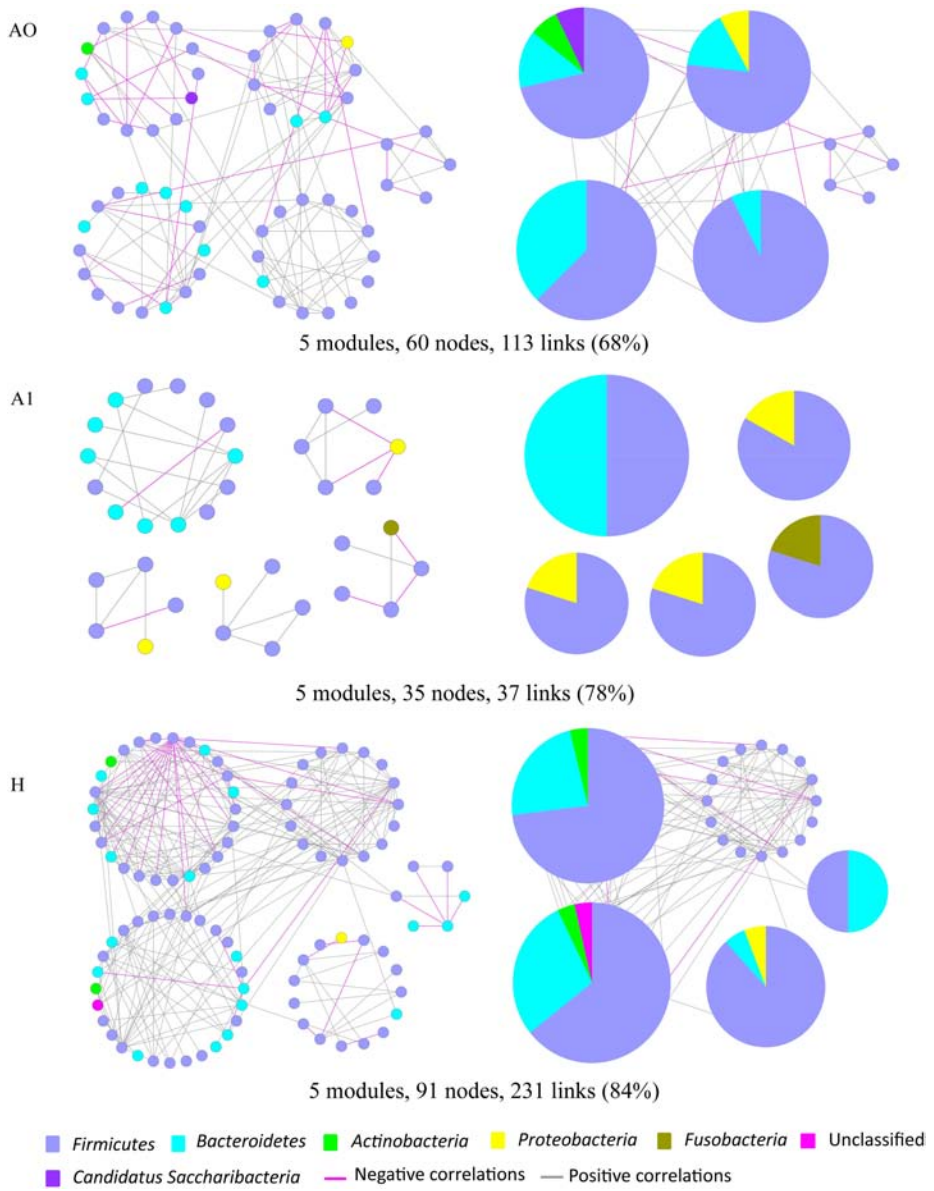

FIGURE 5 | Highly connected modules of gut microbial networks within CRC patients before and after surgery (A0, A1) and healthy individuals (H). The colors of nodes indicate different major phyla; pie charts represent the composition of modules with ≥ 2 phyla. A pink link indicates negative correlations between two individual nodes, whereas a gray link indicates positive correlations. The percentage in parentheses indicates the ratio of positive correlations.

differed from that of healthy individuals ($P < 0.05$). Generally, the gut microbiota in healthy individuals is dominated by the phyla *Firmicutes* and *Bacteroidetes* (Consortium, 2012), whereas *Proteobacteria*, *Actinobacteria*, *Verrucomicrobia*, and *Fusobacteria* are less abundant (Bäckhed et al., 2005). The relative abundance of phylum *Proteobacteria* was significantly higher in A1 than that in A0 and H ($P < 0.05$, **Figure 2A** and **Supplementary Table S6**). Imbalanced gut microbiota often results from a sustained increase in *Proteobacteria*, and human gut microbiota normally contains a minor proportion of this phylum (Shin et al., 2015). A bloom of *Proteobacteria* in the gut often reflects an unstable structure of the gut microbial community, which was often observed in the disease states (Morgan et al., 2012). *Proteobacteria* was often associated with dysbiosis and was a potential diagnostic criterion for disease (Shin et al., 2015). The relative abundance of phylum *Fusobacteria* was significantly increased in A0 than that in A1 and H ($P < 0.05$, **Figure 2B**). At the genus level, *Klebsiella* played more significantly key roles in A1 than that in A0 ($P < 0.05$, **Supplementary Figure S6**). However, the relative abundance of *Klebsiella pneumoniae* was not significantly changed based on the real-time qPCR (**Supplementary Figure S7**). The reasons were probably ascribed to the small sample size, followed by the low abundance in sample itself, DNA degradation of human feces, the

sensitivity and specificity of primer, reaction condition of qPCR. In addition, *Clostridium XlVa*, *Parvimonas*, *Peptostreptococcus*, and *Fusobacterium* played significantly important roles in A0 ($P < 0.05$, **Figure 2A**). *Parvimonas* was frequently and significantly increased in stools from CRC patients (Shah et al., 2017). *Peptostreptococcus* played a key role in the dysbiosis of mucosa-associated microbiota in CRC patients (Shah et al., 2017). It was reported that *Fusobacterium* species led the development of CRC (Kostic et al., 2012). The qPCR results also showed that *Fusobacterium nucleatum* in A0 was significantly higher than that in H ($P < 0.05$, **Supplementary Figure S7**). *Fusobacterium nucleatum* infection is prevalent in human CRC (Castellarin et al., 2012). Furthermore, we found that *Fusobacterium* (*Fusobacteria*, *Fusobacteriia*, *Fusobacteriales*, *Fusobacteriaceae*) in A0 was significantly correlated with lymphatic invasion and tumor marker CA199 ($P < 0.05$, **Supplementary Table S9**), similar to Castellarin et al. (2012) results that indicated that high relative abundance of *Fusobacterium* was more likely to have regional lymph node metastases. Therefore, gut microbiota from fecal samples was increasingly possible to be considered as potential diagnostic biomarkers of dysbiosis for CRC patients (Zackular et al., 2014).

Potential function and metabolism of gut microbiota in CRC patients were greatly changed in response to the surgery. Although great differences were observed in the taxonomic composition of gut microbiota in different individuals, the metabolic pathways are considerably more consistent across people (Consortium, 2012). A healthy microbiota may contain specific microbial combinations, metabolic modules, and regulatory pathways that together maintain a stable host-associated ecology (Martiny et al., 2015). The housekeeping functions are necessary for all microbial life, such as 'replication and repair' and 'cell growth and death' (Consortium, 2012). Our results demonstrated that the housekeeping functions were significantly associated with gut microbiota in A0, whereas the gut microbiota in A1 was more closely involved with the functions of infectious diseases and xenobiotics biodegradation and metabolism (**Figure 3**). The *Klebsiella* in A1 was determined to be closely associated with infectious diseases (**Figure 4**). *Klebsiella* is an opportunistic pathogen routinely found in human gut that causes diarrhea, pneumonia, and bloodstream infections (Yan et al., 2017). It was reported that overgrowth of *Klebsiella* often foreshadowed gut flora dysbiosis (Garrett et al., 2010) and markedly increased the rates of treatment failure and death (Yan et al., 2017). Furthermore, *Klebsiella* (*Proteobacteria*, *Gammaproteobacteria*, *Enterobacteriales*, *Enterobacteriaceae*) in A1 was significantly correlated with lymphatic invasion ($P < 0.05$, **Supplementary Table S9**). Therefore, the gut microbiota in post-surgery CRC patients maybe presented a weaker robustness when random and specific perturbations influence its functional stability.

Molecular ecological networks of gut microbiota in CRC patients were also greatly changed in response to the surgery. In network biology, a group of microbial species strongly interacting with one another constructs a module, which may reflect physical contact, divergent selection, functional association, and/or the phylogenetic clustering of closely related species (Olesen et al., 2007). Considering the characteristic of a smaller and looser network module in A1 (**Figure 5**), it implied that A1 had a weaker coupling between gut microbes than A0 and H. This could partially be explained by some sharply growing pathogenic bacterium, such as the phylum *Proteobacteria*, influencing the microbial community structure (**Figure 2** and **Supplementary Table S6**). Therefore, the gut microbiota in post-surgery patients probably had a higher sensitivity in response to external changes.

The age, sex, BMI, bowel treatment and diet were considered as the important influencing factors in changing the gut microbiota of CRC patients. However, we found that there were no significant correlations between these factors (age, sex, BMI, and bowel treatment) and gut microbiota based on the mantel test (**Supplementary Table S8**). Comprehensive information on microbial species across a great number of samples is essential in identifying the changes among microbial communities (Barberán et al., 2012). Sample sets should ideally be ample to achieve sufficient variability (Barberán et al., 2012). However, the number of patients in the treatment group was relatively small and individual differences were evident (**Supplementary Figure S8**). Therefore, there was not statistical power to adequately examine these relationships between these factors (age, sex, BMI, and bowel treatment) and gut microbiota. Therefore, we could not scale the results to all the situations with only a few samples. In addition, samples from the post-surgery patients were also influenced by the colonoscopy. More attentions should be paid on these correlative factors in the future. Yet, this pilot study would provide better understanding of the responses of gut microbiota to the surgical removal of lesions for CRC patients (**Supplementary Figure S9**). The gut microbiota probably plays a key role in identifying the condition for post-surgery CRC patients. Additional sampling efforts, colonoscopy effects, and diet records combined with clinical follow-up are required to further obtain unique insight into gut microbial changes in post-surgery CRC patients to predict disease states and develop therapies to correct dysbiosis.

CONCLUSION

In summary, this pilot study explored the changes of gut microbiota in CRC patients following the surgery. The gut microbial taxonomic compositions in post-surgery CRC patients were significantly different from those in pre-surgery CRC patients and healthy individuals. The gut microbiota in post-surgery CRC patients had a significantly lower alpha diversity and a looser ecological interaction network. Most post-surgery CRC patients had more abundances of *Klebsiella*. The *Klebsiella* in post-surgery CRC patients was significantly associated with lymphatic invasion. These results indicated that gut microbiota was probably considered to be the valuable biomarkers in evaluating the condition of post-surgery CRC patients. More attentions should be paid to advance our understanding of the

role of gut microbiota in recovering the intestinal health of post-surgery CRC patients.

AVAILABILITY OF DATA AND MATERIAL

Sequencing data are accessible in NCBI SRA database with Accession No. SRP133809 (https://www.ncbi.nlm.nih.gov/sra/SRP133809).

ETHICS STATEMENT

The Affiliated Hospital of Qingdao University Institutional Review Board approved this study, and all study subjects provided informed consent.

AUTHOR CONTRIBUTIONS

All authors were involved in the design of the study. DL, HZ, and CH collected fecal samples. JjZ, TL, CZ, HL, KL, ZT, and JlZ analyzed the data. All authors interpreted the data. JC participated in all the work including writing the manuscript. All authors reviewed and revised the manuscript, and approved the final version of the manuscript.

FUNDING

This study was supported by funding from Project funded by China Postdoctoral Science Foundation (2016M602094), Qingdao Postdoctoral Application Research Project (2016047), Youth Research Fund Project, and Taishan Scholar Foundation (201502061).

ACKNOWLEDGMENTS

The authors thank the CRC patients and healthy volunteers for providing the fecal samples that were used in this study.

SUPPLEMENTARY MATERIAL

The Supplementary Material for this article can be found online at: https://www.frontiersin.org/articles/10.3389/fmicb.2018.02777/full#supplementary-material

REFERENCES

Bachmann, R., Leonard, D., Delzenne, N., Kartheuser, A., and Cani, P. D. (2017). Novel insight into the role of microbiota in colorectal surgery. *Gut* 66, 739–749. doi: 10.1136/gutjnl-2016-312569

Bäckhed, F., Ley, R. E., Sonnenburg, J. L., Peterson, D. A., and Gordon, J. I. (2005). Host-bacterial mutualism in the human intestine. *Science* 307, 1915–1920. doi: 10.1126/science.1104816

Balamurugan, R., Rajendiran, E., George, S., Samuel, G. V., and Ramakrishna, B. S. (2008). Real-time polymerase chain reaction quantification of specific butyrate-producing bacteria, *Desulfovibrio* and *Enterococcus faecalis* in the feces of patients with colorectal cancer. *J. Gastroenterol. Hepatol.* 23, 1298–1303. doi: 10.1111/j.1440-1746.2008.05490.x

Barberán, A., Bates, S. T., Casamayor, E. O., and Fierer, N. (2012). Using network analysis to explore co-occurrence patterns in soil microbial communities. *ISME J.* 6, 343–351. doi: 10.1038/ismej.2011.119

Bernstein, H., Bernstein, C., Payne, C. M., and Dvorak, K. (2009). Bile acids as endogenous etiologic agents in gastrointestinal cancer. *World J. Gastroenterol.* 15, 3329–3340. doi: 10.3748/wjg.15.3329

Berstad, P., Løberg, M., Larsen, I. K., Kalager, M., Holme, Ø, Botteri, E., et al. (2015). Long-term lifestyle changes after colorectal cancer screening: randomized controlled trial. *Gut* 64, 1268–1276. doi: 10.1136/gutjnl-2014-307376

Castellarin, M., Warren, R. L., Freeman, J. D., Dreolini, L., Krzywinski, M., Strauss, J., et al. (2012). *Fusobacterium nucleatum* infection is prevalent in human colorectal carcinoma. *Genome Res.* 22, 299–306. doi: 10.1101/gr.126516.111

Consortium, H. M. P. (2012). Structure, function and diversity of the healthy human microbiome. *Nature* 486, 207–214. doi: 10.1038/nature11234

Deng, Y., Jiang, Y. H., Yang, Y., He, Z., Luo, F., and Zhou, J. (2012). Molecular ecological network analyses. *BMC Bioinformatics* 13:113. doi: 10.1186/1471-2105-13-113

Dethlefsen, L., and Relman, D. A. (2011). Incomplete recovery and individualized responses of the human distal gut microbiota to repeated antibiotic perturbation. *Proc. Natl. Acad. Sci. U.S.A.* 108(Suppl. 1), 4554–4561. doi: 10.1073/pnas.1000087107

Devillard, E., Mcintosh, F. M., Duncan, S. H., and Wallace, R. J. (2007). Metabolism of linoleic acid by human gut bacteria: different routes for biosynthesis of conjugated linoleic acid. *J. Bacteriol.* 189, 2566–2570. doi: 10.1128/JB.01359-06

Eckburg, P. B., Bik, E. M., Bernstein, C. N., Purdom, E., Dethlefsen, L., Sargent, M., et al. (2005). Diversity of the human intestinal microbial flora. *Science* 308, 1635–1638. doi: 10.1126/science.1110591

Edgar, R. C. (2010). Search and clustering orders of magnitude faster than BLAST. *Bioinformatics* 26, 2460–2461. doi: 10.1093/bioinformatics/btq461

Flemer, B., Lynch, D. B., Brown, J. M. R., Jeffery, I. B., Ryan, F. J., Claesson, M. J., et al. (2017a). Original article: tumour-associated and non-tumour-associated microbiota in colorectal cancer. *Gut* 66, 633–643. doi: 10.1136/gutjnl-2015-309595

Flemer, B., Lynch, D. B., Brown, J. M. R., Jeffery, I. B., Ryan, F. J., Claesson, M. J., et al. (2017b). Tumour-associated and non-tumour-associated microbiota in colorectal cancer. *Gut* 66, 633–643. doi: 10.1136/gutjnl-2015-309595

Flores, G. E., Caporaso, J. G., Henley, J. B., Rideout, J. R., Domogala, D., Chase, J., et al. (2014). Temporal variability is a personalized feature of the human microbiome. *Genome Biol.* 15, 1–13. doi: 10.1186/s13059-014-0531-y

Gao, Z., Guo, B., Gao, R., Zhu, Q., and Qin, H. (2015). Microbiota disbiosis is associated with colorectal cancer. *Front. Microbiol.* 6:20. doi: 10.3389/fmicb.2015.00020

Garrett, W. S., Gallini, C. A., Yatsunenko, T., Michaud, M., Dubois, A., Delaney, M. L., et al. (2010). *Enterobacteriaceae* act in concert with the gut microbiota to induce spontaneous and maternally transmitted colitis. *Cell Host Microbe* 8, 292–300. doi: 10.1016/j.chom.2010.08.004

Guimerà, R., Sales-Pardo, M., and Amaral, L. A. N. (2007). Classes of complex networks defined by role-to-role connectivity profiles. *Nat. Phys.* 3, 63–69. doi: 10.1038/nphys489

Huycke, M. M., and Gaskins, H. R. (2004). Commensal bacteria, redox stress, and colorectal cancer: mechanisms and models. *Exp. Biol. Med.* 229, 586–597. doi: 10.1177/153537020422900702

Jemal, A., Bray, F., Center, M. M., Ferlay, J., Ward, E., and Forman, D. (2011). Global cancer statistics. *Cancer J. Clin.* 61, 69–90. doi: 10.3322/caac.20107

Kalliomäki, M., and Isolauri, E. (2003). Role of intestinal flora in the development of allergy. *Curr. Opin. Allergy Clin. Immunol.* 3, 15–20. doi: 10.1097/00130832-200302000-00003

Kong, Y. (2011). Btrim: a fast, lightweight adapter and quality trimming program for next-generation sequencing technologies. *Genomics* 98, 152–153. doi: 10.1016/j.ygeno.2011.05.009

Kostic, A. D., Gevers, D., Pedamallu, C. S., Michaud, M., Duke, F., Earl, A. M., et al. (2012). Genomic analysis identifies association of Fusobacterium

with colorectal carcinoma. *Genome Res.* 22, 292–298. doi: 10.1101/gr.126573.111

Langille, M. G., Zaneveld, J., Caporaso, J. G., Mcdonald, D., Knights, D., Reyes, J. A., et al. (2013). Predictive functional profiling of microbial communities using 16S rRNA marker gene sequences. *Nat. Biotechnol.* 31, 814–821. doi: 10.1038/nbt.2676

Magoč, T., and Salzberg, S. L. (2011). FLASH: fast length adjustment of short reads to improve genome assemblies. *Bioinformatics* 27, 2957–2963. doi: 10.1093/bioinformatics/btr507

Martiny, J. B., Jones, S. E., Lennon, J. T., and Martiny, A. C. (2015). Microbiomes in light of traits: a phylogenetic perspective. *Science* 350:aac9323. doi: 10.1126/science.aac9323

Morgan, X. C., Tickle, T. L., Sokol, H., Gevers, D., Devaney, K. L., Ward, D. V., et al. (2012). Dysfunction of the intestinal microbiome in inflammatory bowel disease and treatment. *Genome Biol.* 13:R79. doi: 10.1186/gb-2012-13-9-r79

Nadal, I., Donat, E., Ribes-Koninckx, C., Calabuig, M., and Sanz, Y. (2007). Imbalance in the composition of the duodenal microbiota of children with coeliac disease. *J. Med. Microbiol.* 56, 1669–1674. doi: 10.1099/jmm.0.47410-0

Nicholson, J. K., Holmes, E., and Wilson, I. D. (2005). Gut microorganisms, mammalian metabolism and personalized health care. *Nat. Rev. Microbiol.* 3, 431–438. doi: 10.1038/nrmicro1152

O'Brien, C. L., Allison, G. E., Grimpen, F., and Pavli, P. (2013). Impact of colonoscopy bowel preparation on intestinal microbiota. *PLoS One* 8:e62815. doi: 10.1371/journal.pone.0062815

Olesen, J. M., Bascompte, J., Dupont, Y. L., and Jordano, P. (2007). The modularity of pollination networks. *Proc. Natl. Acad. Sci. U.S.A.* 104, 19891–19896. doi: 10.1073/pnas.0706375104

Parks, D. H., Tyson, G. W., Hugenholtz, P., and Beiko, R. G. (2014). STAMP: statistical analysis of taxonomic and functional profiles. *Bioinformatics* 30, 3123–3124. doi: 10.1093/bioinformatics/btu494

Ryuk, J. P., Choi, G. S., Park, J. S., Kim, H. J., Park, S. Y., Yoon, G. S., et al. (2014). Predictive factors and the prognosis of recurrence of colorectal cancer within 2 years after curative resection. *Ann. Surg. Treat. Res.* 86, 143–151. doi: 10.4174/astr.2014.86.3.143

Saleh, M., and Trinchieri, G. (2011). Innate immune mechanisms of colitis and colitis-associated colorectal cancer. *Nat. Rev. Immunol.* 11, 9–20. doi: 10.1038/nri2891

Scanlan, P. D., Shanahan, F., and Marchesi, J. R. (2009). Culture-independent analysis of desulfovibrios in the human distal colon of healthy, colorectal cancer and polypectomized individuals. *FEMS Microbiol. Ecol.* 69, 213–221. doi: 10.1111/j.1574-6941.2009.00709.x

Scharlau, D., Borowicki, A., Habermann, N., Hofmann, T., Klenow, S., Miene, C., et al. (2009). Mechanisms of primary cancer prevention by butyrate and other products formed during gut flora-mediated fermentation of dietary fibre. *Mutat. Res.* 682, 39–53. doi: 10.1016/j.mrrev.2009.04.001

Shah, M. S., Desantis, T. Z., Weinmaier, T., Mcmurdie, P. J., Cope, J. L., Altrichter, A., et al. (2017). Leveraging sequence-based faecal microbial community survey data to identify a composite biomarker for colorectal cancer. *Gut* 67, 882–891. doi: 10.1136/gutjnl-2016-313189

Shin, N. R., Whon, T. W., and Bae, J. W. (2015). *Proteobacteria*: microbial signature of dysbiosis in gut microbiota. *Trends Biotechnol.* 33, 496–503. doi: 10.1016/j.tibtech.2015.06.011

Sobhani, I., Sobhani, J., Roudot-Thoraval, F., Roperch, J. P., Letulle, S., Letulle, P., et al. (2011). Microbial dysbiosis in colorectal cancer (CRC) patients. *PLoS One* 6:e16393. doi: 10.1371/journal.pone.0016393

Sun, F., Wu, D., Qiu, Z., Jin, M., Wang, X., and Li, J. (2010). Development of real-time PCR systems based on SYBR Green for the specific detection and quantification of *Klebsiella pneumoniae* in infant formula. *Food Control* 21, 487–491. doi: 10.1016/j.foodcont.2009.07.014

Sun, J., and Kato, I. (2016). Gut microbiota, inflammation and colorectal cancer. *Annu. Rev. Microbiol.* 3, 130–143. doi: 10.1016/j.gendis.2016.03.004

Wang, Q., Garrity, G. M., Tiedje, J. M., and Cole, J. R. (2007). Naïve Bayesian classifier for rapid assignment of rRNA sequences into the new bacterial taxonomy. *Appl. Environ. Microbiol.* 73, 5261–5267. doi: 10.1128/AEM.00062-07

Willing, B. P., Dicksved, J., Halfvarson, J., Andersson, A. F., Lucio, M., Zheng, Z., et al. (2010). A pyrosequencing study in twins shows that gastrointestinal microbial profiles vary with inflammatory bowel disease phenotypes. *Gastroenterology* 139, 1844–1854. doi: 10.1053/j.gastro.2010.08.049

Wu, X., Zhang, H., Chen, J., Shang, S., Wei, Q., Yan, J., et al. (2016). Comparison of the fecal microbiota of dholes high-throughput Illumina sequencing of the V3–V4 region of the 16S rRNA gene. *Appl. Microbiol. Biotechnol.* 100, 3577–3586. doi: 10.1007/s00253-015-7257-y

Xiao, Y., Liu, X., Meng, D., Tao, J., Gu, Y., Yin, H., et al. (2018). The role of soil bacterial community during winter fallow period in the incidence of tobacco bacterial wilt disease. *Appl. Microbiol. Biotechnol.* 102, 2399–2412. doi: 10.1007/s00253-018-8757-3

Yan, Q., Gu, Y., Li, X., Yang, W., Jia, L., Chen, C., et al. (2017). Alterations of the gut microbiome in hypertension. *Front. Cell. Infect. Microbiol.* 7:381. doi: 10.3389/fcimb.2017.00381

Zackular, J. P., Rogers, M. A., and Schloss, P. D. (2014). The human gut microbiome as a screening tool for colorectal cancer. *Cancer Prev. Res.* 7, 1112–1121. doi: 10.1158/1940-6207.CAPR-14-0129

Zeller, G., Tap, J., Voigt, A. Y., Sunagawa, S., Kultima, J. R., Costea, P. I., et al. (2014). Potential of fecal microbiota for early-stage detection of colorectal cancer. *Mol. Syst. Biol.* 10:766. doi: 10.15252/msb.20145645

Zheng, Z., Zhong, W., Liu, L., Wu, C., Zhang, L., Cai, S., et al. (2016). Bioinformatics approaches for human gut microbiome research. *Infect. Dis. Transl. Med.* 2, 69–79.

Conflict of Interest Statement: The authors declare that the research was conducted in the absence of any commercial or financial relationships that could be construed as a potential conflict of interest.

frontiers in Microbiology

ORIGINAL RESEARCH
published: 08 January 2019
doi: 10.3389/fmicb.2018.03246

A Comparison of Homogenization vs. Enzymatic Lysis for Microbiome Profiling in Clinical Endoscopic Biopsy Tissue Samples

Chao Zhang[1,2†], *Prashant V. Thakkar*[2†], *Sarah Ellen Powell*[2], *Prateek Sharma*[3], *Sreekar Vennelaganti*[3], *Doron Betel*[1,2] *and Manish A. Shah*[2*]

[1] *Institute for Computational Biomedicine, Weill Cornell Medicine, New York, NY, United States,* [2] *Division of Hematology and Medical Oncology, Department of Medicine, Weill Cornell Medicine, New York, NY, United States,* [3] *Veterans Affairs Medical Center and University of Kansas School of Medicine, Kansas City, MO, United States*

OPEN ACCESS

Edited by:
Nezar Al-hebshi, Temple University, United States

Reviewed by:
Gary Moran, Trinity College Dublin, Ireland
Mohammed A. Ibrahim Al-Obaide, Texas Tech University Health Science Center School of Medicine at Amarillo, United States
Nur A. Hasan, University of Maryland, College Park, United States

***Correspondence:**
Manish A. Shah
mas9313@med.cornell.edu

†These authors have contributed equally to this work

Specialty section:
This article was submitted to Systems Microbiology, a section of the journal Frontiers in Microbiology

Received: *03 July 2018*
Accepted: *14 December 2018*
Published: *08 January 2019*

Citation:
Zhang C, Thakkar PV, Powell SE, Sharma P, Vennelaganti S, Betel D and Shah MA (2019) A Comparison of Homogenization vs. Enzymatic Lysis for Microbiome Profiling in Clinical Endoscopic Biopsy Tissue Samples. Front. Microbiol. 9:3246. doi: 10.3389/fmicb.2018.03246

Identification of the human microbiome has proven to be of utmost importance with the emerging role of bacteria in various physiological and pathological processes. High throughput sequencing strategies have evolved to assess the composition of the microbiome. To identify possible bias that may exist in the processing of tissue for whole genome sequencing (WGS), it is important to evaluate the extraction method on the overall microbial content and composition. Here we compare two different methods of extraction, homogenization vs. enzymatic lysis, on gastric, esophageal and colorectal biopsies and survey the microbial content and composition using WGS and quantitative PCR (qPCR). We examined total bacterial content using universal 16S rDNA qPCR as well as the abundance of three phyla (*Actinobacter*, *Firmicutes*, *Bacteroidetes)* and one genus (*Fusobacterium)*. We found minimal differences between the two extraction methods in the overall community structure. Furthermore, based on our qPCR analysis, neither method demonstrated preferential extraction of any particular clade of bacteria, nor significantly altered the detection of Gram-positive or Gram-negative organisms. However, although the overall microbial composition remained very similar and the most prevalent bacteria could be detected effectively using either method, the precise community structure and microbial abundances between the two methods were different, primarily due to variations in detection of low abundance genus. We also demonstrate that the homogenization extraction method provides higher microbial DNA content and higher read counts from human tissue biopsy samples of the gastrointestinal tract.

Keywords: gastrointestinal tract, whole genome sequencing, quantitative PCR, microbiome, clinical biopsy, metagenomics, DNA extraction

INTRODUCTION

The human microbiota is an integral part of human physiology, influencing human development, host immunity, and nutrition (Shreiner et al., 2015). Despite extensive studies conducted on the human microbiome over the past decade, the precise ecological relationship between microbial constituents and their human hosts is not fully understood. An important step in the evaluation of

the human microbiome is to accurately extract and quantify microbial content from human tissues (Rossmanith and Wagner, 2011).The human microbiome is remarkably diverse, not only among different individuals but also between anatomic sites within a single host (Human Microbiome Project, 2012).

Differences in extraction methodology may lead to differences in microbial identification due to differences in cell wall structures and susceptibility of certain microbial species to various lysis strategies. Different enzymes lead to variable cell lysis efficiencies for different species (Yuan et al., 2012). Peptide cross-links in peptidoglycan layers within cell walls determine the extent to which some bacteria are more or less resistant to lysing methods vs. mechanical ones (Moore et al., 2004; Lazarevic et al., 2013). As such, there is no single "gold standard" by which to determine microbial composition, especially for low-abundance human biopsy samples from differing anatomic sites.

Most of the upper gastrointestinal (GI) tract, especially the stomach, is a notoriously depauperate environment in terms of microbial composition and diversity, as compared to the oral cavity and the lower gastrointestinal tract. The stomach is a particularly unique and challenging locale from which to isolate and examine microbial constituents because of increased acidity and mucus production, which generally discourages microbial colonization. A number of methods are described in the literature with varied results in diversity, species selection and abundance (Wu et al., 2010; Yuan et al., 2012; Crandall et al., 2016). Few studies to date have addressed the optimal extraction methodology specifically for low-microbial abundance clinical samples. Furthermore, due to cost and efficacy, existing comparisons are predominantly based on sequencing data of 16S rDNA conserved regions of bacterial nucleic acids (Bik et al., 2010). It is unclear how extraction methods affect observed microbial community structure and downstream sequencing analyses, particularly with the advent of whole genome sequencing (WGS) and metagenomic analyses.

This paper examines two microbial DNA isolation protocols for human gastric, esophageal, and colorectal biopsies: a mechanical disruption homogenization protocol and a prolonged enzymatic lysis with lysozyme and proteinase K digestion. We compared these two protocols in terms of microbial yield and capture from low abundance anatomic sites by whole genome analysis. From resulting qPCR and WGS data, we conclude that the extraction methods appear similar when determining overall community structure within low abundance gastric and esophageal biopsy samples. Each method identified similar bacterial populations, for example 26 out of the 36 most prevalent bacterial species identified by WGS could be detected using either method. The minimal differences observed in the other 10 species were not in any generalizable fashion and mostly low abundance. The homogenization method does result in higher bacterial content than enzymatic lysis, resulting in higher bacterial read counts, when undergoing WGS.

RESULTS

We examined a total of 17 biopsy samples from 12 patients, including three gastric samples, four esophageal samples, five colorectal cancer samples and five matching normal colon tissue samples. DNA extracted from these samples, using either the homogenization method or the lysis method, were then compared using qPCR quantitation. Of these, five samples (e.g., three gastric and two esophageal samples) were further examined by WGS.

qPCR Quantification of All Samples

We first evaluated the total bacterial content from different tissues based on the qPCR quantification measured by universal 16S rDNA primers (**Figure 1**). Gastric samples had approximately a 10-fold lower bacterial abundance than colorectal and esophageal tissue confirming previous observations (Bik et al., 2006). Total bacterial content from both protocols are highly consistent in most samples. Eleven out of Seventeen samples show no significant difference between qPCR quantification of two protocols by student t-test ($p > 0.05$). Although the total bacterial contents are different in six samples (C233-Normal and Tumor, C244-Normal and Tumor, C238-Tumor, and E756) when extracted using homogenization vs. lysis method, no specific extraction protocol provided consistently higher yields. This suggests both methods have comparable efficiency in extracting bacterial DNA from human tissue (**Figure 1**).

We then asked if there was a specific preference for either method to extract the Gram-positive or Gram-negative clade. To evaluate this, we used phyla-specific primers to evaluate the extraction of three dominant bacterial phyla in the human GI tract, namely *Actinobacter* (Gram positive), *Firmicutes* (generally Gram positive), and *Bacteroidetes* (Gram negative) using each method (**Figure 2**). In addition, we also quantified a specific genus *Fusobacterium* which is a common bacterium in GI tract albeit with low relative abundance. We assessed abundance of each of the above-mentioned bacterial clade relative to total 16S rDNA quantitation.

Consistent with low total bacterial content, we found low relative abundance of *Firmicutes* as well as *Fusobacterium* in all gastric cancer samples examined and this difference was not significant between the two extraction methods. Whereas, samples G005 and G011 showed significantly higher abundance of *Bacteroidetes* using the lysis method, the homogenization method yielded a higher *Bacteroidetes* proportion in sample G008. We also found significantly different quantitation of *Actinobacter* in all three gastric samples ($p < 0.05$), although this difference was not consistently in favor of one method or the other (**Figure 2**). In esophageal samples, we found no significant difference in the relative abundance of *Fusobacterium*, *Firmicutes*, or *Actinobacter* between the two extraction methods in any of the samples. Only two out of four esophageal samples (E756 and E758) showed a significantly higher abundance of *Bacteroidetes* using the homogenization method which was also in contrast to the lysis method that yielded higher abundance in gastric cancer samples (**Figure 2**).

The colon tumor and normal samples demonstrated greater variability in bacterial quantification (5 out 10 samples differed significantly, $p<0.05$ by student t-test). Notably, despite these differences in bacterial abundances, there was no trend as to which extraction method would routinely provide the greatest bacterial yield. For example, C233 tumor

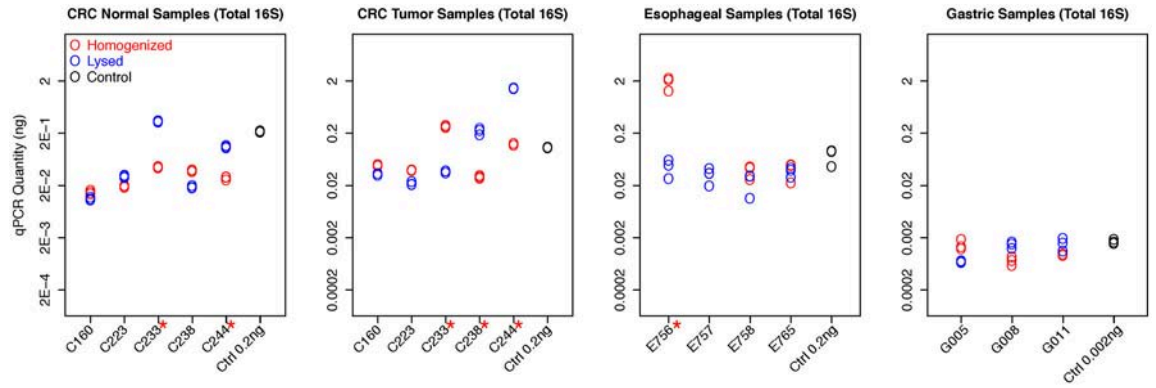

FIGURE 1 | qPCR quantifications of total bacterial content for all samples. The qPCR quantification of each experiment, including replicates, was plotted for each sample with different colors to distinguish two protocols. The readouts of replicates from the same sample are highly consistent. The control samples with known concentration also have been included in all experiments as the reference, demonstrating high accuracy for bacteria quantification. Six samples show significant difference between qPCR quantification of two protocols by student *t*-test (with red * mark).

appears to have significantly greater total bacterial content with the homogenization extraction method (**Figure 1**), with significantly greater amounts of *Fusobacterium* (9 out of 10 colon samples were not significantly different for *Fusobacterium*) (**Figure 2**) whereas the lysis method identified higher amounts of *Bacteroidetes*. In contrast, the C233 normal tissue sample seems to have greater bacterial content with the lysis extraction method (**Figure 1**), whereas significantly more *Bacteroidetes* was identified in this sample using the homogenization method and no difference in quantitation of *Fusobacterium*. Moreover, none of the colon normal and tumor pairs displayed any difference in relative abundance of either *Firmicutes,* or *Actinobacter* (**Figure 2**). While 7 out the 10 colon samples showed significantly different values for *Bacteroidetes* quantitation, once again, this difference wasn't specific to a particular method of extraction.

Overall, no specific method consistently provides higher yields for either of above phyla/genus, and we found near equal quantitation between two methods of most clades across all three types of cancers. Of the 68 samples tested across four different primer sets, 53 samples show no significant difference in quantitation ($p > 0.05$).

Comparison of WGS Data and Microbial Identification Between Two Protocols

We next quantified bacterial content by shallow WGS (10X coverage of human genome) of the full DNA content of the biopsy. Read counts and mapping rates to hg19 (95.773% $\pm$ 0.309) are comparable among all samples (**Table S1**). The remaining reads after multiple steps for filtering human DNA are used for microbial identification. The homogenization extraction method yielded a greater proportion of reads that mapped to bacterial species (3 of the 5 samples had a 2-fold or greater proportion of bacterial mapped reads after filtering, **Table S1**).

Overall, both methods were effective at capturing the most prevalent bacterial species within the samples, for example 26 out of the 36 most prevalent bacterial species identified by WGS could be detected using either method (cosine similarity $p < 0.001$) (**Table S2**). Since the microbial content in biopsy samples is generally low, there may be variable species identification between samples collected from the same patient. We summarized the identification results based on taxonomic genus and order. Considering WGS involves more experimental steps, we expected subtle differences in the community structure from the two methods, and hence we used bacterial absence/presence to measure the profile similarity for the same sample between two different extraction methods. The presence of microbiome at genus level from all five samples, including esophageal tissue E765 and E757, *Helicobacter pylori* negative gastric sample G005, and *H. pylori* positive gastric samples G008 and G011 are all highly consistent between the two extraction methods (cosine similarity $p < 0.05$) (**Figure 3**). Although, as expected, the precise community structure and abundances between the two methods were different, these differences were specifically limited to the low abundance genus. The homogenizing method was more effective in capturing *H. pylori*, consistent with our previous studies in which the homogenization method can identify the presence of *H. pylori* in gastric mucosa of patients with either active or prior *H. pylori* infection (Zhang et al., 2015). The prolonged lysis method appears to identify *Bifidobacterium* sp. and *Pantoea* sp. to a greater extent (**Figure 3**).

Overall, Gram-negative and Gram-positive bacteria were represented by both extraction methods with similar efficiency, with some subtle differences (**Figure S1**). For example, Bacteroidales was detected at low fraction by homogenization method in G008 but not in G011, whereas the detection was inversed in the lysis method. Propionibacteriales is more readily identified using the homogenization method which can yield more reads and higher relative proportion in four out of five samples. Other than Propionibacteriales, there are essentially no other significant difference between any other clades cross all five samples.

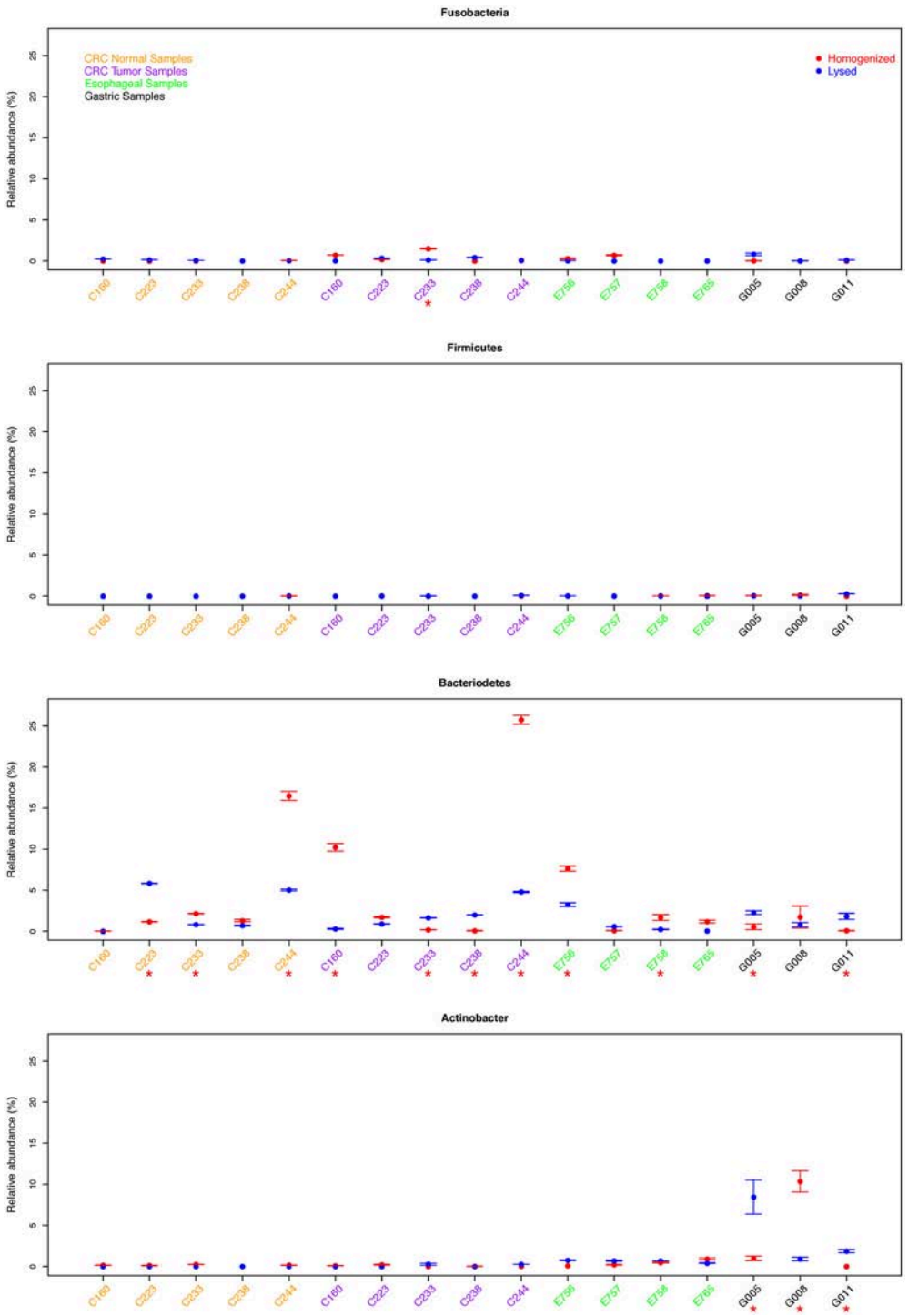

FIGURE 2 | Comparison of relative abundance of *Fusobacterium* sp. and three phyla for all samples. We assessed abundance of each of the above-mentioned bacterial clade relative to total 16S rDNA qPCR quantitation. Samples with significant difference between two protocols were marked with red *.

DISCUSSION

Study of the gut microbiome is of increasing importance with numerous studies identifying the role of microbiota in diseases such as cancer. Various protocols have been employed by the scientific community to extract bacterial DNA from human biopsies, which are then analyzed using next generation sequencing methods. In order to ensure that

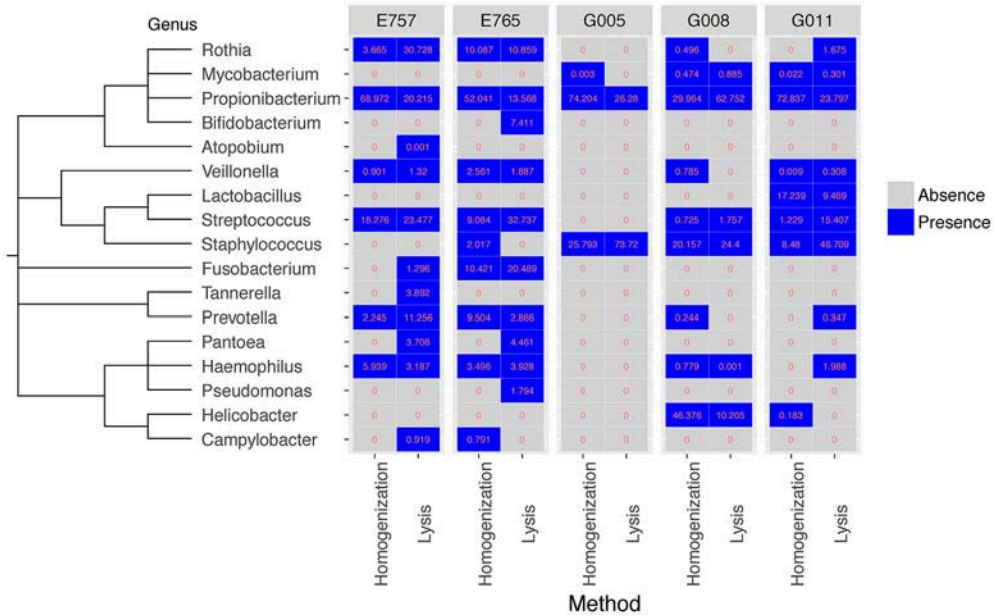

FIGURE 3 | Comparison of bacteria identified from WGS data for five samples at genus level between two extraction methods. Both the homogenization method and the enzymatic lysis method can generate a similar set of microbial genus in all five samples (cosine similarity $p < 0.05$). Values represent percentage of bacteria reads found in each sample.

such an analysis of the gut microbiome is not biased due to the method of extraction, we analyzed and compared two widely used DNA extraction protocols, namely the mechanical disruption (homogenization) vs. the enzymatic lysis method. Furthermore, to account for the vast diversity of the human microbiome, it is important that such an analysis is performed on human biopsies, as opposed to preclinical samples. In order to realistically gauge the influence of a particular extraction method on the complexity of the human gut microbiome, we assessed 5 normal and 12 tumor samples across three different cancer types including gastric, esophageal, and colon cancer. Based on qPCR quantification, no single method consistently generated higher total bacterial content. There were a total of six samples that showed significant differences in the overall bacterial content between the homogenization and the lysis method, as assessed by absolute abundance of 16S rDNA using qPCR quantitation. However, this difference was not in favor of one particular extraction protocol. Moreover, it is possible that these differences may be intrinsic, since different regions of the same biopsy were used to extract DNA using the two protocols. To account for these intrinsic differences, we assessed abundance of three different phyla (*Actinobacter*, *Firmicutes*, and *Bacteroidetes*) as well as *Fusobacterium* relative to total 16S rDNA quantitation. Based on our qPCR results, no single method consistently generated higher readouts for any single clade across all samples. Our results therefore indicate that either extraction method, homogenization or prolonged lysis, can be successfully used to detect bacteria without introducing a significant bias when examining bacteria by qPCR.

We also performed WGS on these samples in parallel to better understand the impact of the extraction method on the bacteria community structure. Whole genome data from gastric and esophageal biopsies did not reveal a significant difference in overall community structure between extraction methods. This is in concordance with studies examining salivary samples and insect gut microbiota whereby 16S rRNA gene amplicons are affected by extraction method but overall community structure is not (Lazarevic et al., 2013; Rubin et al., 2014). In our previous studies, we successfully employed the homogenization method to assess the microbiome composition in gastric mucosa of patients with no infection vs. prior or active *H. pylori* infection (Zhang et al., 2015). Our current analysis further validates that the results obtained previously accurately reflect the predominant bacteria absence/presence in the gastric mucosa, and was not skewed due to the choice of extraction method. However, the relative abundances of some clades do significantly differ by two different methods (**Figure S1**) as we expected. Considering both read counts and relative proportions, the homogenization extraction method yielded notable higher quantity of Campylobacterales for only sample G008 and Propionibacteriales for four out of five samples. Unlike qPCR or 16S rDNA sequencing which are only quantifying bacteria directly, WGS of biopsies contains extremely high abundance of host DNA which makes bacterial identification challenging (Zhang et al., 2015) and the results very sensitive. Besides two different DNA extraction methods, many other potential confounding factors could easily alter the bacterial relative compositions of WGS, for example, different sequencing batches, different commercial kits, and the

microbiome from two split parts of biopsy might not be equally distributed. Then figuring out the exact reasons leading to the bacterial quantification differences between two extraction methods will be very difficult, but even with those variances all predominant clades can be detected by both methods and the quantification of most clades are not in favor of one particular method.

Gram-positive bacteria contain a single layer of peptidoglycan in their cell wall whereas gram-negative organisms contain an additional layer of lipopolysaccharide referred to as the outer membrane. In order to determine, if gram-negative vs. positive bacteria show differential susceptibilities toward lysis or homogenization methods, owing to their different cell wall composition, we compared bacterial yields using qPCR quantitation of 16S rDNA from *Actinobacter* phyla (gram positive), *Firmicutes* (generally gram-positive organisms) and *Bacteroidetes* phyla (gram-negative organisms) relative to total 16S rDNA quantiation. We found very similar yields from *Actinobacter* as well as from other phyla, irrespective of differences in their cell wall composition. Together, our data suggest that both extraction methods can be successfully employed in assessing the overall microbiome composition and content in human biopsies without skewing results due to the choice of extraction method.

The homogenization extraction method does have some favorable characteristics. As a standard protocol for human DNA processing, the homogenizing method has been widely used in many large-scale studies, including large scale cancer project (https://cancergenome.nih.gov/). In our previous study, we successfully retrieved the microbiome information from TCGA samples with our computational pipeline (Zhang et al., 2015). Although the prolonged lysis method might be the preferred way to extract DNA in many microbiome projects (Mann et al., 2014), in many clinical studies, small tissue biopsy samples may not yield sufficient DNA for multiple experiments. For example, separate tissues may be required for both metagenomics analysis with the lysis method and host genomics analysis with the homogenization method. In this study, we show that DNA extraction by the homogenization method is comparable for microbiome profiling as the prolonged enzymatic lysis method. Thus, the homogenization method could allow us to assess microbial and host genomics simultaneously from small clinical biopsy specimens. In addition, the homogenizing method is a faster and more cost-effective method than enzymatic lysis as well as yields higher read counts in WGS. It is further possible that other existing methods such as using a combination of enzymes (lyticase, mutanolysin, lysostaphin) for enzymatic lysis with bead beating process may increase the overall yield and further diversify the community structure (Yuan et al., 2012; Goldschmidt et al., 2014). However, our results suggest that the most abundant bacterial species could still be identified using the above two methods, even in low-bacteria tissue samples. Overall, based on generally equivalent microbiome profiles, but greater versatility for host genomic studies, the homogenizing method on small clinical biopsies or samples with low-bacterial contents for DNA extraction is likely to provide greater tissue utility.

MATERIALS AND METHODS

Sample Collection

This study was performed under one of two clinical tissue acquisition studies approved by the Weill Cornell Medical College Institutional Review Board (IRB). All participants provided written informed consent for use of their tissue samples in accordance with the declaration of Helsinki prior to study enrollment. Patients were enrolled in one of two studies—Weill Cornell Medical College Gastric Cancer and H. pylori Research Database and Tissue Repository (IRB 1203012274), and the NYPH-Weill Cornell Digestive Disease Registry (IRB 0908010582).

Colorectal Cancer Samples

A total of five colorectal tumor and matching normal pairs were obtained from the colorectal cancer biobank supported by the Translational Research Program at WCMC Pathology and Laboratory Medicine. For each sample, 3–4 frozen cores of 1.5 mm diameter each were obtained. One core for each of the samples was used for DNA extraction by either the homogenization or the lysis method. The DNA was subsequently used for qPCR and WGS studies.

Gastric Samples

Three gastric mucosal biopsy pairs were obtained from the Weill Cornell Medicine Gastric Cancer Center and *H. pylori* Research Database, a registry and tissue repository to examine the natural history of *H. pylori* infection in patients with and without gastric cancer. Gastric biopsy samples were sourced from fundus or proximal body sections of the stomach from patients without gastric carcinoma. Biopsies were obtained using the Bard Precisor EXL® coated disposable biopsy forceps (Bard International, Murray Hill, NJ, USA) and were immediately placed into individual sterile cryovials on dry ice and flash frozen while still in the endoscopic suite. The samples were then transferred to liquid nitrogen for prolonged storage.

Esophageal Samples

Esophageal cancer and pre-cancer tissue biopsies were sent to us by our collaborators at University of Kansas School of Medicine, Kansas City, KS. These biopsy samples were obtained from the esophagus at about 2–3 cm above gastroesophageal junction. Tissues were first stored in RNA later solution overnight at 4°C prior to freezing and were shipped to us on dry ice. The DNA from the biopsies was then extracted either using the homogenization method or the enzymatic lysis method as described.

DNA Extraction

Non-paired biopsies from the same tissue were equally cut prior to gDNA isolation to enable extraction using the two extraction methods illustrated below.

Extraction Method 1: Homogenization (Mechanical Disruption)

Frozen biopsy samples (∼3–5 mg) were placed in a 2 ml sterile Eppendorf tube containing 350 μl of RLT lysis buffer (Qiagen®).

Samples were then homogenized individually on ice for 20–30 s using a pre-sterilized homogenizer (Pro250® Pro Scientific) until tissue was uniformly disrupted. gDNA was subsequently isolated according to manufacturer's instructions from Qiagen Allprep Micro DNA/RNA kit (Qiagen-Hilden, Germany). Briefly, the homogenized lysate were loaded on Allprep DNA mini spin column (Qiagen®) and was centrifuged briefly at 10,000 x g in a table top centrifuge. This step allows binding of DNA to the column. After subsequent washing steps with buffers AW1 (Qiagen®) and AW2 (Qiagen®), DNA is eluted using the elution buffer provided in the kit. Homogenizer was cleaned and sterilized before and after each individual sample with separate 15 ml falcon tubes containing 10% bleach, 70% EtOH, and RNAse/DNAse free sterile water.

Extraction Method 2: Enzymatic Lysis and Incubation

Frozen biopsy tissue (∼3–5 mg) was placed in a 1.5 ml centrifuge tube and 180 µl of lysozyme (Gold Biotechnology Cat no: L-040-10) (20 mg/ml stock concentration prepared in TE) was added. Lysozyme was pre-warmed to 37°C prior to its addition to the sample. Samples were then incubated at 37°C for 1 h. Proteinase K (20 µl of 20 mg/ml stock concentration; Thermo Scientific Cat no: EO0491) was added after the incubation. And sample was incubated at 56°C on a heat block and periodically vortexed until complete lysis of tissue was observed (4–6 h). Samples were then incubated in 200 µl Buffer AL from QIAamp DNA Mini kit (Qiagen) for 30 min at 70°C before continuing extraction using QIAamp DNA mini kit (Qiagen) according to manufacturer's instructions (Viljoen et al., 2015). Briefly, after the 30 min incubation at 70°C, sample was loaded on QIAamp DNA spin column (Qiagen®) and was centrifuged briefly at 10,000 x g in a table top centrifuge. The column is then washed with buffers AW1 (Qiagen®) and AW2 (Qiagen®) and DNA is eluted using the elution buffer provided in the kit.

Quantitation and Quality Control

DNA concentrations and quality were measured using the Qubit™ dsDNA high sensitivity assay kit (Invitrogen®) and a Qubit™ 2.0 Fluorometer (Life Technologies, Grand Island, NY, USA).

To validate that the two kits used in the above two mentioned protocols themselves did not contribute to any variation, we re-extracted 1 µg of DNA from one of the gastric cancer samples using Allprep DNA/RNA micro kit as well as QIAamp DNA mini kit. This re-purified DNA from the two kits (5 ng each) was then subjected to qPCR using the 16S rDNA gene primer set to check for bacterial abundance. Furthermore, to prove that the columns itself were not a source of any contamination, we performed parallel purifications using water and subjected the eluate to qPCR against the 16S rDNA gene primer set (**Figure S2**).

Real-time PCR (qPCR)

To corroborate total bacterial abundance (measured by highly conserved 16S rDNA sequences) and *Fusobacterium* sp. abundances, genomic DNA was initially analyzed via qPCR. Reactions were carried out on a StepOne® 48-well thermocycler (Applied Biosystems). Primers used were FAM-labeled Genesig® 16S Eubacteria quantification primer/probe set (Proprietary sequence-PrimerDesign®) to determine total bacterial composition and a custom FAM-MGB *Fusobacterium* primer/probe (Applied biosystems) for *Fusobacterium* quantitation: Forward: 5′–AAGCGCGTCTAGGTGGTTATGT-3′; Reverse: 5′-TGTAGTTCCGCTTACCTCTCCAG-3′; Probe:FAM CAACGCAATACAGAGTTGAGCCCTGCATT (Martin et al., 2002). Phylla-specific primers used for detection of organisms from *Bacteroidetes* were adapted from (Yang et al., 2015) and those for *Actinobacter* and *Firmicutes* were adapted from (Pfeiffer et al., 2014). All three of these primer sets have been validated for both specificity and sensitivity toward each of these phylla in these above-mentioned manuscripts.

Real-time PCR reactions were performed in triplicate on MicroAmp® fast-optical 48 well (0.1 ml) reaction plates (Applied Biosystems). Each reaction contained 1–2 µl template DNA, 0.5ul of 20X ABI primer/probe assay, 5 µl Taqman® Gene Expression Mastermix (Applied Biosystems), and RNase/DNase free water to a total volume of 10 µl

Cycling conditions included an initial denaturation at 50°C for 2 min and 95°C for 10 min followed by 40 cycles of 95°C for 15 s and 60°C for 1 min.

Absolute quantification was performed using a standard reference curve and controls prepared using known concentrations *Escherichia coli* gDNA (ATCC®) for 16S total quantitation and *Fusobacterium nucleatum* gDNA (ATCC® Strain VPI-4355) for *Fusobacterium* sp. quantitation.

Whole Genome Sequencing (WGS)

Genomic DNA (200–500 ng) was submitted from each sample to the Weill Cornell Medicine Epigenomics Core for library preparation and subsequent WGS using an Illumina TruSeq DNA-seq® DNA sample preparation kit and the Illumina HiSeq 2500® platform. Each sample was sequenced on a single flow cell lane as 50-bp paired-end reads at roughly 10x coverage to Human genome. Homopolymers, adapters and distribution of base quality of raw sequences from each sample were investigated using FastQC (version 0.10.1). In order to estimate the potential contaminations from experiment, two control samples containing only RNase/DNase free water went through two extraction procedures along with biopsies samples, and were similarly sequenced as the clinical samples. There were no bacteria detected by either qPCR or WGS in those two control samples.

Computational Pipeline for Bacterial Identification

The bacterial content of each WGS sample was identified with our in-house computational pipeline (Zhang et al., 2015), which is designed to quantify microbiome from WGS data of small clinical sample with following steps:

1) Filtering human DNA: All reads from WGS data were aligned to corresponding Human DNA databases with four different aligners (BWA, RepeatMasker, BLAST, MegaBlast) step by step. Any reads mapped to Human DNA databases were removed and the remaining reads were used as the input for bacteria identification.

2) Mapping to bacterial genomes: 1,421 non-redundant bacterial genomes were collected from NCBI. Bowtie2 was used as the aligner to map the read to each bacterial genome, and each read was labeled as either uniquely mapped, unmapped or ambiguous (multiple genomic mapping).
3) Genome coverage evaluation: For any bacteria with more than ten uniquely mapped reads we compute a genomic coverage measure to further remove false identifications.
4) Calculating the relative abundance: Based on the identified bacteria from step 3, we applied a Bayesian statistical framework to assign all mapped reads to the most probable bacterial source genome (Wood and Salzberg, 2014). Finally, the relative abundances of bacteria were calculated for each sample.

Statistical Analyses

In qPCR data analysis, to determine the total bacterial content difference in particular sample between two extraction methods, we calculated absolute[log2(Homogenization qPCR readout/Lysis qPCR readout)] for each experiment and each sample individually, and then performed a one-tailed one-sample *t*-test with H0: $\mu < 2$ across all samples. Statistical significance was defined as $p \leq 0.05$. For each particular phyla/genus, we assessed relative abundance difference between two extraction methods, and then performed a one-tailed one-sample *t*-test with H0: $\mu < 1\%$ across all samples. Statistical significance was defined as $p \leq 0.05$. For WGS data, cosine similarity was applied to measure the similarity of microbiome absence/presence detection between two extraction methods, and corresponding permutation test was used to evaluate statistical significance (Smirnov et al., 2016).

AUTHOR CONTRIBUTIONS

MS, DB, and CZ conceived and designed project. PT and SP extracted DNA and performed the experiments. PS and SV collected clinical samples. CZ and DB performed the bioinformatic analyses. MS, PT, CZ, and DB interpreted the results. CZ, PT, SP, DB, and MS wrote the manuscript. All authors contributed to final revisions of the manuscript.

FUNDING

This work was supported by the DeGregorio Family Foundation for Gastroesophageal Malignancies and by an internal grant from the Center for Advanced Digestive Care at Weill Cornell Medical College.

ACKNOWLEDGMENTS

The authors greatly acknowledge the contribution of the Weill Cornell Epigenomics Core facility and computing support from the Applied Bioinformatics Core at Weill Cornell as well as Eric Pamer, MD PhD for his comments.

SUPPLEMENTARY MATERIAL

The Supplementary Material for this article can be found online at: https://www.frontiersin.org/articles/10.3389/fmicb.2018.03246/full#supplementary-material

Figure S1 | Comparison of bacteria identified from WGS data for five samples at order level between two extraction methods (Similar to **Figure 3**).

Figure S2 | Comparison of the Qiagen Allprep Micro DNA/RNA kit used with the homogenization protocol and the QIAamp DNA mini kit (Qiagen) that was employed with the Lysis protocol. Overall bacterial abundance (ng) using 16S rDNA primer set is represented. The two different kits used with two different extraction protocols themselves did not contribute to any differences as demonstrated by equal abundance of bacterial DNA in the sample re-extracted using the two kits.

Table S1 | Mapping statistics of WGS samples.

Table S2 | Species-level identification results of WGS samples.

REFERENCES

Bik, E. M., Eckburg, P. B., Gill, S. R., Nelson, K. E., Purdom, E. A., Francois, F., et al. (2006). Molecular analysis of the bacterial microbiota in the human stomach. *Proc. Natl. Acad. Sci. U.S.A.* 103, 732–737. doi: 10.1073/pnas.0506655103

Bik, E. M., Long, C. D., Armitage, G. C., Loomer, P., Emerson, J., Mongodin, E. F., et al. (2010). Bacterial diversity in the oral cavity of 10 healthy individuals. *ISME J.* 4, 962–974. doi: 10.1038/ismej.2010.30

Crandall, K. A., Freishtat, R. J., and Pérez-Losada, M. (2016). Comparison of two commercial DNA extraction kits for the analysis of nasopharyngeal bacterial communities. *AIMS Microbiol.* 2, 108–119. doi: 10.3934/microbiol.2016.2.108

Goldschmidt, P., Degorge, S., Merabet, L., and Chaumeil, C. (2014). Enzymatic treatment of specimens before DNA extraction directly influences molecular detection of infectious agents. *PLoS ONE* 9:e94886. doi: 10.1371/journal.pone.0094886

Human Microbiome Project, C. (2012). Structure, function and diversity of the healthy human microbiome. *Nature* 486, 207–214. doi: 10.1038/nature11234

Lazarevic, V., Gaia, N., Girard, M., Francois, P., and Schrenzel, J. (2013). Comparison of DNA extraction methods in analysis of salivary bacterial communities. *PLoS ONE* 8:e67699. doi: 10.1371/journal.pone.0067699

Mann, E., Pommer, K., Mester, P., Wagner, M., and Rossmanith, P. (2014). Quantification of Gram-positive bacteria: adaptation and evaluation of a preparation strategy using high amounts of clinical tissue. *BMC Vet Res.* 10:53. doi: 10.1186/1746-6148-10-53

Martin, F. E., Nadkarni, M. A., Jacques, N. A., and Hunter, N. (2002). Quantitative microbiological study of human carious dentine by culture and real-time PCR: association of anaerobes with histopathological changes in chronic pulpitis. *J. Clin. Microbiol.* 40, 1698–1704. doi: 10.1128/JCM.40.5.1698-1704.2002

Moore, E., Arnscheidt, A., Krüger, A., Strömpl, C., and Mau, M. (2004). "Section 1 update: Simplified protocols for the preparation of genomic DNA from bacterial cultures," in *Molecular Microbial Ecology Manual,* eds G. A. Kowalchuk, F. J. De Bruijn, I. M. Head, A. D. Akkermans and J. D. Van Elsas (Dordrecht: Springer Netherlands), 1905–1919.

Pfeiffer, S., Pastar, M., Mitter, B., Lippert, K., Hackl, E., Lojan, P., et al. (2014). Improved group-specific primers based on the full SILVA 16S rRNA gene reference database. *Environ. Microbiol.* 16, 2389–2407. doi: 10.1111/1462-2920.12350

Rossmanith, P., and Wagner, M. (2011). Aspects of systems theory in the analysis and validation of innovative molecular-biological based food pathogen detection methods. *Trends Food Sci. Technol.* 22, 61–71. doi: 10.1016/j.tifs.2010.12.004

Rubin, B. E., Sanders, J. G., Hampton-Marcell, J., Owens, S. M., Gilbert, J. A., and Moreau, C. S. (2014). DNA extraction protocols cause differences in 16S rRNA

amplicon sequencing efficiency but not in community profile composition or structure. *Microbiologyopen* 3, 910–921. doi: 10.1002/mbo3.216

Shreiner, A. B., Kao, J. Y., and Young, V. B. (2015). The gut microbiome in health and in disease. *Curr. Opin. Gastroenterol.* 31, 69–75. doi: 10.1097/MOG.0000000000000139

Smirnov, P., Safikhani, Z., El-Hachem, N., Wang, D., She, A., Olsen, C., et al. (2016). PharmacoGx: an R package for analysis of large pharmacogenomic datasets. *Bioinformatics* 32, 1244–1246. doi: 10.1093/bioinformatics/btv723

Viljoen, K. S., Dakshinamurthy, A., Goldberg, P., and Blackburn, J. M. (2015). Quantitative profiling of colorectal cancer-associated bacteria reveals associations between fusobacterium spp., enterotoxigenic Bacteroides fragilis (ETBF) and clinicopathological features of colorectal cancer. *PLoS ONE* 10:e0119462. doi: 10.1371/journal.pone.0119462

Wood, D. E., and Salzberg, S. L. (2014). Kraken: ultrafast metagenomic sequence classification using exact alignments. *Genome Biol.* 15:R46. doi: 10.1186/gb-2014-15-3-r46

Wu, G. D., Lewis, J. D., Hoffmann, C., Chen, Y. Y., Knight, R., Bittinger, K., et al. (2010). Sampling and pyrosequencing methods for characterizing bacterial communities in the human gut using 16S sequence tags. *BMC Microbiol.* 10:206. doi: 10.1186/1471-2180-10-206

Yang, Y. W., Chen, M. K., Yang, B. Y., Huang, X. J., Zhang, X. R., He, L. Q., et al. (2015). Use of 16S rRNA gene-targeted group-specific primers for real-time PCR analysis of predominant bacteria in mouse feces. *Appl. Environ. Microbiol.* 81, 6749–6756. doi: 10.1128/AEM.01906-15

Yuan, S., Cohen, D. B., Ravel, J., Abdo, Z., and Forney, L. J. (2012). Evaluation of methods for the extraction and purification of DNA from the human microbiome. *PLoS ONE* 7:e33865. doi: 10.1371/journal.pone.0033865

Zhang, C., Cleveland, K., Schnoll-Sussman, F., Mcclure, B., Bigg, M., Thakkar, P., et al. (2015). Identification of low abundance microbiome in clinical samples using whole genome sequencing. *Genome Biol.* 16:265. doi: 10.1186/s13059-015-0821-z

Conflict of Interest Statement: The authors declare that the research was conducted in the absence of any commercial or financial relationships that could be construed as a potential conflict of interest.

frontiers in Microbiology

HYPOTHESIS AND THEORY
published: 29 April 2019
doi: 10.3389/fmicb.2019.00846

Potential Role of Biofilm Formation in the Development of Digestive Tract Cancer With Special Reference to *Helicobacter pylori* Infection

*Cosmeri Rizzato[1], Javier Torres[2], Elena Kasamatsu[3], Margarita Camorlinga-Ponce[2], Maria Mercedes Bravo[4], Federico Canzian[5] and Ikuko Kato[6]**

[1] Department of Translation Research and of New Technologies in Medicine and Surgery, University of Pisa, Pisa, Italy, [2] Unidad de Investigación en Enfermedades Infecciosas, Unidades Médicas de Alta Especialidad Pediatría, Instituto Mexicano del Seguro Social, Mexico City, Mexico, [3] Instituto de Investigaciones en Ciencias de la Salud, National University of Asunción, Asunción, Paraguay, [4] Grupo de Investigación en Biología del Cáncer, Instituto Nacional de Cancerología, Bogotá, Colombia, [5] Genomic Epidemiology Group, German Cancer Research Center (DKFZ), Heidelberg, Germany, [6] Department of Oncology and Pathology, Wayne State University School of Medicine, Detroit, MI, United States

OPEN ACCESS

Edited by:
Nezar Al-hebshi, Temple University, United States

Reviewed by:
Rossella Grande, Università degli Studi G. d'Annunzio Chieti e Pescara, Italy
Mun Fai Loke, University of Malaya, Malaysia

***Correspondence:**
Ikuko Kato
katoi@karmanos.org

Specialty section:
This article was submitted to Systems Microbiology, a section of the journal Frontiers in Microbiology

Received: *04 January 2019*
Accepted: *02 April 2019*
Published: *29 April 2019*

Citation:
Rizzato C, Torres J, Kasamatsu E, Camorlinga-Ponce M, Bravo MM, Canzian F and Kato I (2019) Potential Role of Biofilm Formation in the Development of Digestive Tract Cancer With Special Reference to Helicobacter pylori Infection. Front. Microbiol. 10:846. doi: 10.3389/fmicb.2019.00846

Bacteria are highly social organisms that communicate via signaling molecules and can assume a multicellular lifestyle to build biofilm communities. Until recently, complications from biofilm-associated infection have been primarily ascribed to increased bacterial resistance to antibiotics and host immune evasion, leading to persistent infection. In this theory and hypothesis article we present a relatively new argument that biofilm formation has potential etiological role in the development of digestive tract cancer. First, we summarize recent new findings suggesting the potential link between bacterial biofilm and various types of cancer to build the foundation of our hypothesis. To date, evidence has been particularly convincing for colorectal cancer and its precursor, i.e., polyps, pointing to several key individual bacterial species, such as *Bacteroides fragilis, Fusobacterium nucleatum*, and *Streptococcus gallolyticus* subsp. *Gallolyticus.* Then, we further extend this hypothesis to one of the most common bacterial infection in humans, *Helicobacter pylori* (*Hp*), which is considered a major cause of gastric cancer. Thus far, there has been no direct evidence linking *in vivo Hp* gastric biofilm formation to gastric carcinogenesis. Yet, we synthesize the information to support an argument that biofilm associated-*Hp* is potentially more carcinogenic, summarizing biological characteristics of biofilm-associated bacteria. We also discuss mechanistic pathways as to how *Hp* or other biofilm-associated bacteria control biofilm formation and highlight recent findings on *Hp* genes that influence biofilm formation, which may lead to strain variability in biofilm formation. This knowledge may open a possibility of developing targeted intervention. We conclude, however, that this field is still in its infancy. To test the hypothesis rigorously and to link it ultimately to gastric pathologies (e.g., premalignant lesions and cancer), studies are needed to learn more about *Hp* biofilms, such as compositions and biological properties of extracellular polymeric substance (EPS), presence of non-*Hp* microbiome and geographical distribution of biofilms in relation to gastric gland types

and structures. Identification of specific *Hp* strains with enhanced biofilm formation would be helpful not only for screening patients at high risk for sequelae from *Hp* infection, but also for development of new antibiotics to avoid resistance, regardless of its association with gastric cancer.

Keywords: *Helicobacter pylori*, biofilm, persistent infection, cancer, virulence

INTRODUCTION

Over the past two decades, it has been increasingly appreciated that bacteria present in most biological systems exist in biofilms, which are defined as matrix-enclosed microbial accretions adhering to biological or non-biological surfaces and to each other (Hall-Stoodley et al., 2004; Gabrilska and Rumbaugh, 2015; Flemming et al., 2016). Biofilm formation is a key factor for survival in diverse environments and is viewed as an ancient and integral component of the prokaryotic life cycle, as researchers found biofilm formation early in fossil records (∼3.25 billion years ago) (Hall-Stoodley et al., 2004). In biofilms, unicellular bacteria assume a temporary multicellular lifestyle through prolific intercellular interactions, both social and physical, immersing in a complex and specialized matrix formed by both the bacteria and the host (Kostakioti et al., 2013; Watters et al., 2016). These group behaviors represent a microbial social support system to foster survival in hostile environments, share limited resources, favor long-term persistent colonization and maintain the ability to colonize to new niches (Hall-Stoodley et al., 2004; Majumdar and Pal, 2017). Accordingly, this specific mode of living provides strong fitness advantage to biofilm-associated bacteria compared to their planktonic counterparts (Gabrilska and Rumbaugh, 2015; Liu et al., 2016). In particular, biofilm-associated bacteria exhibit increased resistance to chemical disinfectants, antibiotic therapies and human immune responses and thus are associated with long-term persistence (Elias and Banin, 2012; Kostakioti et al., 2013). The self-produced extracellular polymeric substance (EPS) matrix, which is typically composed of polysaccharides, carbohydrate-binding proteins, lipids, extracellular DNA (eDNA), pili, flagella, and other adhesive fibers (Kostakioti et al., 2013; Flemming et al., 2016), plays an important role in antibiotic resistance, enhanced horizontal gene transfer as well as altered gene expressions within the biofilm community, which results in enhanced bacterial virulence (Elias and Banin, 2012; Madsen et al., 2012; Flemming et al., 2016). Furthermore, it has been described that some extracellular pathogens adopt intracellular lifestyle through the formation of bacterial communities with biofilm-like properties, enabling them to persist inside the host cells (Kostakioti et al., 2013). Thus, these biofilm-associated infections in humans on both abiotic (medical devices) and biotic surfaces (e.g., gum, heart valves, lungs, etc.) pose significant challenges to the medical community (Costerton et al., 1999; Hall-Stoodley et al., 2004; Kostakioti et al., 2013).

Chronic inflammation, often caused by chronic microbial infection, has been decisively linked to several stages of carcinogenesis (Grivennikov et al., 2010; Armstrong et al., 2018). A recent estimate also suggests that about 15% of worldwide incident cases of cancer are attributable to chronic infection (Plummer et al., 2016). As discussed above, one way for bacteria to achieve persistent colonization in the hosts is to form biofilms. Despite well-established causal links between certain infectious agents, such as *Helicobacter pylori* (*Hp*), and cancer (Plummer et al., 2016), knowledge concerning the association between bacterial biofilm formation and cancer development has been sparse.

Despite the well-founded association between persistent *Hp* infection and gastric carcinogenesis and growing knowledge concerning unique properties of biofilm-associated bacteria, little is known about biological consequence of *Hp in vivo* biofilm formation beyond antibiotic resistance. In the subsequent sections, we present our hypothesis that biofilm formation has potential etiological role in the development of digestive tract cancer, which may be particularly relevant to infection-associated cancer, such as *Hp*-induced gastric cancer. We synthesize recent new findings suggesting the potential link between bacterial biofilm and various types of cancer, as well as the information to support an argument that biofilm associated-*Hp* is potentially more carcinogenic. We also discuss technical details and challenges in *Hp* biofilm studies to aid interpretation of the results from various different experimental platforms and designing future studies and highlight recent findings on *Hp* genes and virulence factors that influence biofilm formation.

EVIDENCE TO SUPPORT POSSIBLE LINKS BETWEEN BIOFILM FORMATION AND HUMAN CANCER

Recently, a group from Johns Hopkins University in the US published a series of studies addressing the potential link between biofilm-associated bacteria and colorectal cancer and its precursor, i.e., polyps. The investigators found more frequent polymicrobial biofilm formation in colorectal mucosa of the patients with colorectal cancer or adenoma, compared with that of control subjects who had negative findings at screening colonoscopy. This phenomenon was striking for the right sided tumors compared to left sided lesions (Dejea et al., 2014; Drewes et al., 2017). Importantly, biofilms were present not only on tumors but also at normal surgical margins. Furthermore, biofilm formation was associated with diminished epithelial cell E-cadherin, enhanced IL-6 and Stat3 activation, and increased crypt cell proliferation in normal mucosa (Dejea et al., 2014). The subsequent analysis revealed that these tumor-associated biofilms were enriched with *Bacteroides fragilis (Bf)* and several periodontal pathogens, including *Fusobacterium nucleatum*

(Fn) and *Peptostreptococcus stomatits*, and accompanied with altered functions, compared to those in planktonic bacteria, e.g., increases in cytoskeletal proteins, peptidoglycan (PG) biosynthesis and sporulation, and a decrease in flagellar assembly (Drewes et al., 2017). Biofilms were detected also in colorectal mucosa of genetically predisposed individuals, i.e., familial polyposis coli patients, regardless of the locations at the colorectum, but their appearance and composition were different (Dejea et al., 2018). They were rather patchy (as opposed to continuous as observed for sporadic cases) and primarily composed of *Bf* and polyketide-peptide genotoxin producing *pks* island positive *Escherichia coli,* with little periodontal pathogens (Dejea et al., 2018). It was also reported previously that *Bf* was the main component of inflammatory bowel disease-associated biofilms (Swidsinski et al., 2005).

Another piece of corroborative information arises from growing recognition of the association between oral microbiome, specifically *Fn,* and colorectal cancer (Sun and Kato, 2016), which was predominantly observed for proximal colon tumors (Hussan et al., 2017). *Fn* is a normal residential member of dental plaques (biofilms) and well-known periodontal pathogen (Larsen and Fiehn, 2017). *Fn* is considered to be a co-aggregation expert, with an ability of co-aggregating with a broad range of bacteria, nearly all bacterial species involved in oral plaque formation (Kolenbrander et al., 1989; Allen-Vercoe et al., 2011), a very important property in biofilm formation. Moreover, *Fn* can bind to and transport otherwise non-invasive bacterial species into host cells, acting as a shuttle in this respect (Edwards et al., 2006). *Fn* produces outer membrane vesicles (OMV) to facilitate coaggregation and isolated OMVs alone have been shown to exert an equivalent ability to coaggregate other bacteria compared to whole bacterial culture (Kinder and Holt, 1993). OMV production appears to depend on external stimuli and resulting changes in biofilm formation are strain-specific (Musrati et al., 2016). In this context, the putative association with colorectal cancer may be a function of the microbes that *Fn* gathers in its biofilms, rather than a direct effect of its own virulence. In fact, Flemer et al. (2018) more recently reported that several microbes commonly found in oral biofilms were enriched in colonic mucosa from colorectal cancer patients. Finally, *Fn* has recently found to be one of the gut microbes linked to pancreatic cancer (del Castillo et al., 2019), although little has been known about biofilm formation in the pancreatic ducts.

Moreover, growing evidence suggest a link between colorectal cancer and *Streptococcus gallolyticus* subsp. *Gallolyticus (SGG),* formerly known as *S. bovis,* an opportunistic pathogen causing biofilm-associated infections, e.g. infective endocarditis on cardiac valves (Boleij et al., 2010, 2012; Sun and Kato, 2016; Butt et al., 2018; Jans and Boleij, 2018). Martins el al. have revealed that this bacterium exploits Pil3 pilus for adhesion to colonic mucus and for colonization of mouse distal colon (Danne et al., 2011; Martins et al., 2016), while Pil1 pilus allows *S. gallolyticus* to bind to collagen type I and plays a role in biofilm formation (Danne et al., 2011; Martins et al., 2016). Pil3 pilus has been shown to bind not only to human colonic mucins and to human stomach mucins, but also to human fibrinogen (Martins et al., 2016). Accordingly, both pilus proteins play an important role in biofilm formation. Binding to fibrinogen is also known to contribute to increased biofilm formation in other *Streptococcus* species (Bedran et al., 2013). Comparative genomics of 8 *SGG* strains form human blood and feces recently revealed that complete *pil1-3* loci are only present in virulent strains, causing bacteremia and/or endocarditis translocated through impaired mucosal barrier, while other fecal *SGG*s do not carry these full *pil1-3* loci (Jans and Boleij, 2018). Interestingly, several epidemiological studies, including our own, have found that individuals who express high antibody titers to several *S. gallolyticus* pilus proteins have increased risk of colorectal cancer (Boleij et al., 2012; Butt et al., 2016; Butt et al., 2018).

Gallbladder is another potential niche where bacteria can form biofilm. In fact, certain strains of *Salmonella typhi* are known to produce biofilms on the surfaces of cholesterol gallstone (Crawford et al., 2010; Gonzalez-Escobedo and Gunn, 2013), which is in support of the known etiological link between the carriages of *S. typhi* and gallstones and the development of gallbladder cancer (Di Domenico et al., 2017).

Gastric lumen is one of the most hostile environments in human body, which kills many bacteria within a few minutes. *Hp* survives in this environment with its urease activity that neutralizes gastric acid (Abadi, 2017), whereas biofilm formation may be more vital for its persistent colonization. Surprisingly, to date, little has been known about *in vivo* biofilm formation on human gastric mucosa. Three pioneer studies employed high powered electron microscope and demonstrated dense clusters of *Hp* (Carron et al., 2006; Coticchia et al., 2006; Cellini et al., 2008), primarily in coccoid forms, which are known to be viable but non-cultivable (Cellini, 2014; Percival and Suleman, 2014). It is interesting to note that *Hp* isolated from gastric cancer patients is often non-cultivable, despite the fact that the bacteria are detectable by other methods (i.e., PCR or histology), and that coccoid forms have been indeed more frequently found in gastric mucosa of gastric cancer patients than in that of peptic ulcer patients (Chan et al., 1994).

EVIDENCE TO SUPPORT *Hp* ABILITY IN *IN VITRO* AND *IN VIVO* BIOFILM FORMATION

In vitro Abiotic Models

In 1999, Stark et al. (1999) reported the formation of biofilm by *Hp* in a continuous culture of *Hp* NCTC 11637 in Brucella broth supplemented with B-cyclodextrin and glucose in a glass fermentor. *Hp* formed a biofilm containing polysaccharides at the air-liquid interface. Later, Cole et al. (2004) and Bellack et al. (2006) described the progression of biofilm formation with clinical isolates of *Hp* showing that all strains tested were able to form biofilm at the air-liquid interface on a glass surface, although *Hp* biofilms have also been detected by molecular methods on the surface of environmental water supply system. Further studies have clarified that biofilms are not simply passive aggregates of

cells attached to a surface, but they do complex communitarian functions and should be considered as biological systems.

The ability of *in vitro* biofilm formation by *Hp* has been described in several systems. These studies have demonstrated important differences in the *in vitro* growth conditions of the bacteria and in the abiotic surfaces used in the assay. Microtiter polystyrene plates are the most commonly-used substrate (Azeredo et al., 2017). The biomass attached to the surface of the wells and the formed biofilm is quantitated by staining with violet crystal (Wilson et al., 2017). Yonezawa et al. (2009) observed biofilm formation at the air-liquid interface of microtiter plates. More specific pieces of information regarding the structure of *Hp* biofilms *in vitro* on abiotic surface have also been made available by use of scanning electron microscopy (SEM) (Queralt and Araujo, 2007; Yonezawa et al., 2009, 2013). These include *Hp* morphological changes associated with biofilm formation in an aquatic culture model as well as how culture conditions and nutrient supply affect biofilm density, structures and abundance of OMVs. It is worth noting that OMVs have been found to enhance oxidative stress and genomic damages to host cells and thus possess carcinogenic potential in *in vitro* culture systems (Chitcholtan et al., 2008). Using transmission electron microscope analysis (TEM), Grande et al. demonstrated the presence of eDNA, which was associated with OMVs and plays a role in Hp aggregation (Grande et al., 2015).

To demonstrate the interaction of bacteria and the role of cellular appendices in the formation of biofilm using SEM, we cultured *Hp* on glass cover slips for 48 h in RPMI medium (JT, MC, and J Girón, unpublished results). We observed a dense growth of bacteria attached to the substrate (**Figure 1A**), with an extensive expression of flagella. The images suggest that flagella might have a role in both, adhesion to the substrate and in the interaction between bacteria (**Figures 1A,B**). Images also show a high formation of smaller pili by bacteria forming the biofilm (**Figure 1C**). The role of flagella and other pili in the formation of biofilm has been well documented in other bacteria (Belas, 2014; Maldarelli et al., 2016; Zeng et al., 2017).

In vitro Biotic Models

Hp forms biofilms not only on abiotic surfaces, but also on biotic surfaces. Human cell lines may mimic the *in vivo* cell behavior and can be used for *ex vivo* biofilm assays. *Ex vivo* models also include biofilm growth on natural tissues in a minimally altered environment, offering more strictly controlled experimental conditions than those of *in vivo* models, which allows more detailed studies. The *ex vivo* models also facilitate studies of biofilm association with virulence, or therapeutic assays for experimental antibiofilm treatments and biofilm inhibition (Salas-Jara et al., 2016; Magana et al., 2018).

One environmental condition to which *Hp* is reactive is the endogenously produced quorum-sensing molecule autoinducer-2 (AI-2) that *Hp* senses as a chemorepellent. Anderson et al. (2015) studied the role of AI-2 chemotactic responses during *Hp* biofilm formation on biotic and abiotic surfaces. In the biotic assay, they adapted an *in vivo* model, with conditions similar to those previously described (Tan et al., 2011) using polarized Madin Darby canine kidney (MDCK) epithelial cells seeded onto a transwell filter. Experimental inoculation of *Hp* strains resulted in the formation of microcolonies on MDCK monolayers, in an AI-2 chemotaxis- dependent manner; similar results were observed in an abiotic model. Salas-Jara et al. (2016) evaluated

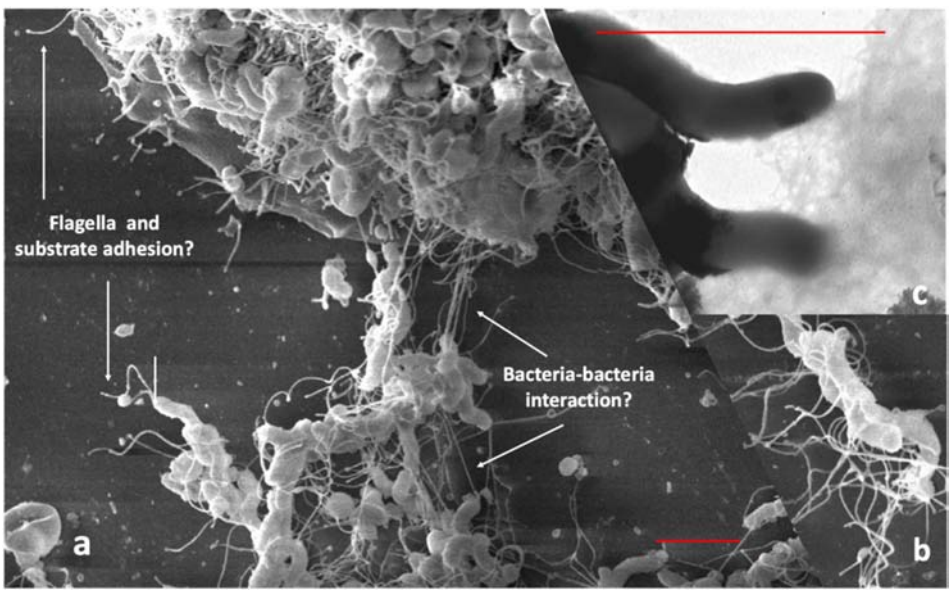

FIGURE 1 | Scanning electron microscopy of *Hp* strain ATCC 43504 biofilm on a glass substrate. A bacterial suspension of 3×10^8 CFU/ml in Brucella broth was applied to a glass slide in a 24-well plate, incubated, dried, fixed with methanol and processed for SEM, **(a)** Images showing flagella probably adhering to the substrate; **(b)** possible bacteria-bacteria interaction with the flagella; **(c)** pilli produced by *H. pylori* during biofilm formation. Red bars in **(a,c)** indicate approximately three-micrometer scale.

biofilm formation of two probiotic strains, *L. fermentum* UCO-979C and *L. casei Shirota*, on the surfaces of two gastrointestinal cell lines, AGS and Caco cells. Sterile glass coverslips were placed in a 24-well polystyrene plate. The coverslips were treated with poly-L-lysine at 1 mg ml^{-1} to improve cell adhesion. Subsequently *Lactobacillus* strains were inoculated and the highest biofilm density was observed 12 h later. The biofilm formed by either *L. fermentum* UCO-979C or *L. casei Shirota* strains inhibited the adherence of *Hp* ATCC 43504 to both cells lines. SEM images of the formed biofilms are shown in their paper (Salas-Jara et al., 2016).

In vivo Biofilm Formation in Animals

A recent study evaluated the potential of isolates of *Hp* to form biofilm in the stomach of C57BL/6J mice model. Mice were infected through gastric gavage with 10^8 UFC of *Hp* strain. Infected mice were examined after 1 and 2 weeks. One week after the last challenge, the mice were sacrificed. For examination, the stomachs were removed and fixed in 4% paraformaldehyde (PFA) and *Hp* biofilm was demonstrated by immunofluorescence and SEM (Attaran et al., 2016).

Detection of Biofilm-Associated *Hp* in Human Gastric Mucosa

The first evidence of biofilm formation by *Hp* during colonization in human gastric mucosa was photographic documentation by Carron et al. (2006). Using endoscopically obtained biopsy specimens and SEM analyses, they demonstrated the presence of dense mature biofilm-associated bacteria, attached to the cell surface of *Hp*-positive specimens. *Hp*-negative specimens, in contrast, had smooth mucosa with little evidence of a bacterial community (Carron et al., 2006). SEM also was used to quantify bacterial biofilm density on human gastric mucosa. Among patients with peptic ulcer disease, surface area covered by biofilms was 97.3% in *Hp*-positive patients, as compared to only 1.64% in *Hp*-negative patients (Coticchia et al., 2006).

To assess the biofilm-associated *Hp* in gastric biopsy specimens it is necessary to use methods other than routine ancillary stains, such as immunohistochemistry and fluorescence *in situ* hybridization (FISH). Preservation of three-dimensional structure is critical in order to analyze the spatial organization of the gut microbiota relative to mucin, host tissue and luminal contents (Hasegawa et al., 2017). Therefore, one of the crucial steps for gastrointestinal pathological laboratory is the fixation and embedment. The most common fixative is formaldehyde, an aqueous fixative, but several authors report that this fixative results in collapse or loss of the mucus layer and a widely used protocol is to process samples with non-aqueous Carnoy fixation to preserve the mucus layer for detection of bacteria adherent to the mucosal surface (Swidsinski et al., 2005; Johansson and Hansson, 2012). Johansson and Hansson (2012) observed a thick inner mucus layer firmly attached to the intestinal epithelia in non-aqueous Carnoy fixative, in contrast with a thin streak of collapsed mucus of less than 1 μm on the same tissue processed with formaldehyde fixative. Using confocal microscopy, Hasegawa et al. (2017) compared preservation of three-dimensional structure of four different embedding media: paraffin wax; polyester wax; optimal cutting temperature (OCT) compound; and glycol methacrylate resin. They conclude that hydrophobic embedding materials as paraffin require organic solvents to remove embedding resin and redistribution, collapse or loss of luminal contents could have occurred. In summary, although all of the examined embedments were capable of producing two-dimensional images, only glycol methacrylate resin enabled both retention and visualization of the three-dimensional luminal distribution of bacteria and food particles (Hasegawa et al., 2017).

The gastric surface mucous cells and gland mucous cells express secretory mucins, MUC5AC and MUC6, respectively. On the other hand, aberrant expression of the secretory mucin MUC2 in gastric mucosa is closely related to intestinal metaplasia and intestinal goblet cells (Ho et al., 1995; Reis et al., 1999; Babu et al., 2006; Matsuda et al., 2008). *Hp* may inhibit MUC5AC expression by the human gastric epithelium, and thus facilitate colonization. In contrast, increased MUC6 expression may help inhibiting colonization due to its antibiotic properties (Niv, 2015). FISH combines the molecular identification of bacteria with the direct visualization of the bacteria and the mucosa, which provides a significant advantage over culture, PCR, and histological methods alone (Swidsinski et al., 2005). Hasegawa et al. (2017) evaluated microbial FISH and two mucus labeling methods simultaneously to visualize microbial cells and host-derived mucus in intestinal sections following both Carnoy and PFA fixation and embedded in methacrylate or paraffin. Mucus was visualized with a fluorescent wheat germ agglutinin (WGA) and by indirect immunofluorescence using a primary antibody raised against mouse colonic mucin and both fixation methods allowed the visualization of intestinal mucus layers (Hasegawa et al., 2017).

We attempted to obtain additional evidence of *Hp* biofilm formation in human gastric mucosa fixed in Carnoy, using FISH and *confocal laser scanning microscopy* (CLSM). We showed that *Hp* colonization is not limited to the surface of the human gastric glands, but can colonize deep in the glands, particularly in the region of the neck where cells are in constant proliferation and interestingly, also at the bottom of the glands, in intimate contact with the stem cells (Sigal et al., 2015). The identification of colonization of niches deep in the glands was possible because we studied large pieces of stomach coming from patients subjected to bypass surgery for control of weight. Using the same approach, we have confirmed the ability of *Hp* to form large aggregates suggestive of biofilm formation in the surface of the glands (**Figure 2A**), in the neck in close contact with proliferative cells and deep in the glands (**Figure 2B**), in the vicinity of stem cells (**Figure 2C**). In these studies, *Hp* was stained with antibodies specific to the bacteria, and confirmed the observed *in vivo* microbial aggregates were formed exclusively by *Hp*.

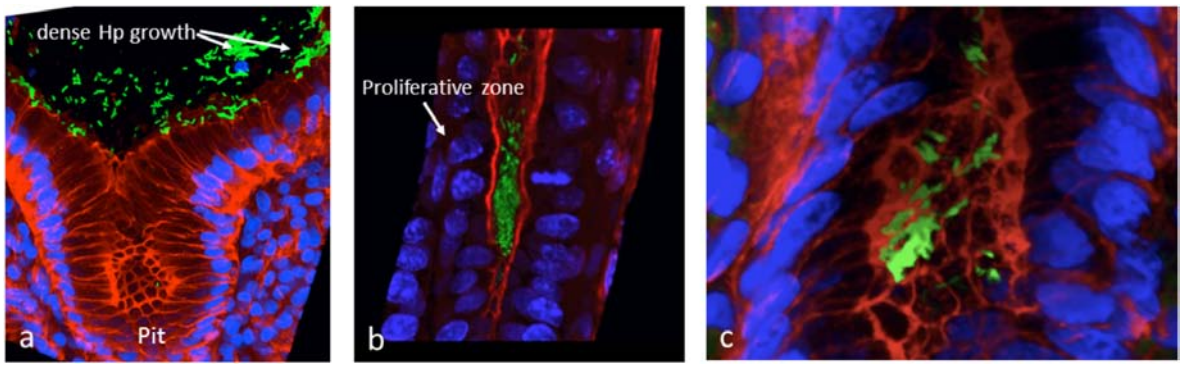

FIGURE 2 | *In vivo* evidences suggestive of biofilm formation by *H. pylori* in the gastric glands of humans. **(a)** Large aggregates of *H. pylori* colonizing the surface of gastric glands; **(b)** *H. pylori* aggregates colonizing the neck of gastric glands, with proliferative cells; **(c)** colonies of *H. pylori* deep in the gland, in the vicinity of stem cells. *H. pylori* in green, actin in red and DNA nucleus in blue.

However, it was not determined whether these aggregates were embedded in host mucins, bacterial EPSs or their combination. The challenge still remains to study the nature of the biofilm formation by *Hp in vivo*, in the gastric mucosa of humans and its role in the decades-lasting persistent colonization. The mechanisms of interaction of this biofilm-communities with the gastric mucosa at different niches in the glands may help us understand why in a few cases (<2%) the outcome of this interaction may be a severe disease such as gastric cancer. In particular, our observation of large aggregates of *Hp* growing in intimate contact with stem cells raises the possibility of damage to these cells as a result of direct interaction with the bacteria.

Quantification of Mucosal Biofilms in Clinical Specimens

Quantification of mucosal biofilm bacteria is rather complex, and it has been performed almost exclusively for gut mucosal biofilms (Swidsinski et al., 2005; Dejea et al., 2014), Swidsinski et al. defined three distinct microscopic fields of the biofilm: (1) adherent bacteria (±1 μm of the epithelial border); (2) mucus-scattered bacteria present within mucus next to the epithelial surface; and (3) mucus ceiling bacteria present in the outer portions of the mucus, at least 10 μm away from the epithelial surface, and found marked increases in fields (1) and (3) for patients with inflammatory bowel disease, using several arithmetic assumptions (Swidsinski et al., 2005). Their data suggest that the average biofilm density in healthy gut mucosa is in a range of 1–5 × 10^8 per ml (Swidsinski et al., 2005; Dejea et al., 2014), which reflects the fact that the inner mucus layer of normal human colon is impenetrable to bacteria (Matsuo et al., 1997; Johansson et al., 2008; Johansson et al., 2014). This number in healthy gastric mucosa may be even lower due to the high acidity, but to date, exact quantitation of *in vivo* biofilm in human stomach is lacking. We would need adjustment to the mathematical formula and bacterial probes used for gut biofilms in order to quantify *Hp* gastric biofilm.

GENETIC REGULATORY PATHWAYS OF *Hp* BIOFILM FORMATION

Candidate Genes Involved in Biofilm Formation

Yonezawa et al. (2010) and Wong et al. (2016) report substantial *Hp* strain variability identifying strong biofilm producers and poor biofilm producers in both reference strains as well as clinical isolates. These strain differences are likely to reflect variability in bacterial genes involved in biofilm formation and may be important for targeted intervention to reduce consequences from such infection. Existing literature suggests that three essential traits are required for bacteria to form and grow in biofilm *in vivo*: (1) inter-bacterial communication, (2) coordinated movements, and (3) aggregation. Furthermore, genes that control bacterial shape to fit biofilm environment may have an additional role in biofilm formation and maintenance.

Inter-bacterial communication is mediated through quorum sensing (QS) system, which is mediated by production and release of chemical signaling molecules in response to cell density and other physiological conditions (Elias and Banin, 2012; Gölz et al., 2012; Majumdar and Pal, 2017). These signaling molecules alter the expression of bacterial QS dependent genes to induce bacterial phenotype changes in virulence, motility, chemotaxis and biofilm formation, thus contributing to adaptation and colonization to the host (Elias and Banin, 2012; Gölz et al., 2012; Majumdar and Pal, 2017). To date, multiple systems based on different groups of molecules have been identified, some very bacteria-specific and others more general. Among those, signaling molecules called autoinducers (AI), AI-2 system, are most universally used by many bacteria, including *Hp* (Elias and Banin, 2012; Gölz et al., 2012; Majumdar and Pal, 2017). Another molecule produced by multiple bacterial families is N-acylhomoserine lactone (AHL) (He and Zhang, 2008; Elias and Banin, 2012; Papenfort and Bassler, 2016), although there have been no data to support that *Hp* utilizes the AHL-based QS. The other group of molecules more recently discovered is termed diffusible signal factor (DSF) that consists of fatty

acids of various chain lengths and branching and is known to be used by several groups of bacteria (He and Zhang, 2008; Elias and Banin, 2012; Papenfort and Bassler, 2016). One well-characterized DSF is 2-(Z)-tetradecenoic acid (TDA) produced by the xylem-limited plant pathogen *Xylella fastidiosa* (Ryan and Dow, 2011; Ryan et al., 2015). Recently, Yamashita et al. reported two self-growth-inhibiting compounds in *Hp* and one of them was identified as 7-(Z)-TDA (Yamashita et al., 2015). Although it has not been reported as a DSF, 2-(Z)-TDA is a positional isomer of 7-(Z)-TDA. Thus, 7-(Z)-TDA probably also acts as a signaling molecule to control the cell density of *Hp*. Currently, it is not known which *Hp* genes are responsible for synthesizing this compound. There are no other *Hp*-specific QS molecules characterized thus far. Several studies have also revealed that signaling pathways induced by QS molecules are followed by the phospho-relay cascade transmitted from the membrane-bound receptors to the cytosolic second-messenger system (Bharati and Chatterji, 2013; Wolska et al., 2016; Jakobsen et al., 2017). Second messengers based on mono (cAMP and cGMP) and di-cyclic or modified nucleotide (ppGpp, c-di-GMP and c-di-AMP) play a crucial role in transmitting the signals received from the surface receptor to the target molecule in the cell. Cyclic dimeric guanosine monophosphate (c-di-GMP) has evolved as a key activator of biofilm formation in almost all bacteria (Römling and Balsalobre, 2012; Bharati and Chatterji, 2013; Wolska et al., 2016; Jakobsen et al., 2017). c-di-GMP is synthesized by the GGDEF domain proteins and degraded by the unrelated EAL and HD-GYP domain proteins. The c-di-GMP signaling network is the most complex secondary signaling system found in bacteria with more than 100 c-di-GMP-metabolizing proteins in some species. This signaling network is especially prominent in γ-Proteobacteria, including the major human pathogens *Pseudomonas aeruginosa, Salmonella typhimurium*, *Escherichia coli,* and *Vibrio cholerae*, but little is known about this network in *Hp* (Römling and Balsalobre, 2012).

After bacteria reach a suitable niche to live, guided by chemotaxis, bacterial congregation requires adhesive materials, known as EPS. EPS are mostly produced by bacteria and consist of polysaccharides, proteins, enzymes, nucleic acids, lipids, other biopolymers, extracellular bacterial structures such as flagella, pili, fimbriae, and OMV (Flemming and Wingender, 2010). Interestingly, in contrast to many other bacteria, proteins appear to be the central player in *Hp* biofilm matrix (Windham et al., 2018). Recent studies also indicate that these three processes are not only controlled by *Hp* protein-coding genes, but also by a number of non-coding small regulatory RNAs (Mika and Hengge, 2013; Fazli et al., 2014; Bak et al., 2015; Wolska et al., 2016). Finally, it is also noteworthy that host molecules may contribute to EPS and host-bacterial co-aggregation. Specifically, secretory immunoglobulin A (IgA) has been shown to facilitate biofilm formation by normal gut flora in human tissue culture and by *Escherichia coli* in an intestinal cell line (Randal et al., 2003), as well as in a mouse model mono-infected with commensal *Bacteroides fragilis* (Donaldson et al., 2018). Interestingly, a higher systemic IgA response has been reported in mice infected with a high biofilm producing *Hp* than in those infected with low biofilm producing *Hp* strain, although mucosal secretory IgA levels were not quantified (Attaran et al., 2016).

Biofilm-Associated *Hp* Genes

Inter-bacterial Communication (QS Molecules)

AI-2 is produced as a metabolic byproduct of the reaction carried out by LuxS, which cleaves S-ribosylhomocysteine, producing homocysteine and 4,5-dihydroxy-2,3-pentanedione (DPD) and AI-2 as a metabolic byproduct of this reaction. DPD undergoes rapid dehydration and cyclization, existing in equilibrium as several molecules collectively termed as AI-2 (Schauder et al., 2001). LuxS uses methionine as a reduced sulfur source in the processes of *de novo* cysteine biosynthesis pathway. The *luxS* gene maps within an operon encoding *cysK*, *metB,* and *luxS*, which are necessary for the *de novo* cysteine biosynthesis pathway (Doherty et al., 2010). Some *luxS* mutants show reduced motility, and present a reduced number and length of each flagella. These differences result from a reduced transcription of genes of the flagella biosynthesis pathway (such as *flaA, flgE, motA, motB, flhA,* and *fliI* but not *flaB* genes) (Osaki et al., 2006; Rader et al., 2007; Shen et al., 2010). Gölz and colleagues demonstrated that a normal motility could be restored by adding AI-2. All described defects affecting motility of *Hp luxS* mutants were restored by the addition of AI-2 or DPD (Gölz et al., 2012). In *Hp*, AI-2 functions as a signaling molecule up-stream of the flagellar regulator *flhA*. High amounts of AI-2 increases motility, but it also reduces biofilm formation by *Hp*, thereby leading to colonization of niches with a small number of bacteria, but with a better provision of nutrients. AI-2 influences flagellar gene expression up-stream of *flhA* (Tsang and Hoover, 2014) and functions as chemorepellant via TlpB (Gölz et al., 2012). Both mechanisms obviously contribute to regulation of biofilm formation vs. planktonic growth, which in turn promotes bacterial colonization and persistence in the stomach (Rader et al., 2011).

The *Hp* genome carries few regulatory elements. Three of those are Fur, regulating the ferric uptake; NikR, regulating the response to the presence of nickel response regulator; and ArsRS, a two component system, which responses to an acid environment (Danielli and Scarlato, 2010). In particular, ArsR is essential for *in vitro* survival (Loh et al., 2010). Mutation studies of ArsS have been performed by mutating *arsR* into a non-phosphorylatable form (ArsR-D52N mutant). Involvement of ArsS in biofilm formation has been suggested by proteomic analysis and because ArsS mutants have a significant increase cellular aggregation and adherence to the flask at the air-liquid interface. Further studies showed that strains carrying ArsRD52N mutation or a combination of *nikR* and *arsS* deletions had a quicker transition to the coccoid form. Similar to biofilm formation, the transition to the coccoid form is known to happen in case of environmental stressors, such as nutrient deprivation. In summary, the data of these studies suggest that the lack of ArsRS system increases stress response, leading to an increased and faster biofilm formation. The simultaneous deletion of *arsS* and *nikR* genes decreases the normal *Hp* functionality and results in increasing of the coccoid forms and increased biofilm

formation (Servetas et al., 2016). This hyper-biofilm forming phenotype of *arsS* mutants is found to be mediated by an outer membrane protein, *homB* (Servetas et al., 2018).

Chemotaxis That Guides Movement to Reach the Right Position

In the colonization of gastric mucosa by *Hp*, coordinated movements are required to reach and position in the right topology of the stomach horizontally and vertically to form stable biofilms, guided by chemotaxis and powered by flagella and pili (Harshey, 2003; Howitt et al., 2011; Persat et al., 2015). In fact, aflagellated *Hp* mutants exhibit impaired biofilm formation (Hathroubi et al., 2018b). *Hp* species regulate their motility by chemotactic signaling systems, which allow the bacteria to follow favorable chemical gradients in their host environment. A number of transcriptional factors are known to be involved in these processes (De la Cruz et al., 2017). For chemotactic signal transduction, four different groups of proteins are necessary: (1) chemoreceptors, (2) core signal proteins, (3) accessory proteins, and (4) flagellar switch proteins (Lertsethtakarn et al., 2011). In *Hp*, the chemotactic behavior to low pH is dependent on the chemoreceptor TlpB (Croxen et al., 2006). A *luxS* mutant of *Hp* strain G27 showed a reduced stopping frequency in liquid media, which was restored by the addition of AI-2 or DPD (Rader et al., 2011). Analyzing the chemotactic behavior of double and single mutants, these authors confirmed that AI-2 is perceived as a chemorepellant signal via TlpB. In fact, an *Hp* strain deficient for the chemoreceptor TlpB failed to move away from a source of synthetic DPD and did not display increased stopping behavior upon addition of synthetic DPD. These behaviors were restored upon genetic complementation of the *tlpB* gene. *Hp* chemoreceptor TlpB is required for recognition of AI-2, which confirms its role in negative pH taxis (Rader et al., 2011). ChePep mediates another signaling system that controls the flagellar switching in a chemotaxis signaling protein-dependent manner. ChePep localizes to the flagellar pole of *Hp*, and chePep mutants show aberrant flagellar rotation, although flagella are correctly assembled and motile. In fact, ChePep does not control directly flagellar switching, but functions as a chemotaxis regulator, as it has been shown by studying *Hp* chemotactic behavior in a pH gradient. *Hp* cells increase their turning frequency in presence of a chemorepellent (i.e., acid) because of a predicted increase in phosphate signaling in the chemotaxis system. ChePep mutants constantly switch flagellar rotation also in normal culture condition and respond to acid condition by increasing their turning frequency. This behavior can be explained by high levels of phosphorylated CheY protein as obtained in some enteric bacteria by the mutation of CheZ and CheB that normally function as chemotaxis regulators by reducing the phosphorylation state of CheY (Howitt et al., 2011).

Extracellular Matrix, Outer Membrane Vehicle, and Adhesins Involved in Biofilm Formation

The Tol Pal gene cluster has been extensively studied in other organism such as *Escherichia (E) coli* and its role in the formation of OMV and in bacterial cell integrity is well known. *Hp* genomes encode homologous genes to *E. coli tolB* and *pal* (*HP1126* and *HP1125*, respectively), but no *Hp* homolog for *tolA* has been described (Turner et al., 2015). Moreover, *Hp* possesses two coding regions (*HP1127* and *HP1128*), with no known homologs in the databases, and other two coding sequences, *HP1130* and *HP1129*, putative homologs of *tolQ* and *tolR*, respectively. *Hp tolB* mutants displayed extensive "blebbing" and had very few flagella, which were markedly shorter in length and appeared to form clumps, suggesting a division defect. The morphology of the double mutant *tolB-pal* was not very different to that of wild type (WT) bacteria, although mutants lacked flagella completely. This phenotype could be due to the fact that the peptidoglycan-associated outer membrane proteins, including those of the Pal family, share sequence homology in the C-terminal region with the *E. coli* motility protein, MotB (Mot and Vanderleyden, 1994). This region of MotB is particularly important in anchoring the flagella structure to the peptidoglycan. It is therefore possible that any disruption of either the TolB or Pal protein may affect the functioning of the Tol-Pal complex as a whole, thereby altering flagella synthesis or hindering the anchoring of the flagella to the peptidoglycan layer. Furthermore, *Hp* ΔtolB and Δpal mutants produce >600- and 22-fold more OMVs than WT bacteria, suggesting a strong co-regulation of flagella and OMV (Turner et al., 2015).

Efflux pump functions in the formation of biofilms and multidrug resistance (Soto, 2013). *gluP* has been shown to be involved in the biofilm formation and multidrug resistance of *Hp* and the expression of *gluP* is upregulated by SpoT, which is a known global regulator (Ge et al., 2018). In addition to *SpoT*, there are other genes involved in both biofilm formation and multidrug resistance in *Hp,* which is mostly mediated through an increased expression of RND efflux pump genes (Yonezawa et al., 2013; Attaran et al., 2017). Furthermore, The *gluP* encodes a glucose/galactose transporter that belongs to the major facilitator superfamily of the efflux pump machinery (Tomb et al., 1997), which is mainly responsible for the physiological uptake of sugars, such as D-glucose (Psakis et al., 2009). Its inactivation has also the effect to alter the biofilm formation because glucose is a component of polysaccharides (Limoli et al., 2015) that are part of biofilm matrix (Ge et al., 2018).

Using nuclear magnetic resonance, Yang et al. (2011) identified mannose-related proteoglycans (proteomannans) as a major contributor to *Hp* EPS in *in vitro* culture. They detected the presence of NapA protein upregulation in the biofilm, suggesting a mechanism to increase adhesiveness of *Hp* biofilm. An isogenic mutant of *napA* revealed an altered biofilm structure with reduced aggregates, when compared to the WT. Adhesins are another class of genes involved in biofilm and the *Hp* genome contains two adjacent homolog genes, *alpA-alpB*, annotated as *omp20-omp21* and *hopC-hopB* in the 26695 and G27 genomes, respectively, that may be involved in biofilm formation. A recent study (Yonezawa et al., 2017) compared OMV protein profiles between a *Hp* strain and its spontaneous weak biofilm-forming mutants and demonstrated that AlpB was an important protein for biofilm formation. *alpB* mutants derived from various strains have also been shown to be incapable of inducing cell aggregation (Senkovich et al., 2011; Yonezawa et al., 2017).

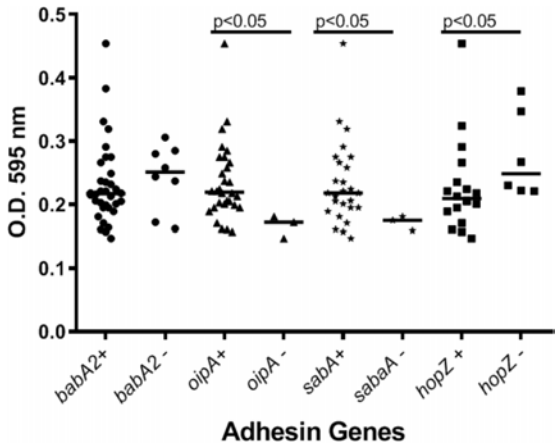

FIGURE 3 | The presence of adhesins in *H. pylori* strains may influence the formation of biofilm. See text for details on the assay.

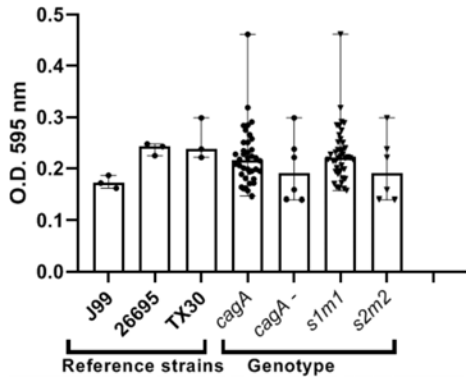

FIGURE 4 | *cagA* or *vacA* genotypes did not influence the capacity to form biofilm by *H. pylori* strains. See text for details on the assay.

Furthermore, these studies suggest that particularly the variable region of *alpB* is involved in the attachment to various substrates, including gastric cells.

Our preliminary studies on several known *Hp* virulence genotypes and biofilm formation *in vitro* support potential involvement of some adhesins. We tested a total of 45 clinical isolates from Mexican patients, including 15 each for non-atrophic gastritis, intestinal metaplasia and gastric cancer, using 96-well polystyrene microtiter plates. Each well was filled with 135 μl of Brucella broth. The formation of biofilm was started by inoculating 15 μl of pre-cultured bacterial suspension with 3×10^8 CFU/ml into each well. The cultures were incubated under microaerobic conditions during 48 h, at 37°C and 10% of CO_2. Uninoculated Brucella broth served as a negative control. After incubation, the supernatant was removed, the plates were washed 3 times with PBS and dried for 30 min. One hundred and fifty microliter of 0.1% crystal violet was added to each well and the plate was incubated at room temperature for 20 min. The excess crystal violet stain was removed, and the plate washed 3 times with PBS. The crystal violet staining biofilm was extracted with 150 μl of ethanol (70%) and measured at OD 595 nm. The assay was done 3 times and the final results were the mean of absorbance values. We tested strains positive or negative for adhesins reported important for *Hp* colonization. Strains lacking either *oipA* or *sabA* showed a significantly reduced ability to form biofilm. In contrast, strains lacking *hopZ* were in fact more efficient producing biofilm (**Figure 3**), and we found no differences between strains with or without the *babA2* gene. These results need to be confirmed with the study of additional strains, including isogenic strains mutated in the gene under study. On the other hand, our initial results indicate that *cagA* and *vacA* genotype may have no influence in the intensity of biofilm formation (**Figure 4**); formation of biofilm was similar in both, *cagA*-postive strains (J99 and 26695) and *cagA*-negative strains (TX30). Formation was also similar between *vacA* s1 and s2, or m1 and m2 strains; although we observed a tendency for reduced biofilm formation by m2 *Hp* strains (**Figure 4**). These observations ensure that the observed association with some adhesines was not mediated through the correlation with the presence of *cagA* and *vacAs1m1* genotypes.

Genes Regulating the Shape of *Hp*

The morphological transition of *Hp* leads from a spiral rod–shaped organism to a coccoid organism by changes in the peptidoglycan of the bacterial cell wall, These modifications are mediated by AmiA (Chaput et al., 2006, 2016). Moreover these changes influence the ability of the coccoid form to escape the immune system. Studies have shown that peptidases Csd1-4 and Csd6, as well as potential regulators Csd5 and CcmA are required to tailor the PG layer to generate the helical cell shape characteristic of *Hp* (Sycuro et al., 2010, 2012, 2013). Csd4 cleaves the gamma-D-Glu^2-*m*DAP^3 bond of the muramyl tripeptide to produce the muramyl dipeptide (member of M14 metallopeptidase family, Zn^{2+}-dependent). Csd3 (also known as HdpA, member of the M23 metallopeptidase family) has D,Dendopeptidase and D,D-carboxypeptidase (D,D-CPase) activities. Csd6 (*HP0518)* belongs to the peptidoglycan trimming pathway and also influences the cell shape of *Hp*. Disruption of the *csd6* gene by transposon-induced mutation or its deletion resulted in a straight rod shape and in an increase in tetrapeptide-containing muropeptides (Kim et al., 2015).

More recently Blair et al. (2018) studied the mechanisms by which Csd5 promotes helical cell shape. It has been shown that the N-terminal cytoplasmic (NT) and transmembrane (TM) domains, together with a C-terminal SH3 domain in Csd5 are each required to promote helical shape. Csd5 interacts directly with peptidoglycan via its C-terminal SH3 domain, whereas the N-terminal transmembrane domain promotes interactions with CcmA, MurF that catalyzes the synthesis of a PG precursor, and F_1F_0 ATP synthase. The recognition of the interaction of Csd5 protein with CcmA, a known cell-shape protein and putative cytoskeletal bactofilin, and with MurF, a known cell elongation factor, was unexpected but not surprising given the connections between PG synthesis, cell shape and intermediate filament proteins in helical organisms. Another study investigated the cholesteryl glucosides (CGs), one of the major components of the cell wall, by the deletion of the *hp0421* gene, which encodes

cholesteryl α–glucoside transferase that integrates (CGs) into the cell wall of *Hp*. This determines a deficiency of cholesterol, an alteration in the morphology and shape ("c"-shaped cells were prevalent), and of cell walls components like LPS, which leads to less virulent strain and an increasing of susceptibility to antibiotics (Qaria et al., 2018).

Hp Genetic Variabilities in Biofilm-Associated Genes

To elucidate the diversity of biofilm-associated genes among *Hp* strain, we used whole genome data (Muñoz-Ramírez et al., 2017) of 74 Latin American *Hp* strains to analyze 33 genes reported to be involved in biofilm formation (**Table 1**). This analysis revealed a mean variation of 6.78% in the amino-acidic sequence, ranging from a minimum of 0.39% in *motA* gene (*HP0815*, 1 non-synonymous variant in 258 amino acids) to a maximum of 23.12% in *chePep* gene (*HP0322*; 318 non-synonymous variants in 506 aa). For *luxS* (*HP0105*) that encodes an enzyme to produce AI-2 (He and Zhang, 2008; Gölz et al., 2012; Wolska et al., 2016), we found 10 non-synonymous variants with a variant frequency >10% on a total of 453 bp. Further phylogenetic

TABLE 1 | Variation analysis in *Hp* biofilm related genes.

Gene name	26695 gene code	Non-synonymous variants > 1% frequency	Non-synonymous variants > 10% frequency	Gene length (bp)	Potential pathways and functional categories (see footnotes)/additional references for genes not referred in the text
luxS	*HP0105*	36	10	453	(1)
arsR	*HP0166*	18	18	683	(1)
aibB	*HP0473*	114	36	753	(1), (2)/(Anderson et al., 2015)
aibA	*HP0298*	120	34	1658	(1), (2) /(Anderson et al., 2015)
fur	*HP1027*	18	4	454	(1), (2)
rpoN	*HP0714*	135	29	1247	(2)
tlpB	*HP0103*	224	33	1700	(2)
fliA	*HP1032*	61	20	804	(2)/(De la Cruz et al., 2017)
flgR	*HP0703*	45	17	1147	(2)/(De la Cruz et al., 2017)
chePep	*HP0322*	322	318	1518	(2)
cheW	*HP0391*	23	5	498	(2)
cheY	*HP1021*	69	7	897	(2)
	HP1067	21	2	375	
cheA	*HP0392*	61	22	2412	(2)
flaA	*HP0601*	52	8	1571	(2)
flgE	*HP0908*	30	8	1818	(2)
	HP0870	27	6	2160	
motA	*HP0815*	32	1	774	(2)
motB	*HP0816*	41	11	779	(2)
flhA	*HP1041*	42	12	2202	(2)
nikR	*HP1338*	52	8	447	(3)
tolB	*HP1126*	104	20	1255	(3)
HP0840/ JHP0778	*HP0840*	42	13	1024	(3)/(Burrows et al., 2000)
futA	*HP0379*	193	196	1278	(3)/(Wong et al., 2016)
futB	*HP0651*	218	241	1431	(3) /(Wong et al., 2016)
homD	*HP1453*	278	84	2303	(3) /(Wong et al., 2016)
napA	*HP0243*	29	5	435	(3)
amiA	*HP0772*	101	27	1323	(4)
ccmA	*HP1542*	24	5	411	(4)
csd1	*HP1543*	103	13	948	(4)
csd2	*HP1544*	87	27	928	(4)
csd4	*HP1075*	127	39	1317	(4)
csd5	*HP1250*	104	27	579	(4)
csd3	*HP0506*	200	33	1281	(4)
csd6	*HP0518*	100	20	983	(4)
murF	*HP0740*	162	54	1485	(4)
cgt	*HP0421*	53	53	1170	(4)

Functional categories: (1) Sensing and communications, quorum sensing molecules, (2) Movement/positioning, chemotaxis, flagella, (3) Extracellular matrix production, polysaccharide metabolism, outer membrane vehicle synthesis, (4) Cell shape control.

analysis of the 33 genes in the 74 *Hp* strains did not show evidence of geographical clustering by country for most of these genes with the only exception of the *murF* gene (*HP0740*), which clearly formed separated clusters for Mexico and Colombia (**Figure 5**). This result would suggests that *murF* is under constant positive selection to adapt to the human host population they are colonizing. Whether this diversity in *murF* contributes to differential gastric cancer risk in these two populations is something that deserves further studies.

FUNCTIONAL AND MORPHOLOGICAL CHANGES ASSOCIATED WITH BIOFILM FORMATION

Growth Rate

Slow growth rate has been recognized as one of the major contributing factors to antibiotic resistance of biofilm-associated bacteria (Stewart, 2015). Matured biofilms are known to contain variable fractions of slow growing or non-dividing metabolically inactive cells, which gives rise to persistent colonization (Lewis, 2005; Kostakioti et al., 2013). *In vitro* mono-microbial biofilm studies demonstrated that *Streptococcus mutans* biofilms grew about 35% slower than planktonic culture before the stationary phase (Welch et al., 2012). Using transcriptional profiles, Folsom et al. estimated that *Pseudomonas aeruginosa* grew at just 10% of planktonic growth rate in the stationary biofilms (Folsom et al., 2010). Applying an agarose gel as artificial EPS, Pabst et al. confirmed that the growth rate of *Staphylococcus aureus* in the stationary biofilms was also about 10% of that of planktonic culture (Pabst et al., 2016). Altered gene expression leading to reduced transcription and to translation and DNA replication arrest, has been identified as molecular characteristics of the stationary biofilm-associated cells (Lewis, 2005; Stewart, 2015). Others suggest that bacterial synthesis of antibacterial compounds against own or neighboring organisms (Elias and Banin, 2012; Yamashita et al., 2015) may also contribute to the slow growth of biofilm-associated bacteria. To date, however, there have been no direct *in vitro* or *in vivo* data to support that *Hp* forming stationary biofilms exhibits a reduced growth rate.

Metabolism

Biofilms are formed by groups of cells in different states, growing or non-growing and metabolically active or inactive in variable fractions, depending on maturity and on chemical gradients

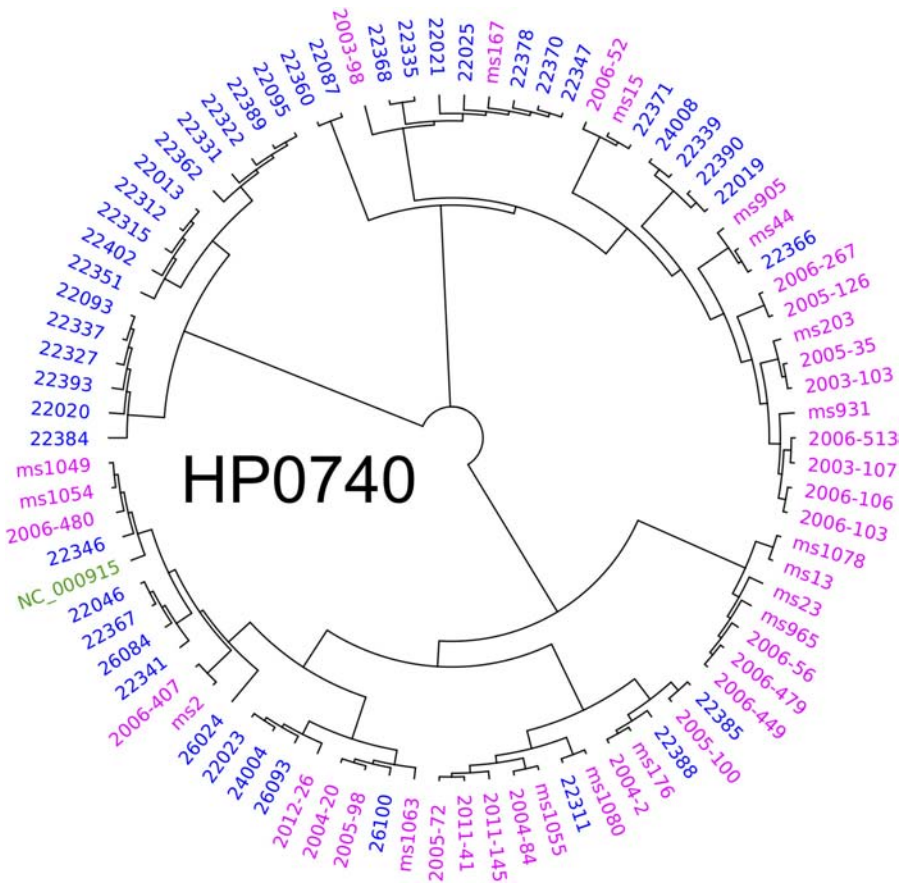

FIGURE 5 | Phylogenetic analyses of *HP0740* for 74 Mexican and Colombian strains. The alignment and graphics was produced with Geneious and graphically modified with Inkscape software.

(O_2 and nutrients) of the biofilms (Stewart, 2015; Flemming et al., 2016). It has been postulated that dormant non-growing metabolically inactive cells reach these metabolic states in order to reduce cell permeability and protect themselves against oxidative stress (Stewart, 2015). Bacterial cells in stationary biofilms have also been reported to increase synthesis of pili, fimbriae and exopolysaccharides as well as lipopolysaccharide modification and production of stress-response enzymes (Prigent-Combaret et al., 1999; Folsom et al., 2010). Wong et al. recently profiled metabolites of high and low biofilm forming *Hp* strains from Malaysia using liquid chromatography/quadrupole time-of-flight mass spectrometry (Wong et al., 2018). The study compared four high and four low biofilm forming strains cultured up to 3 days in duplicate. Interestingly, low-biofilm-formers produced more metabolites than high-biofilm-formers, consistent with lower overall metabolic activities in biofilm-associated bacteria. Further analysis indicated that the metabolites significantly lower in high biofilm producers belonged to major categories of lipids, with an important role in bacterial-bacterial communications, and metabolites involved in prostaglandin synthesis (Wong et al., 2018).

Morphology

A morphological change described as small colony variants (SCVs) has been linked to various biofilm associated infections, such as cystic fibrosis, osteomyelitis and device-related infections (Proctor et al., 2006). Since its first description for *Salmonella enterica serovar typhi* (*S. typhi*) almost 100 years ago, SCVs have now been reported for a wide range of bacterial genera and species, including *Staphylococci, Escherichia coli, Pseudomonas aeruginosa, Vibrio cholerae, Shigella* spp., *Lactobacillus acidophilus*, and *Neisseria gonorrhoeae* (Proctor et al., 2006). Currently, the connection between the SCV phenotype and persistent, recurrent infections has become a hot topic in clinical microbiology. Phenotypically, the size of SCVs are about one tenth of that in regular colonies, with a slow growth rate, atypical colony morphology and unusual biochemical characteristics and are less susceptible to antibiotics than their wild-type counterparts. An altered cellular morphology in the cell wall structure and the emergence of intercellular EPS have also been demonstrated for SCVs from *Staphylococcus aureus*. These characteristics have been associated with mutations in the *nupC* gene that encodes a protein involved in thymidine uptake and in the *thyA* gene that encodes thymidylate synthase (Proctor et al., 2006). A group of Norwegian researchers reported spontaneous appearance of *Hp* SCVs, although they did not clarify its size relative to normal colonies (Bukholm et al., 1997). This variant was induced by acid exposure and showed enhanced adherence and invasion to epithelial cells (Bukholm et al., 1997; Tannæs et al., 2001). It was found that these morphological changes are a consequence of a shift in cell wall lipid composition, specifically, an increase in lysophospholipids, due to phase variation in the *pldA* gene, resulting in production of an active form of the outer membrane phospholipase A (OMPLA) (Bukholm et al., 1997; Tannæs et al., 2001). Another colony variant associated with biofilm is the rough colony variant arising from smooth colonies of *P. putida* (Hansen et al., 2007; Elias and Banin, 2012). This was caused by two independent mutations in *wapH (PP4943)*, a gene involved in lipopolysaccharide (LPS) biosynthesis (Hansen et al., 2007). Rough/smooth phenotype variants due to altered LPS composition were also observed for *Hp*, yet its association with biofilm formation and virulence is unclear (Bertram-Drogatz et al., 1999).

At the cellular level, the best-described morphological change in *Hp* associated with biofilm *in vivo* is coccoid transformation (Carron et al., 2006; Coticchia et al., 2006; Cellini et al., 2008). Coccoid transformation is considered a common feature of Gram-negative rod bacteria under conditions of stress (Andersen and Rasmussen, 2009; van Teeseling et al., 2017; Krzyzek and Gosciniak, 2018). *In vitro*, coccoid forms of *Hp* can be induced by prolonged culture or use of suboptimal levels of antibiotics (Krzyzek and Gosciniak, 2018; Poursina et al., 2018). The *Hp* coccoid forms have been defined as viable but non-culturable (VBNC), thus undetectable by conventional cultures, and are known to have an increased capacity to aggregate into monomicrobial clusters embedded in thick EPS (Cellini et al., 2008; Cellini, 2014; Krzyzek and Gosciniak, 2018). In many ways, VBNC coccoid *Hp* resembles the characteristics of persister cells documented in biofilms of other bacteria (Lewis, 2005; Pinto et al., 2015) and they can survive up to 1 year just in fresh water (Cellini, 2014; Percival and Suleman, 2014). An accumulation of N-acetylglucosaminyl-N-acetylmuramyl–l-Ala–d-Glu in PG of the cell wall (Costa et al., 1999), catalyzed by AmiA (PG hydrolase), has been described to precede this morphological transformation and also to lead to immune evasion by escaping from NOD1 detection (Chaput et al., 2006). Yet, since PG dictates bacterial cell shape (Rubin and Trent, 2013; van Teeseling et al., 2017) and since many other PG remodeling enzymes have been described (Caccamo and Brun, 2018), genes other than *amiA* are likely to be involved in this process. In fact, genes encoding the enzymes, *pgp1* and *pgp2 for Campylobacter* spp, and *csd1, csd2, csd3, csd4, csd6, murF* and related non-enzymatic proteins, *csd5* and *ccmA* for *Hp* have been identified to be critical in the maintenance of helical shape (Sycuro et al., 2010, 2012, 2013; Kim et al., 2015; Esson et al., 2016; Blair et al., 2018) as detailed in the previous section. In addition, coccoid *Hp* harvested *in vitro* from clinical isolates overexpressed *spoT,* a global transcriptional regulator for stress responses (Poursina et al., 2018). A homologous gene in *Mycobacterium smegmatis* has been linked to its cell shape control (Gupta et al., 2016) and a *Hp spoT*-mutant exhibits a reduced ability to form biofilm (Ge et al., 2018). To date, despite these growing observations, it remains to be elucidated whether coccoid transformation indeed prompts biofilm formation, or whether biofilm formation promotes *Hp* coccoid transformation.

Virulence Factors

It is yet unknown whether biofilm-associated bacteria exert virulence more potently than those living planktonically. There are several factors that affect virulence of biofilm-associated bacteria. As discussed above, the stage (maturity) of biofilms, chemical composition (O_2, acidity and nutrients gradients) and microbial (mono- vs. poly-biofilms) environment within biofilms are important determinants of bacterial gene expression

(Lewis, 2005; Folsom et al., 2010; Stewart, 2015). In addition, how to quantify or compare virulence is not so straightforward, because life expectancy of bacteria living in biofilms and that of planktonic bacteria are different, as the former is expected to live longer causing persistent infection (Lewis, 2005; Pinto et al., 2015). Furthermore, even if biofilm-associated bacteria express lower virulence per time compared with planktonic bacteria, cumulative effects on host cells may be higher. In addition, aggregative nature of biofilm-forming bacteria may enhance virulence through increased adherence to host cells, even if the same amount and potency of virulence molecules are produced or released. Part of biofilm-associated virulence is also derived from surrounding EPS, not bacterial cells themselves. EPS contains secreted enzymes, toxins and outer membrane vehicles (Flemming and Wingender, 2010; Hathroubi et al., 2018a) and can activate neutrophils without opsonization to induce inflammatory reactions and exert cytotoxicity (Meyle et al., 2012; Fulsundar et al., 2015; Susanne et al., 2015; Kim et al., 2016; Nascimento et al., 2016).

Pinto et al. reviewed virulence of VBNC bacteria predominantly found in biofilms (Pinto et al., 2015). They concluded that most bacteria continue to express their virulence and toxin genes, but expression levels are downregulated or protein secretion may not be detectable. However, altered gene/protein expression seems to vary with types of bacteria, types of virulence genes, or co-colonization with other bacteria. For example, when *Pseudomonas aeruginosa* and methicillin-resistant *Staphylococcus aureus* (MRSA) were grown together as a mixed culture, biofilm development was accelerated and production of *P. aeruginosa* exotoxin A was increased by 1839-fold in comparison to their respective monocultures (Goldsworthy, 2008). Moreover, *P. aeruginosa* exoproduct 4-hydroxy-2-heptylquinoline-*N*-oxide (HQNO) was found to stimulate *S. aureus* biofilm and SCV formation, leading to an increase in the expression of the fibronectin-binding protein A and a decrease in the expression of the α-hemolysin gene (Mitchell et al., 2010). It was also demonstrated that a spontaneous SCV of *Hp* released VacA and urease from the cells, while its parent large colony cells retain these toxins within the cells (Bukholm et al., 1997).

Other studies specific to *Hp* have attempted to identify differential virulence profiles between coccoid and helical/spiral forms. A proteomic study by Bumann et al. (2004) reported differential virulence profiles, i.e., *cagA*/*vacA* dominance in helical and *ureA/B* and *groEL* dominance in coccoid forms. The lack of CagA protein expression in coccoid *Hp* was consistent with an earlier report by Roe et al. (1999). However, a more recent high resolution proteomic study reached a different conclusion (Loke et al., 2016). When compared with helical forms, coccoid forms of *Hp* were found to express higher levels of proteins that are involved in virulence and carcinogenesis, such as secretion system machinery proteins, CagE, CagV, and YidC and proinflammatory proteins, such as OipA and Hps. Poursina et al. tested the mRNA expression of two *Hp* virulence genes, *babA* and *cagE* in coccoid forms harvested *in vitro* and concluded that both genes were expressed but in lower rates than those of helical forms. Also, coccoid forms of clinical isolates from peptic ulcer patients showed higher *cagE* expression than the reference *Hp* strain 26695, indicating the presence of strain variability (Poursina et al., 2013). More recently, Hirukawa et al. (2018) found that all forms of *Hp* (helical, coccoid and fragmented) expressed certain pathogenic proteins, including CagA, other components of the cag−Type IV secretion system (VirB7 and VirB9), the blood group antigen−binding adhesin BabA, and UreA, to similar levels. However, phosphorylation of CagA in gastric cancer cells was only seen by the helical form (Hirukawa et al., 2018). In contrast, Segal et al. (1996) reported, using the same cells but a different strain, that coccoid *Hp* was capable of binding and inducing cellular changes of the same sort as spiral *Hp*, including tyrosine phosphorylation of host proteins and that coccoid *Hp* induced a stronger cytoskeletal rearrangement than spiral *Hp*. Co-culture of a gastric non-cancer epithelial cell line with coccoid or helical forms of *Hp* revealed that helical *Hp* led to more severe inflammatory and apoptotic responses, while coccoid *Hp* maintained host cell in a high proliferation rate (Liu et al., 2006). Interestingly, in animal models, colonization efficiency of *Hp* mutants in coccoid associated genes, *aimA* and *spoT,* was markedly reduced (Sun et al., 2012; Chaput et al., 2016). Despite substantial contrasting findings in the observations, overall, accumulated data suggest that coccoid *Hp* retains virulence, can survive better *in vivo* and may contribute to carcinogenesis, while helical *Hp* can be more easily eliminated by acute host immunoinflammatory responses.

The toxin–antitoxin (TA) systems have emerged as important virulence factors in many pathogenic bacteria, which have been described to be beneficial in bacterial fitness, persistence, and virulence (Kędzierska and Hayes, 2016). Importantly, we recently documented the presence of a novel TA system in *Hp* encoded by *HP0968-HP0967* (Cárdenas-Mondragón et al., 2016), which was strongly expressed in bacteria forming mature biofilm on abiotic surface, but not in planktonic growth. In addition, the expression of this TA was significantly increased after contact with gastric epithelial cell line AGS. These results suggest that *HP0968-HP0967* may be expressed in the gastric mucosa and have a role in the gastric carcinogenic pathways.

POTENTIAL ROLE OF POLYMICROBIAL BIOFILMS IN CARCINOGENESIS

Gastric Microbiome of *Hp*-Infected Humans

Bacterial-bacterial interactions are a major driver of pathophysiological consequences of poly-microbial biofilms, as observed in niches like oral cavity and intestine (Larsen and Fiehn, 2017; Li et al., 2017). It is not known whether this is also the case for the stomach, although there is evidence that supports the presence of such interactions in animal models. Interestingly, in *Hp*-infected INS-GAS mouse models, gastric intraepithelial neoplasia (GIN) developed much earlier in the presence of commensals, than in mice lacking commensals (Lofgren et al., 2011). A subsequent study confirmed that the presence of only a few other bacterial species had a similar

impact to that of full commensals on GIN development (Lertpiriyapong et al., 2014) and that co-infection specifically promoted progression of metaplasia and foveolar hyperplasia to dysplasia (Pinzon-Guzman et al., 2018). However, to date clinical observations or *in vitro* and *in vivo* experiments for *Hp* biofilm studies have been primarily limited to be mono-microbial, exclusively to *Hp*. There are only a couple of studies that demonstrated the presence of non-*Hp* bacterial aggregates in the gastric mucus layer and crypts of the patients during acid suppression treatment or with gastric primary lymphoma, using chemical and immunochemical staining (Jonkers et al., 1997; Sanduleanu et al., 2001). These studies reported that almost two thirds of the patients harbored non-*Hp* bacteria and that co-existence of *Hp* and non-*Hp* bacteria was common (Jonkers et al., 1997; Sanduleanu et al., 2001), although the presence of EPS between bacteria was not examined.

Recent studies based on *16S* rRNA gene sequencing or other high dimensional approaches to characterize the gastric microbiome have revealed that the gastric lumen is inhabited by a wide range of commensal bacteria, contrary to the previous belief that high gastric acidity kills most microorganisms (Alarcón et al., 2017; Yu et al., 2017). Gastric microbiome comprises commensals from the ororespiratory tract through ingestion, as well as in a smaller fraction from the intestinal tract by biliary reflux (Sanduleanu et al., 2001; Yu et al., 2017). Some of these bacteria are just transient, and data pointing to which are truly resident of the gastric mucosa, other than *Hp*, are still limited. Multiple studies have found that the dominant genera in the gastric mucosa comprise *Streptococcus, Lactobacillus, Rothia, Prevotella, Veillonella, Neisseria,* and *Haemophilus,* including over 100 species (Sheh and Fox, 2013; Alarcón et al., 2017; Yu et al., 2017). There is also a consensus that *Hp* infection, especially before the development of gastric atrophy, substantially reduces diversity and richness of gastric microbiome by dominating others (Alarcón et al., 2017; Parsons et al., 2017). Yet, these studies raise the possibility that some non-*Hp* gastric bacteria may cohabit with *Hp* in biofilms and that the interactions between them may play a role in gastric carcinogenesis. Differential compositions of non-*Hp* gastric microbiome have been reported between normal individuals, pre-malignant lesions and gastric cancer, although the data have been inconsistent concerning specific bacteria associated with the stage of gastric lesions and it is still unclear whether the observed differences in microbiota are a cause or consequence of carcinogenesis (Sheh and Fox, 2013; Aviles-Jimenez et al., 2014; Dias-Jacome et al., 2016; Alarcón et al., 2017). This could suggest a progressive shift in gastric microbiota structure in carcinogenesis, possibly resulting from a complex cross-talk between gastric microbiota and *Hp*, which are likely to occur within biofilms where they live in proximity. In fact, abundance of non-*Hp* bacteria may not be important if they act like a keystone pathogen, as it is well known for *Porphyromonas gingivalis* in dental biofilms (Hajishengallis et al., 2011; Lamont and Hajishengallis, 2015). Keystone pathogens are typically present at very low abundance in a particular microbial niche; still, they can alter commensal structure to become a dysbiotic community and by attracting more pathogenic microbes (Hajishengallis et al., 2011; Lamont and Hajishengallis, 2015). Such biofilms are thought to promote host inflammatory responses and immune suppression, leading to tissue damage and development of precancerous lesions.

Commensal-*Hp* Interactions

Potential interactions between *Hp* and other commensals or pathogens have been investigated mainly in co-culture studies and also by virtual bioinformatic models. Das et al. analyzed 16S rRNA gene pyrosequencing data from 39 Indian patients with suspected *Hp* infection using a network analyses (Das et al., 2017). Their results suggest that *Hp* has negative interactions with most members of the gastric microbiota, while other microbes interacted positively with each other, showing frequent intra-cluster co-occurrence/co-operation and increased network density. Major microbes that showed negative interactions with *Hp* include *Ralstonia, Bradyrhizobium, Cloacibacterium, Acidovorax, Aeromonas, Halomonas, Bacillus, Methylobacterium,* and *Meiothermus.* On the other hand, Krausse et al. (2005) examined the effects of other bacteria found in the gastric lumen on the growth of 30 *Hp* clinical isolates and one reference strain, using cross-streak *in vitro* culture. Among 29 bacteria tested, *Staphylococcus epidermidis, Staphylococcus aureus, Pseudomonas aeruginosa, Stenotrophomonas maltophilia, Morganella morganii, Serratia marcescens, Bf, Fn,* and *Clostridium difficile* showed the strongest growth inhibition, with varied degree on the different *Hp* strains (Krausse et al., 2005). Other researchers have focused on bacteria more common in oral cavity, *Streptococcus* and *Lactobacillus*. When a *cagA* positive *Hp* strain was co-cultured with human monocyte-derived dendritic cells (DC) in the presence of *Lactobacillus*, maturation of DC was stimulated, producing more inflammatory cytokines, compared with *Hp* alone (Wiese et al., 2015). This suggests that lactic acid producing bacteria may enhance gastric inflammatory reactions caused by *Hp* and may also promote *Hp*-induced carcinogenesis. These results were consistent with a gastric microbiome study in humans showing increased abundance of *Lactobacillus* in *Hp*-associated intestinal metaplasia and intestinal type of gastric cancer, compared with non-atrophic gastritis (Aviles-Jimenez et al., 2014) as well as the increased gastric *Lactobacillus* population in INS-GAS mouse model co-infected with *Hp* and limited commensals (*Bacteroides, Clostridium,* and *Lactobacillus*) that developed GIN (Lertpiriyapong et al., 2014). However, others have reported a probiotic *Lactobacillus* strain that inhibited the colonization of *Hp* in a Mongolian gerbil model (Merino et al., 2018). More relevant to biofilm-associated *Hp*, Khosravi et al. (2014) reported that *Streptococcus mitis* induced *Hp* conversion to coccoid cells in co-culture studies and their proteomic analysis revealed a metabolic crosstalk between these two bacteria, suggesting a probable impact on *Hp*-associated carcinogenesis (Khosravi et al., 2016; Krzyżek, 2017). Furthermore, a recent animal experiment demonstrated that INS-GAS mice co-infected with *Hp* and *Streptococcus salivarius* developed more severe inflammation, hyperplasia, and dysplasia

in the stomach when compared with *Hp* only at 5 months post-infection. These studies address only a small fraction of possible interactions between *Hp* and other bacteria, but provide evidence suggesting that bacterial-bacterial interactions may modify *Hp*-associated carcinogenesis (Shen et al., 2018).

Importantly, biofilms are considered to foster horizontal gene transfer between and within species through transduction and transformation and increase fitness of organisms (Madsen et al., 2012). Mixed infection with multiple *Hp* strains has been found to produce biofilms with higher adherent capacity compared with each strain alone (Grande et al., 2012). Indeed, *Hp* exhibits high homologous recombination rates (Suerbaum et al., 1998; Falush et al., 2001) and is competent for DNA uptake (Chattopadhyay et al., 2018) as the genome often contains pathogenicity islands (cagPAI) to encode a DNA transfer apparatus, such as *tfs4*, to facilitate conjugation (Fischer et al., 2010; Fernandez-Gonzalez and Backert, 2014). Conjugative DNA transfer occurred between *Campylobacter jejuni and Hp* in an experimental system (Oyarzabal et al., 2007) and inter-species horizontal gene transfer and DNA recombinatorial events have been demonstrated within *Hp* species or with closely related genera (Eppinger et al., 2004; Saunders et al., 2005). Thus, such heightened genetic exchanges are likely to promote bacterial persistence and virulence, as evidenced by acquisition of cagPAI more than 60,000 years ago (Grande et al., 2012; Fernandez-Gonzalez and Backert, 2014).

CONCLUDING REMARKS

As discussed above, emerging evidence suggests that certain low abundance gut bacteria, such as *Fn* and *SGG,* which are capable of causing biofilm-associated infection, may promote the development of colorectal cancer in humans. This notion is supported by not only epidemiological studies, but also biological data to corroborate molecular pathways to mediate biofilm formation and bacterial aggregation. On the other hand, despite a substantial number of studies to support the ability of *Hp* to form biofilms in *in vitro* environments (Garcia et al., 2014; Hathroubi et al., 2018a), *in vivo* observations of gastric biofilms from human subjects are still very sparse. Studies based on other anatomic niches, such as gut and oral cavity indicate that behavior of biofilm-associated bacteria is different from that of planktonic counterparts (Gabrilska and Rumbaugh, 2015; Liu et al., 2016) and that bacterial-bacterial and host-bacterial interactions taking place in the biofilm community enhance virulence and adverse host responses, probably contributing to cancer initiation and progression (Li et al., 2017). Accordingly, it is highly plausible that the presence of *Hp* biofilms predisposes individuals to progression to gastric cancer, compared to infection with planktonic *Hp*, directly through altered virulence or/and indirectly through prolonged exposure due to persistent infection. However, information available to date is insufficient to test these hypotheses and thus more clinical observations are urgently needed. New histological techniques to preserve mucus layers of gastro-intestinal mucosa may be explored to gain better resolution and quantitation of *Hp*-biofilms in such studies. Furthermore, we need to accumulate more information regarding characteristics of *Hp* biofilms including compositions and biological properties of EPS and non-*Hp* microbiome, as well as geographical distribution of biofilms in relation to gastric gland types and structures and to gastric pathologies (e.g., premalignant lesions). We need also to address the possible effects of *Hp* morphological changes on host oncogenic signaling pathways. Identification of specific *Hp* gene variants resulting into enhanced biofilm formation would be helpful not only for screening patients at high risk for sequelae from *Hp* infection, but also for development of new antibiotic regimens to avoid resistance, regardless of its association with gastric cancer. Given putative auxiliary functions of type IV secretion system pili in the contact and adhesion to host and other bacterial cells (Backert et al., 2008; Maldarelli et al., 2016) and because of well established oncogenic properties of CagA, studies focused on *cagA*-positive *Hp* in high risk populations would be particularly advantageous in addressing potential effects of *Hp* biofilms on gastric carcinogenesis.

ETHICS STATEMENT

The original clinical studies where human samples were collected were approved by the respective institutional ethical committee in Mexico and Colombia.

AUTHOR CONTRIBUTIONS

IK conceptualized the manuscript. JT and MC-P carried out the experiments presented in **Figures 1–4**. FC, JT, MB, and CR contributed to *Hp* sequence analyses. IK, EK, JT, MC-P, and CR conducted literature review and prepared the first draft. FC and MB participated in editing the draft. All authors approved the final manuscript for submission.

REFERENCES

Abadi, A. T. B. (2017). Strategies used by *Helicobacter pylori* to establish persistent infection. *World J. Gastroenterol.* 23, 2870–2882. doi: 10.3748/wjg.v23.i16.2870

Alarcón, T., Llorca, L., and Perez-Perez, G. (2017). "Impact of the microbiota and gastric disease development by *Helicobacter pylori*," in *Molecular Pathogenesis and Signal Transduction by Helicobacter pylori*, eds N. Tegtmeyer and S. Backert (Cham: Springer), 253–275. doi: 10.1007/978-3-319-50520-6_11

Allen-Vercoe, E., Strauss, J., and Chadee, K. (2011). Fusobacterium nucleatum. *Gut Microbes* 2, 294–298. doi: 10.4161/gmic.2.5.18603

Andersen, L. P., and Rasmussen, L. (2009). *Helicobacter pylori*– coccoid forms and biofilm formation. *FEMS Immunol. Med. Microbiol.* 56, 112–115. doi: 10.1111/j.1574-695X.2009.00556.x

Anderson, J. K., Huang, J. Y., Wreden, C., Sweeney, E. G., Goers, J., Remington, S. J., et al. (2015). Chemorepulsion from the quorum signal autoinducer-2 promotes *Helicobacter pylori* biofilm dispersal. *mBio* 6:e00379. doi: 10.1128/mBio.00379-15

Armstrong, H., Bording-Jorgensen, M., Dijk, S., and Wine, E. (2018). The complex interplay between chronic inflammation, the microbiome, and cancer: understanding disease progression and what we can do to prevent it. *Cancers* 10:E83. doi: 10.3390/cancers10030083

Attaran, B., Falsafi, T., and Ghorbanmehr, N. (2017). Effect of biofilm formation by clinical isolates of *Helicobacter pylori* on the efflux-mediated resistance to commonly used antibiotics. *World J. Gastroenterol.* 23, 1163–1170. doi: 10.3748/wjg.v23.i7.1163

Attaran, B., Falsafi, T., and Moghaddam, A. (2016). Study of biofilm formation in C57Bl/6J mice by clinical isolates of *Helicobacter pylori*. *Saudi J. Gastroenterol.* 22, 161–168. doi: 10.4103/1319-3767.178529

Aviles-Jimenez, F., Vazquez-Jimenez, F., Medrano-Guzman, R., Mantilla, A., and Torres, J. (2014). Stomach microbiota composition varies between patients with non-atrophic gastritis and patients with intestinal type of gastric cancer. *Sci. Rep.* 4:4202. doi: 10.1038/srep04202

Azeredo, J., Azevedo, N. F., Briandet, R., Cerca, N., Coenye, T., Costa, A. R., et al. (2017). Critical review on biofilm methods. *Crit. Rev. Microbiol.* 43, 313–351. doi: 10.1080/1040841X.2016.1208146

Babu, S. D., Jayanthi, V., Devaraj, N., Reis, C. A., and Devaraj, H. (2006). Expression profile of mucins (MUC2, MUC5AC and MUC6) in *Helicobacter pylori* infected pre-neoplastic and neoplastic human gastric epithelium. *Mol. Cancer* 5:10. doi: 10.1186/1476-4598-5-10

Backert, S., Fronzes, R., and Waksman, G. (2008). VirB2 and VirB5 proteins: specialized adhesins in bacterial type-IV secretion systems? *Trends Microbiol.* 16, 409–413. doi: 10.1016/j.tim.2008.07.001

Bak, G., Lee, J., Suk, S., Kim, D., Young Lee, J., Kim, K.-S., et al. (2015). Identification of novel sRNAs involved in biofilm formation, motility, and fimbriae formation in *Escherichia coli*. *Sci. Rep.* 5:15287. doi: 10.1038/srep15287

Bedran, T. B. L., Azelmat, J., Spolidorio, D. P., and Grenier, D. (2013). Fibrinogen-induced *Streptococcus mutans* biofilm formation and adherence to endothelial cells. *BioMed Res. Int.* 2013:431465. doi: 10.1155/2013/431465

Belas, R. (2014). Biofilms, flagella, and mechanosensing of surfaces by bacteria. *Trends Microbiol.* 22, 517–527. doi: 10.1016/j.tim.2014.05.002

Bellack, N. R., Koehoorn, M. W., MacNab, Y. C., and Morshed, M. G. (2006). A conceptual model of water's role as a reservoir in *Helicobacter pylori* transmission: a review of the evidence. *Epidemiol. Infect.* 134, 439–449. doi: 10.1017/S0950268806006005

Bertram-Drogatz, P. A., Sobek-Klocke, I., Moller, C., Wingbermuhle, D., Beil, W., Sewing, K. F., et al. (1999). Growth characteristics and influence of antibiotics on rough/smooth phenotypic variants of *Helicobacter pylori*. *Eur. J. Clin. Microbiol. Infect. Dis.* 18, 490–495. doi: 10.1007/s100960050329

Bharati, B. K., and Chatterji, D. (2013). Quorum sensing and pathogenesis: role of small signalling molecules in bacterial persistence. *Curr. Sci.* 105, 643–656.

Blair, K. M., Mears, K. S., Taylor, J. A., Fero, J., Jones, L. A., Gafken, P. R., et al. (2018). The *Helicobacter pylori* cell shape promoting protein Csd5 interacts with the cell wall, MurF, and the bacterial cytoskeleton. *Mol. Microbiol.* 110, 114–127. doi: 10.1111/mmi.14087

Boleij, A., Roelofs, R., Danne, C., Bellais, S., Dramsi, S., Kato, I., et al. (2012). Selective antibody response to *Streptococcus gallolyticus* pilus proteins in colorectal cancer patients. *Cancer Prev. Res.* 5, 260–265. doi: 10.1158/1940-6207.CAPR-11-0321

Boleij, A., Roelofs, R., Schaeps, R. M., Schulin, T., Glaser, P., Swinkels, D. W., et al. (2010). Increased exposure to bacterial antigen RpL7/L12 in early stage colorectal cancer patients. *Cancer* 116, 4014–4022. doi: 10.1002/cncr.25212

Bukholm, G., Tannæs, T., Nedenskov, P., Esbensen, Y., Grav, H. J., Hovig, T., et al. (1997). Colony variation of *Helicobacter pylori*: pathogenic potential is correlated to cell wall lipid composition. *Scand. J. Gastroenterol.* 32, 445–454. doi: 10.3109/00365529709025079

Bumann, D., Habibi, H., Kan, B., Schmid, M., Goosmann, C., Brinkmann, V., et al. (2004). Lack of stage-specific proteins in coccoid *Helicobacter pylori* cells. *Infect. Immun.* 72, 6738–6742. doi: 10.1128/IAI.72.11.6738-6742.2004

Burrows, L. L., Urbanic, R. V., and Lam, J. S. (2000). Functional conservation of the polysaccharide biosynthetic protein WbpM and its homologues in *Pseudomonas aeruginosa* and other medically significant bacteria. *Infect. Immun.* 68, 931–936. doi: 10.1128/iai.68.2.931-936.2000

Butt, J., Romero-Hernández, B., Pérez-Butt, J., Blot, W. J., Teras, L. R., Visvanathan, K., et al. (2018). Antibody responses to *Streptococcus Gallolyticus* subspecies *Gallolyticus* proteins in a large prospective colorectal cancer cohort consortium. *Cancer Epidemiol. Biomark. Prev.* 27, 1186–1194. doi: 10.1158/1055-9965.EPI-18-0249

Butt, J., Romero-Hernández, B., Pérez-Gómez, B., Willhauck-Fleckenstein, M., Holzinger, D., Martin, V., et al. (2016). Association of *Streptococcus gallolyticus* subspecies *gallolyticus* with colorectal cancer: serological evidence. *Int. J. Cancer* 138, 1670–1679. doi: 10.1002/ijc.29914

Caccamo, P. D., and Brun, Y. V. (2018). The molecular basis of noncanonical bacterial morphology. *Trends Microbiol.* 26, 191–208. doi: 10.1016/j.tim.2017.09.012

Cárdenas-Mondragón, M. G., Ares, M. A., Panunzi, L. G., Pacheco, S., Camorlinga-Ponce, M., Girón, J. A., et al. (2016). Transcriptional profiling of type II toxin–antitoxin genes of *Helicobacter pylori* under different environmental conditions: identification of HP0967–HP0968 system. *Front. Microbiol.* 7:1872. doi: 10.3389/fmicb.2016.01872

Carron, M. A., Tran, V. R., Sugawa, C., and Coticchia, J. M. (2006). Identification of *Helicobacter pylori* biofilms in human gastric mucosa. *J. Gastrointest. Surg.* 10, 712–717. doi: 10.1016/j.gassur.2005.10.019

Cellini, L. (2014). *Helicobacter pylori*: a chameleon-like approach to life. *World J. Gastroenterol.* 20, 5575–5582. doi: 10.3748/wjg.v20.i19.5575

Cellini, L., Grande, R., Di Campli, E., Traini, T., Di Giulio, M., Lannutti, S. N., et al. (2008). Dynamic colonization of *Helicobacter pylori* in human gastric mucosa. *Scand. J. Gastroenterol.* 43, 178–185. doi: 10.1080/00365520701675965

Chan, W. Y., Hui, P. K., Leung, K. M., Chow, J., Kwok, F., and Ng, C. S. (1994). Coccoid forms of *Helicobacter pylori* in the human stomach. *Am. J. Clin. Pathol.* 102, 503–507.

Chaput, C., Ecobichon, C., Cayet, N., Girardin, S. E., Werts, C., Guadagnini, S., et al. (2006). Role of AmiA in the morphological transition of *Helicobacter pylori* and in immune escape. *PLoS Pathog.* 2:e97. doi: 10.1371/journal.ppat.0020097

Chaput, C., Ecobichon, C., Pouradier, N., Rousselle, J.-C., Namane, A., and Boneca, I. G. (2016). Role of the N-Acetylmuramoyl-l-Alanyl Amidase, AmiA, of *Helicobacter pylori* in peptidoglycan metabolism, daughter cell separation, and virulence. *Microb. Drug Resist.* 22, 477–486. doi: 10.1089/mdr.2016.0070

Chattopadhyay, S., Chi, P. B., Minin, V. N., Berg, D. E., and Sokurenko, E. V. (2018). Recombination-independent rapid convergent evolution of the gastric pathogen *Helicobacter pylori*. *BMC Genomics* 19:835. doi: 10.1186/s12864-018-5231-7

Chitcholtan, K., Hampton, M. B., and Keenan, J. I. (2008). Outer membrane vesicles enhance the carcinogenic potential of *Helicobacter pylori*. *Carcinogenesis* 29, 2400–2405. doi: 10.1093/carcin/bgn218

Cole, S. P., Harwood, J., Lee, R., She, R., and Guiney, D. G. (2004). Characterization of monospecies biofilm formation by *Helicobacter pylori*. *J. Bacteriol.* 186, 3124–3132. doi: 10.1128/jb.186.10.3124-3132.2004

Costa, K., Bacher, G., Allmaier, G., Dominguez-Bello, M. G., Engstrand, L., Falk, P., et al. (1999). The morphological transition of *Helicobacter pylori* cells from spiral to coccoid is preceded by a substantial modification of the cell wall. *J. Bacteriol.* 181, 3710–3715.

Costerton, J. W., Stewart, P. S., and Greenberg, E. P. (1999). Bacterial biofilms: a common cause of persistent infections. *Science* 284, 1318–1322. doi: 10.1126/science.284.5418.1318

Coticchia, J. M., Sugawa, C., Tran, V. R., Gurrola, J., Kowalski, E., and Carron, M. A. (2006). Presence and density of *Helicobacter pylori* biofilms in human gastric mucosa in patients with peptic ulcer disease. *J. Gastrointest. Surg.* 10, 883–889. doi: 10.1016/j.gassur.2005.12.009

Crawford, R. W., Reeve, K. E., and Gunn, J. S. (2010). Flagellated but not hyperfimbriated *Salmonella enterica* serovar typhimurium attaches to and forms biofilms on cholesterol-coated surfaces. *J. Bacteriol.* 192, 2981–2990. doi: 10.1128/jb.01620-09

Croxen, M. A., Sisson, G., Melano, R., and Hoffman, P. S. (2006). The *Helicobacter pylori* chemotaxis receptor TlpB (HP0103) is required for pH taxis and for colonization of the gastric mucosa. *J. Bacteriol.* 188, 2656–2665. doi: 10.1128/JB.188.7.2656-2665.2006

Danielli, A., and Scarlato, V. (2010). Regulatory circuits in *Helicobacter pylori*: network motifs and regulators involved in metal-dependent

responses. *FEMS Microbiol. Rev.* 34, 738–752. doi: 10.1111/j.1574-6976.2010.00233.x

Danne, C., Entenza, J. M., Mallet, A., Briandet, R., Debarbouille, M., Nato, F., et al. (2011). Molecular characterization of a *Streptococcus gallolyticus* genomic island encoding a pilus involved in endocarditis. *J. Infect. Dis.* 204, 1960–1970. doi: 10.1093/infdis/jir666

Das, A., Pereira, V., Saxena, S., Ghosh, T. S., Anbumani, D., Bag, S., et al. (2017). Gastric microbiome of Indian patients with *Helicobacter pylori* infection, and their interaction networks. *Sci. Rep.* 7:15438. doi: 10.1038/s41598-017-15510-6

De la Cruz, M. A., Ares, M. A., von Bargen, K., Panunzi, L. G., Martinez-Cruz, J., Valdez-Salazar, H. A., et al. (2017). Gene expression profiling of transcription factors of *Helicobacter pylori* under different environmental conditions. *Front. Microbiol.* 8:615. doi: 10.3389/fmicb.2017.00615

Dejea, C. M., Fathi, P., Craig, J. M., Boleij, A., Taddese, R., Geis, A. L., et al. (2018). Patients with familial adenomatous polyposis harbor colonic biofilms containing tumorigenic bacteria. *Science* 359, 592–597. doi: 10.1126/science.aah3648

Dejea, C. M., Wick, E. C., Hechenbleikner, E. M., White, J. R., Mark Welch, J. L., Rossetti, B. J., et al. (2014). Microbiota organization is a distinct feature of proximal colorectal cancers. *Proc. Natl. Acad. Sci. U.S.A.* 111, 18321–18326. doi: 10.1073/pnas.1406199111

del Castillo, E., Meier, R., Chung, M., Koestler, D. C., Chen, T., Paster, B. J., et al. (2019). The microbiomes of pancreatic and duodenum tissue overlap and are highly subject specific but differ between pancreatic cancer and noncancer subjects. *Cancer Epidemiol. Biomark. Prev.* 28, 370–383. doi: 10.1158/1055-9965.epi-18-0542

Di Domenico, E. G., Cavallo, I., Pontone, M., Toma, L., and Ensoli, F. (2017). Biofilm producing *Salmonella Typhi*: chronic colonization and development of gallbladder cancer. *Int. J. Mol. Sci.* 18:E1887. doi: 10.3390/ijms18091887

Dias-Jacome, E., Libanio, D., Borges-Canha, M., Galaghar, A., and Pimentel-Nunes, P. (2016). Gastric microbiota and carcinogenesis: the role of non-*Helicobacter pylori* bacteria - A systematic review. *Rev. Esp. Enferm. Dig.* 108, 530–540. doi: 10.17235/reed.2016.4261/2016

Doherty, N. C., Shen, F., Halliday, N. M., Barrett, D. A., Hardie, K. R., Winzer, K., et al. (2010). In *Helicobacter pylori*, LuxS is a key enzyme in cysteine provision through a reverse transsulfuration pathway. *J. Bacteriol.* 192, 1184–1192. doi: 10.1128/JB.01372-09

Donaldson, G. P., Ladinsky, M. S., Yu, K. B., Sanders, J. G., Yoo, B. B., Chou, W.-C., et al. (2018). Gut microbiota utilize immunoglobulin A for mucosal colonization. *Science* 360, 795–800. doi: 10.1126/science.aaq0926

Drewes, J. L., White, J. R., Dejea, C. M., Fathi, P., Iyadorai, T., Vadivelu, J., et al. (2017). High-resolution bacterial 16S rRNA gene profile meta-analysis and biofilm status reveal common colorectal cancer consortia. *NPJ Biofilms Microbiomes* 3:34. doi: 10.1038/s41522-017-0040-3

Edwards, A. M., Grossman, T. J., and Rudney, J. D. (2006). *Fusobacterium nucleatum* transports noninvasive *Streptococcus cristatus* into human epithelial cells. *Infect. Immun.* 74, 654–662. doi: 10.1128/IAI.74.1.654-662.2006

Elias, S., and Banin, E. (2012). Multi-species biofilms: living with friendly neighbors. *FEMS Microbiol. Rev.* 36, 990–1004. doi: 10.1111/j.1574-6976.2012.00325.x

Eppinger, M., Baar, C., Raddatz, G., Huson, D. H., and Schuster, S. C. (2004). Comparative analysis of four Campylobacterales. *Nat. Rev. Microbiol.* 2, 872–885. doi: 10.1038/nrmicro1024

Esson, D., Mather, A. E., Scanlan, E., Gupta, S., de Vries, S. P. W., Bailey, D., et al. (2016). Genomic variations leading to alterations in cell morphology of Campylobacter spp. *Sci. Rep.* 6:38303. doi: 10.1038/srep38303

Falush, D., Kraft, C., Taylor, N. S., Correa, P., Fox, J. G., Achtman, M., et al. (2001). Recombination and mutation during long-term gastric colonization by *Helicobacter pylor*: estimates of clock rates, recombination size, and minimal age. *Proc. Natl. Acad. Sci. U.S.A.* 98, 15056–15061. doi: 10.1073/pnas.251396098

Fazli, M., Almblad, H., Rybtke, M. L., Givskov, M., Eberl, L., and Tolker-Nielsen, T. (2014). Regulation of biofilm formation in *Pseudomonas* and *Burkholderia* species. *Environ. Microbiol.* 16, 1961–1981. doi: 10.1111/1462-2920.12448

Fernandez-Gonzalez, E., and Backert, S. (2014). DNA transfer in the gastric pathogen *Helicobacter pylori*. *J. Gastroenterol.* 49, 594–604. doi: 10.1007/s00535-014-0938-y

Fischer, W., Windhager, L., Rohrer, S., Zeiller, M., Karnholz, A., Hoffmann, R., et al. (2010). Strain-specific genes of *Helicobacter pylori*: genome evolution driven by a novel type IV secretion system and genomic island transfer. *Nucleic Acids Res.* 38, 6089–6101. doi: 10.1093/nar/gkq378

Flemer, B., Warren, R. D., Barrett, M. P., Cisek, K., Das, A., Jeffery, I. B., et al. (2018). The oral microbiota in colorectal cancer is distinctive and predictive. *Gut* 67, 1454–1463. doi: 10.1136/gutjnl-2017-314814

Flemming, H.-C., and Wingender, J. (2010). The biofilm matrix. *Nat. Rev. Microbiol.* 8, 623–633.

Flemming, H.-C., Wingender, J., Szewzyk, U., Steinberg, P., Rice, S. A., and Kjelleberg, S. (2016). Biofilms: an emergent form of bacterial life. *Nat. Rev. Microbiol.* 14, 563–575. doi: 10.1038/nrmicro.2016.94

Folsom, J. P., Richards, L., Pitts, B., Roe, F., Ehrlich, G. D., Parker, A., et al. (2010). Physiology of *Pseudomonas aeruginosa* in biofilms as revealed by transcriptome analysis. *BMC Microbiol.* 10:294. doi: 10.1186/1471-2180-10-294

Fulsundar, S., Kulkarni, H. M., Jagannadham, M. V., Nair, R., Keerthi, S., Sant, P., et al. (2015). Molecular characterization of outer membrane vesicles released from *Acinetobacter radioresistens* and their potential roles in pathogenesis. *Microb. Pathog.* 8, 12–22. doi: 10.1016/j.micpath.2015.04.005

Gabrilska, R. A., and Rumbaugh, K. P. (2015). Biofilm models of polymicrobial infection. *Future Microbiol.* 10, 1997–2015. doi: 10.2217/fmb.15.109

Garcia, A., Salas-Jara, M. J., Herrera, C., and Gonzalez, C. (2014). Biofilm and *Helicobacter pylori*: from environment to human host. *World J. Gastroenterol.* 20, 5632–5638. doi: 10.3748/wjg.v20.i19.5632

Ge, X., Cai, Y., Chen, Z., Gao, S., Geng, X., Li, Y., et al. (2018). Bifunctional enzyme SpoT is involved in biofilm formation of *Helicobacter pylori* with multidrug resistance by upregulating efflux pump Hp1174 (gluP). *Antimicrob. Agents Chemother.* 62:e00957-18. doi: 10.1128/AAC.00957-18

Goldsworthy, M. J. H. (2008). Gene expression of *Pseudomonas aeruginosa* and MRSA within a catheter-associated urinary tract infection biofilm model. *Biosci. Horiz.* 1, 28–37. doi: 10.1093/biohorizons/hzn008

Gölz, G., Sharbati, S., Backert, S., and Alter, T. (2012). Quorum sensing dependent phenotypes and their molecular mechanisms in *Campylobacterales*. *Eur. J. Microbiol. Immunol.* 2, 50–60. doi: 10.1556/EuJMI.2.2012.1.8

Gonzalez-Escobedo, G., and Gunn, J. S. (2013). Identification of *Salmonella enterica* serovar typhimurium genes regulated during biofilm formation on cholesterol gallstone surfaces. *Infect. Immun.* 81, 3770–3780. doi: 10.1128/iai.00647-13

Grande, R., Di Campli, E., Di Bartolomeo, S., Verginelli, F., Di Giulio, M., Baffoni, M., et al. (2012). *Helicobacter pylori* biofilm: a protective environment for bacterial recombination. *J. Appl. Microbiol.* 113, 669–676. doi: 10.1111/j.1365-2672.2012.05351.x

Grande, R., Di Marcantonio, M. C., Robuffo, I., Pompilio, A., Celia, C., Di Marzio, L., et al. (2015). *Helicobacter pylori* ATCC 43629/NCTC 11639 outer membrane vesicles (OMVs) from biofilm and planktonic phase associated with extracellular DNA (eDNA). *Front. Microbiol.* 6:1369. doi: 10.3389/fmicb.2015.01369

Grivennikov, S. I., Greten, F. R., and Karin, M. (2010). Immunity, inflammation, and cancer. *Cell* 140, 883–899. doi: 10.1016/j.cell.2010.01.025

Gupta, K. R., Baloni, P., Indi, S. S., and Chatterji, D. (2016). Regulation of Growth, Cell Shape, Cell Division, and Gene Expression by Second Messengers (p)ppGpp and Cyclic Di-GMP in *Mycobacterium smegmatis*. *J. Bacteriol.* 198, 1414–1422. doi: 10.1128/jb.00126-16

Hajishengallis, G., Liang, S., Payne, M. A., Hashim, A., Jotwani, R., Eskan, M. A., et al. (2011). A low-abundance biofilm species orchestrates inflammatory periodontal disease through the commensal microbiota and the complement pathway. *Cell Host Microbe* 10, 497–506. doi: 10.1016/j.chom.2011.10.006

Hall-Stoodley, L., Costerton, J. W., and Stoodley, P. (2004). Bacterial biofilms: from the Natural environment to infectious diseases. *Nat. Rev. Microbiol.* 2, 95–108. doi: 10.1038/nrmicro821

Hansen, S. K., Rainey, P. B., Haagensen, J. A. J., and Molin, S. (2007). Evolution of species interactions in a biofilm community. *Nature* 445, 533–536. doi: 10.1038/nature05514

Harshey, R. M. (2003). Bacterial motility on a surface: many ways to a common goal. *Annu. Rev. Microbiol.* 57, 249–273. doi: 10.1146/annurev.micro.57.030502.091014

Hasegawa, Y., Mark Welch, J. L., Rossetti, B. J., and Borisy, G. G. (2017). Preservation of three-dimensional spatial structure in the gut microbiome. *PLoS One* 12:e0188257. doi: 10.1371/journal.pone.0188257

Hathroubi, S., Servetas, S. L., Windham, I., Merrell, D. S., and Ottemann, K. M. (2018a). *Helicobacter pylori* biofilm formation and its potential role in pathogenesis. *Microbiol. Mol. Biol. Rev.* 82:e00001-18. doi: 10.1128/mmbr.00001-18

Hathroubi, S., Zerebinski, J., and Ottemann, K. M. (2018b). *Helicobacter pylori* biofilm involves a multigene stress-biased response, including a structural role for flagella. mBio 9:e1973-18. doi: 10.1128/mBio.01973-18

He, Y.-W., and Zhang, L.-H. (2008). Quorum sensing and virulence regulation in *Xanthomonas campestris*. *FEMS Microbiol. Rev.* 32, 842–857. doi: 10.1111/j.1574-6976.2008.00120.x

Hirukawa, S., Sagara, H., Kaneto, S., Kondo, T., Kiga, K., Sanada, T., et al. (2018). Characterization of morphological conversion of *Helicobacter pylori* under anaerobic conditions. *Microbiol. Immunol.* 62, 221–228. doi: 10.1111/1348-0421.12582

Ho, S. B., Shekels, L. L., Toribara, N. W., Kim, Y. S., Lyftogt, C., Cherwitz, D. L., et al. (1995). Mucin gene expression in normal, preneoplastic, and neoplastic human gastric epithelium. *Cancer Res.* 55, 2681–2690.

Howitt, M. R., Lee, J. Y., Lertsethtakarn, P., Vogelmann, R., Joubert, L.-M., Ottemann, K. M., et al. (2011). ChePep controls *Helicobacter pylori* infection of the gastric glands and chemotaxis in the Epsilonproteobacteria. *mBio* 2:e00098-11. doi: 10.1128/mBio.00098-11

Hussan, H., Clinton, S. K., Roberts, K., and Bailey, M. T. (2017). *Fusobacterium*'s link to colorectal neoplasia sequenced: a systematic review and future insights. *World J. Gastroenterol.* 23, 8626–8650. doi: 10.3748/wjg.v23.i48.8626

Jakobsen, T., Tolker-Nielsen, T., and Givskov, M. (2017). Bacterial biofilm control by perturbation of bacterial signaling processes. *Int. J. Mol. Sci.* 18:E1970. doi: 10.3390/ijms18091970

Jans, C., and Boleij, A. (2018). The road to infection: host-microbe interactions defining the pathogenicity of *Streptococcus bovis/Streptococcus equinus* complex members. *Front. Microbiol.* 9:603. doi: 10.3389/fmicb.2018.00603

Johansson, M. E. V., Gustafsson, J. K., Holmén-Larsson, J., Jabbar, K. S., Xia, L., Xu, H., et al. (2014). Bacteria penetrate the normally impenetrable inner colon mucus layer in both murine colitis models and patients with ulcerative colitis. *Gut* 63, 281–291. doi: 10.1136/gutjnl-2012-303207

Johansson, M. E. V., and Hansson, G. C. (2012). "Preservation of mucus in histological sections, immunostaining of mucins in fixed tissue, and localization of bacteria with FISH," in *Mucins: Methods and Protocols*, eds M. A. McGuckin and D. J. Thornton (Totowa, NJ: Humana Press), 229–235. doi: 10.1007/978-1-61779-513-8_13

Johansson, M. E. V., Phillipson, M., Petersson, J., Velcich, A., Holm, L., and Hansson, G. C. (2008). The inner of the two Muc2 mucin-dependent mucus layers in colon is devoid of bacteria. *Proc. Natl. Acad. Sci. U.S.A.* 105, 15064–15069. doi: 10.1073/pnas.0803124105

Jonkers, D., Gisbertz, I., De Bruine, A., Bot, F., Arends, J. W., Stobberingh, E., et al. (1997). *Helicobacter pylori* and non-*Helicobacter pylori* bacterial flora in gastric mucosal and tumour specimens of patients with primary gastric lymphoma. *Eur. J. Clin. Invest.* 27, 885–892. doi: 10.1046/j.1365-2362.1997.1940756.x

Kędzierska, B., and Hayes, F. (2016). Emerging roles of toxin-antitoxin modules in bacterial pathogenesis. *Molecules* 21:E790. doi: 10.3390/molecules21060790

Khosravi, Y., Dieye, Y., Loke, M. F., Goh, K. L., and Vadivelu, J. (2014). *Streptococcus mitis* induces conversion of *Helicobacter pylori* to coccoid cells during co-culture in vitro. *PLoS One* 9:e112214. doi: 10.1371/journal.pone.0112214

Khosravi, Y., Loke, M. F., Goh, K. L., and Vadivelu, J. (2016). Proteomics analysis revealed that crosstalk between *Helicobacter pylori* and *Streptococcus mitis* may enhance bacterial survival and reduces carcinogenesis. *Front. Microbiol.* 7:1462. doi: 10.3389/fmicb.2016.01462

Kim, H. S., Im, H. N., An, D. R., Yoon, J. Y., Jang, J. Y., Mobashery, S., et al. (2015). The cell shape-determining Csd6 protein from *Helicobacter pylori* constitutes a new family of L,D-Carboxypeptidase. *J. Biol. Chem.* 290, 25103–25117. doi: 10.1074/jbc.M115.658781

Kim, S. W., Oh, M. H., Jun, S. H., Jeon, H., Kim, S. I., Kim, K., et al. (2016). Outer membrane Protein A plays a role in pathogenesis of *Acinetobacter nosocomialis*. *Virulence* 7, 413–426. doi: 10.1080/21505594.2016.1140298

Kinder, S. A., and Holt, S. C. (1993). Localization of the *Fusobacterium nucleatum* T18 adhesin activity mediating coaggregation with *Porphyromonas gingivalis* T22. *J. Bacteriol.* 175, 840–850. doi: 10.1128/jb.175.3.840-850.1993

Kolenbrander, P. E., Andersen, R. N., and Moore, L. V. (1989). Coaggregation of *Fusobacterium nucleatum*, *Selenomonas flueggei, Selenomonas infelix, Selenomonas noxia*, and *Selenomonas sputigena* with strains from 11 genera of oral bacteria. *Infect. Immun.* 57, 3194–3203.

Kostakioti, M., Hadjifrangiskou, M., and Hultgren, S. J. (2013). Bacterial biofilms: development, dispersal, and therapeutic strategies in the dawn of the Postantibiotic Era. *Cold Spring Harb. Perspect. Med.* 3: a010306. doi: 10.1101/cshperspect.a010306

Krausse, R., Piening, K., and Ullmann, U. (2005). Inhibitory effects of various micro-organisms on the growth of *Helicobacter pylori*. *Lett. Appl. Microbiol.* 40, 81–86. doi: 10.1111/j.1472-765X.2004.01632.x

Krzyżek, P. (2017). Commentary: proteomics analysis revealed that crosstalk between *Helicobacter pylori* and *Streptococcus mitis* may enhance bacterial survival and reduces carcinogenesis. *Front. Microbiol.* 8:2381. doi: 10.3389/fmicb.2017.02381

Krzyzek, P., and Gosciniak, G. (2018). A proposed role for diffusible signal factors in the biofilm formation and morphological transformation of *Helicobacter pylori*. *Turk. J. Gastroenterol.* 29, 7–13. doi: 10.5152/tjg.2017.17349

Lamont, R. J., and Hajishengallis, G. (2015). Polymicrobial synergy and dysbiosis in inflammatory disease. *Trends Mol. Med.* 21, 172–183. doi: 10.1016/j.molmed.2014.11.004

Larsen, T., and Fiehn, N. E. (2017). Dental biofilm infections - an update. *APMIS* 125, 376–384. doi: 10.1111/apm.12688

Lertpiriyapong, K., Whary, M. T., Muthupalani, S., Lofgren, J. L., Gamazon, E. R., Feng, Y., et al. (2014). Gastric colonisation with a restricted commensal microbiota replicates the promotion of neoplastic lesions by diverse intestinal microbiota in the *Helicobacter pylori* INS-GAS mouse model of gastric carcinogenesis. *Gut* 63, 54–63. doi: 10.1136/gutjnl-2013-305178

Lertsethtakarn, P., Ottemann, K. M., and Hendrixson, D. R. (2011). Motility and chemotaxis in *Campylobacter* and *Helicobacter*. *Annu. Rev. Microbiol.* 65, 389–410. doi: 10.1146/annurev-micro-090110-102908

Lewis, K. (2005). Persister cells and the riddle of biofilm survival. *Biochemistry* 70, 267–274. doi: 10.1007/s10541-005-0111-6

Li, S., Konstantinov, S. R., Smits, R., and Peppelenbosch, M. P. (2017). Bacterial biofilms in colorectal cancer initiation and progression. *Trends Mol. Med.* 23, 18–30. doi: 10.1016/j.molmed.2016.11.004

Limoli, D. H., Jones, C. J., and Wozniak, D. J. (2015). Bacterial extracellular polysaccharides in biofilm formation and function. *Microbiol. Spectr.* 3. doi: 10.1128/microbiolspec.MB-0011-2014

Liu, W., Røder, H. L., Madsen, J. S., Bjarnsholt, T., Sørensen, S. J., and Burmølle, M. (2016). Interspecific bacterial interactions are reflected in multispecies biofilm spatial organization. *Front. Microbiol.* 7:1366. doi: 10.3389/fmicb.2016.01366

Liu, Z.-F., Chen, C.-Y., Tang, W., Zhang, J.-Y., Gong, Y.-Q., and Jia, J.-H. (2006). Gene-expression profiles in gastric epithelial cells stimulated with spiral and coccoid *Helicobacter pylori*. *J. Med. Microbiol.* 55, 1009–1015. doi: 10.1099/jmm.0.46456-0

Lofgren, J. L., Whary, M. T., Ge, Z., Muthupalani, S., Taylor, N. S., Mobley, M., et al. (2011). Lack of commensal flora in *H. pylori*-infected INS-GAS mice reduces gastritis and delays intraepithelial neoplasia. *Gastroenterology* 140, 210.e–220.e. doi: 10.1053/j.gastro.2010.09.048

Loh, J. T., Gupta, S. S., Friedman, D. B., Krezel, A. M., and Cover, T. L. (2010). Analysis of protein expression regulated by the *Helicobacter pylori* ArsRS two-component signal transduction system. *J. Bacteriol.* 192, 2034–2043. doi: 10.1128/JB.01703-08

Loke, M. F., Ng, C. G., Vilashni, Y., Lim, J., and Ho, B. (2016). Understanding the dimorphic lifestyles of human gastric pathogen *Helicobacter pylori* using the SWATH-based proteomics approach. *Sci. Rep.* 6:26784. doi: 10.1038/srep26784

Madsen, J. S., Burmølle, M., Hansen, L. H., and Sørensen, S. J. (2012). The interconnection between biofilm formation and horizontal gene transfer. *FEMS Immunol. Med. Microbiol.* 65, 183–195. doi: 10.1111/j.1574-695X.2012.00960.x

Magana, M., Sereti, C., Ioannidis, A., Mitchell, C. A., Ball, A. R., Magiorkinis, E., et al. (2018). Options and limitations in clinical investigation of bacterial biofilms. *Clin. Microbiol. Rev.* 31:e00084-16. doi: 10.1128/cmr.00084-16

Majumdar, S., and Pal, S. (2017). Bacterial intelligence: imitation games, time-sharing, and long-range quantum coherence. *J. Cell Commun. Signal.* 11, 281–284. doi: 10.1007/s12079-017-0394-6

Maldarelli, G. A., Piepenbrink, K. H., Scott, A. J., Freiberg, J. A., Song, Y., Achermann, Y., et al. (2016). Type IV pili promote early biofilm formation by *Clostridium difficile*. *Pathog. Dis.* 74:ftw061. doi: 10.1093/femspd/ftw061

Martins, M., Porrini, C., du Merle, L., Danne, C., Robbe-Masselot, C., Trieu-Cuot, P., et al. (2016). The Pil3 pilus of *Streptococcus gallolyticus* binds to intestinal mucins and to fibrinogen AU - Martins, Mariana. *Gut Microbes* 7, 526–532. doi: 10.1080/19490976.2016.1239677

Matsuda, K., Yamauchi, K., Matsumoto, T., Sano, K., Yamaoka, Y., and Ota, H. (2008). Quantitative analysis of the effect of *Helicobacter pylori* on the expressions of SOX2, CDX2, MUC2, MUC5AC, MUC6, TFF1, TFF2, and TFF3 mRNAs in human gastric carcinoma cells. *Scand. J. Gastroenterol.* 43, 25–33. doi: 10.1080/00365520701579795

Matsuo, K., Ota, H., Akamatsu, T., Sugiyama, A., and Katsuyama, T. (1997). Histochemistry of the surface mucous gel layer of the human colon. *Gut* 40, 782–789. doi: 10.1136/gut.40.6.782

Merino, J. S., Garcia, A., Pastene, E., Salas, A., Saez, K., and Gonzalez, C. L. (2018). Lactobacillus fermentum UCO-979C strongly inhibited *Helicobacter pylori* SS1 in Meriones unguiculatus. *Benef. Microbes* 9, 625–627. doi: 10.3920/bm2017.0160

Meyle, E., Brenner-Weiss, G., Obst, U., Prior, B., and Hänsch, G. M. (2012). Immune defense against *S. epidermidis* biofilms: components of the extracellular polymeric substance activate distinct bactericidal mechanisms of phagocytic cells. *Int. J. Artif. Organs* 35, 700–712. doi: 10.5301/ijao.5000151

Mika, F., and Hengge, R. (2013). Small regulatory RNAs in the control of motility and biofilm formation in *E. coli* and *Salmonella*. *Int. J. Mol. Sci.* 14:4560. doi: 10.3390/ijms14034560

Mitchell, G., Séguin, D. L., Asselin, A.-E., Déziel, E., Cantin, A. M., Frost, E. H., et al. (2010). *Staphylococcus aureus* sigma B-dependent emergence of small-colony variants and biofilm production following exposure to *Pseudomonas aeruginosa* 4-hydroxy-2-heptylquinoline-N- oxide. *BMC Microbiol.* 10:33. doi: 10.1186/1471-2180-10-33

Mot, R., and Vanderleyden, J. (1994). The C-terminal sequence conservation between OmpA-related outer membrane proteins and MotB suggests a common function in both Gram-positive and Gram-negative bacteria, possibly in the interaction of these domains with peptidoglycan. *Mol. Microbiol.* 12, 333–334. doi: 10.1111/j.1365-2958.1994.tb01021.x

Muñoz-Ramírez, Z. Y., Mendez-Tenorio, A., Kato, I., Bravo, M. M., Rizzato, C., Thorell, K., et al. (2017). Whole genome sequence and phylogenetic analysis show *Helicobacter pylori* strains from latin america have followed a unique evolution pathway. *Front. Cell. Infect. Microbiol.* 7:50. doi: 10.3389/fcimb.2017.00050

Musrati, A. A., Fteita, D., Paranko, J., Könönen, E., and Gürsoy, U. K. (2016). Morphological and functional adaptations of *Fusobacterium nucleatum* exposed to human neutrophil Peptide-1. *Anaerobe* 39, 31–38. doi: 10.1016/j.anaerobe.2016.02.008

Nascimento, R., Gouran, H., Chakraborty, S., Gillespie, H. W., Almeida-Souza, H. O., Tu, A., et al. (2016). The type II secreted lipase/esterase LesA is a key virulence factor required for *Xylella fastidiosa* Pathogenesis in Grapevines. *Sci. Rep.* 6:18598. doi: 10.1038/srep18598

Niv, Y. (2015). *Helicobacter pylori* and gastric mucin expression: a systematic review and meta-analysis. *World J. Gastroenterol.* 21, 9430–9436. doi: 10.3748/wjg.v21.i31.9430

Osaki, T., Hanawa, T., Manzoku, T., Fukuda, M., Kawakami, H., Suzuki, H., et al. (2006). Mutation of luxS affects motility and infectivity of *Helicobacter pylori* in gastric mucosa of a Mongolian gerbil model. *J. Med. Microbiol.* 55(Pt 11), 1477–1485. doi: 10.1099/jmm.0.46660-0

Oyarzabal, O. A., Rad, R., and Backert, S. (2007). Conjugative transfer of chromosomally encoded antibiotic resistance from *Helicobacter pylori* to *Campylobacter jejuni*. *J. Clin. Microbiol.* 45, 402–408. doi: 10.1128/jcm.01456-06

Pabst, B., Pitts, B., Lauchnor, E., and Stewart, P. S. (2016). Gel-Entrapped *Staphylococcus aureus* bacteria as models of biofilm infection exhibit growth in dense aggregates, oxygen limitation, antibiotic tolerance, and heterogeneous gene expression. *Antimicrob. Agents Chemother.* 60, 6294–6301. doi: 10.1128/aac.01336-16

Papenfort, K., and Bassler, B. L. (2016). Quorum sensing signal–response systems in Gram-negative bacteria. *Nat. Rev. Microbiol.* 14, 576–588. doi: 10.1038/nrmicro.2016.89

Parsons, B. N., Ijaz, U. Z., D'Amore, R., Burkitt, M. D., Eccles, R., Lenzi, L., et al. (2017). Comparison of the human gastric microbiota in hypochlorhydric states arising as a result of *Helicobacter pylori*-induced atrophic gastritis, autoimmune atrophic gastritis and proton pump inhibitor use. *PLoS Pathog.* 13:e1006653. doi: 10.1371/journal.ppat.1006653

Percival, S. L., and Suleman, L. (2014). Biofilms and *Helicobacter pylori*: dissemination and persistence within the environment and host. *World J. Gastrointest. Pathophysiol.* 5, 122–132. doi: 10.4291/wjgp.v5.i3.122

Persat, A., Nadell, C. D., Kim, M. K., Ingremeau, F., Siryaporn, A., Drescher, K., et al. (2015). The mechanical world of bacteria. *Cell* 161, 988–997. doi: 10.1016/j.cell.2015.05.005

Pinto, D., Santos, M. A., and Chambel, L. (2015). Thirty years of viable but nonculturable state research: unsolved molecular mechanisms. *Crit. Rev. Microbiol.* 41, 61–76. doi: 10.3109/1040841X.2013.794127

Pinzon-Guzman, C., Meyer, A. R., Wise, R., Choi, E., Muthupalani, S., Wang, T. C., et al. (2018). Evaluation of lineage changes in the gastric mucosa following infection with *Helicobacter pylori* and specified intestinal flora in INS-GAS mice. *J. Histochem. Cytochem.* 67:002215541878562. doi: 10.1369/0022155418785621

Plummer, M., de Martel, C., Vignat, J., Ferlay, J., Bray, F., and Franceschi, S. (2016). Global burden of cancers attributable to infections in 2012: a synthetic analysis. *Lancet Glob. Health* 4, e609–e616. doi: 10.1016/S2214-109X(16)30143-7

Poursina, F., Faghri, J., Moghim, S., Zarkesh-Esfahani, H., Nasr-Esfahani, B., Fazeli, H., et al. (2013). Assessment of *cagE* and *babA* mRNA expression during morphological conversion of *Helicobacter pylori* From spiral to coccoid. *Curr. Microbiol.* 66, 406–413. doi: 10.1007/s00284-012-0280-7

Poursina, F., Fagri, J., Mirzaei, N., and Safaei, H. G. (2018). Overexpression of spoT gene in coccoid forms of clinical *Helicobacter pylori* isolates. *Folia Microbiol.* 63, 459–465. doi: 10.1007/s12223-017-0557-0

Prigent-Combaret, C., Vidal, O., Dorel, C., and Lejeune, P. (1999). Abiotic surface sensing and biofilm-dependent regulation of gene expression in *Escherichia coli*. *J. Bacteriol.* 181, 5993–6002.

Proctor, R. A., von Eiff, C., Kahl, B. C., Becker, K., McNamara, P., Herrmann, M., et al. (2006). Small colony variants: a pathogenic form of bacteria that facilitates persistent and recurrent infections. *Nat. Rev. Microbiol.* 4, 295–305. doi: 10.1038/nrmicro1384

Psakis, G., Saidijam, M., Shibayama, K., Polaczek, J., Bettaney, K. E., Baldwin, J. M., et al. (2009). The sodium-dependent d-glucose transport protein of *Helicobacter pylori*. *Mol. Microbiol.* 71, 391–403. doi: 10.1111/j.1365-2958.2008.06535.x

Qaria, M. A., Kumar, N., Hussain, A., Qumar, S., Doddam, S. N., Sepe, L. P., et al. (2018). Roles of cholesteryl-α-glucoside transferase and cholesteryl glucosides in maintenance of *Helicobacter pylori* morphology, cell wall integrity, and resistance to antibiotics. *mBio* 9:e01523-18. doi: 10.1128/mBio.01523-18

Queralt, N., and Araujo, R. (2007). Analysis of the survival of *H. pylori* within a laboratory-based aquatic model system using molecular and classical techniques. *Microb. Ecol.* 54, 771–777. doi: 10.1007/s00248-007-9242-1

Rader, B. A., Campagna, S. R., Semmelhack, M. F., Bassler, B. L., and Guillemin, K. (2007). The quorum-sensing molecule autoinducer 2 regulates motility and flagellar morphogenesis in *Helicobacter pylori*. *J. Bacteriol.* 189, 6109–6117. doi: 10.1128/JB.00246-07

Rader, B. A., Wreden, C., Hicks, K. G., Sweeney, E. G., Ottemann, K. M., and Guillemin, K. (2011). *Helicobacter pylori* perceives the quorum-sensing molecule AI-2 as a chemorepellent via the chemoreceptor TlpB. *Microbiology* 157, 2445–2455. doi: 10.1099/mic.0.049353-0

Randal, B. R., Everett, M. L., Palestrant, D., Love, S. D., Lin, S. S., and Parker, W. (2003). Human secretory immunoglobulin A may contribute to biofilm formation in the gut. *Immunology* 109, 580–587. doi: 10.1046/j.1365-2567.2003.01700.x

Reis, C. A., David, L., Correa, P., Carneiro, F., Bolós, C. D., Garcia, E., et al. (1999). Intestinal metaplasia of human stomach displays distinct patterns of mucin (MUC1, MUC2, MUC5AC, and MUC6) expression. *Cancer Res.* 59, 1003–1007.

Roe, I. H., Son, S. H., Oh, H. T., Choi, J., Shin, J. H., Lee, J. H., et al. (1999). Changes in the evolution of the antigenic profiles and morphology during coccoid conversion of *Helicobacter pylori*. *Korean J. Intern. Med.* 14, 9–14. doi: 10.3904/kjim.1999.14.1.9

Römling, U., and Balsalobre, C. (2012). Biofilm infections, their resilience to therapy and innovative treatment strategies. *J. Intern. Med.* 272, 541–561. doi: 10.1111/joim.12004

Rubin, E. J., and Trent, M. S. (2013). Colonize, evade, flourish. *Gut Microbes* 4, 439–453. doi: 10.4161/gmic.25721

Ryan, R. P., An, S.-Q., Allan, J. H., McCarthy, Y., and Dow, J. M. (2015). The DSF family of cell–cell signals: an expanding class of bacterial virulence regulators. *PLoS Pathog.* 11:e1004986. doi: 10.1371/journal.ppat.1004986

Ryan, R. P., and Dow, J. M. (2011). Communication with a growing family: diffusible signal factor (DSF) signaling in bacteria. *Trends Microbiol.* 19, 145–152. doi: 10.1016/j.tim.2010.12.003

Salas-Jara, M. J., Sanhueza, E. A., Retamal-Diaz, A., Gonzalez, C., Urrutia, H., and Garcia, A. (2016). Probiotic *Lactobacillus fermentum* UCO-979C biofilm formation on AGS and Caco-2 cells and *Helicobacter pylori* inhibition. *Biofouling* 32, 1245–1257. doi: 10.1080/08927014.2016.1249367

Sanduleanu, S., Jonkers, D., De Bruine, A., Hameeteman, W., and Stockbrügger, R. W. (2001). Non-*Helicobacter pylori* bacterial flora during acid-suppressive therapy: differential findings in gastric juice and gastric mucosa. *Aliment. Pharmacol. Ther.* 15, 379–388. doi: 10.1046/j.1365-2036.2001.00888.x

Saunders, N. J., Boonmee, P., Peden, J. F., and Jarvis, S. A. (2005). Inter-species horizontal transfer resulting in core-genome and niche-adaptive variation within *Helicobacter pylori*. *BMC Genomics* 6:9. doi: 10.1186/1471-2164-6-9

Schauder, S., Shokat, K., Surette, M. G., and Bassler, B. L. (2001). The LuxS family of bacterial autoinducers: biosynthesis of a novel quorum-sensing signal molecule. *Mol. Microbiol.* 41, 463–476. doi: 10.1046/j.1365-2958.2001.02532.x

Segal, E. D., Falkow, S., and Tompkins, L. S. (1996). *Helicobacter pylori* attachment to gastric cells induces cytoskeletal rearrangements and tyrosine phosphorylation of host cell proteins. *Proc. Natl. Acad. Sci. U.S.A.* 93, 1259–1264. doi: 10.1073/pnas.93.3.1259

Senkovich, O. A., Yin, J., Ekshyyan, V., Conant, C., Traylor, J., Adegboyega, P., et al. (2011). *Helicobacter pylori* AlpA and AlpB bind host laminin and influence gastric inflammation in gerbils. *J. Infect. Immun.* 79, 3106–3116. doi: 10.1128/IAI.01275-10

Servetas, S. L., Carpenter, B. M., Haley, K. P., Gilbreath, J. J., Gaddy, J. A., and Merrell, D. S. (2016). Characterization of key *Helicobacter pylori* regulators identifies a role for ArsRS in biofilm formation. *J. Bacteriol.* 198, 2536–2548. doi: 10.1128/jb.00324-16

Servetas, S. L., Doster, R. S., Kim, A., Windham, I. H., Cha, J.-H., Gaddy, J. A., et al. (2018). ArsRS-dependent regulation of homB contributes to *Helicobacter pylori* biofilm formation. *Front. Microbiol.* 9:1497. doi: 10.3389/fmicb.2018.01497

Sheh, A., and Fox, J. G. (2013). The role of the gastrointestinal microbiome in *Helicobacter pylori* pathogenesis. *Gut Microbes* 4, 505–531. doi: 10.4161/gmic.26205

Shen, F., Hobley, L., Doherty, N., Loh, J. T., Cover, T. L., Sockett, R. E., et al. (2010). In *Helicobacter pylori* auto-inducer-2, but not LuxS/MccAB catalysed reverse transsulphuration, regulates motility through modulation of flagellar gene transcription. *BMC Microbiol.* 10:210. doi: 10.1186/1471-2180-10-210

Shen, Z., Dzink-Fox, J., Wilson, K. T., Whary, M. T., Muthupalani, S., Piazuelo, M. B., et al. (2018). Tu1288 - co-colonization of *Helicobacter Pylori* with *Staphylococcus Epidermidis* or *Streptococcus Salivarius* differ in the progression of gastritis in ins-gas mice. *Gastroenterology* 154(6, Suppl. 1), S–924–S–925. doi: 10.1016/S0016-5085(18)33114-7

Sigal, M., Rothenberg, M. E., Logan, C. Y., Lee, J. Y., Honaker, R. W., Cooper, R. L., et al. (2015). *Helicobacter pylori* activates and expands Lgr5+ stem cells through direct colonization of the gastric glands. *Gastroenterology* 148, 1392.e–1404.e. doi: 10.1053/j.gastro.2015.02.049

Soto, S. M. (2013). Role of efflux pumps in the antibiotic resistance of bacteria embedded in a biofilm. *Virulence* 4, 223–229. doi: 10.4161/viru.23724

Stark, R. M., Gerwig, G. J., Pitman, R. S., Potts, L. F., Williams, N. A., Greenman, J., et al. (1999). Biofilm formation by *Helicobacter pylori*. *Lett. Appl. Microbiol.* 28, 121–126. doi: 10.1046/j.1365-2672.1999.00481.x

Stewart, P. S. (2015). Antimicrobial tolerance in biofilms. *Microbiol. Spectr.* 3. doi: 10.1128/microbiolspec.MB-0010-2014

Suerbaum, S., Smith, J. M., Bapumia, K., Morelli, G., Smith, N. H., Kunstmann, E., et al. (1998). Free recombination within *Helicobacter pylori*. *Proc. Natl. Acad. Sci. U.S.A.* 95, 12619–12624. doi: 10.1073/pnas.95.21.12619

Sun, J., and Kato, I. (2016). Gut microbiota, inflammation and colorectal cancer. *Genes Dis.* 3, 130–143. doi: 10.1016/j.gendis.2016.03.004

Sun, Y., Li, X., Li, W., Zhao, M., Wang, L., Liu, S., et al. (2012).). Proteomic analysis of the function of spot in *Helicobacter pylori* anti-oxidative stress *in vitro* and colonization *in vivo*. *J. Cell. Biochem.* 113, 3393–3402. doi: 10.1002/jcb.24215

Susanne, M., Philippe, F., Eva, M., Birgit, P., Gertrud, M. H., and Ulrike, D. (2015). Activation of neutrophils by the extracellular polymeric substance of *S.epidermidis* biofilms is mediated by the bacterial heat shock protein Groel. *J. Biotechnol. Biomater.* 5:176. doi: 10.4172/2155-952x.1000176

Swidsinski, A., Weber, J., Loening-Baucke, V., Hale, L. P., and Lochs, H. (2005). Spatial organization and composition of the mucosal flora in patients with inflammatory bowel disease. *J. Clin. Microbiol.* 43, 3380–3389. doi: 10.1128/jcm.43.7.3380-3389.2005

Sycuro, L. K., Pincus, Z., Gutierrez, K. D., Biboy, J., Stern, C. A., Vollmer, W., et al. (2010). Peptidoglycan crosslinking relaxation promotes *Helicobacter pylori*'s helical shape and stomach colonization. *Cell* 141, 822–833. doi: 10.1016/j.cell.2010.03.046

Sycuro, L. K., Rule, C. S., Petersen, T. W., Wyckoff, T. J., Sessler, T., Nagarkar, D. B., et al. (2013). Flow cytometry-based enrichment for cell shape mutants identifies multiple genes that influence *Helicobacter pylori* morphology. *Mol. Microbiol.* 90, 869–883. doi: 10.1111/mmi.12405

Sycuro, L. K., Wyckoff, T. J., Biboy, J., Born, P., Pincus, Z., Vollmer, W., et al. (2012). Multiple peptidoglycan modification networks modulate *Helicobacter pylori*'s cell shape, motility, and colonization potential. *PLoS Pathog.* 8:e1002603. doi: 10.1371/journal.ppat.1002603

Tan, S., Noto, J. M., Romero-Gallo, J., Peek, R. M. Jr., and Amieva, M. R. (2011). *Helicobacter pylori* perturbs iron trafficking in the epithelium to grow on the cell surface. *PLoS Pathog.* 7:e1002050. doi: 10.1371/journal.ppat.1002050

Tannæs, T., Dekker, N., Bukholm, G., Bijlsma, J. J. E., and Appelmelk, B. J. (2001). Phase variation in the *Helicobacter pylori* phospholipase a gene and its role in acid adaptation. *Infect. Immun.* 69, 7334–7340. doi: 10.1128/iai.69.12.7334-7340.2001

Tomb, J.-F., White, O., Kerlavage, A. R., Clayton, R. A., Sutton, G. G., Fleischmann, R. D., et al. (1997). The complete genome sequence of the gastric pathogen *Helicobacter pylori*. *Nature* 388, 539–547.

Tsang, J., and Hoover, T. R. (2014). Themes and variations: regulation of RpoN-dependent flagellar genes across diverse bacterial species. *Scientifica* 2014:681754. doi: 10.1155/2014/681754

Turner, L., Praszkier, J., Hutton, M. L., Steer, D., Ramm, G., Kaparakis-Liaskos, M., et al. (2015). Increased outer membrane vesicle formation in a *Helicobacter pylori tolB* mutant. *Helicobacter* 20, 269–283. doi: 10.1111/hel.12196

van Teeseling, M. C. F., de Pedro, M. A., and Cava, F. (2017). Determinants of bacterial morphology: from fundamentals to possibilities for antimicrobial targeting. *Front. Microbiol.* 8:1264. doi: 10.3389/fmicb.2017.01264

Watters, C., Fleming, D., Bishop, D., and Rumbaugh, K. P. (2016). Host responses to biofilm. *Prog. Mol. Biol. Transl. Sci.* 142, 193–239. doi: 10.1016/bs.pmbts.2016.05.007

Welch, K., Cai, Y., and Strømme, M. (2012). A method for quantitative determination of biofilm viability. *J. Funct. Biomater.* 3, 418–431. doi: 10.3390/jfb3020418

Wiese, M., Eljaszewicz, A., Helmin-Basa, A., Andryszczyk, M., Motyl, I., Wieczyska, J., et al. (2015). Lactic acid bacteria strains exert immunostimulatory effect on *H. pylori*-induced dendritic cells. *J. Immunol. Res.* 2015:106743. doi: 10.1155/2015/106743

Wilson, C., Lukowicz, R., Merchant, S., Valquier-Flynn, H., Caballero, J., Sandoval, J., et al. (2017). Quantitative and qualitative assessment methods for biofilm growth: a mini-review. *Res. Rev. J. Eng. Technol.* 6.

Windham, I. H., Servetas, S. L., Whitmire, J. M., Pletzer, D., Hancock, R. E. W., and Merrell, D. S. (2018). *Helicobacter pylori* biofilm formation is differentially affected by common culture conditions, and proteins play a central role in the biofilm matrix. *Appl. Environ. Microbiol.* 84:e00391-18. doi: 10.1128/aem.00391-18

Wolska, K. I., Grudniak, A. M., Rudnicka, Z., and Markowska, K. (2016). Genetic control of bacterial biofilms. *J. Appl. Genet.* 57, 225–238. doi: 10.1007/s13353-015-0309-2

Wong, E. H. J., Ng, C. G., Chua, E. G., Tay, A. C. Y., Peters, F., Marshall, B. J., et al. (2016). Comparative genomics revealed multiple *helicobacter pylori* genes associated with biofilm formation in vitro. *PLoS One* 11:e0166835. doi: 10.1371/journal.pone.0166835

Wong, E. H. J., Ng, C. G., Goh, K. L., Vadivelu, J., Ho, B., and Loke, M. F. (2018). Metabolomic analysis of low and high biofilm-forming *Helicobacter pylori* strains. *Sci. Rep.* 8:1409. doi: 10.1038/s41598-018-19697-0

Yamashita, S., Igarashi, M., Hayashi, C., Shitara, T., Nomoto, A., Mizote, T., et al. (2015). Identification of self-growth-inhibiting compounds lauric acid and 7-(Z)-tetradecenoic acid from *Helicobacter pylori*. *Microbiology* 161, 1231–1239. doi: 10.1099/mic.0.000077

Yang, F.-L., Hassanbhai, A. M., Chen, H.-Y., Huang, Z.-Y., Lin, T.-L., Wu, S.-H., et al. (2011). Proteomannans in biofilm of *Helicobacter pylori* ATCC 43504. *Helicobacter* 16, 89–98. doi: 10.1111/j.1523-5378.2010.00815.x

Yonezawa, H., Osaki, T., Fukutomi, T., Hanawa, T., Kurata, S., Zaman, C., et al. (2017). Diversification of the AlpB outer membrane protein of *Helicobacter pylori* affects biofilm formation and cellular adhesion. *J. Bacteriol.* 199:e00729-16. doi: 10.1128/JB.00729-16

Yonezawa, H., Osaki, T., Hanawa, T., Kurata, S., Ochiai, K., and Kamiya, S. (2013). Impact of *Helicobacter pylori* biofilm formation on clarithromycin susceptibility and generation of resistance mutations. *PLoS One* 8:e73301. doi: 10.1371/journal.pone.0073301

Yonezawa, H., Osaki, T., Kurata, S., Fukuda, M., Kawakami, H., Ochiai, K., et al. (2009). Outer membrane vesicles of *Helicobacter pylori* TK1402 are involved in biofilm formation. *BMC Microbiol.* 9:197. doi: 10.1186/1471-2180-9-197

Yonezawa, H., Osaki, T., Kurata, S., Zaman, C., Hanawa, T., and Kamiya, S. (2010). Assessment of *in vitro* biofilm formation by *Helicobacter pylori*. *J. Gastroenterol. Hepatol.* 25, S90–S94. doi: 10.1111/j.1440-1746.2009.06213.x

Yu, G., Torres, J., Hu, N., Medrano-Guzman, R., Herrera-Goepfert, R., Humphrys, M. S., et al. (2017). Molecular characterization of the human stomach microbiota in gastric cancer patients. *Front. Cell. Infect. Microbiol.* 7:302. doi: 10.3389/fcimb.2017.00302

Zeng, L., Zhang, L., Wang, P., and Meng, G. (2017). Structural basis of host recognition and biofilm formation by *Salmonella* Saf pili. *eLife* 6:e28619. doi: 10.7554/eLife.28619

Conflict of Interest Statement: The authors declare that the research was conducted in the absence of any commercial or financial relationships that could be construed as a potential conflict of interest.

frontiers in Microbiology

ORIGINAL RESEARCH
published: 07 May 2019
doi: 10.3389/fmicb.2019.01008

Chemotherapy Alters the Phylogenetic Molecular Ecological Networks of Intestinal Microbial Communities

*Jing Cong[1,2], Jingjuan Zhu[1], Chuantao Zhang[1], Tianjun Li[1], Kewei Liu[1], Dong Liu[1,2], Na Zhou[1,2], Man Jiang[1,2], Helei Hou[1,2] and Xiaochun Zhang[1,2]**

[1] Department of Medical Oncology, The Affiliated Hospital of Qingdao University, Qingdao University, Qingdao, China, [2] Cancer Institute, Qingdao, China

Intestinal microbiota is now widely known to play key roles in nutritional uptake, metabolism, and regulation of human immune responses. There are multiple studies assessing intestinal microbiota changes in response to chemotherapy. In this study, microbial phylogenetic molecular ecological networks (pMENs) were firstly used to study the effects of chemotherapy on the intestinal microbiota of colorectal cancer (CRC) patients. Based on the random network model, we demonstrated that overall network structures and properties were significantly changed by chemotherapy, especially in average path length, average clustering coefficient, average harmonic geodesic distance and modularity ($P < 0.05$). The taxa in the module tended to co-exclude rather than co-occur in CRC patient networks, indicating probably competition relationships. The co-exclude correlations were decreased by 37.3% from T0 to T5 in response to chemotherapy. Significantly negative correlations were observed in positive/negative OTU degree and tumor markers ($P < 0.05$). Furthermore, the topological roles of the OTUs (module hubs and connectors) were changed with the chemotherapy. For example, the OTU167, OTU8, and OTU9 from the genera *Fusobacterium*, *Bacteroides*, and *Faecalibacterium*, respectively, were identified as keystone taxa, which were defined as either "hubs" or OTUs with highest connectivity in the network. These OTUs were significantly correlated with tumor markers ($P < 0.05$), suggesting that they probably were influenced by chemotherapy. The pMENs constructed in this study predicted the potential effects of chemotherapy on intestinal microbial community co-occurrence interactions. The changes may have an effect on the therapeutic effects. However, larger clinical samples are required to identify the conclusion.

Keywords: intestinal microbiota, phylogenetic molecular ecological networks, high-throughput sequencing, chemotherapy, colorectal cancer

OPEN ACCESS

Edited by:
Nezar Al-hebshi, Temple University, United States

Reviewed by:
Yuji Naito, Kyoto Prefectural University of Medicine, Japan
Leah M. Pyter, The Ohio State University, United States

****Correspondence:***
Xiaochun Zhang
zhangxiaochun9670@126.com

Specialty section:
This article was submitted to Systems Microbiology, a section of the journal Frontiers in Microbiology

Received: *30 November 2018*
Accepted: *23 April 2019*
Published: *07 May 2019*

Citation:
Cong J, Zhu J, Zhang C, Li T, Liu K, Liu D, Zhou N, Jiang M, Hou H and Zhang X (2019) Chemotherapy Alters the Phylogenetic Molecular Ecological Networks of Intestinal Microbial Communities. Front. Microbiol. 10:1008. doi: 10.3389/fmicb.2019.01008

INTRODUCTION

Colorectal cancer (CRC) is a major killer of people around the world despite continuing medical advances on several fronts. Chemotherapy continues to be the mainstay therapy for most CRC patients, and the related treatment response is unpredictable. Personalized cancer therapies are now emerging, and targeted therapies have promoted revolutionary outcomes in CRC (Mirnezami et al., 2012). However, novel problems such as idiosyncratic adverse effects, acquired resistance and high costs are still present (Kantarjian et al., 2013; Welsh et al., 2016). Recent studies have

implicated intestinal microbiota at the species level in influencing the drug response and toxicity of CRC patients (Haiser et al., 2013). Drug metabolism by intestinal microbiota has been well recognized since the 1960s (Scheline, 1968). Intestinal microbiota plays a key role in confirming the efficacy and toxicity of a broad range of drugs (Li et al., 2016). With the development of high-throughput sequencing, the importance of intestinal microbiota for drug modulation and discovery is increasingly recognized (Jia et al., 2008). Scott et al. (2017) reported that intestinal microbiota influenced fluoropyrimidines, which are the first-line treatment for CRC through drug interconversion involving bacterial vitamin B6 and B9 and ribonucleotide metabolism. Guthrie et al. (2017) suggested that metagenomic mining of the microbiome, which is associated with metabolomics, was considered as a non-invasive approach to develop biomarkers for CRC treatment outcomes. As a consequence, intestinal microbiota can be leveraged for therapeutic interventions (Ross et al., 2016) and to improve therapeutic effects (Wallace et al., 2010).

Microbes coexist in complex environments in which interactions among individuals are indispensable for community assembly and ecosystem function (Fuhrman, 2009; Hallam and Mccutcheon, 2015). However, few studies have explored the interactions among intestinal microbiota or determined which individuals share niches within the intestinal environment. Therefore, identifying and defining the interactions that occur among intestinal microbiota contributes to understanding the role of intestinal microbiota to provide a possibility for better therapeutic interventions. Molecular ecological network analysis provides a promising future for exploring the dynamics of microbial interactions and niches (Faust and Raes, 2012). In recent years, molecular ecological network analysis has been used as a tool to determine complex microbial assemblages in various environments such as in humans (Faust et al., 2012), groundwater (Deng et al., 2016), and soil (Jing et al., 2015). Network analysis can identify putative keystone taxa that are important for maintaining community structure and function (Power et al., 1996).

To identify intestinal microbial assemblages that potentially interact with or share niches within the intestine, we constructed the phylogenetic molecular ecological networks (pMENs) for healthy volunteers and CRC patients during the chemotherapy based on the 16S rRNA sequencing data (Deng et al., 2012). We studied intestinal microbiota using fecal samples from CRC patients and healthy volunteers. High-throughput sequencing of 16S rRNA gene amplicons was used to describe the intestinal bacterial assemblages. We mainly examined the changes in intestinal microbiota during the treatment based on the pMENs. The following research questions were addressed based on the intestinal microbial phylogenetic data: (i) whether chemotherapy affects the intestinal microbial molecular network structure, (ii) what the potential "keystone taxa" in the network are and how they change in response to chemotherapy, and (iii) what the relationships are among key OTUs in the network and clinical variables. Our work identifies a previously undocumented dimension of intestinal microbiota and offers insights into the species-species interaction networks of intestinal microbiota associated with CRC patients in response to chemotherapy.

MATERIALS AND METHODS

Experiment Description

Twenty-two CRC patients from the Affiliated Hospital of Qingdao University (Qingdao, China), aged 34–73 years, were enrolled in our study (**Table 1**). This study was selected based on the histopathological diagnosis of primary CRC, newly diagnosed and untreated, and no history of other tumors. Twenty-one healthy volunteers, aged 27–64 years, were selected as controls. During a routine physical examination, all the participants who had used antibiotics within the past 2 months or were regularly using non-steroidal anti-inflammatory drugs, probiotics, or statins before sampling, were excluded from the study. Other exclusions included chronic bowel disease, food allergies, dietary restrictions, and other signs of infections. Based on the national comprehensive cancer network (NCCN) guidelines, the CRC patients were treated with standard chemotherapy, and follow-up samples were obtained from CRC patients before the treatment of every stage. The interval time between two treatments is about 21 $\pm$ 3 days. However, individuals had different starting time at the first chemotherapy. The sampling time followed the treatment time for about six times. In total, 123 fecal samples from the CRC patients and 21 fecal samples from healthy individuals were collected. The demographic, clinical and technical details of study subjects were shown in **Table 1** and **Supplementary Table S1**. All these participants had been local residents of Qingdao city for more than 5 years. This study was approved by the Ethics Committee of the Affiliated Hospital of Qingdao University and all study participants gave written informed consent before participation. These fresh fecal samples from healthy individuals were collected into 5 ml tubes in the morning at home. Then they were sent into our lab within 3 h after defecation, and were reserved by ice bag during the transportation, and were immediately frozen at −80°C. These samples from CRC patients were collected in the morning in the hospital, then they were immediately frozen at −80°C after defecation until the day of analysis. The collected samples from the healthy individuals and CRC patients were named by H and T, respectively. In addition, these samples from CRC patients before the first chemotherapy, before the second chemotherapy, before the third chemotherapy, before the fourth chemotherapy, and before the fifth chemotherapy were named by T0, T1, T2, T3, T4, and T5, respectively.

DNA Extraction, Purification, Sequencing, and Data Processing

Microbial DNA was extracted from fecal samples with the QIAamp Fast DNA Stool Mini Kit as previously reported (Wu et al., 2016). The freshly extracted DNA was purified by 1% melting point agarose gel followed by phenol chloroform-butanol extraction. The V3-V4 region of the 16S rRNA gene from each sample was amplified by the bacterial universal primers (forward primer, 5′-ACTCCTACGGGRSGCAGCAG-3′, and reverse primer, 5′-GGACTACVVGGGTATCTAATC-3′). PCR amplification was performed in a 30 μl reaction containing 15 μl 2 × KAPA HiFi Hotstart ReadyMix, 10 ng template

DNA, 1 μl of each primer (forward and reverse primers), and ddH_2O. The reaction mixtures were amplified using the following conditions: denaturation at 95°C for 1 min; 12 cycles of 98°C for 15 s, 72°C for 10 s, 94°C for 20 s, 65°C for 10 s, and 72°C for 10 s; 11 cycles of 94°C for 20 s, 58°C for 30 s, and 72°C for 30 s; and a final extension at 72°C for 150 s. The PCR amplification products were purified using an AxyPrep DNA Gel Extraction Kit (Axygen, United States), eluted in 30 μl water, and aliquoted into three PCR tubes. DNA quality and quantity were assessed by the 260/280 and 260/230 nm ratios, and the final DNA contents were quantified with a Qubit® dsDNA HS Assay Kit (Invitrogen, United States). Finally, we sequenced the bacterial DNA amplicons from each fecal sample using an Illumina Hiseq 2500.

Raw sequences were separated into samples by barcodes. After raw data quality control, the clean reads were first sorted by abundance from large to small, followed by the removal of singletons. Using the Usearch software, the reads were clustered and chimeras were removed based on 97% standard similarity. The reads from each sample were randomly pumped to extract the corresponding Operational Taxonomic Unit (OTU) sequences. Each OTU is considered to represent a species. The taxonomic assignment was performed by the ribosomal database project (RDP) classifier (Wang et al., 2007). Random resampling was conducted on 39,796 sequences per fecal sample.

Network Construction and Analysis

In this study, we took 22 CRC patients and 21 healthy individuals as biological replicates to infer the possible co-occurrence relationship between intestinal microbes in response to chemotherapy. Networks were constructed for intestinal microbiota based on the OTU relative abundance. Each stage of chemotherapy was considered as one treatment/group. Only OTUs detected in more than 50% of replicate samples in each group were used for network construction. The microbial phylogenetic data were converted to a similarity matrix. The similarity matrix measures the degree of concordance between the abundance of OTUs across various samples by obtaining the absolute values of the Pearson correlation matrix (Horvath and Dong, 2008). The microbial communities can be predicted by the Poisson distribution, which reflects the non-random properties, system-specific of a complex system, and the Gaussian orthogonal ensemble (GOE) statistics, which is involved in the random properties of a complex system (Luo et al., 2007). The random matrix theory (RMT), which is a reliable, sensitive and robust tool for analyzing high-throughput genomics data (Deng et al., 2012), was used to automatically determine the appropriate similarity threshold (St) for identifying modular networks and elucidating network interactions. The St represents the minimal strength of the connections between each pair of nodes (Zhou et al., 2011). Subsequently, an adjacency matrix was derived from the similarity matrix based on the St (Luo et al., 2007). These transitions are indicated by the existence of the same St (**Table 2**). Global network properties were characterized according to previous research (Deng et al., 2012). Modules reflect divergent selection regimes, clusters of phylogenetically and closely related species, habitat heterogeneity and the key unit of species co-evolution (Olesen et al., 2007). Modularity is used to demonstrate a network that is naturally divided into distinct sub-groups (Deng et al., 2012). The average degree represents the complexity of the network. Harmonic geodesic distance represents the state (close or dispersive) of the nodes in the network. The average clustering coefficient describes how well a node is linked to its neighbors. The modular topological roles are explained by peripherals, connectors, module hubs and network hubs, which are defined by two parameters, the within-module connectivity (*Zi*) and among-module connectivity (*Pi*) (Deng et al., 2012; Jing et al., 2015). The *Zi* reflects how close a node is connected to other nodes within its own module, and *Pi* describes how close a node contacts with different modules. Module hubs have the nodes with $Pi \leq 0.62$ and $Zi > 2.5$, connectors with $Pi > 0.62$ and $Zi \leq 2.5$, and network hubs with $Pi > 0.62$ and $Zi > 2.5$, peripheral nodes with $Pi \leq 0.62$ and $Zi \leq 2.5$. In an ecological perspective, peripherals tend to have the role of specialists, whereas connectors and module hubs are considered as generalists and network hubs as super-generalists (Olesen et al., 2007).

In the RMT-based molecular ecological network approach, the phylogenetic molecular ecological networks constructed should be ensured that the co-occurrence patterns are statistically significant rather than a random process (Zhou et al., 2011). Only one network was constructed by combining 21/22 samples under each group; therefore, we cannot compare the network indices between CRC patients with chemotherapy and healthy individuals statistically. Thus, random networks were generated to assess the significance of network indices based on a null

TABLE 1 | Summary information of individuals in this study (Fecal sample's demographic, clinical, and technical details).

Group	Healthy volunteers	Colorectal cancers patients	*P* value	Sample collection	Sequencing platform
Sample size	21	22	NA	Prior to each treatment	Sequencing Platform: Illumina Hiseq PE250; Sequencing Target Depth: 5 GB; read length: 500 bp
Male/Female	4/17	14/8	0.003		
Age, year, median	54 (26–64)	57 (34–73)	0.098		
BMI, median	23.2	23.4	0.913		

TABLE 2 | Topological properties of the empirical molecular ecological networks (MENs) of intestinal microbial community from healthy individuals and colorectal cancer (CRC) patients during the different treatment stages and their associated random MENs.

Sample		H	T0	T1	T2	T3	T4	T5
Empirical Network	No. of original OTU[a]	655	778	727	793	814	788	758
	Network size[b]	105	99	102	103	80	103	103
	Total links	110	238	228	239	173	210	231
	Average degree	2.095	4.808	4.471	4.641	4.325	4.078	4.485
	Average path distance	5.942[d]	2.893[d]	2.982[d]	3.216[d]	3.403[d]	3.701[d]	3.210[d]
	Average clustering coefficient	0.07[e]	0.191[e]	0.209[e]	0.175[e]	0.140[e]	0.119[e]	0.240[e]
	Average harmonic geodesic distance	4.165[f]	2.488[f]	2.539[f]	2.759[f]	2.717[f]	3.022[f]	2.668[f]
	Identical threshold	0.660	0.660	0.660	0.660	0.660	0.660	0.660
	R^2 of power-law	0.786	0.794	0.724	0.821	0.808	0.861	0.870
	Modularity	0.773[g]	0.429[g]	0.450[g]	0.475[g]	0.405[g]	0.500[g]	0.498[g]
Random networks[c]	Average path distance	5.584 ± 0.467	2.693 ± 0.045	2.705 ± 0.047	3.02 ± 0.052	2.883 ± 0.068	3.228 ± 0.069	3.022 ± 0.064
	Average clustering coefficient	0.014 ± 0.010	0.209 ± 0.025	0.200 ± 0.024	0.101 ± 0.018	0.139 ± 0.022	0.077 ± 0.017	0.102 ± 0.018
	Average harmonic geodesic distance	4.318 ± 0.254	2.401 ± 0.026	2.415 ± 0.026	2.635 ± 0.031	2.509 ± 0.042	2.803 ± 0.043	2.647 ± 0.039
	Modularity	0.731 ± 0.015	0.355 ± 0.010	0.381 ± 0.010	0.393 ± 0.011	0.380 ± 0.011	0.434 ± 0.012	0.396 ± 0.011

**Random networks were generated by resetting all of the links of a matching empirical network with the same nodes and links. Data were generated from 100 random runs and SD indicates the standard deviation from the 100 runs. [a]Numbers of OTUs that originally used for network construction using the RMT-based approach. [b]Number of OTUs (i.e., nodes) in a network. [c]The random networks were generated by rewiring all of the links of a MEN with the identical numbers of nodes and links to the corresponding empirical MEN. [d]Significant difference ($P < 0.05$) in average path distance between healthy individuals and CRC patients based on the Students t-test with standard deviations derived from corresponding random networks. [e]Significant difference ($P < 0.05$) in average clustering coefficients between healthy individuals and CRC patients based on the Students t-test with standard deviations derived from corresponding random networks. [f]Significant difference ($P < 0.05$) in average harmonic geodesic distance between healthy individuals and CRC patients based on the Students t-test with standard deviations derived from corresponding random networks. [g]Significant difference ($P < 0.05$) in modularity between healthy individuals and CRC patients based on the Students t-test with standard deviations derived from corresponding random networks.*

model (Sergei and Kim, 2002). Total of 100 random networks were generated in each identified network, and all network indices were calculated individually. The average and standard deviation value of all random networks were obtained (Zhou et al., 2011). The network indices between CRC patients and healthy individuals were compared based on the Student *t*-test with standard deviations derived from corresponding random networks.

Statistical Analyses

All network analyses were performed based on the Molecular Ecological Network Analyses (MENA) Pipeline[1] and networks were graphed using the Cytoscape 2.8.3 (Killcoyne et al., 2009) and Gephi 0.9.1 software (Eck and Waltman, 2014). The Pearson and Spearson correlation by IBM SPSS statistic 19.0 were used to determine the significance of the differences and the clinical correlates.

RESULTS

Effects of Chemotherapy on pMENs

The pMENs were constructed for CRC patients in response to different therapy stages to determine the effect of chemotherapy on intestinal microbial community (**Table 2**). The CRC patients had unique ecological network models that varied during different treatment stages (**Supplementary Figure S1**). Identical threshold values of 0.66 were imposed on the T and H samples. The network sizes, links, connectivity, and module numbers were calculated for intestinal microbial community in the CRC patients and healthy individuals. Random networks were generated to test the statistical significance of the constructed network indices (**Table 2**). All the constructed networks showed scale-free characteristics, which means that only a few nodes in the network have many connections, whereas most nodes have no or few connections (Barabási, 2009), as proven by the power law R^2 ranging from 0.72 to 0.87 (**Table 2**).

The intestinal microbial networks were significantly different for CRC patients and healthy individuals, which were proven by multiple network topological properties, such as average path length, average clustering coefficient, average harmonic geodesic distance, and modularity ($P < 0.05$, **Table 2** and **Supplementary Figure S1**). Lower modularity values (0.40–0.50) in the T samples indicated that these networks could be impossibly isolated into multiple modules. Healthy assemblages formed larger networks with more nodes than the CRC patient networks (**Table 2**). However, the CRC patient networks contained more links between nodes than healthy individual networks, which increased the density of the connections and created more intricate network patterns (**Supplementary Figure S1** and **Table 2**). The increased complexity of the T networks was also reflected by the shorter harmonic geodesic distances and the increased average degree (Deng et al., 2012). In addition, the CRC patient networks presented distinctly different from T0 to T5, identified by the changes in multiple network indices (**Table 2**). The average path length, average clustering coefficient, average harmonic geodesic distance and modularity, were significantly different between T0 and T5 samples ($P < 0.05$). As the treatment stages progressed, the nodes in the CRC patients increased, ranging from 99 to 103, except for T3 (80). Collectively, the above results indicated that other than the significant differences with the healthy individual networks, overall network structures of the intestinal microbial communities in CRC patients were significantly changed under the chemotherapy.

Modularity in CRC Intestinal Communities

To identify microbial assemblages that potentially share or interact with intestinal niches during the CRC patient treatment process, we focused on representative networks from CRC patients with five treatment stages. We focused on modules with at least five nodes and visualized the phylogeny for these modules (**Figure 1**). The intestinal microbiota in CRC patients formed more complex networks than healthy individuals, as determined by more kinds of phyla in each sub-module (**Figure 1**). Eight modules were detected in the healthy individuals. There were 6, 6, 5, 6, 7, and 7 modules in the T0, T1, T2, T3, T4, and T5 networks, respectively (**Supplementary Table S2**). Networks from all CRC patients contained modules with modularity values $\leq$0.50 (**Table 2**). Overall, taxa tended to co-exclude (negative correlations, pink lines) rather than co-occur (positive correlations, blue lines); negative correlations accounted for 47–75% of the potential interactions observed at each treatment stage (**Figure 2**). The negative correlations in CRC patients decreased by 37.3% from T0 to T5; however, they were still more than those in healthy individuals (45%).

The composition of the modules differed within each network and changed over the treatment time (**Figure 1**). *Firmicutes* almost dominated all the modules from each treatment stage in CRC patients. The phylum *Fusobacteria* presented in the modules before the treatment (T0), before the second treatment (T1), and before the fifth treatment (T4). The phylum *Fusobacteria*, which was supposed to be more relevant to dysbiosis and CRC progression (Geng et al., 2014; Flemer et al., 2017), was primarily co-excluded with *Firmicutes*, *Bacteroidetes*, and *Proteobacteria* in the module during the different treatment stage.

Visualization of Topological Roles of Individual Nodes in CRC Patients

To evaluate the possible topological roles of the taxa in the networks, we organized these nodes into four categories based on the among-module connectivity (*Pi*) and within-module connectivity (*Zi*) values, including the module hubs, connectors, peripherals, and network hubs (Deng et al., 2012) (**Figure 2** and **Supplementary Tables S3–S5**). Structurally, the loss of peripherals could influence the functions of ecological networks, while losing the connectors, module hubs or network hubs would result in the deterioration of the entire network (Roger and Nunes Amaral, 2005). The nodes in each network were mainly peripherals, with most of their links inside their modules. Module hubs and connectors have been proposed

[1] http://ieg2.ou.edu/MENA/

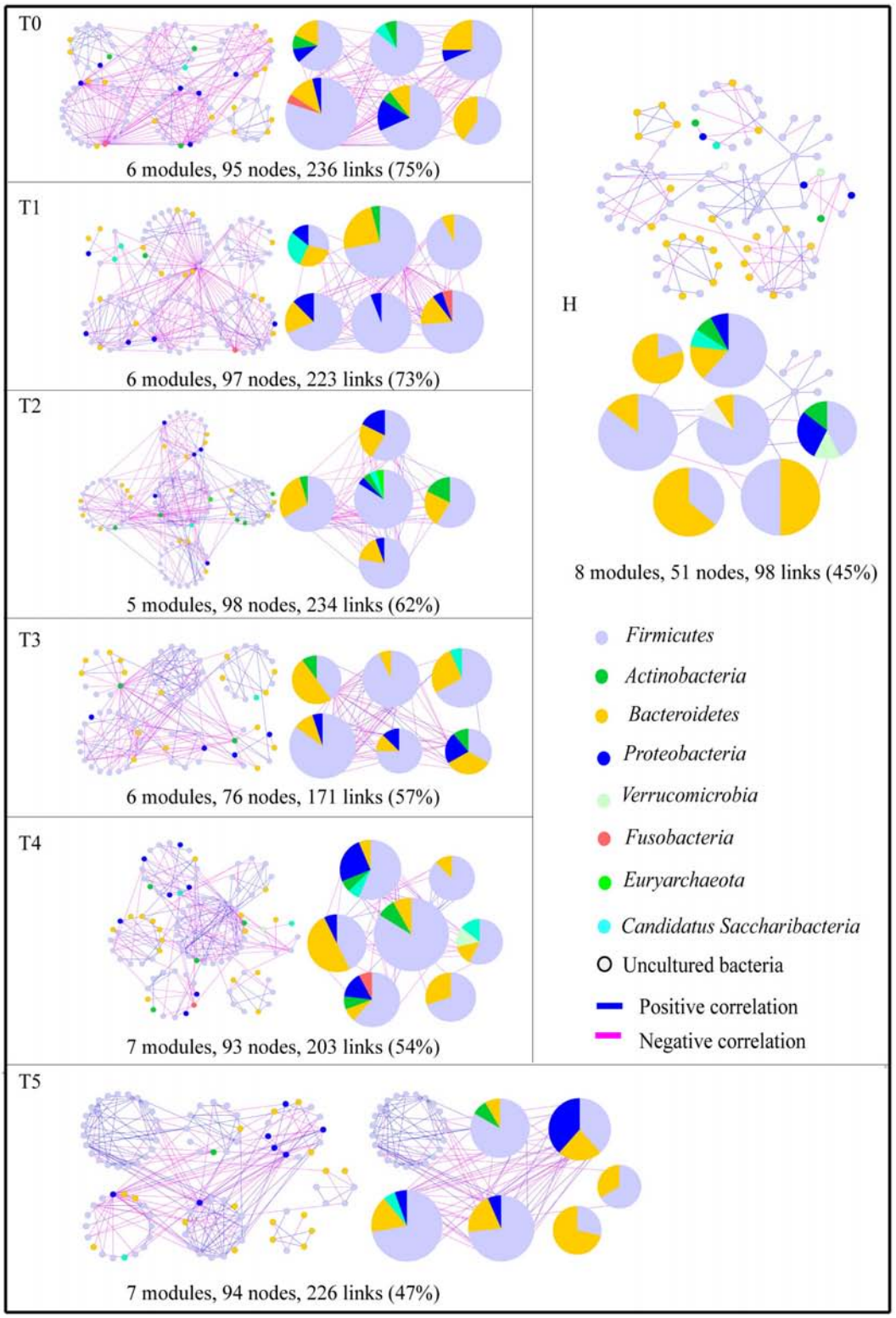

FIGURE 1 | Highly connected modules within intestinal networks of colorectal cancer patients in response to the five stages of chemotherapy. Node colors represent different major phyla; pie charts represent the composition of the modules with >1 phyla. A blue link indicates a positive relationship between two individual nodes, whereas a pink link indicates a negative relationship. The number in bracket means the ratio of negative links accounting for the total links.

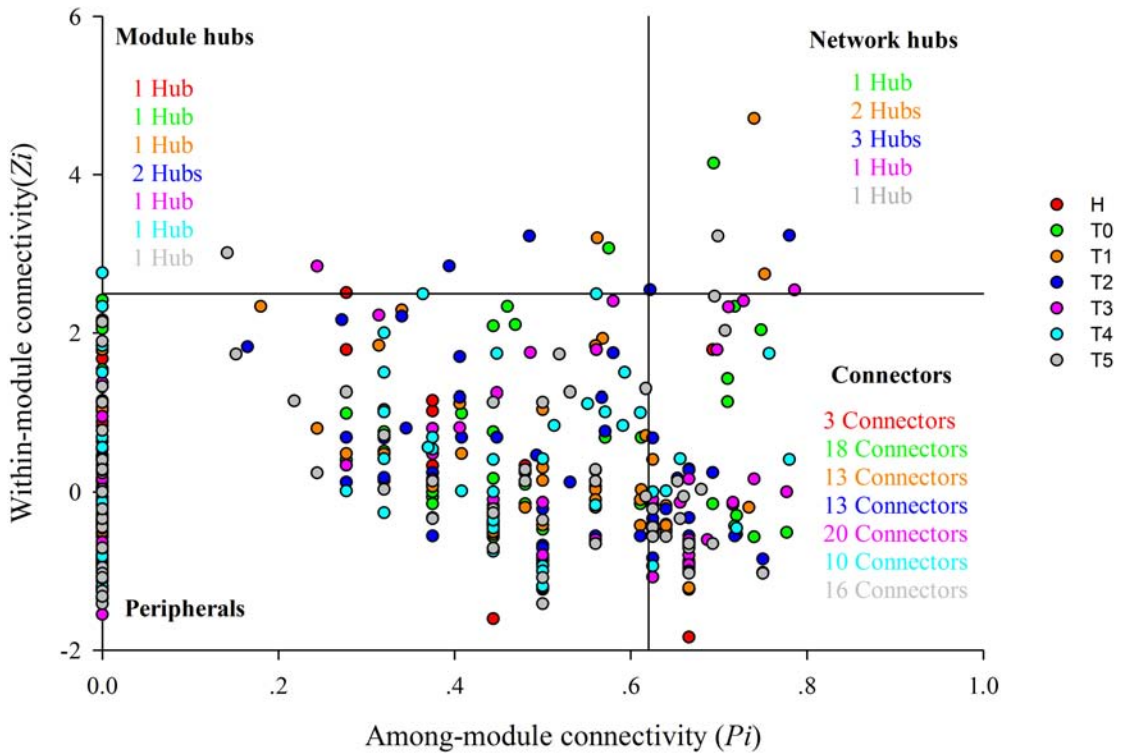

FIGURE 2 | Z-P plot showing the classification of nodes to identify putative keystone species in healthy individuals and colorectal cancer patients in response to chemotherapy. Each symbol represents an OTU. Different colors represent different groups, namely, red for healthy individuals (H), green for CRC patients before the first treatment (T0), orange for CRC patients before the second treatment (T1), blue for CRC patients before the third treatment (T2), pink for CRC patients before the fourth treatment (T3), water blue for CRC patients before the fifth treatment (T4), and gray for CRC patients before the sixth treatment (T5). Module hubs have the nodes with $Pi \leq 0.62$ and $Zi > 2.5$, connectors with $Pi > 0.62$ and $Zi \leq 2.5$, and network hubs with $Pi > 0.62$ and $Zi > 2.5$, peripheral nodes with $Pi \leq 0.62$ and $Zi \leq 2.5$. There are 1, 1, 1, 2, 1, 1, and 1 module hub in H, T0, T1, T2, T3, T4, and T5, respectively. There are 1, 2, 3, 1, and 1 network hub in T0, T1, T2, T3, and T5, respectively. There are 3, 18, 13, 13, 20, 10, and 16 connectors in H, T0, T1, T2, T3, T4, and T5, respectively.

to be keystone taxa because of their important roles in the network topology (Deng et al., 2012). In this study, the module hubs and connectors were detected in all networks. There were one or two nodes in each treatment stage classified as module hubs in the T networks. The module hubs identified in the T networks originated from a variety of taxonomic groups. The module hubs in T0 and T1 were from the genera *Klebsiella* and *Fusobacterium*, respectively (**Supplementary Table S3**), which are pathogens routinely found in the human intestine that cause diarrhea and bloodstream infections and markedly increase the rates of treatment failure and death (Yan et al., 2017). Two taxa from the genus *Bacteroides* and *Atopobium* were classified as module hubs in T2. The module hubs in T3, T4, and T5 were from *Faecalibacterium*, *Bacteroides*, and *Faecalibacterium*, respectively (**Supplementary Table S3**). Compared with the H network, the T networks had more connectors during the different treatment stages. Most of the connectors in each network originated from *Firmicutes*, while the others were from the *Actinobacteria*, *Bacteroidetes*, *Proteobacteria*, and *Candidatus Saccharibacteria* (**Supplementary Table S4**). In addition, there were also network hubs in the T networks, however, not in the H network. Therefore, the topological roles of the taxa were different and the keystone taxa were changed for CRC patients during the chemotherapy.

Association of Network Structure With Clinical Variables

Spearman correlation analysis was performed between OTU degree and tumor markers (CA242, CEA, CA199, and CA724) to determine the relationships between microbial network interactions and clinical variables (**Supplementary Material 1**). The OTU degree was calculated by summing the strengths of the links of each node with all of the other connected nodes in the network. OTU degree represents how strong an OTU is connected to other OTUs, which is one of the most commonly used network indices (Deng et al., 2012). Significantly negative correlations ($P < 0.05$) were observed in positive/negative OTU degree and CA199 and CEA (**Table 3**). This means that changes of interactive relationships of pMENs between species were probably closely correlated with tumor markers in CRC patients. In addition, based on the topological roles of individual nodes in the pMENs of CRC patients, we also selected some key nodes (OTU787, OTU167, OTU8, OTU238, OTU9, OTU2, OTU847, OTU488, and OTU16) and

TABLE 3 | The Spearman correlation of tumor markers and OTU degree.

Tumor marker	OTU degree (r, *P*)	Negative OTU degree (r, *P*)	Positive OTU links (r, *P*)
CA242	0.09, 0.87	0.31, 0.54	−0.43, 0.40
CEA	0.49, 0.33	**0.83, 0.04**	**−0.94, 0.01**
CA199	0.37, 0.47	**0.89, 0.02**	**−0.94, 0.01**
CA724	−0.03, 0.96	0.09, 0.87	−0.31, 0.54

"r" means the Spearman's correlation coefficient; "P" means the significant results. CA242, carbohydrae antigen 242; CEA, carcino-embryonic antigen; CA199, carbohydrae antigen 199; CA724, carbohydrae antigen 724. The bold values means the significant correlation between two parameters.

tumor markers (CA242, CEA, CA199, and CA724) for Spearman correlation analysis to further explore the linkages between the microbial correlation networks and clinical chemotherapeutic effects. The results showed that the relative abundances of OTU167, OTU8, and OTU9 were significantly correlated with CEA, CA724, and CA242, respectively ($P < 0.05$, **Supplementary Table S6**). The OTU167, OTU8, and OTU9 were from the genera *Fusobacterium*, *Bacteroides*, and *Faecalibacterium*, respectively. These significant OTUs, which were classified into module hubs or network hubs in T0, T1, T2, and T3, were conspicuous in ecological networks. These results showed that microbial interaction networks were closely related with tumor markers, indicating that they were extremely influenced by chemotherapy. However, the relative abundance of these keystone taxa were almost not significantly correlated with chemotherapy stages (**Supplementary Figure S2**).

DISCUSSION

Chemotherapy remains the mainstay treatment for patients with CRC, except for available surgical debulking (Yu et al., 2017). In recent years, the changes that occur to the intestinal microbiota in response to cancer chemotherapy have been gradually understood (van Vliet et al., 2009; Jutta et al., 2011; Stringer et al., 2013; Marin et al., 2014; Cammarota and Ianiro, 2017). Chemotherapy can damage the mucus layer and disrupt the mucosal barrier in the intestine. Afterward, some intestinal microbiota probably penetrate the lamina propria, leading to life-threatening systemic infections that activate the innate immune system, which may influence the efficacy of chemotherapy (Marin et al., 2014; Cammarota and Ianiro, 2017). A previous study reported that chemotherapy severely influenced the homeostasis of intestinal microbiota (Montassier et al., 2015); in turn, intestinal microbiota modulated the efficacy and toxicity through key mechanisms, such as the translocation, immunomodulation, metabolism, reduced diversity, and ecological variation (Alexander et al., 2017). Previous studies mainly analyzed the composition and structure of intestinal microbiota influenced by chemotherapy. Here, we firstly explored the intestinal microbial interactive networks from the feces of CRC patients in response to the five stages of chemotherapy based on the molecular ecological network analysis.

Microbes in the intestine are not independent individuals but complex inter-connected ecological communities. Microbes compete for resources or exchange genetic material, influencing the microbial composition and host health. Therefore, understanding microbial interactions is important to understand their functions. Although the chemotherapy is known to exert profound effects on intestinal microbiota (Emmanuel et al., 2014), the effects on the microbial ecological networks were first explored in this study. In our study, network properties significantly changed in CRC patients in response to chemotherapy ($P < 0.05$). For example, connectivity (average degree), which shows that how strong a node is connected to other nodes, was decreased by 6.7% in T5 than in T0. However, these CRC patients were still increased by 56.4, 53.1, 54.9, 51.6, 48.6, and 58.6% in T0, T1, T2, T3, T4, and T5, respectively, compared with healthy individuals (**Table 1**). It suggested that intestinal microbiota were linked with each other very tightly in CRC patients with chemotherapy. Modularity, which provides information on the extent to which nodes possess more links with their own modules, was higher by 16.1% in T5 than in T0. However, these CRC patients were lower by 44.5, 41.8, 38.6, 47.6, 35.3, and 35.6% in T0, T1, T2, T3, T4, and T5, respectively, compared with H (**Table 1**). These indicated that the pMENs in CRC patients were changed greatly under the chemotherapy. Previous study found that the changes of the connectivity and modularity were consistent (Liang et al., 2016). In our study, the inconsistency between the connectivity and modularity probably revealed that overall intestinal micro-ecosystem was in a seriously unbalanced state. Findings revealed that the overall phylogenetic network structures were changed, thereby suggesting a potential change in the organization of intestinal microbial communities (Faust and Raes, 2012). This change may result in the potential switching of roles of intestinal microbial species and ecological functions, which may influence therapeutic effects of chemotherapy.

The identified modules within the networks probably arise from microbes–microbes interactions in response to shared niches in the intestine. The links in the ecological network could explain the co-occurrence or co-exclusion of two nodes caused by the species performing similar or complementary and contrary or exclusive functions (Zhou et al., 2011). This study results showed that the links of modules in T5 were distinctly decreased than that in T0, but still higher than that in H (**Figure 1**), indicating that interspecies interactions within the ecological network were changed by chemotherapy, and the more complex and compact of modules were in CRC patients. Positive interactions often indicate that nodes

complement or cooperate with one another, while negative interactions signify predation or competition between the taxa. In a relatively healthy intestine, cooperation probably linked with stability was found to be the primary interaction among symbiotic intestinal communities (Jain and Krishna, 2001; Schluter and Foster, 2012). Our results showed that more negative correlations were in CRC patients (**Figure 1**). The previous study experimentally demonstrated that external disturbance promoted microbial species-species competition (Cyrille et al., 2010). After five stages of therapy, the negative links decreased distinctly in T5 than in T0, suggesting that chemotherapy could have key effects on species-species interactions of intestinal microbiota.

Identifying the key OTUs in a community is a challenge, because of the uncultured status and high diversity of microbes (Faust and Raes, 2012). In this study, pMENs analysis provided information on keystone OTUs that were most important to the structures and functions of microbial ecosystem in CRC patients during the different treatment stage. The keystone OTUs included that the module hubs (those highly linked to numerous OTUs in their own modules), and connectors (those highly connected to several modules). Module hubs and connectors have been proposed to be keystone taxa because losing them would result in the deterioration of the entire network (Deng et al., 2012). Topologically, different OTUs play individual roles in the ecological networks (Guimerà et al., 2007). The topological roles of the taxa were different and the keystone taxa were changed for CRC patients during the chemotherapy. We found that these keystone taxa (OTU787, OTU167, OTU8, OTU238, OTU9, OTU2, OTU847, OTU488, and OTU16) were not significantly correlated with types of chemotherapy, except for the OTU787 (P = 0.003), which was from the genus *Klebsiella* (**Supplementary Table S6**). One important reason was that most CRC patients used the same XELOX as the treatment protocols (**Supplementary Table S1**). The OTU167, OTU8, and OTU9 were classified into module hubs or networks hubs in T0, T1, T2, and T3, which were significantly correlated with tumor markers ($P < 0.05$, **Supplementary Table S6**). Therefore, these OTUs were probably extremely influenced by chemotherapy, which also may influence the chemotherapy efficacy. However, intestinal microbiota exerts both direct and indirect effects on chemotherapy efficacy by a large suite of ways. Not only are the intestinal microbiota niche-specific, but their ecology is also dynamic (Alexander et al., 2017). For example, intestinal structural ecology of CRC patients at old age might be perturbed by the exposure to a lifetime of environmental modifiers. The chemotherapy may create a state of dysbiosis, exaggerate the influence of deleterious bacteria, reduce efficacy, and further exacerbate any dysbiotic state rather than correct it (Claesson et al., 2011). Therefore, the actual roles of keystone taxa must be elucidated by co-culture experiments or more biological replicates in the further work.

It is very important to detect the interactive relationships among microbial communities across relatively large numbers of samples using network analysis (Barberán et al., 2012). We could not scale the results to all the conditions with only 22 samples, however, constructing a pMEN is important to determine the potential interactions among different microbes. The study results would provide a better understanding of the responses of intestinal microbial communities to chemotherapy. Additional larger sampling efforts are required to reduce the variables, such as age, sex, types of chemotherapy, antibiotic, and probiotics usage, to obtain more fundamental insight into intestinal microbial ecological networks in complex intestinal environment.

CONCLUSION

An ecological molecular network is considered an effective way to systematically evaluate intestinal microbial homeostasis and provides novel insights into the intestinal microbiota for CRC patients in response to chemotherapy. In this study, we concluded that the intestinal microbiota of CRC patients were changed greatly under the chemotherapy based on the ecological molecular network analysis. These changes may influence the therapeutic effects of chemotherapy. However, further studies are needed to provide for more evidence to support this idea.

AUTHOR CONTRIBUTIONS

JC analyzed the data and wrote the manuscript. DL, NZ, and MJ collected samples and analyzed the data. JZ, CZ, TL, KL, HH, and XZ reviewed and revised the manuscript. All the authors were involved in the design of the study, interpreted the data, and read and approved the final manuscript.

FUNDING

This study was supported by funding from Project funded by China Postdoctoral Science Foundation (2016M602094), Qingdao Application Research Project (2016047), and Taishan Scholar Foundation (201502061).

ACKNOWLEDGMENTS

We would like to thank the CRC patients and healthy volunteers for providing the fecal samples that were used in this study. We would also like to thank Yuguang Zhang for reviewing and correcting errors and providing feedback on manuscript drafts.

SUPPLEMENTARY MATERIAL

The Supplementary Material for this article can be found online at: https://www.frontiersin.org/articles/10.3389/fmicb.2019.01008/full#supplementary-material

REFERENCES

Alexander, J. L., Wilson, I. D., Teare, J., Marchesi, J. R., Nicholson, J. K., and Kinross, J. M. (2017). Gut microbiota modulation of chemotherapy efficacy and toxicity. *Nat. Rev. Gastroenterol. Hepatol.* 14, 356–365. doi: 10.1038/nrgastro.2017.20

Barabási, A. L. (2009). Scale-free networks: a decade and beyond. *Science* 325, 412–413. doi: 10.1126/science.1173299

Barberán, A., Bates, S. T., Casamayor, E. O., and Fierer, N. (2012). Using network analysis to explore co-occurrence patterns in soil microbial communities. *ISME J.* 6, 343–351. doi: 10.1038/ismej.2011.119

Cammarota, G., and Ianiro, G. (2017). Gut microbiota and cancer patients: a broad-ranging relationship. *Mayo Clin. Proc.* 92, 1605–1607. doi: 10.1016/j.mayocp.2017.09.009

Claesson, M. J., Cusack, S., O'Sullivan, O., Greene-Diniz, R., De Weerd, H., Flannery, E., et al. (2011). Composition, variability, and temporal stability of the intestinal microbiota of the elderly. *Proc. Natl. Acad. Sci. U.S.A.* 108, 4586–4591. doi: 10.1073/pnas.1000097107

Cyrille, V., Zhichao, P., and Lin, J. (2010). Experimental demonstration of the importance of competition under disturbance. *Proc. Natl. Acad. Sci. U.S.A* 107, 12925–12929. doi: 10.1073/pnas.1000699107

Deng, Y., Jiang, Y. H., Yang, Y., He, Z., Luo, F., and Zhou, J. (2012). Molecular ecological network analyses. *BMC Bioinformatics* 13:113. doi: 10.1186/1471-2105-13-113

Deng, Y., Zhang, P., Qin, Y., Tu, Q., Yang, Y., He, Z., et al. (2016). Network succession reveals the importance of competition in response to emulsified vegetable oil amendment for uranium bioremediation. *Environ. Microbiol.* 18, 205–218. doi: 10.1111/1462-2920.12981

Eck, N. J. V., and Waltman, L. (2014). "Visualizing bibliometric network," in *Measuring Scholarly Impact*, eds Y. Ding, R. Rousseau, and D. Wolfram (Cham: Springer).

Emmanuel, M., Eric, B., Sébastien, M., Thomas, G., Thomas, C., Jocelyne, C., et al. (2014). 16S rRNA gene pyrosequencing reveals shift in patient faecal microbiota during high-dose chemotherapy as conditioning regimen for bone marrow transplantation. *Microb. Ecol.* 67, 690–699. doi: 10.1007/s00248-013-0355-4

Faust, K., and Raes, J. (2012). Microbial interactions: from networks to models. *Nat. Rev. Microbiol.* 10, 538–550. doi: 10.1038/nrmicro2832

Faust, K., Sathirapongsasuti, J. F., Izard, J., Segata, N., Gevers, D., Raes, J., et al. (2012). Microbial co-occurrence relationships in the human microbiome. *PLoS Comput. Biol.* 8:e1002606. doi: 10.1371/journal.pcbi.1002606

Flemer, B., Lynch, D. B., Brown, J. M. R., Jeffery, I. B., Ryan, F. J., Claesson, M. J., et al. (2017). Tumour-associated and non-tumour-associated microbiota in colorectal cancer. *Gut* 66, 633–643. doi: 10.1136/gutjnl-2015-309595

Fuhrman, J. A. (2009). Microbial community structure and its functional implications. *Nature* 459, 193–199. doi: 10.1038/nature08058

Geng, J., Song, Q., Tang, X., Xiao, L., Hong, F., Peng, H., et al. (2014). Co-occurrence of driver and passenger bacteria in human colorectal cancer. *Gut Pathog.* 6:26. doi: 10.1186/1757-4749-6-26

Guimerà, R., Sales-Pardo, M., and Amaral, L. A. N. (2007). Classes of complex networks defined by role-to-role connectivity profiles. *Nat. Phys.* 3, 63–69. doi: 10.1038/nphys489

Guthrie, L., Gupta, S., Daily, J., and Kelly, L. (2017). Human microbiome signatures of differential colorectal cancer drug metabolism. *NPJ Biofilms Microbiomes* 3:27. doi: 10.1038/s41522-017-0034-1

Haiser, H. J., Gootenberg, D. B., Chatman, K., Sirasani, G., Balskus, E. P., and Turnbaugh, P. J. (2013). Predicting and manipulating cardiac drug inactivation by the human gut bacterium eggerthella lenta. *Science* 341, 295–298. doi: 10.1126/science.1235872

Hallam, S. J., and Mccutcheon, J. P. (2015). Microbes don't play solitaire: how cooperation trumps isolation in the microbial world. *Environ. Microbiol. Rep.* 7, 26–28. doi: 10.1111/1758-2229.12248

Horvath, S., and Dong, J. (2008). Geometric interpretation of gene coexpression network analysis. *PLoS Comput. Biol.* 4:e1000117. doi: 10.1371/journal.pcbi.1000117

Jain, S., and Krishna, S. (2001). A model for the emergence of cooperation, interdependence, and structure in evolving networks. *Proc. Natl. Acad. Sci. U.S.A.* 98, 543–547. doi: 10.1073/pnas.021545098

Jia, W., Li, H., Zhao, L., and Nicholson, J. K. (2008). Gut microbiota: a potential new territory for drug targeting. *Nat. Rev. Drug Discov.* 7, 123–129. doi: 10.1038/nrd2505

Jing, C., Yang, Y., Liu, X., Hui, L., Xiao, L., Zhou, J., et al. (2015). Analyses of soil microbial community compositions and functional genes reveal potential consequences of natural forest succession. *Sci. Rep.* 5:10007. doi: 10.1038/srep10007

Jutta, Z., Cornelia, L., Berit, H., Angelika, P., Switzeny, O. J., Marlene, R., et al. (2011). Changes in human fecal microbiota due to chemotherapy analyzed by TaqMan-PCR, 454 sequencing and PCR-DGGE fingerprinting. *PLoS One* 6:e28654. doi: 10.1371/journal.pone.0028654

Kantarjian, H. M., Fojo, T., Mathisen, M., and Zwelling, L. A. (2013). Cancer drugs in the United States: justum Pretium—the just price. *J. Clin. Oncol.* 31, 3600–3604. doi: 10.1200/jco.2013.49.1845

Killcoyne, S., Carter, G. W., Smith, J., and Boyle, J. (2009). Cytoscape: a community-based framework for network modeling. *Methods. Mol. Biol.* 563, 219–239. doi: 10.1007/978-1-60761-175-2_12

Li, H., He, J., and Jia, W. (2016). The influence of gut microbiota on drug metabolism and toxicity. *Expert. Opin. Drug Metab. Toxicol.* 12, 31–40. doi: 10.1517/17425255.2016.1121234

Liang, Y., Zhao, H., Deng, Y., Zhou, J., Li, G., and Sun, B. (2016). Long-term oil contamination alters the molecular ecological networks of soil microbial functional genes. *Front. Microbiol.* 7:60. doi: 10.3389/fmicb.2016.00060

Luo, F., Yang, Y., Zhong, J., Gao, H., Khan, L., Thompson, D. K., et al. (2007). Constructing gene co-expression networks and predicting functions of unknown genes by random matrix theory. *BMC Bioinformatics* 8:299. doi: 10.1186/1471-2105-8-299

Marin, M., Gudiol, C., Ardanuy, C., Garcia-Vidal, C., Calvo, M., Arnan, M., et al. (2014). Bloodstream infections in neutropenic patients with cancer: differences between patients with haematological malignancies and solid tumours. *J. Infect.* 69, 417–423. doi: 10.1016/j.jinf.2014.05.018

Mirnezami, R., Nicholson, J., and Darzi, A. (2012). Preparing for precision medicine. *N. Engl. J. Med.* 366, 489–491.

Montassier, E., Gastinne, T., Vangay, P., Alghalith, G. A., Bruley, D. V. S., Massart, S., et al. (2015). Chemotherapy-driven dysbiosis in the intestinal microbiome. *Aliment. Pharmacol. Ther.* 42, 515–528. doi: 10.1111/apt.13302

Olesen, J. M., Jordi, B., Dupont, Y. L., and Pedro, J. (2007). The modularity of pollination networks. *Proc. Natl. Acad. Sci. U.S.A* 104, 19891–19896. doi: 10.1073/pnas.0706375104

Power, M. E., Tilman, D., Estes, J. A., Menge, B. A., Bond, W. J., Mills, L. S., et al. (1996). Challenges in the quest for keystones. *Bioscience* 46, 609–620. doi: 10.2307/1312990

Roger, G., and Nunes Amaral, L. A. (2005). Functional cartography of complex metabolic networks. *Nature* 433, 895–900. doi: 10.1038/nature03288

Ross, C. L., Spinler, J. K., and Savidge, T. C. (2016). Structural and functional changes within the gut microbiota and susceptibility to Clostridium difficile infection. *Anaerobe* 41, 37–43. doi: 10.1016/j.anaerobe.2016.05.006

Scheline, R. R. (1968). Drug metabolism by intestinal microorganisms. *J. Pharm. Sci.* 57, 2021–2037. doi: 10.1002/jps.2600571202

Schluter, J., and Foster, K. R. (2012). The evolution of mutualism in gut microbiota via host epithelial selection. *PLoS Biol.* 10:e1001424. doi: 10.1371/journal.pbio.1001424

Scott, T. A., Quintaneiro, L. M., Norvaisas, P., Lui, P. P., Wilson, M. P., Leung, K. Y., et al. (2017). Host-microbe co-metabolism dictates cancer drug efficacy in C.Â *elegans*. *Cell* 169, 442–456. doi: 10.1016/j.cell.2017.03.040

Sergei, M., and Kim, S. (2002). Specificity and stability in topology of protein networks. *Science* 296, 910–913. doi: 10.1126/science.1065103

Stringer, A. M., Al-Dasooqi, N., Bowen, J. M., Tan, T. H., Radzuan, M., Logan, R. M., et al. (2013). Biomarkers of chemotherapy-induced diarrhoea: a clinical study of intestinal microbiome alterations, inflammation and circulating matrix metalloproteinases. *Support. Care Cancer* 21, 1843–1852. doi: 10.1007/s00520-013-1741-7

van Vliet, M. J., Tissing, W. J., and dun, C. A. (2009). Chemotherapy treatment in pediatric patients with acute myeloid leukemia receiving antimicrobial prophylaxis leads to a relative increase of colonization with potentially pathogenic bacteria in the gut. *Clin. Infect. Dis.* 49, 262–270. doi: 10.1086/599346

Wallace, B. D., Wang, H., Lane, K. T., Scott, J. E., Orans, J., Koo, J. S., et al. (2010). Alleviating cancer drug toxicity by inhibiting a bacterial enzyme. *Science* 330, 831–835. doi: 10.1126/science.1191175

Wang, Q., Garrity, G. M., Tiedje, J. M., and Cole, J. R. (2007). Naïve bayesian classifier for rapid assignment of rrna sequences into the new bacterial taxonomy. *Appl. Environ. Microbiol.* 73, 5261–5267. doi: 10.1128/aem.00062-07

Welsh, S. J., Rizos, H., Scolyer, R. A., and Long, G. V. (2016). Resistance to combination BRAF and MEK inhibition in metastatic melanoma: where to next? *Eur. J. Cancer* 62, 76–85. doi: 10.1016/j.ejca.2016.04.005

Wu, X., Zhang, H., Chen, J., Shang, S., Wei, Q., Yan, J., et al. (2016). Comparison of the fecal microbiota of dholes high-throughput Illumina sequencing of the V3–V4 region of the 16S rRNA gene. *Appl. Microbiol. Biotechnol.* 100, 3577–3586. doi: 10.1007/s00253-015-7257-y

Yan, Q., Gu, Y., Li, X., Yang, W., Jia, L., Chen, C., et al. (2017). Alterations of the gut microbiome in hypertension. *Front. Cell. Infect. Microbiol.* 7:381. doi: 10.3389/fcimb.2017.00381

Yu, T., Guo, F., Yu, Y., Sun, T., Ma, D., Han, J., et al. (2017). *Fusobacterium nucleatum* promotes chemoresistance to colorectal cancer by modulating autophagy. *Cell* 170, 548–563. doi: 10.1016/j.cell.2017.07.008

Zhou, J., Deng, Y., Luo, F., He, Z., and Yang, Y. (2011). Phylogenetic molecular ecological network of soil microbial communities in response to elevated CO2. *mBio* 2:e00122–11. doi: 10.1128/mBio.00122-11

Conflict of Interest Statement: The authors declare that the research was conducted in the absence of any commercial or financial relationships that could be construed as a potential conflict of interest.

frontiers in Microbiology

ORIGINAL RESEARCH
published: 05 June 2019
doi: 10.3389/fmicb.2019.01261

Mucosa-Associated Microbiota in Gastric Cancer Tissues Compared With Non-cancer Tissues

*Xiao-Hui Chen[1,2,3], Ang Wang[1,2,3], Ai-Ning Chu[1,2,3], Yue-Hua Gong[1,2,3] and Yuan Yuan[1,2,3]**

[1] Tumor Etiology and Screening Department of Cancer Institute and General Surgery, The First Hospital of China Medical University, Shenyang, China, [2] Key Laboratory of Cancer Etiology and Prevention in Liaoning Education Department, The First Hospital of China Medical University, Shenyang, China, [3] Key Laboratory of GI Cancer Etiology and Prevention in Liaoning Province, The First Hospital of China Medical University, Shenyang, China

The link between microbiota and gastric cancer (GC) has attracted widespread attention. However, the phylogenetic profiles of niche-specific microbiota in the tumor microenvironment is still unclear. Here, mucosa-associated microorganisms from 62 pairs of matched GC tissues and adjacent non-cancerous tissues were characterized by 16S rRNA gene sequencing. Functional profiles of the microbiota were predicted using PICRUSt, and a co-occurrence network was constructed to analyze interactions among gastric microbiota. Results demonstrated that mucosa-associated microbiota from cancerous and non-cancerous tissues established micro-ecological systems that differed in composition, structure, interaction networks, and functions. Microbial richness and diversity were increased in cancerous tissues, with the co-occurrence network exhibiting greater complexity compared with that in non-cancerous tissue. The bacterial taxa enriched in the cancer samples were predominantly represented by oral bacteria (such as *Peptostreptococcus*, *Streptococcus*, and *Fusobacterium*), while lactic acid-producing bacteria (such as *Lactococcus lactis* and *Lactobacillus brevis*) were more abundant in adjacent non-tumor tissues. Colonization by *Helicobacter pylori*, which is a GC risk factor, also impacted the structure of the microbiota. Enhanced bacterial purine metabolism, carbohydrate metabolism and denitrification functions were predicted in the cancer associated microbial communities, which was consistent with the increased energy metabolism and concentration of nitrogen-containing compounds in the tumor microenvironment. Furthermore, the microbial co-occurrence networks in cancerous and non-cancerous tissues of GC patients were described for the first time. And differential taxa and functions between the two groups were identified. Changes in the abundance of certain bacterial taxa, especially oral microbiota, may play a role in the maintenance of the local microenvironment, which is associated with the development or progression of GC.

Keywords: gastric cancer, microbiota, 16S rDNA, cancer microenvironment, risk

OPEN ACCESS

Edited by:
Gary Moran,
Trinity College Dublin, Ireland

Reviewed by:
Robert J. Moore,
RMIT University, Australia
Suleyman Yildirim,
Istanbul Medipol University, Turkey

***Correspondence:**
Yuan Yuan
yuanyuan@cmu.edu.cn

Specialty section:
This article was submitted to Systems Microbiology, a section of the journal Frontiers in Microbiology

Received: *20 December 2018*
Accepted: *21 May 2019*
Published: *05 June 2019*

Citation:
Chen X-H, Wang A, Chu A-N, Gong Y-H and Yuan Y (2019) Mucosa-Associated Microbiota in Gastric Cancer Tissues Compared With Non-cancer Tissues. Front. Microbiol. 10:1261. doi: 10.3389/fmicb.2019.01261

INTRODUCTION

Gastric cancer (GC) is one of the most common malignant cancers and the third leading cause of cancer-associated death worldwide (Ferlay et al., 2015; Torre et al., 2015). The incidence of GC varies by region and race, with a high rate in East Asia. Both host factors (such as genetic susceptibility) and environmental factors (such as microbial infections) play crucial roles in gastric tumorigenesis (Compare et al., 2010). It is widely accepted that chronic *Helicobacter pylori* infection, which leads to enhanced inflammation and disorders of epithelial structure and function, is closely related to precancerous lesions such as atrophic gastritis. Nevertheless, only 1–3% of *H. pylori*-infected patients develop GC, and GC could not be completely prevented by the eradication of *H. pylori* (Wroblewski et al., 2010). Additionally, during the progression of GC, *H. pylori* colonization gradually decreases and even disappears (El-Omar et al., 1997). Therefore, biological factors other than *H. pylori* colonization may play an important role in the development of cancer and the maintenance of the local lesion microenvironment.

In recent years, the development of culture-independent technologies for characterizing microbiota composition has shed light on the profile of gastric microbiota. Studies have demonstrated the significant role played by non-*H. pylori* microbiota in gastric carcinogenesis in mice (Lofgren et al., 2011; Lertpiriyapong et al., 2014). In human studies, chronic *H. pylori* infection or the use of drugs such as omeprazole resulted in an elevated intragastric pH level by reducing the secretion of gastric acid, which allowed the proliferation and colonization of other bacteria (Mowat et al., 2000; Plottel and Blaser, 2011). As a result, the microbial balance of the gastric mucosa ecological niche was disrupted, and increased nitrosating species raised nitrite and *N*-nitrosamine levels in the stomach (Leach et al., 1987). Together, these findings highlighted the potential role of microbiota other than *H. pylori* in the development of GC.

Thus far, our understanding of the complex gastric flora in human is still limited. A few studies have revealed differences in the composition and function of the gastric microbiota between GC patients and control groups. However, there is no consensus on specific microbial taxa that play important roles in the pathogenesis of GC. In addition, microbial changes in the tumor microenvironment remain unclear. Unlike most previous studies that compared two groups of individuals, our research focused on the microbiota in the tumor microenvironment by comparing matched samples from GC patients. In this condition, the influence of the external environment and the genetic effects of the host would be controlled to some extent. We characterized the variations in the composition, interaction network and functions of gastric microbiota in cancerous and patient-matched non-cancerous tissues, aiming to explore the differential distribution profile of microbiota in the tumor microenvironment. Our findings will help to explore the role of mucosa-associated microbiota in carcinogenesis and in the maintenance of the local microenvironment in GC patients.

MATERIALS AND METHODS

Study Population and Specimen Collection

A total of 124 gastric tissue samples, consisting of cancerous and paired non-cancerous tissues, were obtained from 62 GC patients who underwent subtotal gastrectomy at The First Hospital of China Medical University between 2012 and 2014. Patients who had received medical treatment (including probiotics, proton pump inhibitors, antibiotics, and H_2 receptor antagonists) within 1 month, or those who had received chemotherapy or radiotherapy prior to the surgery were excluded. Gastric mucosa tissues, collected from the cancerous lesions and neighboring noncancerous sites (at least 5 cm away from the tumor site), were immediately frozen after surgical resections and stored at −80°C until further use. Epidemiologic information was obtained through questionnaire.

DNA Extraction, PCR Amplification, and 16S rRNA Gene Sequencing

Total DNA was extracted using methods as previously described (Chen et al., 2017). After treating the mucosal samples with lysozyme, proteinase K, and SDS, we purified the DNA through multiple steps with phenol-chloroform-isoamylalcohol, then precipitated the DNA with glycogen, sodium acetate, and cold isopropanol, followed by cleaning the DNA with 70% ethanol. Finally, the DNA was dissolved in TE buffer and stored at −20°C. The V4–V5 regions of the 16S rRNA gene were amplified by primers 515F, 5′-barcode-GTGCCAGCMGCCGCGGTAA-3′ and 907R, 5′-barcode CCGTCAATTCMTTTRAGTTT-3′ (Liu et al., 2018), using the PCR kit (TransGenAP221-02, Peking; containing the high fidelity enzyme). PCR was performed as follows: 95°C for 5 min, followed by 34 cycles of 94°C for 60 s, 57°C for 45 s, and 72°C for 60 s, with final extension at 72°C for 10 min. In order to avoid possible contamination, DNA extraction and PCR set up were performed in a laminar air flow bench, illuminated with a UV lamp before use. Two negative controls (containing DNA extraction reagents and PCR kit reagents) were amplified and sequenced to assess contamination. The concentration and length of the PCR amplicons were detected by 2% agarose gel electrophoresis. PCR products with bright main strip (approximately 400–450 bp) were chosen for further experiments. The amplicons in the target region were purified with Qiagen Gel Extraction Kit (Qiagen, Germany). Sequencing libraries were generated by using DNA PCR-Free Sample Preparation Kit (Illumina, San Diego, CA, United States) following manufacturers recommendations and index codes were added. The library quality was assessed on the Qubit@2.0 Fluorometer (Thermo Scientific) and Agilent Bioanalyzer 2100 system. The libraries were sequenced on the Illumina Hiseq 2500 platform and 250 bp paired-end reads were generated. The sequence data have been deposited in the NCBI Sequence Read Archive (SRA) database with the accession number PRJNA532731.

Processing of Sequencing Results and Taxonomical Annotation

The sequencing data were processed using the Quantitative Insights Into Microbial Ecology (QIIME, V1.9.1) pipeline as previously reported (Caporaso et al., 2010). Raw sequencing reads were assigned to each sample based on the unique barcode and identified as valid sequences. The low quality and short sequences were filtered out with the following criteria (Gill et al., 2006; Fadrosh et al., 2014): sequence reads with average Phred score ≤19, length less than 150 bp; paired reads having at least one with length less than 75% of their original length; reads with ambiguous bases; reads containing mononucleotide repeats more than 8 bp. Paired-end reads were assembled using FLASH (version 1.2.7) (Magoč and Salzberg, 2011). Chimeras were filtered out using UCHIME (v4.2.40) (Edgar et al., 2011). Sequence clustering analysis was performed using UPARSE pipeline (Edgar, 2013). Tags with at least 97% identity were clustered into the same operational classification unit (OTU; **Supplementary Table S1**). The Silva Database was used to annotate taxonomic information for OTU representative sequences by the ribosome database project (RDP) Classifier v.2.2.

Microbial Diversity Analysis and Network Construction

QIIME (V1.9.1) was used to calculate diversity parameters. Alpha diversity analysis was performed to describe the richness and diversity of the microbiota in each sample. The Chao1 and ACE indices were used to estimate community richness, and the Shannon and phylogenetic diversity (PD) whole tree indices were applied to measure microbial diversity. Good's coverage was used to evaluate the coverage quality of sequencing results. Beta diversity was measured by weighted UniFrac distance matrices and Bray–Curtis, and visualized via principal coordinate analysis (PCoA) and non-metric multidimensional scaling (NMDS) plots. Co-occurrence networks were structured by Spearman's correlation analysis and visualized using the Cytoscape software (V.3.0.2., United States).

Functional Prediction of Mucosal-Associated Microbiota

Functions of mucosal-associated microbiota were predicted using PICRUSt (Langille et al., 2013). Accuracy of the predicted metagenomes was evaluated by the nearest sequenced taxon index (NSTI; Langille et al., 2013). The enrichment analysis of pathways was performed based on Kyoto Encyclopedia of Genes and Genomes (KEGG) database. Additionally, predicted functional genes were also categorized into clusters of orthologous groups (COG), and compared across cancer and non-cancer groups by STAMP (Parks et al., 2014) to identify gene functions that differentiated bacterial communities in the two-group comparison.

Statistical Analysis

Continuous variables that were not normally distributed were represented by inter-quartile range (IQR). Mann–Whitney *U* test was used to examine the correlation between alpha diversity parameters and epidemiological risk factors of GC. Tests were performed with SPSS 22.0 software (SPSS Inc., Chicago, IL, United States). Analysis of similarity (ANOSIM) and permutational multivariate analysis of variance (PERMANOVA) were performed to test the dissimilarity of beta diversity between groups by using ANOSIM and Adonis functions of vegan package in R (version 3.4.1). Linear discriminant analysis effect size (LEfSe) algorithm (Segata et al., 2011) was used to identify specific microbial taxa and functions that differed significantly between groups. Differences with linear discriminant analysis (LDA) scores >2.0 were considered significant. The analysis of differences in the abundance of the microbiota between two groups were also performed using the DESeq. 2 package in R (Weiss et al., 2017). The White's non-parametric *t*-test was applied to determine statistical differences of COG between groups by STAMP. *P*-values were adjusted by Benjamini-Hochberg false discovery rate correction for multiple comparisons. $P < 0.05$ was considered statistically significant.

RESULTS

Sequencing Results and Basic Characteristics of the Study Subjects

After PCR amplification, no bands were observed in the negative controls on the gel. The negative controls both had <130 reads, and the sequences could not be assembled. After sequencing and quality control, libraries of 16S rRNA gene V4–V5 region amplicon sequences from 61 cancerous and 62 adjacent non-cancerous tissue samples were used for further analysis, with an average of 67,958 effective tags per sample. The number of raw reads and effective tags for each sample are shown in **Supplementary Table S2**. At the 3% dissimilarity level, the number of OTUs were 152 (119-200) [median (IQR)] for the non-cancer group and 221 (177-350) for the cancer group. Good's coverage was estimated to ensure quality assessment. All samples had a value >0.99, suggesting that the sequencing results were sufficient to represent the bacterial diversity of the bacteria in the gastric mucosa.

Detailed information regarding individuals included in the study is provided in **Table 1**. All cases were diagnosed as gastric adenocarcinoma. The median age of the patients was 60 years old. Samples with relative abundance of *H. pylori* more than 1% were identified as *H. pylori* sequencing positive, while others with relative abundance less than 1% were identified as *H. pylori* sequencing negative as previously proposed (Kim et al., 2015). Among the patients, *H. pylori* sequencing-positive cases accounted for 29%.

Characteristics of Mucosa-Associated Microbiota in Cancerous Tissues

Microbial Community Profile of Cancerous Tissues

Proteobacteria was the predominant phylum in the cancerous samples, followed by *Firmicutes*, *Bacteroidetes*, *Actinobacteria*, *Acidobacteria*, and *Fusobacteria* (**Table 2**). Overall, 90% of cancerous samples were dominated by *Proteobacteria*, with relative abundance >50% in each case. Four samples were dominated by *Firmicutes* or *Bacteroidetes*, while the remaining two samples had no obviously dominant phylum (**Supplementary Figure S1**).

Correlation Between Cancerous Tissue Microbiota and GC Risk Factors

We next analyzed the association between GC-related epidemiological risk factors (such as age, gender, smoking, alcohol consumption, family history, and *H. pylori* colonization status) and the microbiota. Results showed that in tumor tissues, the alpha diversity of the microbiota, estimated by Shannon index and PD whole tree, was significantly increased in GC patients aged over 60 years old compared with that of younger patients (P = 0.043, 0.022, respectively, **Supplementary Table S3**). No significant differences in the microbial richness or community structure were discovered in relation to the other risk factors.

TABLE 1 | Baseline characteristics of the study subjects (n = 62).

Characteristics	Median (IQR)/number (%)
Age (years)	60 (52–68)
<60	26 (42%)
≥60	36 (58%)
Gender	
Male	46 (74%)
Female	16 (26%)
Family history	
Yes	20 (32%)
No	42 (68%)
Drinking	
Nondrinker	38 (61%)
Drinker	24 (39%)
Smoking	
Never smoker	32 (52%)
Ever smoker	30 (48%)
***H. pylori* colonization status**	
Sequencing positive	18 (30%)
Sequencing negative	44 (70%)

IQR, inter-quartile range.

TABLE 2 | The relative abundances of major bacterial phyla in cancerous and adjacent non-cancerous tissues.

Taxonomy	Non-cancer group (%)	Cancer group (%)	*P*
Proteobacteria	83.691	78.434	0.084
Firmicutes	1.907	5.568	0.000
Bacteroidetes	0.518	2.339	0.000
Actinobacteria	0.080	0.741	0.000
Fusobacteria	0.041	0.257	0.000
Acidobacteria	0.004	0.314	0.000

The P-value is calculated using Wilcoxon signed-ranks test.

Ecological Network of Gastric Microbiota in Cancerous Tissues

Co-occurrence network analysis was used to describe the interactions among the microbiota in the complex gastric microbial population. As shown in **Figure 1A**, the interactions across the mucosa-associated microbiota mainly occurred among taxa belonging to the phyla *Firmicutes* and *Proteobacteria*, the two predominant phyla in the taxonomic profiles. Collectively, co-occurrence interactions dominated in the networks. In addition, co-occurrence interactions between *Helicobacter* and *Lachnoclostridium* and between *Helicobacter* and *Ezakiella* were also observed in the cancer tissue network. No co-exclusion interaction was identified in strong correlations ($r > 0.6$ or < -0.6).

Characteristics of Mucosa-Associated Microbiota in Non-cancerous Tissues

Microbial Community Profile of Non-cancerous Tissues

The gastric microbiota in non-cancerous tissues was also dominated by *Proteobacteria* and consisted mainly of the six main phyla observed in the cancer group. However, the ranking of phyla differed slightly (**Table 2**), with a decreased abundance of *Firmicutes*, *Bacteroidetes*, *Actinobacteria*, *Acidobacteria*, *Fusobacteria* (all $P < 0.01$), but an increased abundance of *Proteobacteria* (P = 0.084) when compared with the cancer group.

Correlation Between Non-cancerous Tissue Microbiota and GC Risk Factors

Unlike the cancer group, *H. pylori* colonization significantly impacted the composition of the microbiota in the non-cancerous samples. The *H. pylori* sequencing-positive group showed greater bacterial diversity (Shannon index) than the sequencing-negative group (P = 0.022, **Supplementary Table S4**). The differences in microbial structure were assessed by Bray–Curtis and weighted UniFrac distance matrices. PERMANOVA showed significant differences between *H. pylori* sequencing positive and negative group (Bray–Curtis, P = 0.001; weighted UniFrac distance matrices, P = 0.004). No significant association was found between microbial richness or community structure and the other risk factors.

LEfSe analysis (Segata et al., 2011) was conducted to further explore the taxa correlated with *H. pylori* colonization status in non-tumor tissues (**Supplementary Figure S2**). In the *H. pylori* sequencing-positive group, the enrichment of 15 genera was observed other than *Helicobacter*. Among them, *Serratia*, *Lactobacillus*, and *Streptococcus* were abundant in all non-cancerous tissues, ranking in the top 20 abundant genera. In comparison, *Pseudomonas aeruginosa* and its higher level taxa from genus to phylum were significantly more abundant in the *H. pylori* negative group. In summary, *H. pylori* colonization

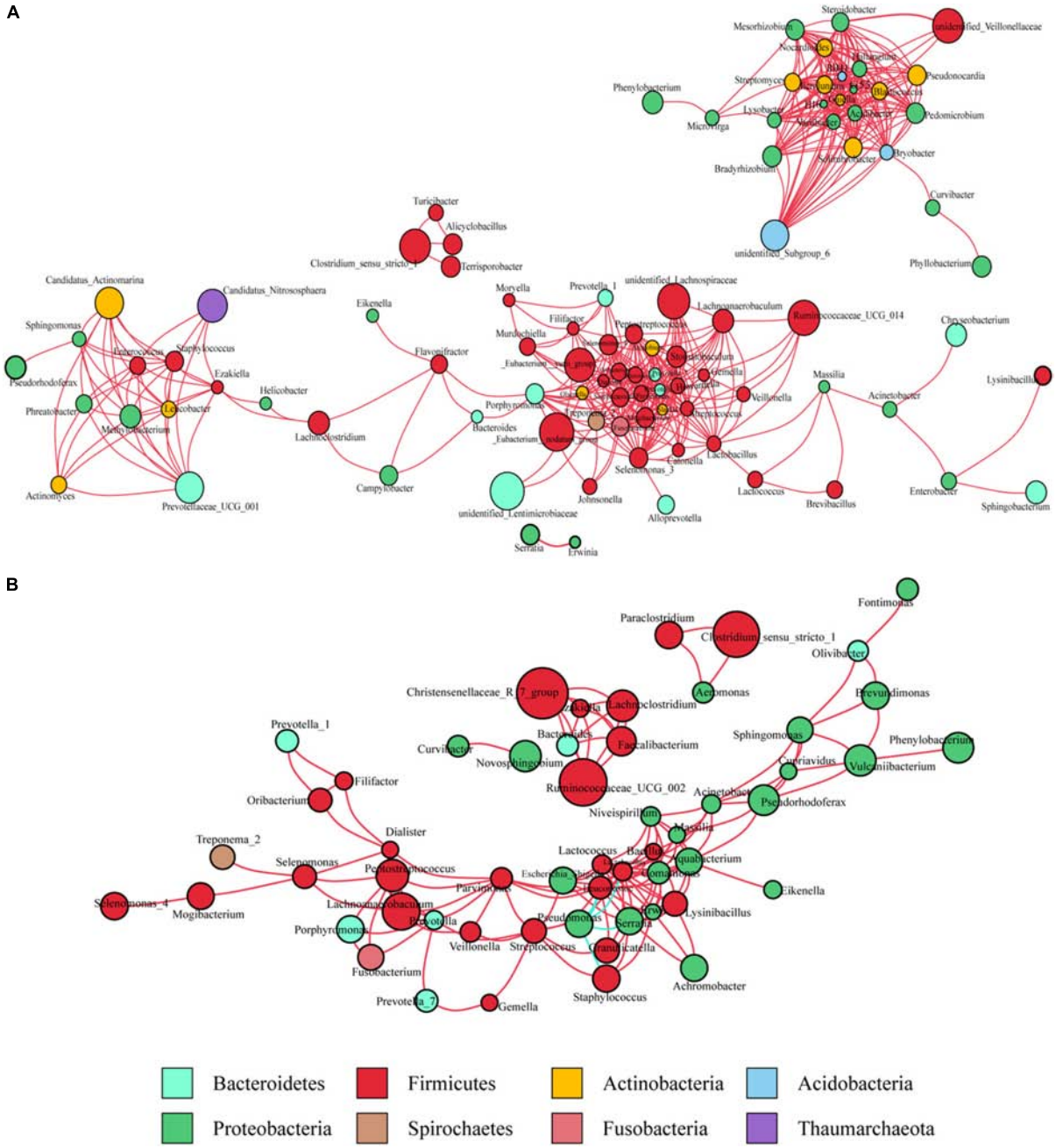

FIGURE 1 | Co-occurrence network analysis of gastric bacterial genera with correlation coefficient >0.6 or < –0.6 **(A)** in cancer tissues and **(B)** non-cancer tissues. The nodes represent different genera, whose colors indicates different phyla. The size of node shows relative abundance of the genus. Positive and negative correlations are drawn in red and blue, respectively.

status, which is a well-known epidemiological risk factor for GC, was closely associated with the composition and structure of the gastric microbiota.

Ecological Network of Gastric Microbiota in Non-cancerous Tissues

As observed in the cancerous tissue samples, the interactions within the microbiota of the non-cancerous samples also occurred mainly in the two taxonomically dominant phyla, *Firmicutes* and *Proteobacteria*; however, fewer phyla were involved. The network diagram revealed denser and more complicated co-occurrence interactions across the microbiota in the cancerous tissues compared with the non-cancerous tissues, especially with regard to oral bacteria (such as *Streptococcus*, *Peptostreptococcus*, *Fusobacterium*, *Dialister*, and *Prevotella*) (**Figures 1A,B**). However, several co-exclusion interactions

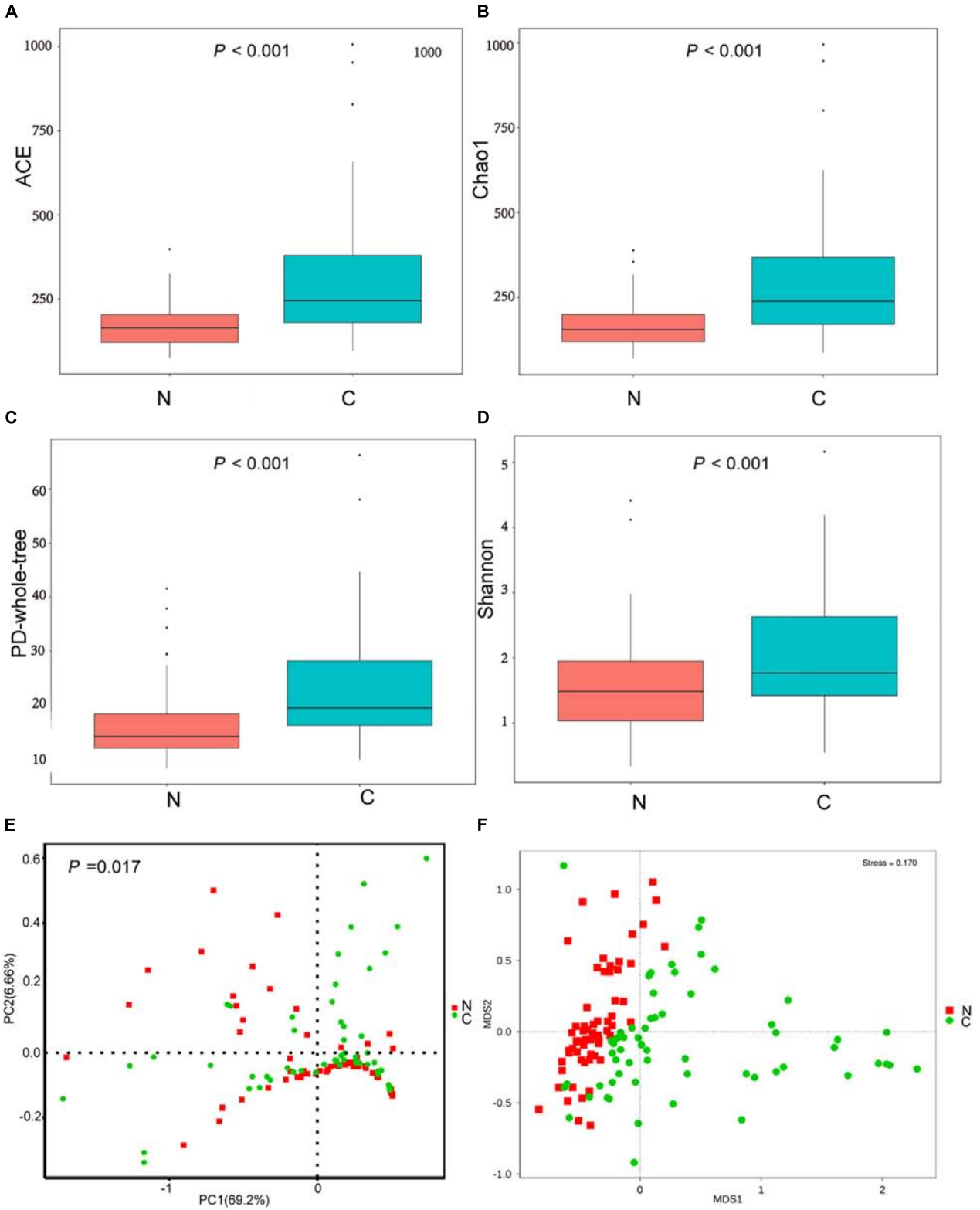

FIGURE 2 | (A–D) The alpha diversity of the microbial communities in cancer and non-cancer groups. The global microbial structure differs between the two groups in **(E)** PCoA plot and **(F)** NMDS plot. C, cancer group; N, non-cancer group.

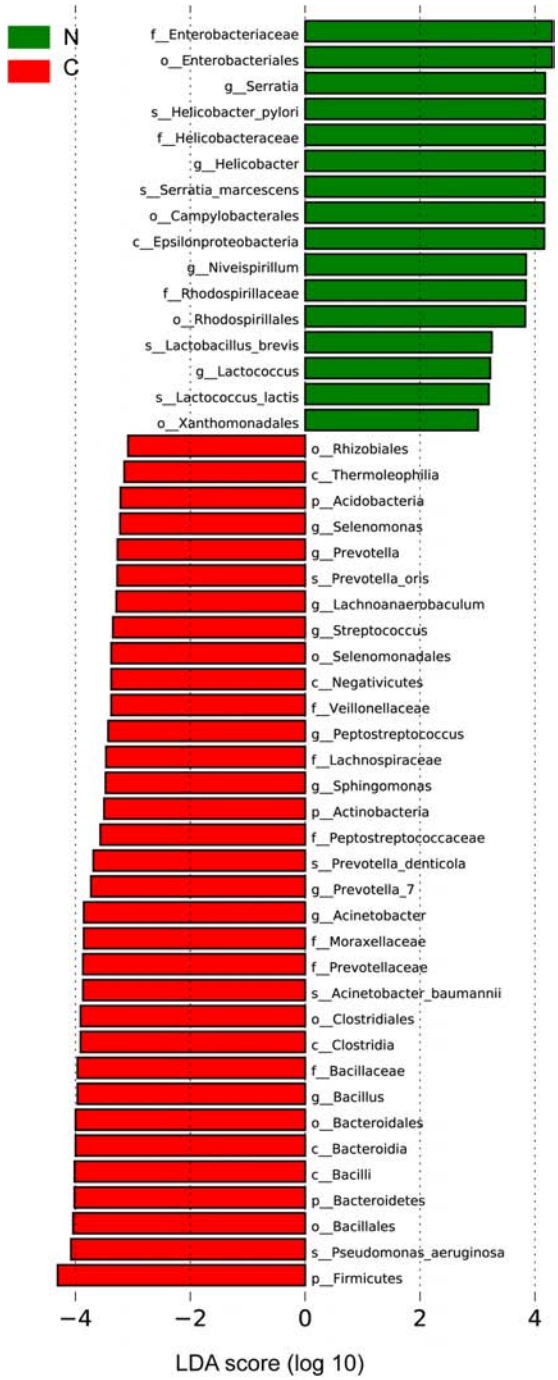

FIGURE 3 | Differential bacteria between the two groups by LEfSe analysis (LDA scores >3.0). Green indicates taxa enriched in non-cancerous tissues and red indicates taxa enriched in cancerous tissues. C, cancer group; N, non-cancer group.

were observed in the non-cancerous tissue network, with *Pseudomonas* as the interaction node. These interactions occurred among *Pseudomonas and Serratia*, *Lactobacillus*, *Lactococcus*, *Staphylococcus*, as well as *Leuconostoc*.

Differential Microbial Taxa of the GC Tissues Compared With the Non-cancerous Tissues

Bacterial Taxonomic Richness and Diversity

The cancerous tissues had a significantly higher number of OTUs than the non-cancer tissues (219 versus 148 OTUs; $P < 0.05$). In terms of alpha diversity (**Figures 2A–D**), compared with non-cancerous tissues, cancer samples had significantly increased community richness, which was estimated by Chao1 and ACE index (both $P < 0.001$), and diversity, which was estimated by Shannon index and PD whole tree (both $P < 0.001$).

Bacterial Community Structure

To analyze differences in microbial community structure between groups, we assessed the beta diversity (**Figures 2E,F**). The overall differences were visualized using PCoA and NMDS plots. The diversity described in the PCoA plots by the top two principal coordinates was 75.86% based on weighted UniFrac phylogenetic distance matrices. The non-cancerous and cancerous samples were clustered separately, with a significant difference confirmed by ANOSIM ($P = 0.017$, **Figure 2E**). The results of NMDS analysis based on OTU level also divided samples into two separate clusters (**Figure 2F**), suggesting significant differences in the overall community structure of mucosal microorganisms between the cancer and non-cancer groups.

Specific Microbial Taxa Associated With GC in the Cancer Microenvironment

We sought to identify the differential microbiota between the two sample groups, using two different methods. First, the LEfSe analysis (Segata et al., 2011) was conducted to identify the specific taxa responsible for the statistically significant differences (**Figure 3**). Overall, 49 taxa were identified as being differentially abundant between the cancer and non-cancer samples at the phylum, class, order, family, genus, and species levels (LDA = 3). 33 of them were enriched in the cancer group, including the genera *Streptococcus*, *Peptostreptococcus*, *Prevotella*, *Prevotella_7*, *Acinetobacter*, *Bacillus*, *Selenomonas*, *Lachnoanaerobaculum*, and *Sphingomonas* and the species *Acinetobacter baumannii*, *P. aeruginosa*, *Prevotella oris*, and *Prevotella denticola*, most of which were oral microbiota. 16 taxa were enriched in the non-cancer group, including the genera *Serratia*, *Helicobacter*, *Niveispirillum*, and *Lactococcus*, and the species *H. pylori*, *Serratia marcescens*, *Lactococcus lactis*, and *Lactobacillus brevis*.

Then, we used the DESeq. 2 package to calculate and compare the top 20 abundant genera with a median relative abundance >0.1% between the two groups. In addition to the eight genera (*Peptostreptococcus*, *Streptococcus*, *Acinetobacter*, *Bacillus*, *Bacteroides*, *Sphingomonas*, *Prevotella_1*, and *Prevotella_7*) described above as being enriched in the cancer group, *Fusobacterium* was also shown to be significantly more abundant in cancerous tissues. On the other hand, *Helicobacter* and *Lactobacillus* showed significant increase in the adjacent non-cancerous tissues (**Supplementary Table S5**).

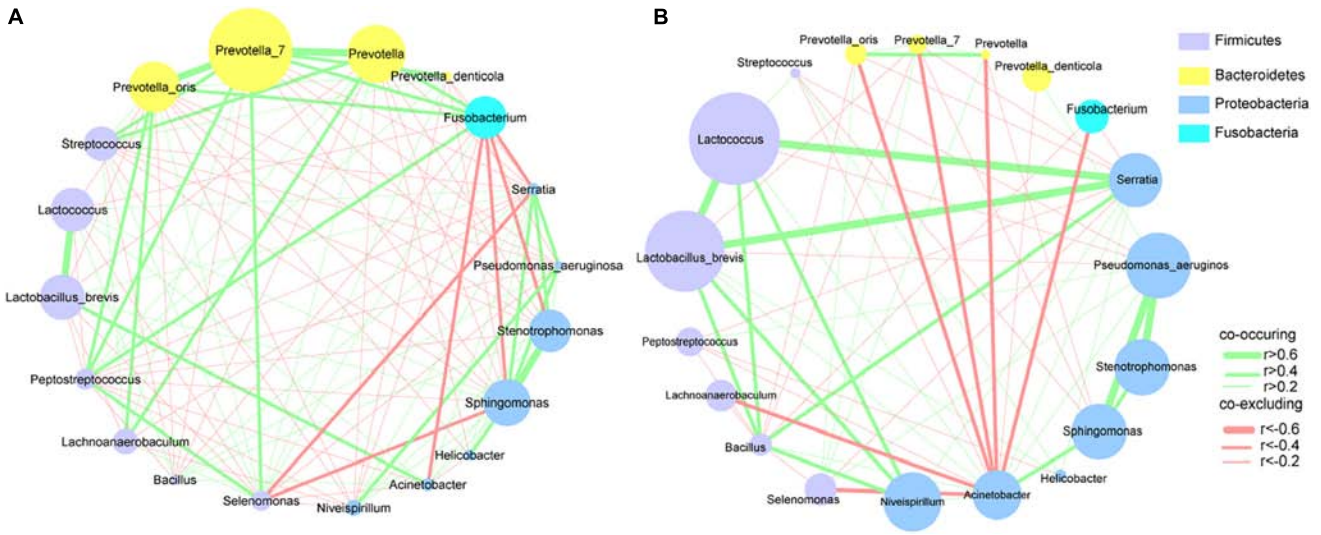

FIGURE 4 | Correlation networks of differential bacteria **(A)** in cancer and **(B)** non-cancer tissues. A subset of significant correlations with strengths of at least 0.2 were selected for visualization. The size of the nodes correspond to weighted node connectivity (WNC) scores.

To explore the interactions among these differential bacteria, the network within each group was constructed (**Figures 4A,B**). We found that co-occurrence and co-excluding interactions were significantly different between the two groups. Oral microbiota including *Prevotella*, *Prevotella_7*, *Peptostreptococcus*, *Streptococcus*, and *Fusobacterium* had higher weighted node connectivity (WNC) scores in cancerous tissues (**Figure 4A**), while *Serratia*, *Lactococcus*, and *L. brevis*, which were identified above as being enriched in non-cancer group, had higher WNC scores in non-cancer tissues (**Figure 4B**). Higher WNC scores indicated centralities and their important roles in the interaction network.

Functional Prediction of Mucosal-Associated Microbiota

Based on 16S rRNA gene sequencing data, PICRUSt was performed to predict the functional profiling of microbial communities using the KEGG databases (Langille et al., 2013). The NSTI scores (0.02–0.13) (Langille et al., 2013) demonstrated a reasonable prediction accuracy (**Supplementary Table S6**). The LEfSe algorithm was used to detect differences in the functional pathways of the microbiota between the cancer and non-cancer groups. Several metabolic pathways were enriched in the cancerous samples, including those involved in nucleotide metabolism (pyrimidine and purine metabolism), energy metabolism (methane metabolism), carbohydrate metabolism (e.g., glycolysis and gluconeogenesis), etc. (**Supplementary Figure S3**), while other predicted pathways were significantly increased in the non-cancerous samples, such as bacterial motility (motility proteins and chemotaxis), membrane transport (e.g., secretion system and phosphotransferase system), lipopolysaccharide biosynthesis and signal transduction (two component system), etc. (**Supplementary Figure S3**).

Given that the accumulation of nitrogen-containing compounds such as nitrate and nitrite in the stomach can increase the risk of GC and promote the malignant transformation of cells in the stomach (Correa, 1992; Alarcon et al., 2017), we focused on the microbial functions relevant to the metabolism of nitrogen-containing compounds in the cancerous and non-cancerous tissues. Compared with the non-cancer group, metabolic enzymes related to denitrification, including nitrate reductase (COG1116) and nitrous oxide reductase (COG4263), were enriched in the gastric microbiota of the cancer group (**Supplementary Table S7**).

DISCUSSION

Microbial communities have been universally considered as an important biological factor in the occurrence and development of GC. Recent studies have shown the changes in the microbial populations of GC patients compared with control groups (Eun et al., 2014; Coker et al., 2018; Ferreira et al., 2018; Hsieh et al., 2018). However, microbial profiles in the tumor microenvironment were still unclear. Our findings confirmed that gastric mucosa-associated microbiota from cancerous and adjacent non-cancerous tissues established distinct micro-ecological systems. We observed significant microbial community disturbances in the cancer lesions, where the richness and diversity of the microbial communities increased significantly, the interaction network exhibited greater complexity, and the relative abundance of *H. pylori* decreased compared with non-cancerous tissues. The bacterial taxa enriched in the cancer group mostly consisted of oral bacteria (such as *Peptostreptococcus*, *Streptococcus*, and *Fusobacterium*), while lactic acid-producing bacteria (such as *L. lactis*, and *L. brevis*) were more abundant in the adjacent non-tumor tissues.

These results suggest that the occurrence and development of GC disturbs the structure of the endogenous bacterial community, and that *H. pylori* might play a limited role in the development and/or progression of malignant tumors.

Characteristics of Mucosal-Associated Microbiota in GC and Non-cancerous Tissues

Changes in localized niches in GC patients result from long-term interactions among microorganisms, the host, and the environment. Shifts in gastric acidity and nutrient availability, as well as the innate immune response all contribute to the disruption of the microbial ecological balance in GC patients, leading to the colonization and overgrowth of non-*H. pylori* bacteria (Brawner et al., 2014). Gastric microbiota in cancerous and adjacent non-cancerous tissues were both dominated by *Proteobacteria* at the phylum level. The significant differences between the two groups mainly occurred at the genus and species level. Oral bacteria such as *Fusobacterium*, *Streptococcus*, *Peptostreptococcus*, and *Prevotella* were enriched in cancerous tissues. On the other hand, *Serratia* and lactic acid producing bacteria such as *Lactococcus* and *Lactobacillus* were more abundant in non-cancer group. Importantly, we identified some differential taxa that have not been reported in gastric microbiota studies before, such as *P. denticola*, *P. aeruginosa*, and *Serratia*. Although *Streptococcus*, *Peptostreptococcus*, *Fusobacterium*, and *Lactobacillus* have been discussed in recent studies of GC (Castano-Rodriguez et al., 2017; Hsieh et al., 2018), our research is the first to identify their abundance differences in the tumor microenvironment.

Our results highlight the possible pathogenic role of oral microbiota in GC. The changed acidity environment of GC may provide increased opportunities for oral bacteria to colonize the gastrointestinal tract. Previous studies have shown that oral bacteria were associated with colorectal cancer (CRC; Nakatsu et al., 2015) and pancreatic cancer (Michaud, 2013), which attracted widespread attention. Patients with certain oral pathogens had a higher risk of developing pancreatic cancer (Ertz-Archambault et al., 2017). There has been no studies directly analyzing changes in the oral microbiota of GC patients. A more in-depth investigation is needed to characterize its role as a driver or passenger in carcinogenicity. Whether oral microbes could be used as a non-invasive diagnostic marker for GC requires further studies.

It is noteworthy that *Fusobacterium* was more abundant in GC specimens than non-cancerous tissues. *Fusobacterium* is a genus of anaerobic bacteria closely related to CRC. Increasing evidence has shown its roles in carcinogenesis, diagnosis, progression and prognosis of CRC (Zhang et al., 2018). A recent report revealed that *Fusobacterium* species were over-represented in GC patients, and that it could be used as a diagnostic marker for GC. It supported our findings, despite being based on a relatively small cohort (11 GC patients vs. 16 controls) (Hsieh et al., 2018).

Previous reports had shown the significant increase in the abundance of *Lactobacillus* species in GC compared with the control population (Aviles-Jimenez et al., 2014; Eun et al., 2014; Wang et al., 2016; Castano-Rodriguez et al., 2017). However, changes in lactic acid producing bacteria in the tumor microenvironment were previously unknown. We observed an obvious enrichment of lactic acid producing bacteria (such as *L. lactis* and *L. brevis*) in non-cancerous tissues compared with cancerous tissues. *Lactococcus* and *Lactobacillus* species are generally thought of as probiotics and considered beneficial to the host. Reports show that lactic acid production has immunomodulative, anti-cancer and anti-inflammatory activities, and is conducive to the eradication therapy of *H. pylori* (Kim et al., 2014; Han et al., 2015; Kanayama et al., 2018). Another noteworthy taxon enriched in the non-cancer tissues here was *S. marcescens*, which has not been reported in cancer-related microbiota research before. Prodigiosin, a secondary metabolite of *S. marcescens*, could induce GC cell apoptosis and inhibit human oral squamous carcinoma cell growth *in vitro* (Diaz-Ruiz et al., 2001; Cheng et al., 2017).

Correlation Between Microbial Community Characteristics and GC Risk Factors

Results of association analyses between epidemiological risk factors and gastric microbiota revealed an increased Shannon's diversity in the older patients (≥60 years old). This may be due to the overall decline in immunity associated with age, and the elevated pH caused by local mucosal atrophy, both of which are conducive to bacterial growth (Sheh and Fox, 2013). We also showed that sex, smoking, drinking, and family history of upper gastrointestinal cancer were not significantly associated with microbial community characteristics. In addition, *H. pylori* colonization changed the microbial community structure, with a significant increase in alpha diversity, which was observed in *H. pylori* sequencing-positive group compared with negative group. This finding is supported by a previous report showing that the abundance of *H. pylori* can remarkably affect the diversity of the gastric microbiota (Wang et al., 2016). How *H. pylori* impacts on the diversity and structure of the gastric microbiota is not yet understood. Nevertheless, it is plausible that changes in the gastric niche induced by *H. pylori* may influence the colonization and growth of other microbes.

Ecological Networks of Microbial Taxa in Cancer and Adjacent Mucosal Tissues

The microbiota inhabiting the mucosal surface affects the development of cancer by altering the metabolome and regulating cell proliferation and tumor growth (Johnson et al., 2015). A niche-specific microbial network could affect the disease-associated microenvironment. A study has shown stronger interactions among differential OTUs in the microbiota of GC patients compared with those in patients with precancerous lesions (superficial gastritis, atrophic gastritis, intestinal metaplasia) (Coker et al., 2018). We extended previous work by delineating the interaction networks of microbiota in cancerous and adjacent non-cancerous tissues. Our results revealed that the distribution of microbial interactions differed between cancerous and adjacent non-cancerous mucosae. In the strong correlation network ($r > 0.6$ or $r < -0.6$), compared with the non-cancer group, more microbial taxa

were involved in the cancer group. And they formed a denser and more complex association network, in which only co-occurrence interactions were observed. This may be due to the decrease in abundance of *H. pylori*, the increased abundance of other microbes in cancerous tissues, and shifts of the local pathogenic microenvironment. The enrichment of a larger number of microbial taxa, particularly oral microbes, in the cancerous samples contributed to the formation of a disease-specific interaction network. Further, the markedly increased symbiotic interactions in the cancer group might also contribute to the maintenance of the tumor microenvironment and even affect further disease development. Interestingly, strong co-occurrence interactions formed by *Streptococcus*, *Peptostreptococcus*, *Fusobacterium*, *Dialister*, and *Prevotella*, showed the centralities of these taxa in the whole cancer group network. They also played significant roles in the network constructed of the differentially abundant bacteria. These results suggest that these oral microbiota may have major impact on the structure of the microbiota in GC patients, which deserves further investigations. On the other hand, several co-exclusion interactions presented in the whole non-cancer group network, occurred separately between *Serratia*, *Lactobacillus*, *Lactococcus* with *Pseudomonas* (as the interaction node). Moreover, *Serratia*, *Lactobacillus*, and *Lactococcus* exhibited their centralities in the network constructed of the differentially abundant bacteria. These findings show their potential protective effects.

Functional Analysis of Mucosal-Associated Microbiota in GC and Non-cancer Tissues

Our work showed differences in the predicted microbiota functions in cancerous and adjacent non-cancerous tissues. Purines are rich in the cancer microenvironment, with the capability of regulating immune cell responses and the release of cytokines (Di Virgilio, 2012). In this study, the purine metabolism pathways were enriched in the cancer group, indicating the metabolism of released purines in tumor microenvironment by GC microbiota (Coker et al., 2018). In addition, the microbiota in cancerous tissues had an increase in denitrification functions compared with non-cancerous tissues. The abundant nitrate reductase (COG1116) is associated with bacterial-mediated N-nitrosylation (Hillman, 2004), while the N-nitroso compound is a causative factor in carcinogenesis. Additionally, several pathways that facilitated host cell recognition were decreased in the microbiota of cancerous tissues, such as bacterial movement (bacterial motor proteins and chemotaxis) and bacterial signal transduction (membrane transport, etc.). To develop a deeper understanding of gastric carcinogenesis, further studies are needed to examine the significance of microbial functional variations in the GC microenvironment.

Advantages and Limitations

In this study, gastric mucosa samples were obtained from GC patients undergoing surgical treatment, thus avoiding possible oral microbial contamination that may occur during upper digestive endoscopy sampling. Our work provided insights into the composition, function and interaction network of the mucosa-associated bacterial community in the tumor microenvironment, and its links with GC risk factors. We identified specific genera and species that may be involved in gastric carcinogenesis and the maintenance of the tumor microenvironment. However, this study had several limitations. Firstly, PICRUSt, which was used for microbial functional assessment, is a predictive method by nature. Although it has been widely applied in studies of disease-associated microorganisms, this approach may not fully reflect the biological functions of the microorganisms. Furthermore, this study did not include gastric tissues from individuals without GC for comparison. However, to a certain extent, this reduced the impact of inter-subject dissimilarity. In addition, our DNA extraction protocol did not include a bead-beating step, which was an extra cell lysis process to destroy the hard-to-break cell membranes of certain species. A previous study had compared DNA extraction methods with and without a bead-beating step. The result demonstrated that the extraction method without a bead-beating step inevitably missed some taxa with hard-to-break cell membranes, however, these taxa were exceedingly rare and would not have a detrimental impact on the final results (Yu et al., 2017). The research revealed the correlation between gastric microbiota and GC, but could not determine the causal relationship. This will require follow-up animal models and cell culture experiments.

CONCLUSION

Compared with non-cancerous tissues, mucosa-associated microbiota in cancer tissues showed significant differences in distribution profile. The alterations in microbial community composition, function and ecological network in GC tissues may be involved in carcinogenesis and the maintenance of local microenvironment of GC. In future studies, we would focus on verification using a larger number of samples and multicentric populations, and extend our work into cell culture systems and animal models to examine the pathogenic roles of microorganisms in GC. These investigations into the mucosa-associated microbiota of GC patients may contribute to the development of new strategies for prevention, diagnosis, early intervention, and treatment of GC.

ETHICS STATEMENT

This study was approved by the Human Ethics Review Committee of The First Hospital of China Medical University (Shenyang, China [2012]115), and written informed consent was obtained from all patients.

AUTHOR CONTRIBUTIONS

YY contributed conceptualization, funding acquisition, project administration, writing–review, and editing. X-HC contributed data curation, investigation, formal analysis, and writing the original draft. AW contributed methodology and software. A-NC partly contributed to the validation. Y-HG contributed resources and supervision.

FUNDING

This work was supported by the National Key R&D Program of China, grant no. 2017YFC0907400 to YY, and grant no. 2017YFC0908300 to Y-HG.

SUPPLEMENTARY MATERIAL

The Supplementary Material for this article can be found online at: https://www.frontiersin.org/articles/10.3389/fmicb.2019.01261/full#supplementary-material

FIGURE S1 | Bacterial profiling plot of relative abundances of operational taxonomic units (OTUs) at the phylum level.

FIGURE S2 | LEfSe analysis in non-cancer tissues with and without *H. pylori* colonization. Green indicates taxa enriched in *H. pylori* positive group and red indicates taxa enriched in *H. pylori* negative group.

FIGURE S3 | Differences in functional compositions between the cancer and non-cancer groups by LEfSe analysis (LDA scores >2.0). Green indicates functions enriched in cancer group and red indicates functions enriched in non-cancer group. C, cancer group; N, non-cancer group.

TABLE S1 | OUT abundance table.

TABLE S2 | Sequencing data.

TABLE S3 | Association between alpha diversity indices of microbiota in cancerous tissues and GC risk factors.

TABLE S4 | Association between alpha diversity indices of microbiota in non-cancerous tissues and GC risk factors.

TABLE S5 | Significantly differential bacteria identified among the top 20 abundant genera of the cancer and non-cancer groups.

TABLE S6 | Nearest sequence taxon index (NSTI) scores for all samples.

TABLE S7 | Comparison for microbial functions associated with nitrogen-containing compound metabolism between cancer and non-cancer groups.

REFERENCES

Alarcon, T., Llorca, L., and Perez-Perez, G. (2017). Impact of the microbiota and gastric disease development by *Helicobacter pylori*. *Curr. Top. Microbiol. Immunol.* 400, 253–275. doi: 10.1007/978-3-319-50520-6_11

Aviles-Jimenez, F., Vazquez-Jimenez, F., Medrano-Guzman, R., Mantilla, A., and Torres, J. (2014). Stomach microbiota composition varies between patients with non-atrophic gastritis and patients with intestinal type of gastric cancer. *Sci. Rep.* 4:4202. doi: 10.1038/srep04202

Brawner, K. M., Morrow, C. D., and Smith, P. D. (2014). Gastric microbiome and gastric cancer. *Cancer J.* 20, 211–216. doi: 10.1097/PPO.0000000000000043

Caporaso, J. G., Kuczynski, J., Stombaugh, J., Bittinger, K., Bushman, F. D., Costello, E. K., et al. (2010). QIIME allows analysis of high-throughput community sequencing data. *Nat. Methods* 7, 335–336. doi: 10.1038/nmeth.f.303

Castano-Rodriguez, N., Goh, K. L., Fock, K. M., Mitchell, H. M., and Kaakoush, N. O. (2017). Dysbiosis of the microbiome in gastric carcinogenesis. *Sci. Rep.* 7:15957. doi: 10.1038/s41598-017-16289-16282

Chen, C., Song, X., Wei, W., Zhong, H., Dai, J., Lan, Z., et al. (2017). The microbiota continuum along the female reproductive tract and its relation to uterine-related diseases. *Nat. Commun.* 8:875.

Cheng, M. F., Lin, C. S., Chen, Y. H., Sung, P. J., Lin, S. R., Tong, Y. W., et al. (2017). Inhibitory growth of oral squamous cell carcinoma cancer via bacterial prodigiosin. *Mar. Drugs* 15:E224. doi: 10.3390/md15070224

Coker, O. O., Dai, Z., Nie, Y., Zhao, G., Cao, L., Nakatsu, G., et al. (2018). Mucosal microbiome dysbiosis in gastric carcinogenesis. *Gut* 67, 1024–1032. doi: 10.1136/gutjnl-2017-314281

Compare, D., Rocco, A., and Nardone, G. (2010). Risk factors in gastric cancer. *Eur. Rev. Med. Pharmacol. Sci.* 14, 302–308.

Correa, P. (1992). Human gastric carcinogenesis: a multistep and multifactorial process–first American cancer society award lecture on cancer epidemiology and prevention. *Cancer Res.* 52, 6735–6740.

Di Virgilio, F. (2012). Purines, purinergic receptors, and cancer. *Cancer Res.* 72, 5441–5447. doi: 10.1158/0008-5472.can-12-1600

Diaz-Ruiz, C., Montaner, B., and Perez-Tomas, R. (2001). Prodigiosin induces cell death and morphological changes indicative of apoptosis in gastric cancer cell line HGT-1. *Histol. Histopathol.* 16, 415–421. doi: 10.14670/HH-16.415

Edgar, R. (2013). UPARSE: highly accurate OTU sequences from microbial amplicon reads. *Nat. Methods* 10, 996–998. doi: 10.1038/nmeth.2604

Edgar, R. C., Haas, B. J., Clemente, J. C., Quince, C., and Knight, R. (2011). UCHIME improves sensitivity and speed of chimera detection. *Bioinformatics* 27, 2194–2200. doi: 10.1093/bioinformatics/btr381

El-Omar, E. M., Oien, K., El-Nujumi, A., Gillen, D., Wirz, A., Dahill, S., et al. (1997). *Helicobacter pylori* infection and chronic gastric acid hyposecretion. *Gastroenterology* 113, 15–24. doi: 10.1016/s0016-5085(97)70075-1

Ertz-Archambault, N., Keim, P., and Von Hoff, D. (2017). Microbiome and pancreatic cancer: a comprehensive topic review of literature. *World J. Gastroenterol.* 23, 1899–1908. doi: 10.3748/wjg.v23.i10.1899

Eun, C. S., Kim, B. K., Han, D. S., Kim, S. Y., Kim, K. M., Choi, B. Y., et al. (2014). Differences in gastric mucosal microbiota profiling in patients with chronic gastritis, intestinal metaplasia, and gastric cancer using pyrosequencing methods. *Helicobacter* 19, 407–416. doi: 10.1111/hel.12145

Fadrosh, D. W., Ma, B., Gajer, P., Sengamalay, N., Ott, S., Brotman, R. M., et al. (2014). An improved dual-indexing approach for multiplexed 16S rRNA gene sequencing on the Illumina MiSeq platform. *Microbiome* 2: 6. doi: 10.1186/2049-2618-2-6

Ferlay, J., Soerjomataram, I., Dikshit, R., Eser, S., Mathers, C., Rebelo, M., et al. (2015). Cancer incidence and mortality worldwide: sources, methods and major patterns in GLOBOCAN 2012. *Int. J. Cancer* 136, E359–E386. doi: 10.1002/ijc.29210

Ferreira, R. M., Pereira-Marques, J., Pinto-Ribeiro, I., Costa, J. L., Carneiro, F., Machado, J. C., et al. (2018). Gastric microbial community profiling reveals a dysbiotic cancer-associated microbiota. *Gut* 67, 226–236. doi: 10.1136/gutjnl-2017-314205

Gill, S. R., Pop, M., Deboy, R. T., Eckburg, P. B., Turnbaugh, P. J., Samuel, B. S., et al. (2006). Metagenomic analysis of the human distal gut microbiome. *Science* 312, 1355–1359. doi: 10.1126/science.1124234

Han, K. J., Lee, N. K., Park, H., and Paik, H. D. (2015). Anticancer and anti-inflammatory activity of probiotic *Lactococcus lactis* NK34. *J. Microbiol. Biotechnol.* 25, 1697–1701. doi: 10.4014/jmb.1503.03033

Hillman, B. (2004). *Role of Gut Bacteria in Human Toxicology and Pharmacology*. Boca Raton, FL: CRC Press.

Hsieh, Y. Y., Tung, S. Y., Pan, H. Y., Yen, C. W., Xu, H. W., Lin, Y. J., et al. (2018). Increased abundance of *Clostridium* and *Fusobacterium* in gastric microbiota of patients with gastric cancer in Taiwan. *Sci. Rep.* 8:158. doi: 10.1038/s41598-017-18596-18590

Johnson, C. H., Dejea, C. M., Edler, D., Hoang, L. T., Santidrian, A. F., Felding, B. H., et al. (2015). Metabolism links bacterial biofilms and colon carcinogenesis. *Cell Metab.* 21, 891–897. doi: 10.1016/j.cmet.2015.04.011

Kanayama, M., Kato, Y., Tsuji, T., Konoeda, Y., Hashimoto, A., Kanauchi, O., et al. (2018). Enhancement of immunomodulative effect of lactic acid bacteria on plasmacytoid dendritic cells with sucrose palmitate. *Sci. Rep.* 8:3147. doi: 10.1038/s41598-018-21527-21522

Kim, J., Kim, N., Jo, H. J., Park, J. H., Nam, R. H., Seok, Y. J., et al. (2015). An appropriate cutoff value for determining the colonization of *Helicobacter pylori* by the pyrosequencing method: comparison with conventional methods. *Helicobacter* 20, 370–380. doi: 10.1111/hel.12214

Kim, J. E., Kim, M. S., Yoon, Y. S., Chung, M. J., and Yum, D. Y. (2014). Use of selected lactic acid bacteria in the eradication of *Helicobacter pylori* infection. *J. Microbiol.* 52, 955–962. doi: 10.1007/s12275-014-4355-y

Langille, M. G., Zaneveld, J., Caporaso, J. G., McDonald, D., Knights, D., Reyes, J. A., et al. (2013). Predictive functional profiling of microbial communities using 16S rRNA marker gene sequences. *Nat. Biotechnol.* 31, 814–821. doi: 10.1038/nbt.2676

Leach, S. A., Thompson, M., and Hill, M. (1987). Bacterially catalysed N-nitrosation reactions and their relative importance in the human stomach. *Carcinogenesis* 8, 1907–1912. doi: 10.1093/carcin/8.12.1907

Lertpiriyapong, K., Whary, M. T., Muthupalani, S., Lofgren, J. L., Gamazon, E. R., Feng, Y., et al. (2014). Gastric colonisation with a restricted commensal microbiota replicates the promotion of neoplastic lesions by diverse intestinal microbiota in the *Helicobacter pylori* INS-GAS mouse model of gastric carcinogenesis. *Gut* 63, 54–63. doi: 10.1136/gutjnl-2013-305178

Liu, Z., Li, J., Liu, H., Tang, Y., Zhan, Q., Lai, W., et al. (2018). The intestinal microbiota associated with cardiac valve calcification differs from that of coronary artery disease. *Atherosclerosis* 284, 121–128. doi: 10.1016/j.atherosclerosis.2018.11.038

Lofgren, J. L., Whary, M. T., Ge, Z., Muthupalani, S., Taylor, N. S., Mobley, M., et al. (2011). Lack of commensal flora in *Helicobacter pylori*-infected INS-GAS mice reduces gastritis and delays intraepithelial neoplasia. *Gastroenterology* 140, 210–220. doi: 10.1053/j.gastro.2010.09.048

Magoč, T., and Salzberg, S. (2011). FLASH: fast length adjustment of short reads to improve genome assemblies. *Bioinformatics* 27, 2957–2963. doi: 10.1093/bioinformatics/btr507

Michaud, D. S. (2013). Role of bacterial infections in pancreatic cancer. *Carcinogenesis* 34, 2193–2197. doi: 10.1093/carcin/bgt249

Mowat, C., Williams, C., Gillen, D., Hossack, M., Gilmour, D., Carswell, A., et al. (2000). Omeprazole, *Helicobacter pylori* status, and alterations in the intragastric milieu facilitating bacterial N-nitrosation. *Gastroenterology* 119, 339–347. doi: 10.1053/gast.2000.9367

Nakatsu, G., Li, X., Zhou, H., Sheng, J., Wong, S. H., Wu, W. K., et al. (2015). Gut mucosal microbiome across stages of colorectal carcinogenesis. *Nat. Commun.* 6:8727. doi: 10.1038/ncomms9727

Parks, D. H., Tyson, G. W., Hugenholtz, P., and Beiko, R. G. (2014). STAMP: statistical analysis of taxonomic and functional profiles. *Bioinformatics* 30, 3123–3124. doi: 10.1093/bioinformatics/btu494

Plottel, C. S., and Blaser, M. J. (2011). Microbiome and malignancy. *Cell Host. Microbe* 10, 324–335. doi: 10.1016/j.chom.2011.10.003

Segata, N., Izard, J., Waldron, L., Gevers, D., Miropolsky, L., Garrett, W., et al. (2011). Metagenomic biomarker discovery and explanation. *Genome Biol.* 12:R60. doi: 10.1186/gb-2011-12-6-r60

Sheh, A., and Fox, J. G. (2013). The role of the gastrointestinal microbiome in *Helicobacter pylori* pathogenesis. *Gut Microbes* 4, 505–531. doi: 10.4161/gmic.26205

Torre, L. A., Bray, F., Siegel, R. L., Ferlay, J., Lortet-Tieulent, J., and Jemal, A. (2015). Global cancer statistics, 2012. *CA Cancer J. Clin.* 65, 87–108. doi: 10.3322/caac.21262

Wang, L., Zhou, J., Xin, Y., Geng, C., Tian, Z., Yu, X., et al. (2016). Bacterial overgrowth and diversification of microbiota in gastric cancer. *Eur. J. Gastroenterol. Hepatol.* 28, 261–266. doi: 10.1097/meg.0000000000000542

Weiss, S., Xu, Z. Z., Peddada, S., Amir, A., Bittinger, K., Gonzalez, A., et al. (2017). Normalization and microbial differential abundance strategies depend upon data characteristics. *Microbiome* 5:27. doi: 10.1186/s40168-017-0237-y

Wroblewski, L. E., Peek, R. M. Jr., and Wilson, K. T. (2010). *Helicobacter pylori* and gastric cancer: factors that modulate disease risk. *Clin. Microbiol. Rev.* 23, 713–739. doi: 10.1128/cmr.00011-10

Yu, G., Torres, J., Hu, N., Medrano-Guzman, R., Herrera-Goepfert, R., Humphrys, M. S., et al. (2017). Molecular characterization of the human stomach microbiota in gastric cancer patients. *Front. Cell. Infect. Microbiol.* 7:302. doi: 10.3389/fcimb.2017.00302

Zhang, S., Cai, S., and Ma, Y. (2018). Association between *Fusobacterium nucleatum* and colorectal cancer: progress and future directions. *J. Cancer* 9, 1652–1659. doi: 10.7150/jca.24048

Conflict of Interest Statement: The authors declare that the research was conducted in the absence of any commercial or financial relationships that could be construed as a potential conflict of interest.

frontiers in Microbiology

REVIEW
published: 25 June 2019
doi: 10.3389/fmicb.2019.01050

Gut Microbiota Shapes the Efficiency of Cancer Therapy

Weidong Ma[1,2,3†], Qixing Mao[1,2†], Wenjie Xia[1,2,4†], Gaochao Dong[1,4], Changhua Yu[3] and Feng Jiang[1,4*]*

[1] Department of Thoracic Surgery, Jiangsu Cancer Hospital, Jiangsu Institute of Cancer Research, Nanjing Medical University Affiliated Cancer Hospital, Nanjing, China, [2] The Fourth Clinical College of Nanjing Medical University, Nanjing, China, [3] Department of Radiotherapy, Huai'an First People's Hospital, Nanjing Medical University, Huai'an, China, [4] Jiangsu Key Laboratory of Molecular and Translational Cancer Research, Nanjing Medical University Affiliated Cancer Hospital, Cancer Institute of Jiangsu Province, Nanjing, China

OPEN ACCESS

Edited by:
Gary Moran,
Trinity College Dublin, Ireland

Reviewed by:
Till Strowig,
Helmholtz Center for Infection Research, Helmholtz Association of German Research Centers (HZ), Germany
Haralampos Hatzikirou,
Helmholtz Center for Infection Research, Helmholtz Association of German Research Centers (HZ), Germany

***Correspondence:**
Changhua Yu
1131603215@qq.com
Feng Jiang
zengnljf@hotmail.com

[†] These authors have contributed equally to this work

Specialty section:
This article was submitted to Systems Microbiology, a section of the journal Frontiers in Microbiology

Received: 12 November 2018
Accepted: 25 April 2019
Published: 25 June 2019

Citation:
Ma W, Mao Q, Xia W, Dong G, Yu C and Jiang F (2019) Gut Microbiota Shapes the Efficiency of Cancer Therapy. Front. Microbiol. 10:1050. doi: 10.3389/fmicb.2019.01050

Systems biology provides an opportunity to discover the role that gut microbiota play in almost all aspects of human health. Existing evidence supports the hypothesis that gut microbiota is closely related to the pharmacological effects of chemical therapy and novel targeted immunotherapy. Gut microbiota shapes the efficiency of drugs through several key mechanisms: metabolism, immunomodulation, translocation, enzymatic degradation, reduction of diversity, and ecological variability. Therefore, gut microbiota have emerged as a novel target to enhance the efficacy and reduce the toxicity and adverse effects of cancer therapy. There is growing evidence to show that cancer therapy perturbs the host immune response and results in dysbiosis of the immune system, which then influences the efficiency of the therapy. Studies suggest that gut microbes play a significant role in cancer therapy by modulating drug efficacy, abolishing the anticancer effect, and mediating toxicity. In this review, we outline the role of gut microbiota in modulating cancer therapy and the implications for improving the efficacy of chemotherapy and immunotherapy in clinical practice. We also summarize the current limitations of the safety and effectiveness of probiotics in cancer therapies such as personalized cancer therapy.

Keywords: gut microbiome, cancer therapy, immunotherapy, chemotherapy, radiotherapy

INTRODUCTION

Microbial communities have evolved into a diverse array of specialized lineages in order to adapt to different habitats and which have shaped the evolution of modern life (Dzutsev et al., 2017). The development of next generation sequencing has made the identification and relative quantitation of species more precise than can be acheieved by traditional methods. Thus, microbiotic responses to microenvironmental changes are being elucidated.

Gut microbes have a role in shaping normal and pathologic immune responses to cancer therapy. A host's mucosal immune system and microbial communities are coevolutionary, and multiple mechanisms have been developed for maintaining homeostasis. However, when pathogenic bacteria disturb this tightly balanced ecosystem, the immune system responds to the bacteria and may also change the immune response to tumors and the tumor microenvironment (Gagliani et al., 2014). As surgical treatment and chemotherapy and radiotherapy regimens become increasingly efficacious, cancer survival rates have dramatically improved in recent decades

(Siegel et al., 2018). For most patients with advanced disease, cytotoxic drugs are the mainstay of medical treatment. However, these drugs can cause considerable treatment-related morbidity and mortality and unpredictable treatment response. Idiosyncratic adverse effects, acquired resistance, and high costs are issues for targeted therapies. Intestinal microbiota can provide a novel way to enhance the efficacy and reduce the toxicity of current chemotherapeutic drugs and improve sensitivity to immunotherapy.

The host's diet feeds and shapes the microbiome to satisfy the nutritional needs of the host (Dzutsev et al., 2017). In the metaorganism, crosstalk between host and commensal microbes is beneficial to the maintenance of physiological homeostasis (Dzutsev et al., 2017). It is widely accepted that microbiota at the epithelial barrier affect host systemic functions such as nutrition, metabolism, energy balance, inflammation, and adaptive immunity (Cryan and Dinan, 2012; Zeevi et al., 2015). The microbiota do not usually elicit a proinflammatory immune response because the host mucosal immune system coevolves with commensal organisms. Hosts have developed multiple mechanisms to maintain ecological balance.

When pathogenic bacteria disturb this balanced ecosystem and impair these mechanisms, the responses of the immune system to the microbiota may also change the immune response. Gut microbes can, therefore, shape normal and pathologic immune responses to cancer therapy. Recent human clinical studies, meta-analyses of clinical studies, and preclinical studies using cell culture and animal models have revealed that gut microbiota play various roles in the host response to different anticancer drugs. One of the central mechanisms may be immunomodulation. Dysbiosis may be both the result of tumor therapy and the cause of differential responses to tumor therapy (Bhatt et al., 2017). Here, we outline how gut bacteria influence the effects of chemotherapy and immunotherapy (**Table 1**).

GUT MICROBIOTA AND THE EFFICIENCY OF CANCER THERAPIES (INCLUDING CHEMOTHERAPY, RADIOTHERAPY, AND IMMUNOTHERAPY)

Immunotherapy

Immunotherapy has been very successful in the treatment of cancer. Identification and killing of tumor cells partly depends on T cell-mediated cellular immunity. T cells, through T cell receptors (TCR), combine with a specific antigen of the major histocompatibility complex (MHC) on the surface of tumor cells. The interaction of TCR and MHC molecules is controlled by a series of immune checkpoints, with costimulatory signals and coinhibitory signals that can activate or inhibit T cells. Cytotoxic T lymphocyte-associated protein 4 (CTLA-4), programmed cell death 1 (PD-1), and PD-1 ligand (PD-L1) are coinhibitory molecules that can restrain the immune response to prevent autoimmune diseases. In the tumor microenvironment, stromal cells and cancer cells often overexpress coinhibitory ligands and receptors. PD1 and its ligand PD-L1 play important roles in immune tolerance. Their binding can transmit coinhibitory signals that inhibit the immune activity of T cells and can cause immune escape of tumor cells (Sharma and Allison, 2015). To date, CTLA-4 and the PD-1/PD-L1 axis (mAb-mediated blockade of two checkpoints) have produced the greatest clinical success (Sharma and Allison, 2015). Monoclonal antibodies against PD-1 (nivolumab), PD-L1 (pembrolizumab), and CTLA-4 (ipilimumab) have already received FDA approval for several cancers. These monoclonal antibodies can reactivate the patient's own immune response against tumors. These antibodies have been highly effective for treating Hodgkin lymphoma, melanomas, kidney cancer, lung cancer, and bladder cancer. Although these findings are promising, patients' responses to checkpoint inhibitors have considerable inter-individual variation, as seen with other cancer therapies (Vétizou et al., 2015; Pitt et al., 2016a,b). The cause of this heterogeneity in response remains unclear, however, and elucidating the cause could boost the efficacy of treatment and expand the respondent population. Interestingly, recent human clinical studies and preclinical trials have suggested that the efficacy of checkpoint inhibitors is affected by patients' gut microbiota. The observed variation in clinical responses may be explained by the interaction between the gut microbiota and immune checkpoint inhibitors (Sivan et al., 2015; Vétizou et al., 2015).

Sivan et al. (2015) used mouse models of melanoma and found that gut microbiota accounted for the variation in clinical responses to immune checkpoint inhibitors. They noted that different laboratory mice had different tumor growth speeds and that tumors grew more slowly and responded more effectively to anti-PD-L1 in Jackson Laboratory (JAX) mice than in Taconic mice. These mice had the same genetic background, but their microbial compositions were distinct. When JAX donors' fecal microbiota was transplanted into Taconic recipients, anti-PD-L1 antitumor efficacy was enhanced. *Bifidobacterium* was identified as being crucial, and feeding *Bifidobacterium* alone could enhance anti-PD-L1 efficacy by reactivating dendritic cells that boosted CD8-positive T cell responses to defeat tumors (Sivan et al., 2015).

Zitvogel et al. (Routy et al., 2018) revealed an interesting phenomenon in which antibiotics made patients relapse sooner and shortened their survival. Patients who did not receive antibiotics before, or soon after, anti-PD1 had a better response to anti-PD-L1 (Routy et al., 2018). Based on an analysis of the microbiota composition of 100 lung and renal cancer patients treated with anti-PD1 gut microbiota in both Europe and the United States, the bacterial species *Akkermansia muciniphila* was shown to be significantly more abundant in anti-PD1 responders (R) than non-responders (NR) (Routy et al., 2018). To determine whether gut microbiota play a key role in the different responses to anti-PD1, the researchers transplanted the patients' fecal microbiota into antibiotic-treated mice or germ-free mice and noted that these mice acquired the same ability to respond to immune checkpoint blockade (ICB). The studies also showed a higher frequency of *Enterococcus hirae* in R patients and a trend of higher representation of *Corynebacterium aurimucosum* and *Staphylococcus haemolyticus* in NR patients (Routy et al., 2018).

TABLE 1 | Summary of the effects of gut microbiota on tumor treatment.

Therapy	Side effect	Relevant mechanism
Irinotecan	Diarrhea	Microbiota can reactivate SN38 by secreting b-glucuronidase enzymes (Lin et al., 2012)
Doxorubicin	Intestinal mucositis	Significant changes in microbiota occur in the oral cavity and the intestinal tract (Napeñas et al., 2010; Rigby et al., 2016)
5-FU	Intestinal dysbiosis	*Staphylococcus* and *Clostridium* species increase and *Bacteroides* and *Lactobacillus* decrease (Stringer et al., 2009b)
Ionizing radiation therapy	Oral mucositis, enteritis, colitis, diarrhea and bone marrow failure	RTX alters the microbiota composition, breaks the intestinal barrier and causes apoptosis in intestinal crypts (Barker et al., 2015)
Total body irradiation	Radiotherapy toxicity	The expression of ANGPTL4 is restrained by the gut microbiota to induce apoptosis in endothelial cells of the intestinal mucosa (Crawford and Gordon, 2005)

NR patients' fecal microbiome could not replicate the mouse response to anti-PD1, but the unresponsiveness could be rescued by gavage with *A. muciniphila* alone or in combination with *E. hirae* (Routy et al., 2018). *A. muciniphila* can cause IL-12 production and increase gut-tropic CD4+ T cells, which express the chemokine receptor CCR9 in tumor beds, tumor-draining lymph nodes, and mesenteric lymph nodes to exert an adjuvant effect on the anti-PD1 response. *A. muciniphila* is an elliptic gram-negative bacterium that preferentially colonizes the mucus layer of the gut. Studies have shown that metformin improves the abundance of intestinal *A. muciniphila* (Lee et al., 2017). These findings suggest that metformin could be used to increase the sensitivity of tumor patients to immune checkpoint inhibitors. Additional research is needed to confirm this finding.

Wargo et al. (Gopalakrishnan et al., 2018) at the MD Anderson Cancer Center explored *Faecalibacterium* species enriched in R patients by 16S rRNA gene sequencing in 25 samples from melanoma patients treated with anti-PD1 (Vétizou et al., 2015; Gopalakrishnan et al., 2018). *Faecalibacterium* showed a significant positive correlation with progression-free survival, while *Bacteroidales* increased the risk of relapse. Patients with a higher abundance of *Faecalibacterium* at the treatment baseline had preexisting anticancer immune responses, and a higher number of cytotoxic CD8 + T cells were found to have infiltrated the tumor bed. This result could be replicated in a mouse model. In a similar case, Gajewskis et al. (Matson et al., 2018) (University of Chicago, IL, United States) analyzed 38 fecal samples from metastatic melanoma patients undergoing anti-PD1 treatment and identified that *Bifidobacterium longum*, *Enterococcus faecium*, and *Collinsella aerofaciens* contributed to a better prognosis. Germ-free mice with an R patient fecal microbiota transfer had better tumor control and responded more strongly to anti-PD-L1 (Matson et al., 2018).

Together, these studies demonstrate that the response to ICB (PD1/PDL1) is regulated by gut microbiota (**Figure 1**). From these studies, we can conclude that at least three species (*Bifidobacterium*, *A. muciniphila*, *Faecalibacterium*) play an immune adjuvant role in the immunotherapy of PD-1. There may be more bacteria that play important roles in promoting or inhibiting the efficacy of checkpoint inhibitors, but these hypotheses need to be further examined. Overall, we can conclude that a healthy and diverse microbiota and the presence of some bacterial species contribute to the antitumor immune response. The efficacy of ICB was reduced when patients received antibiotic treatment before or soon after immune therapy. This finding provides new insight and ideas for the use of antibiotics in clinical treatment. In addition, it is obvious that not only single species but also the ecology and metabolism of the gut microbiota affect the response to immune therapy. It is possible that a new therapy targeting the microbiota could be developed to improve cancer treatment.

In terms of CTLA4, Vétizou et al. (2015) found that the microbiome experienced a rapid change when patients received anti-CTLA-4 and that the abundance of *Bacteroidales* and *Burkholderiales* decreased, while that of *Clostridiales* increased in the gut (Vétizou et al., 2015). Germ-free mice had a minor response to anti-CTLA-4 immunotherapy, but oral feeding of either *Bacteroides thetaiotaomicron* or *Bacteroides fragilis* to germ-free mice restored the therapeutic response to anti-CTLA4. Studies revealed that *B. thetaiotaomicron* and *B. fragilis* can trigger dendritic cell maturation and modulate IL-12–dependent TH 1 responses in the tumor-draining lymph nodes (Cramer and Bresalier, 2017). While the monoclonal antibody against CTLA-4 is effective, ipilimumab can cause subclinical colitis. Many factors contribute to such side effects, such as host homeostasis, immune response, and microbiota. The abundance of *Bacteroidetes* in new-onset, immune-mediated colitis patients who were administered anti-CTLA-4 therapy was significantly lower than in colitis-free individuals receiving ipilimumab (Dubin et al., 2016). The oral feeding of *B. fragilis* and *B. cepacian* to mice can restore the response to anti-CTLA4 and significantly decrease the extent of immune-mediated colitis. However, a single administration of either *B. fragilis* or *B. thetaiotaomicron* failed to produce the same effect. Moreover, Dubin et al. (2016) similarly revealed that the Bacteroidetes phylum plays a protective role against ipilimumab-associated colitis (Dubin et al., 2016). When germ-free mice receiving anti-CTLA-4 mAb were monopolized with *B. fragilis*, plasmacytoid DCs accumulated and matured in mesenteric lymph nodes, which promoted ICOS + Treg cells to proliferate in the lamina propria (Dasgupta et al., 2014; Vétizou et al., 2015). This may be a possible mechanism for the protective role of *B. fragilis* against ipilimumab-associated colitis.

Individual antibiotics play an important role in the immunotherapy of tumors and even affect the curative effects of immune agents by changing the composition of the gut microbiota. For example, when mice were administered vancomycin, the efficacy of CTLA-4 blockade was enhanced because vancomycin preserved the gram-negative

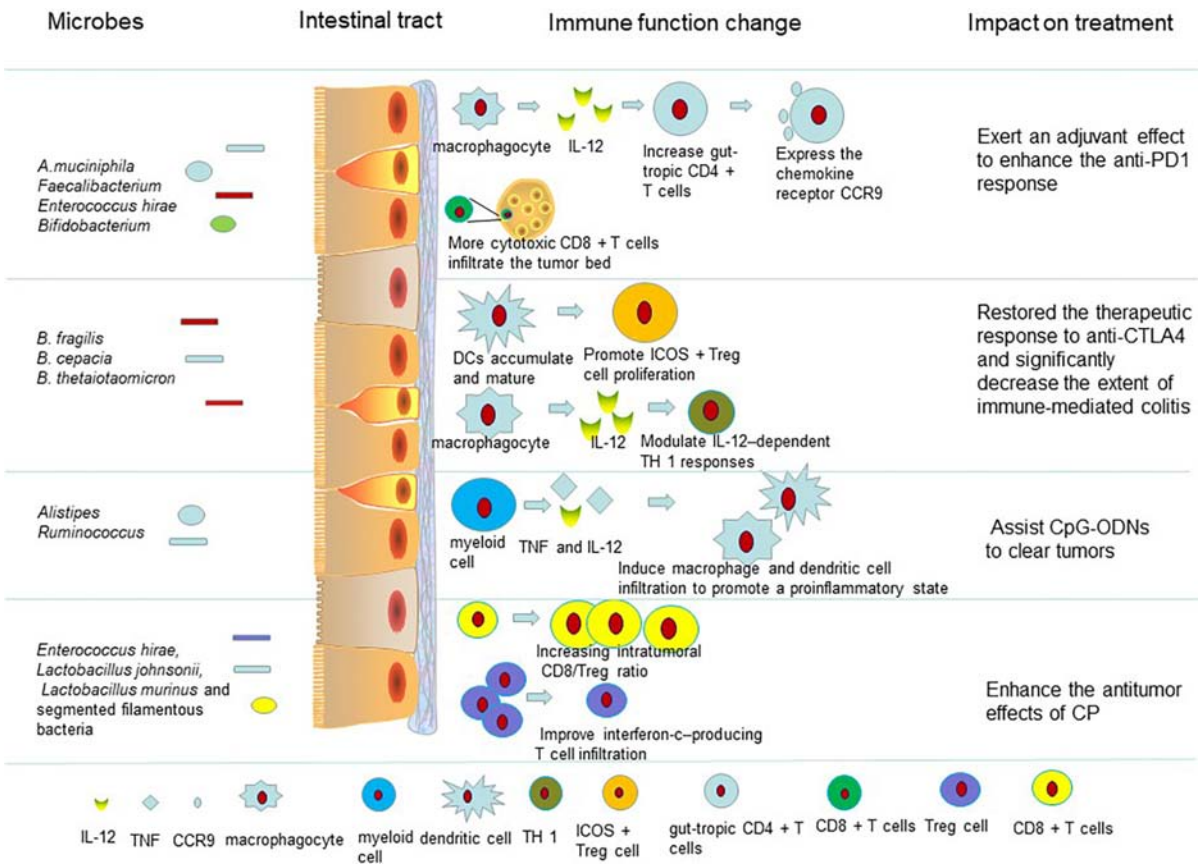

FIGURE 1 | Intestinal microbiota influence the therapeutic effect of drugs on tumors by regulating the immune system. The gut microbiota enhance anti-PD-L1 efficacy by reactivating dendritic cells. Dendritic cells can boost CD8-positive T cell responses and increase the number of gut-tropic CD4 + T cells to defeat tumors. Also the gut microbiota can trigger dendritic cell maturation and modulate IL-12–dependent TH 1 responses to restore the therapeutic response to anti-CTLA4. The microbiota are associated with side effects of immunotherapy (**Supplementary Table S1**). When germ-free mice receiving anti-CTLA-4 mAb were monopolized with *B. fragilis*, plasmacytoid DCs accumulated and matured in mesenteric lymph nodes. Dendritic cells can promote ICOS + Treg cells to proliferate in the lamina propria. The gut microbiota help CpG-ODNs to promote myeloid cells to secrete proinflammatory cytokines such as TNF and IL-12. TNF and IL-12 induce macrophage and dendritic cell infiltration to promote a proinflammatory state (**Supplementary Table S1**). The body develops an antigen-specific adaptive T cell antitumor immunity to clear tumors in this proinflammatory microenvironment. Some of the intestinal microbiota affect the antitumor efficacy of CP. *E. hirae* translocation could improve the intratumoral CD8/Treg ratio. And, the gram-negative *Barnesiella intestinihominis* was found to improve interferon-c–producing T cell infiltration in cancer lesions to enhance the antitumor effects of CP (**Supplementary Table S1**).

Burkholderiales and *Bacteroidales* and decreased gram-positive bacteria in the gut (Vétizou et al., 2015). Zitvogel et al. (Pitt et al., 2017) explored the relationship between microbiota and the efficacy of anti-CTLA-4 treatment (Pitt et al., 2017). They found that the therapeutic efficacy of ipilimumab in germ-free mice largely depended on the gut microbiota, such as the activation of CD4+ T cells with treatment (Pitt et al., 2017). Ipilimumab could alter the composition of microbiota at the genus level in both patients and mice and the dominance of distinct *Bacteroides* spp., such as *B. fragilis*, was necessary for successful treatment of cancer (Pitt et al., 2017). The feces from patients who had received ipilimumab treatment led to the recovery of anti-CTLA-4 therapeutic efficacy in germ-free mice. The researchers found that *B. fragilis* did not induce the side effects of ipilimumab (Pitt et al., 2017). As a result of these observations, we can conclude that *B. fragilis* may be used to modulate the efficacy of anti-CTLA-4 therapy.

Synthetic CpG oligonucleotides (CpG-ON) are ligands for TLR9 on immune cells, which enhance the immune response to cancer cells and induce an antitumor effect. When patients were administered IL-10 receptor antibodies to prevent the immunosuppressive effects of tumor-infiltrating Treg cells, the effect of CpG-ON was potentiated (Guiducci et al., 2005; Stewart et al., 2013). CpG-ONs promote myeloid cells to secrete proinflammatory cytokines such as TNF and IL-12. TNF and IL-12 induce macrophage and dendritic cell infiltration to promote a proinflammatory state and cause rapid hemorrhagic necrosis. The body develops an antigen-specific adaptive T cell antitumor immunity to clear tumors in this proinflammatory microenvironment (Guiducci et al., 2005). In microbiota-depleted mice, CpG-ODNs and anti-IL-10R therapy for subcutaneous tumors are largely inefficient, and tumor-infiltrating myeloid cells cannot produce proinflammatory cytokines. Microbiota-depleted mice also have

no efficient antitumor adaptive immunity and experience strong TNF-dependent hemorrhagic necrosis. However, the expression of genes encoding inflammatory factors and markers such as TNF and IL-12 was a major difference between conventionally raised mice and microbiota-depleted mice when CpG-ODNs were administered in tumor-infiltrating myeloid cell subsets. The frequencies of the gram-positive *Ruminococcus* and the gram-negative *Alistipes* genera favor TNF production. The frequencies of *Lactobacillus* sp., such as *Lactobacillus fermentum*, *Lactobacillus murinum*, and *Lactobacillus intestinalis* are negatively correlated with TNF production (Wallace et al., 2015). After mice were exposed to antibiotics, the recolonization of *Alistipes shahii* induced myeloid cells to produce TNF again in microbiota-depleted mice, but *L. fermentum* transplantation often impaired the TNF production of conventionally raised mice (Iida et al., 2013). These results indicate that different bacterial species can have opposite effects, although completely eliminating the gut microbiota abolishes the 'training' of myeloid cells to respond to CpG-ODNs. Thus, probiotics could help modulate the response to immunotherapies by changing the frequencies of individual species.

Chemotherapy

Not unexpectedly, the microbial composition of patients can be altered by chemotherapy, but it is unclear whether the altered microbiome affects a patients' prognosis. According to previous studies, the efficacy of various conventional chemotherapeutics can be influenced by some specific microbiota. Currently, the goals of the pharmaceutical and biotechnology industries are to improve the efficiency, and reduce the toxicity, of chemotherapy and immunotherapy in clinical practice. In the near future, microbial drug targets have the potential to ease the adverse effects of chemotherapy drugs on the GI tract.

The tumor-retardation effects of oxaliplatin (platinum chemotherapeutic) depend on microbiota. Oxaliplatin efficacy was attenuated due to reduced intratumoral ROS generation in germ-free mice (Iida et al., 2013). Moreover, when people were treated with antibiotics, the recruitment of immune cells that are important for mediating tumor regression was decreased, and their proinflammatory potential also decreased. This finding suggests that the microbiota mediated immunomodulatory effects in response to chemotherapeutic compounds.

Cyclophosphamide (CP) is an alkylating agent commonly used for chemotherapy. CP induces commensals to translocate into secondary lymphoid organs due to the disruption of the intestinal barrier and the decrease of small intestinal villus height. Viaud et al. (2013) found that the antitumor efficacy of CP was attenuated in germ-free mice or antibiotic-treated mice (Viaud et al., 2013). The antibiotics selectively working on gram-positive bacteria significantly reduced CP efficacy compared with antibiotics targeting gram-negative bacteria. Thus, specific gram-positive bacteria (*E. hirae*, *Lactobacillus johnsonii*, *L. murinus*, and segmented filamentous bacteria) were identified as essential to regulate the antitumor efficacy of CP in a non-metastasizing sarcoma mouse model. *E. hirae* translocation has been shown to improve the intra-tumoral CD8/Treg ratio (Iida et al., 2013). At the same time, the gram-negative *Barnesiella intestinihominis* was found to improve interferon-c–producing T cell infiltration in cancer lesions to enhance the antitumor effects of CP (Daillère et al., 2016). Interestingly, when patients with advanced ovarian and lung cancer have a specific TH 1 cell memory response to *B. intestinihominis* and *E. hirae*, they are predicted to have longer progression-free survival. Importantly, more studies should be conducted to find an optimized microbiota cocktail including *Enterococcus* and *Barnesiella* coadministered with CP and other alkylating agents. In the near future, these bacterial compounds or their specific products/metabolites that modulate the immune response may be developed to improve chemotherapeutic efficacy.

THE ROLE OF GUT MICROBIOTA IN THE TOXICITY OF CANCER THERAPY (INCLUDING CHEMOTHERAPY, RADIOTHERAPY, AND IMMUNOTHERAPY)

Chemotherapy

Some side effects resulting from chemotherapeutic compounds are so serious that patients cannot receive a sufficient dose of compounds or a sufficient duration of treatment. Irinotecan (topoisomerase I inhibitor) hinders DNA replication, particularly in rapidly dividing cells, and is administered to treat pancreatic cancer and CRC. The metabolic process of irinotecan *in vivo* is as follows: (1) irinotecan is metabolized from a prodrug into the active working chemotherapeutic agent SN38; (2) the liver glucuronidates SN38 into the inactive form SN38-G and excretes it into the GI tract. In the human gut, microbiota can reactivate SN38 by secreting b-glucuronidase enzymes that hydrolyze the glucuronic acid moiety in the GI lumen. Increased SN38 levels cause serious diarrhea, and patients often need to de-escalate and frequently adjust doses. *Clostridium* species decrease from the initial time of irinotecan therapy to recovery on day 7, but the abundance of *Bifidobacterium* and *Lactobacillus* species is persistently reduced (Lin et al., 2012). Interestingly, germ-free mice can receive more doses of irinotecan and exhibit less GI damage than conventional mice with intact microbiota (Brandi et al., 2006). Small-molecule inhibitors, which are innocuous to either human cells or bacteria, inhibit bacterial b-glucuronidases and do not cross-react with human b-glucuronidases (Wallace et al., 2010, 2015; Roberts et al., 2013). Preclinical studies revealed that mice concurrently administered irinotecan and b-glucuronidase inhibitors were free from irinotecan-induced diarrhea (Wallace et al., 2010). These findings indicate that the side effects of multiple chemotherapeutics may diminish with gut microbiota.

The relationship between intestinal dysbiosis and specific chemotherapeutic agents has been explored in animal models, and 5-fluorouracil (5-FU) is one of the best studied agents in colorectal cancer therapies. 5-FU interferes with the synthesis of thymidylate and inhibits DNA synthesis during DNA replication and repair (Longley et al., 2003). Studies have shown that mice receiving 5-FU chemotherapy exhibit dysbiosis. Specifically, the abundance of *Staphylococcus* and *Clostridium* species increased and that of *Bacteroides* and *Lactobacillus*

decreased after administration with 5-FU (Stringer et al., 2009b). Multiple animal studies showed that the abundance of Enterobacteriaceae (facultative gram-negative bacteria) increased after either irinotecan or 5-FU therapy (Stringer et al., 2009a; Takemura et al., 2014). However, these studies relied on targeted PCR or culture methods and cannot evaluate the influence of chemotherapy on the extensive gut microbiota. It is still a challenge to manipulate probiotics to treat intestinal dysbiosis in 5-FU therapy.

Severe side effects induced by doxorubicin, such as intestinal mucositis and cardiomyopathy, are related to significant changes in the microbiota of the oral cavity and the intestinal tract (Napeñas et al., 2010; Rigby et al., 2016). Studies have revealed that bacterial muramyl dipeptide prevented doxorubicin-induced mucosal damage by stimulating NOD2 (Nigro et al., 2014). Clinical practice shows that adipose tissue and fat metabolism are influenced in many tumor patients, resulting in cachexia (Das et al., 2011; de Matos-Neto et al., 2015). Pancreatic beta-cell mass, uptake of lipids, and adipose tissue inflammation are regulated by the gut microbiota. Cancer therapy can exacerbate the serious effects of cancer-induced cachexia (Antoun et al., 2010; Toledo et al., 2016), but some chemotherapeutic agents can also directly cause muscle wasting and multi-organ failure that resemble cancer-induced cachexia (Garcia et al., 2008; Toledo et al., 2016). We do not completely understand the cachexia mechanism underlying these conditions, but this observation raises the possibility that the close relationship between energy metabolism and gut microbiota could be a therapeutic target, as the microbiota composition could affect the pathogenesis of this condition (Bindels and Delzenne, 2013; Klein et al., 2013; de Matos-Neto et al., 2015). Probiotics can improve body weight in mice and patients with cancer-associated cachexia (Yeh et al., 2013; Varian et al., 2016). Recent studies in mice have found that colonization by the *E. coli* strain O21:H + in the gut protects against muscle wasting induced by intestinal damage (Schieber et al., 2015). Modulation between gut microbiota and homeostasis could be an effective clinical means to treat cancer-associated diseases, such as cachexia and anorexia, and adverse cancer treatment effects. Additional mechanism studies and rigorous clinical trials are necessary.

Radiotherapy

Ionizing radiation therapy (RTX) is an effective way to treat tumors based on its genotoxic effect on tumor cells. Immunogenic tumor cell death can be induced by local irradiation, and systemic immunity and inflammation are also promoted (Demaria and Formenti, 2012; Kroemer et al., 2013). Unfortunately, ionizing radiation also induces some side effects, including genomic instability, bystander effects on nearby cells, and systemic radio-associated immune and inflammatory reactivity (Azzam and Little, 2004). Although there has been considerable progress in the development of ionizing radiation therapy, the main limitations are the safety and effectiveness of RTX and heterogeneity in the therapeutic sensitivity of diverse cancer types and kinds of side effects with RTX (Deng et al., 2014; Baird et al., 2016).

Healthy tissues are also damaged by RTX, which is more obvious in actively proliferating tissues (Barker et al., 2015). RTX alters the microbiota composition, breaks the intestinal barrier, and causes apoptosis in intestinal crypts (Barker et al., 2015). The pathogenesis of oral mucositis, enteritis, colitis, diarrhea, and bone marrow failure in patients and mice receiving RTX is associated with alterations in the epithelial surface microbiota composition (Touchefeu et al., 2014; Ó Broin et al., 2015). The serious oral mucositis and enteropathy induced by RTX may limit therapy completion. Some studies have shown that irradiation-mediated intestinal toxicity is regulated by TLR3 in dsRNA. TLR3 mice receiving ionizing radiation survived longer and suffered less severe intestinal toxicity compared with wild type mice, suggesting that suppression of TLR3 signaling may decrease the gastrointestinal damage induced by radiation (Adams, 2009; Takemura et al., 2014). In contrast, TLR2-activating microorganisms in mice, such as the probiotic *Lactobacillus rhamnosus* GG (Ciorba et al., 2012), have been shown to protect the intestinal mucosa against radiotherapy-induced toxicity by driving cyclooxygenase 2-expressing cells from the intestinal villi to the bottom of the intestinal crypts and producing ROS to activate the cytoprotective NRF2 system (Jones et al., 2013, 2015). In some clinical studies, probiotics have been shown to help prevent radiation-related enteropathy. Preparations containing *B. bifidum*, *L. acidophilus*, *Lactobacillus casei*, and the VSL#3 formulation containing *Streptococcus*, *Lactobacillus*, and *Bifidobacterium* spp. have been proven to reduce radiation-induced gut toxicity, such as diarrhea (Delia et al., 2007; Touchefeu et al., 2014). Head and neck cancer patients who were administered radiation and chemotherapy treatment and received *Lactobacillus brevis* oral-treatments with CD2 lozenges had a lower incidence of mucositis and greater treatment completion. All of these findings raise the possibility that probiotics could become an adjuvant therapy for cancer treatment.

Studies have shown that intestinal microbiota have a significant effect on total body irradiation (Crawford and Gordon, 2005). Irradiation drives fewer endothelial cells of the intestinal mucosa into apoptosis and induces less lymphocyte infiltration in germ-free mice than in conventional mice (Crawford and Gordon, 2005). This finding indicates that gut commensals can play a negative role in resistance to the enteric toxicity of TBI in germ-free mice. However, the production of angiopoietin-like 4 (ANGPTL4), a protein inhibitor of lipoprotein lipase, is one of the major mechanisms resulting in the resistance of germ-free mice to TBI. The expression of ANGPTL4 is restrained by the gut microbiota in conventional mice (Crawford and Gordon, 2005). The transcription of Angptl4 is administered by the PPAR family in response to small chain fatty acid-producing bacteria (Grootaert et al., 2011; Korecka et al., 2013). Further exploration revealed that probiotic bacteria that induce Angptl4 expression include *Streptococcus*, *Lactobacillus*, and *Bifidobacterium* spp. and these render both germ-free mice and conventional mice resistant to radiotherapy toxicity.

We can conclude that gut microbiota regulates the response and repair of irradiation-induced damage. Future research will be invaluable to inform the alleviation of radiotherapy-collateral toxicity, the increase of therapeutic effectiveness to better understand the regulation mechanisms, and the therapeutic manipulation of commensal microbiota.

APPLICATION TO CLINICAL PRACTICE

Several clinical trials are ongoing. The "Intestinal Microflora in Lung Cancer After Chemotherapy" trial was launched by Shandong University to explore how probiotics modulate the gut microflora and immune status in lung cancer patients who need chemotherapy (ClinicalTrials.gov, 2018). Concurrently, the University of Arkansas carried out a project named "Gut Microbiome and Gastrointestinal Toxicities as Determinants of Response to Neoadjuvant Chemo for Advanced Breast Cancer" (ClinicalTrials.gov, 2018). The goal of this research was to study whether normal gut bacteria help the body fight cancer. S&D Pharma Ltd., will conduct a project titled "Prevention of Febrile Neutropenia by Synbiotics in Pediatric Cancer Patients (FENSY)" to find new options for increasing the quality of healthcare for pediatric cancer patients (ClinicalTrials.gov, 2018). Febrile neutropenia (FN) is a major treatment-related complication and a life-threatening condition for cancer patients receiving intensive chemotherapy. One of the main sources of infection during neutropenia is the endogenous flora. According to existing human and animal studies, probiotics probably not only decrease the degree of enrichment of the pathogenic bacteria colonizing the gut but may also reduce the duration of neutropenia. Although a significant number of studies have shown that probiotic treatment is effective, evidence of the safety of probiotics is still insufficient, especially in immunocompromised patients. This new study will explore the safety and practicability of probiotics in cancer treatment (ClinicalTrials.gov, 2018).

PERSPECTIVE

In general, abundant gut microbiota play a regulatory role in tumor therapy, including enhancing the sensitivity of patients to immunotherapy, reducing side effects of chemotherapeutic agents, and lightening radiation injuries. However, the effects of other mucosal barrier microbes on the body are still not clear. Many existing studies have revealed mechanisms of the gut microbiota that affect carcinogenesis, inflammation, immunity, and therapy response at the local level. However, it is still not known how microbiota colonizing distant epithelial barriers regulate not only carcinogenesis and immunity but also the physiological functions of many organs. Most studies investigating how microbiota modulate cancer therapy have been carried out in mice, and how to translate these academic findings to the clinic is still a challenge. The change in the monogenus does not explain the mechanisms behind the body's corresponding changes. The entire body is affected by the gut microbiota. Although mice transplanted with human microbiota have pathological and immune responses similar to humans, they are not identical to those in humans (Smith et al., 2007). For example, *Bifidobacterium* activates immune cells through two different functional innate immune receptors, TLR2 and TLR9, in the mouse, but the cellular expression of TLR9 is very different between mice and humans. TLR9 is expressed on plasmacytoid dendritic cells and B cells in humans, whereas it is expressed in all myeloid and dendritic cells in mice (Kadowaki et al., 2001). Thus, while activation of TLR9 by *Bifidobacterium* spp. in mice has immunostimulating activity, we cannot assume the same is true in humans. Once the most beneficial microbiota compositions in various clinical conditions have been identified, it may be possible to use microbiota composition as a biomarker, a diagnostic tool, or a therapeutic target. Targeted interventions in the microbiome using probiotics may be used for cancer prevention in particularly high-risk populations. Several clinical trials are ongoing. The ultimate goal is to develop a microbe therapy that both promotes anticancer therapy and reduces systemic toxicity. Thus, therapeutic intervention targeting the microbiota will be one of the next frontiers for precise and personalized therapies for cancer treatment.

AUTHOR CONTRIBUTIONS

FJ and CY contributed to the conception of the study and drafted the work for the manuscript framework, and agreed to publish the manuscript and be accountable for all aspects of the work in ensuring that questions related to the accuracy or integrity of any part of the work are appropriately investigated and resolved. GD contributed significantly to manuscript preparation. WM performed the data analyses and wrote the manuscript. QM and WX helped to perform the analysis with constructive discussions. All authors listed have made a substantial, direct and intellectual contribution to the work, and approved it for publication.

FUNDING

This research was supported by the National Natural Science Foundation of China (Nos. 81472702, 81501977, and 81672294), Natural Science Foundation of Jiangsu Province (No. SBK016030028), and the Innovation Capability Development Project of Jiangsu Province (No. BM2015004).

ACKNOWLEDGMENTS

CY would like to express his sincere thanks to all those who have helped him in the course of writing this manuscript. First, CY would like to take this opportunity to show his sincere gratitude to his supervisor, FJ, who has given him so much useful advice on writing. Second, CY would like to thank his classmates, who have offered him references and information. Without their help, it would be much harder for him to finish his study and this manuscript.

SUPPLEMENTARY MATERIAL

The Supplementary Material for this article can be found online at: https://www.frontiersin.org/articles/10.3389/fmicb.2019.01050/full#supplementary-material

REFERENCES

Adams, S. (2009). Toll-like receptor agonists in cancer therapy. *Immunotherapy* 1, 949–964. doi: 10.2217/imt.09.70

Antoun, S., Baracos, V. E., Birdsell, L., Escudier, B., and Sawyer, M. B. (2010). Low body mass index and sarcopenia associated with dose-limiting toxicity of sorafenib in patients with renal cell carcinoma. *Ann. Oncol.* 21, 1594–1598. doi: 10.1093/annonc/mdp605

Azzam, E. I., and Little, J. B. (2004). The radiation-induced bystander effect: evidence and significance. *Hum. Exp. Toxicol.* 23, 61–65. doi: 10.1191/0960327104ht418oa

Baird, J. R., Friedman, D., Cottam, B., Dubensky, T. W., Kanne, D. B., Bambina, S., et al. (2016). Radiotherapy combined with novel STING-targeting oligonucleotides results in regression of established tumors. *Cancer Res.* 76, 50–61. doi: 10.1158/0008-5472.CAN-14-3619

Barker, H. E., Paget, J. T., Khan, A. A., and Harrington, K. J. (2015). The tumour microenvironment after radiotherapy: mechanisms of resistance and recurrence. *Nat. Rev. Cancer* 15, 409–425. doi: 10.1038/nrc3958

Bhatt, A. P., Redinbo, M. R., and Bultman, S. J. (2017). The role of the microbiome in cancer development and therapy. *CA Cancer J. Clin.* 67, 326–344. doi: 10.3322/caac.21398

Bindels, L. B., and Delzenne, N. M. (2013). Muscle wasting: the gut microbiota as a new therapeutic target. *Int. J. Biochem. Cell Biol.* 45, 2186–2190. doi: 10.1016/j.biocel.2013.06.021

Brandi, G., Dabard, J., Raibaud, P., Di, B. M., Bridonneau, C., Pisi, A. M., et al. (2006). Intestinal microflora and digestive toxicity of irinotecan in mice. *Clin. Cancer Res.* 12, 1299–1307. doi: 10.1158/1078-0432.CCR-05-0750

Ciorba, M. A., Riehl, T. E., Rao, M. S., Moon, C., Ee, X., Nava, G. M., et al. (2012). Lactobacillus probiotic protects intestinal epithelium from radiation injury in a TLR-2/cyclo-oxygenase-2-dependent manner. *Gut* 61, 829–838. doi: 10.1136/gutjnl-2011-300367

ClinicalTrials.gov (2018). Available at: https://clinicaltrials.gov/ct2/results?cond=Cancer&term=microbiota+&cntry=&state=&city=&dist=

Cramer, P., and Bresalier, R. S. (2017). Gastrointestinal and hepatic complications of immune checkpoint inhibitors. *Curr. Gastroenterol. Rep.* 19:3. doi: 10.1007/s11894-017-0540-6

Crawford, P. A., and Gordon, J. I. (2005). Microbial regulation of intestinal radiosensitivity. *Proc. Natl. Acad. Sci. U.S.A.* 102, 13254–13259. doi: 10.1073/pnas.0504830102

Cryan, J. F., and Dinan, T. G. (2012). Mind-altering microorganisms: the impact of the gut microbiota on brain and behaviour. *Nat. Rev. Neurosci.* 13, 701–712. doi: 10.1038/nrn3346

Daillère, R., Vétizou, M., Waldschmitt, N., Yamazaki, T., Isnard, C., Poirier-Colame, V., et al. (2016). *Enterococcus hirae* and *Barnesiella intestinihominis* facilitate cyclophosphamide-induced therapeutic immunomodulatory effects. *Immunity* 45, 931–943. doi: 10.1016/j.immuni.2016.09.009

Das, S. K., Eder, S., Schauer, S., Diwoky, C., Temmel, H., Guertl, B., et al. (2011). Adipose triglyceride lipase contributes to cancer-associated cachexia. *Science* 333, 233–238. doi: 10.1126/science.1198973

Dasgupta, S., Erturk-Hasdemir, D., Ochoa-Reparaz, J., Reinecker, H. C., and Kasper, D. L. (2014). Plasmacytoid dendritic cells mediate anti-inflammatory responses to a gut commensal molecule via both innate and adaptive mechanisms. *Cell Host Microbe* 15, 413–423. doi: 10.1016/j.chom.2014.03.006

de Matos-Neto, E. M., Lima, J. D., de Pereira, W. O., Figuerêdo, R. G., Riccardi, D. M., Radloff, K., et al. (2015). Systemic inflammation in cachexia - is tumor cytokine expression profile the culprit. *Front. Immunol.* 6:629. doi: 10.3389/fimmu.2015.00629

Delia, P., Sansotta, G., Donato, V., Frosina, P., Messina, G., De Renzis, C., et al. (2007). Use of probiotics for prevention of radiation-induced diarrhea. *World J. Gastroenterol.* 13, 912–915.

Demaria, S., and Formenti, S. C. (2012). Radiation as an immunological adjuvant: current evidence on dose and fractionation. *Front. Oncol.* 2:153. doi: 10.3389/fonc.2012.00153

Deng, L., Liang, H., Burnette, B., Beckett, M., Darga, T., Weichselbaum, R. R., et al. (2014). Irradiation and anti-PD-L1 treatment synergistically promote antitumor immunity in mice. *J. Clin. Invest.* 124, 687–695. doi: 10.1172/JCI67313

Dubin, K., Callahan, M. K., Ren, B., Khanin, R., Viale, A., Ling, L., et al. (2016). Intestinal microbiome analyses identify melanoma patients at risk for checkpoint-blockade-induced colitis. *Nat. Commun.* 7:10391. doi: 10.1038/ncomms10391

Dzutsev, A., Badger, J. H., Perez-Chanona, E., Roy, S., Salcedo, R., Smith, C. K., et al. (2017). Microbes and cancer. *Annu. Rev. Immunol.* 35, 199–228. doi: 10.1146/annurev-immunol-051116-052133

Gagliani, N., Hu, B., Huber, S., Elinav, E., and Flavell, R. A. (2014). The fire within: microbes inflame tumors. *Cell* 157, 776–783. doi: 10.1016/j.cell.2014.03.006

Garcia, J. M., Cata, J. P., Dougherty, P. M., and Smith, R. G. (2008). Ghrelin prevents cisplatin-induced mechanical hyperalgesia and cachexia. *Endocrinology* 149, 455–460. doi: 10.1210/en.2007-0828

Gopalakrishnan, V., Spencer, C. N., Nezi, L., Reuben, A., Andrews, M. C., Karpinets, T. V., et al. (2018). Gut microbiome modulates response to anti-PD-1 immunotherapy in melanoma patients. *Science* 359, 97–103. doi: 10.1126/science.aan4236

Grootaert, C., Van de Wiele, T., Van Roosbroeck, I., Possemiers, S., Vercoutter-Edouart, A. S., Verstraete, W., et al. (2011). Bacterial monocultures, propionate, butyrate and H2O2 modulate the expression, secretion and structure of the fasting-induced adipose factor in gut epithelial cell lines. *Environ. Microbiol.* 13, 1778–1789. doi: 10.1111/j.1462-2920.2011.02482.x

Guiducci, C., Vicari, A. P., Sangaletti, S., Trinchieri, G., and Colombo, M. P. (2005). Redirecting in vivo elicited tumor infiltrating macrophages and dendritic cells towards tumor rejection. *Cancer Res.* 65, 3437–3446. doi: 10.1158/0008-5472.CAN-04-4262

Iida, N., Dzutsev, A., Stewart, C. A., Smith, L., Bouladoux, N., Weingarten, R. A., et al. (2013). Commensal bacteria control cancer response to therapy by modulating the tumor microenvironment. *Science* 342, 967–970. doi: 10.1126/science.1240527

Jones, R. M., Desai, C., Darby, T. M., Luo, L., Wolfarth, A. A., Scharer, C. D., et al. (2015). Lactobacilli modulate epithelial cytoprotection through the Nrf2 Pathway. *Cell Rep.* 12, 1217–1225. doi: 10.1016/j.celrep.2015.07.042

Jones, R. M., Luo, L., Ardita, C. S., Richardson, A. N., Kwon, Y. M., Mercante, J. W., et al. (2013). Symbiotic lactobacilli stimulate gut epithelial proliferation via Nox-mediated generation of reactive oxygen species. *EMBO J.* 32, 3017–3028. doi: 10.1038/emboj.2013.224

Kadowaki, N., Ho, S., Antonenko, S., Malefyt, R. W., Kastelein, R. A., Bazan, F., et al. (2001). Subsets of human dendritic cell precursors express different toll-like receptors and respond to different microbial antigens. *J. Exp. Med.* 194, 863–869.

Klein, G. L., Petschow, B. W., Shaw, A. L., and Weaver, E. (2013). Gut barrier dysfunction and microbial translocation in cancer cachexia: a new therapeutic target. *Curr. Opin. Support. Palliat. Care* 7, 361–367. doi: 10.1097/SPC.0000000000000017

Korecka, A., de Wouters, T., Cultrone, A., Lapaque, N., Pettersson, S., Doré, J., et al. (2013). ANGPTL4 expression induced by butyrate and rosiglitazone in human intestinal epithelial cells utilizes independent pathways. *Am. J. Physiol. Gastrointest. Liver Physiol.* 304, G1025–G1037. doi: 10.1152/ajpgi.00293.2012

Kroemer, G., Galluzzi, L., Kepp, O., and Zitvogel, L. (2013). Immunogenic cell death in cancer therapy. *Annu. Rev. Immunol.* 31, 51–72. doi: 10.1146/annurev-immunol-032712-100008

Lee, H., Lee, Y., Kim, J., An, J., Lee, S., Kong, H., et al. (2017). Modulation of the gut microbiota by metformin improves metabolic profiles in aged obese mice. *Gut Microbe.* 9, 155–165. doi: 10.1080/19490976.2017.1405209

Lin, X. B., Dieleman, L. A., Ketabi, A., Bibova, I., Sawyer, M. B., Xue, H., et al. (2012). Irinotecan (CPT-11) chemotherapy alters intestinal microbiota in tumour bearing rats. *PLoS One* 7:e39764. doi: 10.1371/journal.pone.0039764

Longley, D. B., Harkin, D. P., and Johnston, P. G. (2003). 5-fluorouracil: mechanisms of action and clinical strategies. *Nat. Rev. Cancer* 3, 330–338. doi: 10.1038/nrc1074

Matson, V., Fessler, J., Bao, R., Chongsuwat, T., Zha, Y., Alegre, M. L., et al. (2018). The commensal microbiome is associated with anti-PD-1 efficacy in metastatic melanoma patients. *Science* 359, 104–108. doi: 10.1126/science.aao3290

Napeñas, J. J., Brennan, M. T., Coleman, S., Kent, M. L., Noll, J., Frenette, G., et al. (2010). Molecular methodology to assess the impact of cancer chemotherapy on the oral bacterial flora: a pilot study. *Oral Surg. Oral Med. Oral Pathol. Oral Radiol. Endod.* 109, 554–560. doi: 10.1016/j.tripleo.2009.11.015

Nigro, G., Rossi, R., Commere, P. H., Jay, P., and Sansonetti, P. J. (2014). The cytosolic bacterial peptidoglycan sensor Nod2 affords stem cell protection and links microbes to gut epithelial regeneration. *Cell Host Microbe* 15, 792–798. doi: 10.1016/j.chom.2014.05.003

Ó Broin, P., Vaitheesvaran, B., Saha, S., Hartil, K., Chen, E. I, Goldman, D., et al. (2015). Intestinal microbiota-derived metabolomic blood plasma markers for prior radiation injury. *Int. J. Radiat. Oncol. Biol. Phys.* 91, 360–367. doi: 10.1016/j.ijrobp.2014.10.023

Pitt, J. M., Vétizou, M., Daillère, R., Roberti, M. P., Yamazaki, T., Routy, B., et al. (2016a). Resistance mechanisms to immune-checkpoint blockade in cancer: tumor-intrinsic and -extrinsic factors. *Immunity* 44, 1255–1269. doi: 10.1016/j.immuni.2016.06.001

Pitt, J. M., Vétizou, M., Waldschmitt, N., Kroemer, G., Chamaillard, M., Boneca, I. G., et al. (2016b). Fine-tuning cancer immunotherapy: optimizing the gut microbiome. *Cancer Res.* 76, 4602–4607. doi: 10.1158/0008-5472.CAN-16-0448

Pitt, J. M., Vétizou, M., Gomperts, B. I., Lepage, P., Chamaillard, M., and Zitvogel, L. (2017). Enhancing the clinical coverage and anticancer efficacy of immune checkpoint blockade through manipulation of the gut microbiota. *Oncoimmunology* 6:e1132137. doi: 10.1080/2162402X.2015.1132137

Rigby, R. J., Carr, J., Orgel, K., King, S. L., Lund, P. K., and Dekaney, C. M. (2016). Intestinal bacteria are necessary for doxorubicin-induced intestinal damage but not for doxorubicin-induced apoptosis. *Gut Microbes* 7, 414–423. doi: 10.1080/19490976.2016.1215806

Roberts, A. B., Wallace, B. D., Venkatesh, M. K., Mani, S., and Redinbo, M. R. (2013). Molecular insights into microbial β-glucuronidase inhibition to abrogate CPT-11 toxicity. *Mol. Pharmacol.* 84, 208–217. doi: 10.1124/mol.113.085852

Routy, B., Le, C. E., Derosa, L., Duong, C. P. M., Alou, M. T., Daillère, R., et al. (2018). Gut microbiome influences efficacy of PD-1-based immunotherapy against epithelial tumors. *Science* 359, 91–97. doi: 10.1126/science.aan3706

Schieber, A. M., Lee, Y. M., Chang, M. W., Leblanc, M., Collins, B., Downes, M., et al. (2015). Disease tolerance mediated by microbiome *E. coli* involves inflammasome and IGF-1 signaling. *Science* 350, 558–563. doi: 10.1126/science.aac6468

Sharma, P., and Allison, J. P. (2015). The future of immune checkpoint therapy. *Science* 348, 56–61. doi: 10.1126/science.aaa8172

Siegel, R. L., Miller, K. D., and Jemal, A. (2018). Cancer statistics, 2018. *CA Cancer J. Clin.* 68, 7–30. doi: 10.3322/caac.21442

Sivan, A., Corrales, L., Hubert, N., Williams, J. B., Aquino-Michaels, K., Earley, Z. M., et al. (2015). Commensal Bifidobacterium promotes antitumor immunity and facilitates anti-PD-L1 efficacy. *Science* 350, 1084–1089. doi: 10.1126/science.aac4255

Smith, K., McCoy, K. D., and Macpherson, A. J. (2007). Use of axenic animals in studying the adaptation of mammals to their commensal intestinal microbiota. *Semin. Immunol.* 19, 59–69. doi: 10.1016/j.smim.2006.10.002

Stewart, C. A., Metheny, H., Iida, N., Smith, L., Hanson, M., Steinhagen, F., et al. (2013). Interferon-dependent IL-10 production by Tregs limits tumor Th17 inflammation. *J. Clin. Invest.* 123, 4859–4874. doi: 10.1172/JCI65180

Stringer, A. M., Gibson, R. J., Logan, R. M., Bowen, J. M., Yeoh, A. S., Hamilton, J., et al. (2009b). Gastrointestinal microflora and mucins may play a critical role in the development of 5-Fluorouracil-induced gastrointestinal mucositis. *Exp. Biol. Med.* 234, 430–441. doi: 10.3181/0810-RM-301

Stringer, A. M., Gibson, R. J., Bowen, J. M., Logan, R. M., Ashton, K., Yeoh, A. S., et al. (2009a). Irinotecan-induced mucositis manifesting as diarrhoea corresponds with an amended intestinal flora and mucin profile. *Int. J. Exp. Pathol.* 90, 489–499. doi: 10.1111/j.1365-2613.2009.00671.x

Takemura, N., Kawasaki, T., Kunisawa, J., Sato, S., Lamichhane, A., Kobiyama, K., et al. (2014). Blockade of TLR3 protects mice from lethal radiation-induced gastrointestinal syndrome. *Nat. Commun.* 5:3492. doi: 10.1038/ncomms4492

Toledo, M., Penna, F., Oliva, F., Luque, M., Betancourt, A., Marmonti, E., et al. (2016). A multifactorial anti-cachectic approach for cancer cachexia in a rat model undergoing chemotherapy. *J. Cachexia Sarcopenia Muscle* 7, 48–59. doi: 10.1002/jcsm.12035

Touchefeu, Y., Montassier, E., Nieman, K., Gastinne, T., Potel, G., Bruley, D. V. S., et al. (2014). Systematic review: the role of the gut microbiota in chemotherapy- or radiation-induced gastrointestinal mucositis - current evidence and potential clinical applications. *Aliment. Pharmacol. Ther.* 40, 409–421. doi: 10.1111/apt.12878

Varian, B. J., Goureshetti, S., Poutahidis, T., Lakritz, J. R., Levkovich, T., Kwok, C., et al. (2016). Beneficial bacteria inhibit cachexia. *Oncotarget* 7, 11803–11816. doi: 10.18632/oncotarget.7730

Vétizou, M., Pitt, J. M., Daillère, R., Lepage, P., Waldschmitt, N., Flament, C., et al. (2015). Anticancer immunotherapy by CTLA-4 blockade relies on the gut microbiota. *Science* 350, 1079–1084. doi: 10.1126/science.aad1329

Viaud, S., Saccheri, F., Mignot, G., Yamazaki, T., Daillère, R., Hannani, D., et al. (2013). The intestinal microbiota modulates the anticancer immune effects of cyclophosphamide. *Science* 342, 971–976. doi: 10.1126/science.1240537

Wallace, B. D., Roberts, A. B., Pollet, R. M., Ingle, J. D., Biernat, K. A., Pellock, S. J., et al. (2015). Structure and inhibition of microbiome β-Glucuronidases essential to the alleviation of cancer drug toxicity. *Chem. Biol.* 22, 1238–1249. doi: 10.1016/j.chembiol.2015.08.005

Wallace, B. D., Wang, H., Lane, K. T., Scott, J. E., Orans, J., Koo, J. S., et al. (2010). Alleviating cancer drug toxicity by inhibiting a bacterial enzyme. *Science* 330, 831–835. doi: 10.1126/science.1191175

Yeh, K. Y., Wang, H. M., Chang, J. W., Huang, J. S., Lai, C. H., Lan, Y. J., et al. (2013). Omega-3 fatty acid-, micronutrient-, and probiotic-enriched nutrition helps body weight stabilization in head and neck cancer cachexia. *Oral Surg. Oral Med. Oral Pathol. Oral Radiol.* 116, 41–48. doi: 10.1016/j.oooo.2013.01.015

Zeevi, D., Korem, T., Zmora, N., Israeli, D., Rothschild, D., Weinberger, A., et al. (2015). Personalized nutrition by prediction of glycemic responses. *Cell* 163, 1079–1094. doi: 10.1016/j.cell.2015.11.001

Conflict of Interest Statement: The authors declare that the research was conducted in the absence of any commercial or financial relationships that could be construed as a potential conflict of interest.

frontiers in Microbiology

ORIGINAL RESEARCH
published: 25 June 2019
doi: 10.3389/fmicb.2019.01458

Analysis of the Relationship Between the Degree of Dysbiosis in Gut Microbiota and Prognosis at Different Stages of Primary Hepatocellular Carcinoma

Jiajia Ni[1,2], Rong Huang[3], Huifang Zhou[4], Xiaoping Xu[1,2]*, Yang Li[1,2], Peihua Cao[1,2], Kebo Zhong[1,2], Mei Ge[1,2], Xiaoxia Chen[1,2], Baohua Hou[5], Min Yu[5], Baogang Peng[6], Qiao Li[6], Peng Zhang[7] and Yi Gao[1,2]**

[1] Department of Hepatobiliary Surgery II, Guangdong Provincial Research Center of Artificial Organ and Tissue Engineering, Zhujiang Hospital of Southern Medical University, Guangzhou, China, [2] State Key Laboratory of Organ Failure Research, Southern Medical University, Guangzhou, China, [3] Department of Neonatal Surgery, Guangdong Women and Children Hospital, Guangzhou, China, [4] Department of Clinical Laboratory, First People's Hospital of Kashi, Kashgar, China, [5] Department of General Surgery, Guangdong General Hospital, Guangdong Academy of Medical Sciences, Guangzhou, China, [6] Department of Hepatic Surgery, The First Affiliated Hospital, Sun Yat-sen University, Guangzhou, China, [7] Department of Organ Transplantation, The Second Affiliated Hospital of Guangzhou Medical University, Guangzhou, China

OPEN ACCESS

Edited by:
Gary Moran,
Trinity College Dublin, Ireland

Reviewed by:
Vishal Singh,
University of Toledo, United States
Aleksandra Barac,
University of Belgrade, Serbia

***Correspondence:**
Jiajia Ni
nijiajia2005@126.com
Xiaoping Xu
xuxp7193@163.com
Yi Gao
gaoyi6146@163.com;
drgaoy@126.com

Specialty section:
This article was submitted to Systems Microbiology, a section of the journal Frontiers in Microbiology

Received: 06 March 2019
Accepted: 11 June 2019
Published: 25 June 2019

Citation:
Ni J, Huang R, Zhou H, Xu X, Li Y, Cao P, Zhong K, Ge M, Chen X, Hou B, Yu M, Peng B, Li Q, Zhang P and Gao Y (2019) Analysis of the Relationship Between the Degree of Dysbiosis in Gut Microbiota and Prognosis at Different Stages of Primary Hepatocellular Carcinoma. Front. Microbiol. 10:1458. doi: 10.3389/fmicb.2019.01458

Gut microbiota dysbiosis is closely associated with primary hepatocellular carcinoma (HCC). Recent studies have evaluated the early diagnosis of primary HCC through analysis of gut microbiota dysbiosis. However, the relationship between the degree of dysbiosis and the prognosis of primary HCC remains unclear. Because primary HCC is accompanied by dysbiosis and dysbiosis usually increases the circulatory concentrations of endotoxin and other harmful bacterial substances, which further increases liver damage, we hypothesized that level of dysbiosis associated with primary HCC increases with the stage of cancer progression. To test this hypothesis, we introduced a more integrated index referred to as the degree of dysbiosis (D_{dys}); and we investigated D_{dys} of the gut microbiota with the development of primary HCC through high-throughput sequencing of 16S rRNA gene amplicons. Our results showed that compared with healthy individuals, patients with primary HCC showed increased pro-inflammatory bacteria in their fecal microbiota. The D_{dys} increased significantly in patients with primary HCC compared with that in healthy controls. Moreover, there was a tendency for the D_{dys} to increase with the development of primary HCC, although no significant difference was detected between different stages of primary HCC. Our findings provide important insights into the use of gut microbiota analysis during the treatment of primary HCC.

Keywords: chronic liver diseases, dysbiosis degree, gut microbiota, primary hepatocellular carcinoma, prognosis

INTRODUCTION

Disruption of the gut microbiota (termed "dysbiosis") is closely associated with the development of chronic liver diseases (CLDs) in humans and rodent models (Aron-Wisnewsky et al., 2013; Grice and Segre, 2013; Kamada et al., 2013; Schnabl, 2013; Bajaj et al., 2014a; Grąt et al., 2016; Houghton et al., 2016; Shen et al., 2017). Several studies have reported that dysbiosis is associated

with CLDs of different etiologies (Quigley et al., 2013; Schnabl, 2013; Xie et al., 2016). For example, patients with chronic hepatitis or decompensated cirrhosis secondary to hepatitis B infection showed reduced numbers of probiotic Bifidobacteria and lactic acid-producing bacteria in the feces, whereas *Enterococcus faecalis* and Enterobacteriaceae numbers were higher than those in asymptomatic carriers and healthy controls (Lu et al., 2011). In addition, using deep high-throughput sequencing of the 16S rRNA gene of bacteria, fecal microbial communities from patients with alcoholic or hepatitis B-related cirrhosis could be clearly distinguished from healthy controls. Increases in Streptococcaceae, Veillonellaceae, and Enterobacteriaceae, accompanied by a decrease in Lachnospiraceae, characterize the gut microbiota in cirrhosis. The relative abundances of the Lachnospiraceae and Streptococcaceae families were negatively and positively related with the Child-Pugh score in patients with cirrhosis, respectively (Chen et al., 2011).

Hepatocellular carcinoma (HCC) is a type of advanced CLD and a long-term consequence of chronic liver injury, inflammation, and fibrosis (Darnaud et al., 2013). HCC is the third leading cause of cancer-related death worldwide (El-Serag and Kanwal, 2014; Yu and Schwabe, 2017). Approximately 29,200 new HCC cases in men and 11,510 new HCC cases in women were reported in the United States of America (USA) in 2017 (Siegel et al., 2017). The incidence in China is worse, with new HCC cases reported in more than 343,000 men and 122,000 women in 2015 (Chen et al., 2016). Gut microbiota dysbiosis is closely associated with HCC, and recently, Ren et al. (2018) reported that 13 genera, including *Gemmiger* and *Parabacteroides*, were enriched in early HCC following progression from cirrhosis to HCC.

Dysbiosis accompanies the occurrence of HCC and usually increases the circulatory concentrations of endotoxin and other harmful bacterial substances, which further increases liver damage (Yu et al., 2010; Darnaud et al., 2013; Yu and Schwabe, 2017; Ma et al., 2018). Therefore, we hypothesized that level of dysbiosis associated with primary HCC increases with the stage of cancer progression, suggesting clinical importance in the prognosis of patients with HCC.

Although dysbiosis is commonly reported in fecal microbiota from patients with HCC and several methods are available to evaluate gut bacterial taxa and quantify the degree of dysbiosis in patients with other CLDs (Lu et al., 2011; Wong et al., 2013; Bajaj et al., 2014b; Grąt et al., 2015), still no viable integrated approach to measure the degree of dysbiosis in patients with HCC. Therefore, it is difficult to assess whether the dysbiosis becomes more serious with the progression of HCC. This study introduced a novel integrated index that could be utilized to determine the degree of dysbiosis in HCC patients. This new index is called the degree of dysbiosis (D_{dys}) and used to identify disparities in the gut microbiota during the development of HCC, via high-throughput sequencing of 16S rRNA gene amplicons. Our findings provide important insights into the use of gut microbiota analysis during the treatment of HCC.

MATERIALS AND METHODS

Inclusion and Exclusion Criteria

The study protocol was approved by the Medical Ethics Committee of Zhujiang Hospital, Southern Medical University (approval number: 2017-GDEK-002) and was performed in accordance with clinical ethics guidelines and the Declaration of Helsinki and Rules of Good Clinical Practice. Patients with primary HCC were age-matched to healthy controls and recruited from five hospitals in Guangzhou, a large modern city in southern China. All patients and healthy controls provided informed consent for their participation in the study. No specific medical intervention was conducted specifically for this study.

Patients with primary HCC were defined as having histological evidence, radiological evidence, or clinical diagnosis of primary HCC (Ye, 2009). Primary HCC samples were staged according to the National Health and Family Planning Commission of the People's Republic of China (Zhou et al., 2018). We excluded patients with an unclear diagnosis of primary HCC, those with inflammatory bowel disease, those with a current infection, those on gut-absorbable antibiotic therapy, those with type 2 diabetes or hypertension, and those with incomplete clinically diagnostic information. If the above criteria were met, participants were enrolled in the study and admitted to hospital following diagnosis. No other therapy was provided to patients in the 2 months before fecal sampling. Analysis of the fecal microbiota profiles was based on prospectively collected stool samples from the pretherapy period and immediately stored at −80°C. The patients were recruited based on their admission time in the hospital during the study period August 1, 2017 to November 30, 2017.

We only included age-matched healthy controls without clinically diagnosable disease and those who had not taken antibiotics or probiotics in the last 2 months. The healthy controls were recruited as volunteers for the out-patient physical examinations occurring during the study period. Analysis of the fecal microbiota profiles was conducted following the initial clinical examination and participants lacking clinically diagnosable disease were accepted for the study as healthy volunteers, and their stool samples were subjected to further analysis.

Two reduplicate fecal samples were collected using fecal collectors synchronously from each participant; one sample was used to analyze microbial composition and the other reserved for further testing.

Fecal DNA Extraction and High-Throughput Sequencing

Fresh fecal pellets (0.3 g) of each participant were used for microbial DNA extraction. Fecal microbial DNA was extracted using a PowerSoil DNA isolation kit (Mobio, United States).

DNA concentration and quality were checked using a NanoDrop spectrophotometer (Thermo Fisher Scientific, United States).

The V4–V5 hypervariable region of the prokaryotic 16S rRNA gene was amplified using the universal primer pair 515F (5′-GTGYCAGCMGCCGCGGTA-3′) and 909R (5′-CCCCGYCAATTCMTTTRAGT-3′), with a 12-nt sample-specific barcode sequence included at the 5′-end of the 515F sequence to distinguish samples (Ni et al., 2017; Huang et al., 2018; Xiang et al., 2018). Polymerase chain reaction (PCR) was performed, and amplicons were sequenced using a MiSeq system at Guangdong Meilikang Bio-Science, Ltd. (China), as described previously (Huang et al., 2018; Xiang et al., 2018).

The raw sequences were merged using FLASH-1.2.8 software (Magoc and Salzberg, 2011) and processed using the QIIME Pipeline 1.9.0 with default parameters (Caporaso et al., 2010). Chimeric sequences were identified and removed using the Uchime algorithm before further analysis (Edgar et al., 2011). The high-quality sequences were clustered into OTUs at 97% identity using UPARSE (Edgar, 2013). Taxonomic assignments of each OTU were determined using the RDP classifier (Wang et al., 2007).

Definition of the Degree of Dysbiosis

In order to quantify the degree of dysbiosis in patients with primary HCC, we compared the ratio of abundance of Firmicutes to Bacteroidetes (Wong et al., 2013), the ratio of abundance of autochthonous taxa to non-autochthonous taxa (Bajaj et al., 2014b), and the ratio of abundance of the genus *Bifidobacterium* to the family Enterobacteriaceae (Lu et al., 2011) at different stages of primary HCC and healthy controls, as these ratios were reported associated with other liver diseases. In addition, we introduced a more integrated index for measuring the dysbiosis. This index was calculated based on the relative abundance of seven types of inherently probiotic bacterial genera with decreased abundance in the fecal microbiota of patients with CLDs (*Anaerostipes*, *Bifidobacterium*, *Coprococcus*, *Faecalibacterium*, *Lactobacillus*, *Oscillibacter*, and *Phascolarctobacterium*) and 13 potentially harmful bacterial genera that generally increased in the fecal microbiota of these patients (*Akkermansia*, *Bacteroides*, *Clostridium*, *Dorea*, *Escherichia*, *Fusobacterium*, *Haemophilus*, *Helicobacter*, *Klebsiella*, *Prevotella*, *Ruminococcus*, *Streptococcus*, and *Veillonella*) (Huang et al., 2004; Fox et al., 2010; Malaguarnera et al., 2010; Zhang et al., 2012; Ren et al., 2018; Zmora et al., 2018). The degree of dysbiosis was then calculated according to the follow formula:

$$D_{dys} = \Sigma(\log_{10}[100 \times RA_{harmful} + 1]) - \Sigma(\log_{10}[100 \times RA_{probiotic} + 1])$$

where D_{dys} was the degree of dysbiosis; $RA_{harmful}$ was the relative abundance of each harmful bacterial genus; and $RA_{probiotic}$ was the relative abundance of each probiotic bacterial genus.

Statistical Analysis

The results for each parameter are presented as the mean ± standard error for each group. Non-parametric Adonis tests (Anderson, 2001) were applied to test the significance of differences among three or more groups using the R vegan package (Dixon, 2003). The indicator value method (McGeoch, 2007) was used to screen potentially significantly different genera among the groups. The values were calculated through the R indicspecies package. Screened genera were verified using the standard non-parametric Kruskal–Wallis test through R with the ggpubr package according to a previous report (Li et al., 2018). The Kruskal–Wallis test was also used to detect the statistical significance of alpha-diversity indices among patients with different stages of HCC and healthy controls. Cladogram layout was drawn using GraPhlAn software (Asnicar et al., 2015). Box plots were drawn to show the relative abundances of significantly different dominant phyla or genera among groups using R software with the ggpubr package. Statistically significant markers were added to the box plots using Adobe Illustrator CS5 software according to the Wilcoxon rank sum test results. Correlation analyses were conducted using R software. Results

TABLE 1 | Basic and physiological data of patients with primary HCC and healthy controls.

Sample ID	HCC-I	HCC-II	HCC-III	HCC-IV*	Healthy
Specimen number	**23**	**13**	**30**	**2**	**18**
Age	52.96 ± 2.49	59.31 ± 2.06	52.47 ± 1.41		50.28 ± 2.28
Height (cm)	163.65 ± 1.42	166.38 ± 1.00	165.22 ± 1.25		165.17 ± 1.71
Weight (kg)	63.04 ± 2.23	60.08 ± 2.42	61.88 ± 1.53		65.33 ± 2.54
Body mass index	23.47 ± 0.67	21.73 ± 0.92	22.64 ± 0.45		23.90 ± 0.80
Systolic pressure	122.21 ± 3.94	124.46 ± 5.06	127.34 ± 2.58		134.72 ± 4.68
Fasting blood glucose (mmol/L)	5.08 ± 0.29^{a}	4.79 ± 0.46^{a}	4.74 ± 0.15^{a}		5.83 ± 0.43^{b}
Total bilirubin (μmol/L)	17.97 ± 2.46^{a}	21.64 ± 3.04^{ab}	42.94 ± 8.85^{b}		12.46 ± 1.07^{a}
Albumin (g/L)	37.34 ± 1.39^{a}	36.46 ± 0.87^{a}	35.21 ± 1.04^{a}		41.53 ± 0.85^{b}
Alanine aminotransferase (IU/L)	51.21 ± 6.84^{a}	50.77 ± 6.76^{a}	66.40 ± 11.86^{a}		27.17 ± 5.19^{b}

*Primary HCC samples were staged as previously described (Zhou et al., 2018). Results with P-values of less than or equal to 0.05 were considered statistically significant. Lowercases at the upper right corner of the mean ± standard error showed the statistical significance. *The samples from patients with stages III and IV HCC were mixed together for further analysis because these stages were considered advanced HCC.*

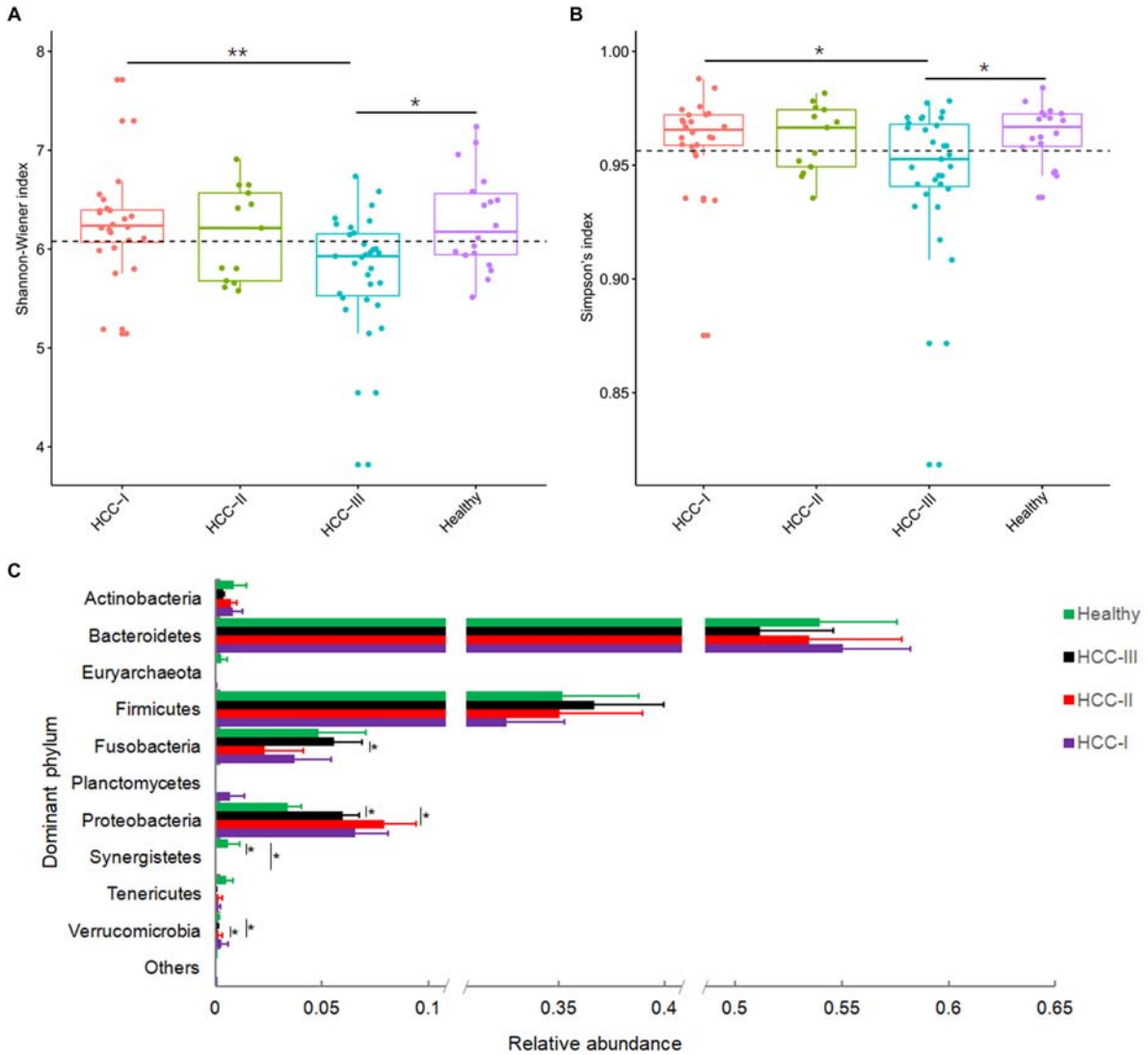

FIGURE 1 | Shannon-Wiener index **(A)**, Simpson's index **(B)**, and relative abundances of the dominant phyla of fecal microbiota from patients with primary hepatocellular carcinoma (HCC) and healthy controls **(C)**. Patients with primary HCC were staged as described previously (Zhou et al., 2018). $^{**}p < 0.01$; $^{*}p < 0.05$.

with *P*-values of less than or equal to 0.05 were considered statistically significant.

Availability of Data

The merged DNA datasets were deposited in the NCBI Sequence Read Archive database (accession number SRP151835).

RESULTS

Baseline Characteristics Examined for All Volunteers

In total, 110 fecal samples were prospectively collected from 110 participants and subjected to MiSeq sequencing, and after a strict exclusion process, 86 samples (23 cases of stage I of primary HCC; 13 cases of stage II of primary HCC; 30 cases of stage III of primary HCC; 2 cases of stage IV of primary HCC; and 18 healthy control individuals) were finally included for further analysis (**Table 1**); other samples did not meet the inclusion criteria. The samples from patients with stages III and IV HCC were grouped together because these stages were considered advanced HCC. No significant differences were detected between the different stages of primary HCC and the healthy controls with regard to age (Kruskal–Wallis test, $\chi^2 = 7.62$, $p = 0.054$), height (Kruskal–Wallis test, $\chi^2 = 1.63$, $p = 0.652$), weight (Kruskal–Wallis test, $\chi^2 = 4.64$, $p = 0.200$), body mass index (BMI, Kruskal–Wallis test, $\chi^2 = 7.29$, $p = 0.063$), and systolic pressure (SP, Kruskal–Wallis test, $\chi^2 = 4.45$, $p = 0.217$). However, fasting blood glucose (FBG, Kruskal–Wallis test, $\chi^2 = 12.62$, $p = 0.006$) and albumin (Kruskal–Wallis test, $\chi^2 = 19.02$, $p < 0.001$) were significantly lower in primary HCC cases with different stages than healthy controls, and alanine

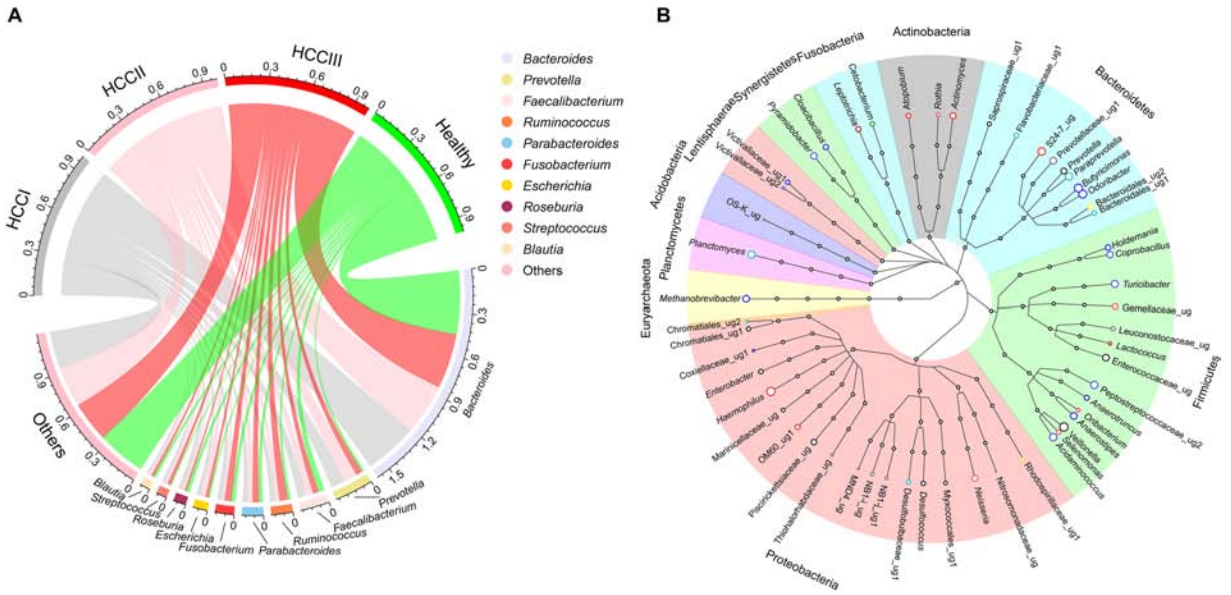

FIGURE 2 | Circular layout **(A)** and Cladogram layout **(B)** depict the top 10 genera found in the fecal microbiota, as well as significantly different genera found in the gut microbiota among patients with different primary HCC stages and the healthy controls. Primary HCC samples were staged as previously described (Zhou et al., 2018). Circle colors in the layout **(B)** show changes in genera within the fecal microbiota of patients expressing different stages of primary HCC, compared with healthy controls. The genera that were enhanced include yellow (stage I), gray (stage II), light red (stage III), pink (stages I and II), red (stages I and III), dark red (stages II and III), and black (stages I, II and III). The genera that were reduced by color bright green (stage I), green (stage II), blue (stage III), pale green (stages I and II), light blue (stages I and III), dark blue (stage II and III), and dark green (stages I, II and III), respectively.

aminotransferase (ALT) was significantly higher (Kruskal–Wallis test, $\chi^2 = 14.99$, $p = 0.002$). In addition, total bilirubin (TB) was significantly higher in stage III of primary HCCs than the healthy controls (**Table 1**).

Proteobacteria Were Increased in the Gut Microbiota of Patients With Primary HCC

After low-quality and chimeric sequences were removed, 5,258,105 (61,140.76 ± 2,723.202) high-quality sequences were obtained. To eliminate the influence of sequencing depth, 20,293 sequences were randomly sampled for further analysis. In total, 7,655 operational taxonomic units (OTUs) from 604 genera were identified at 97% sequence similarity. Although the alpha-diversities of the microbiota from advanced primary HCC (stage III and IV primary HCC) were significantly reduced compared with that in healthy controls (**Figures 1A,B**), no significant differences were detected between early primary HCC and healthy controls (**Figures 1A,B**), consistent with a previous report (Ren et al., 2018), although they found that microbial diversity was markedly increased in early primary HCC versus liver cirrhosis. The OTUs belonged to 38 phyla, with the exception of tiny unclassified sequences (0–0.19%, 0.004 ± 0.002%). However, only 10 phyla, i.e., Actinobacteria, Bacteroidetes, Euryarchaeota, Firmicutes, Fusobacteria, Planctomycetes, Proteobacteria, Synergistetes, Tenericutes, and Verrucomicrobia, were the dominant phyla, with relative abundances of more than 1% in at least one sample (**Figure 1C** and **Supplementary Figure S1**). These phyla accounted for up to 99.92 ± 0.01% of the analyzed high-quality sequences. Although the relative abundances of *Firmicutes* were not significantly changed in patients with primary HCC, these *Proteobacteria* were significantly increased in patients with stages II and III primary HCC compared with that in healthy controls (**Figure 1C**). Because most pro-inflammatory bacteria come from *Proteobacteria* and many probiotic bacteria come from *Firmicutes* (Stecher et al., 2013; Gao et al., 2015), this result implied that pro-inflammatory bacteria accompanied the development of primary HCC. Simultaneously, many pro-inflammatory bacteria in *Proteobacteria*, such as those of Enterobacteriaceae, were indicators of dysbiosis. Therefore, dysbiosis may worsen with the progression of primary HCC. To determine which bacterial species led to the expansion of *Proteobacteria*, we analyzed the gut microbiota at the genus level.

The Degree of Dysbiosis Increased in Patients With Primary HCC

There were 604 genera identified from the 86 fecal samples. *Bacteroides* (39.91 ± 2.01%) was the most dominant genus, followed by *Prevotella* (6.19 ± 1.36%), *Faecalibacterium* (4.83 ± 0.50%), *Ruminococcus* (4.07 ± 0.52%), *Parabacteroides* (3.79 ± 0.43%), *Fusobacterium* (3.58 ± 0.70%), *Escherichia* (2.34 ± 0.43%), *Roseburia* (2.08 ± 0.26%), *Streptococcus* (1.84 ± 0.41%), and *Blautia* (1.76 ± 0.19%). The top 10 genera accounted for up to 71.75 ± 1.63% of

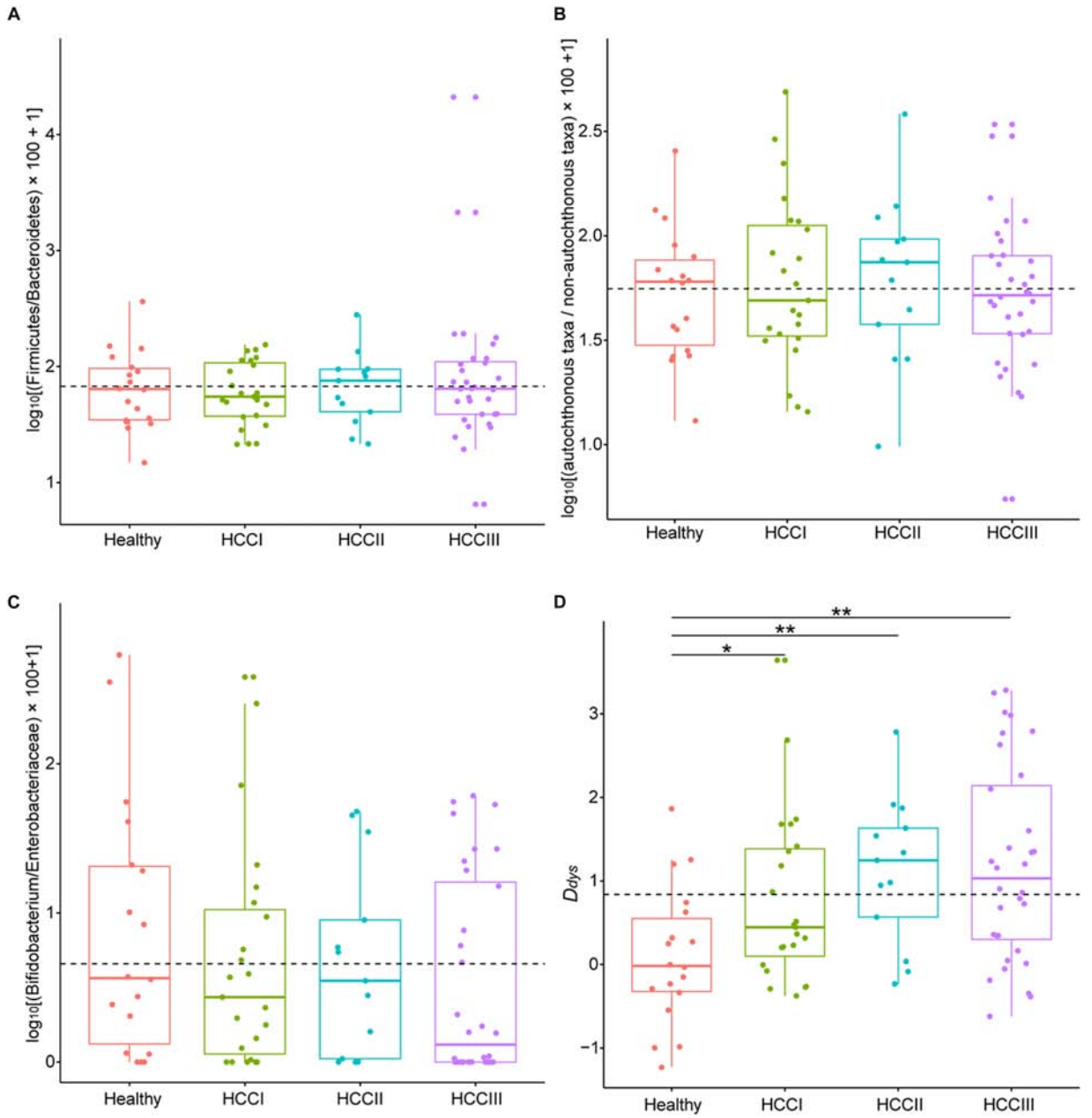

FIGURE 3 | Boxplots showing changes by degree of dysbiosis. Description of indices and how they were calculated **(A)** based on the relative abundance of Firmicutes and those of Bacteroidetes, **(B)** based on the relative abundance of autochthonous taxa and those of non-autochthonous taxa, **(C)** based on the relative abundance of *Bifidobacterium* and those of Enterobacteriaceae, and **(D)** based on seven probiotic bacterial genera (*Anaerostipes*, *Bifidobacterium*, *Coprococcus*, *Faecalibacterium*, *Lactobacillus*, *Oscillibacter*, and *Phascolarctobacterium*) and 13 harmful bacterial genera (*Akkermansia*, *Bacteroides*, *Clostridium*, *Dorea*, *Escherichia*, *Fusobacterium*, *Haemophilus*, *Helicobacter*, *Klebsiella*, *Prevotella*, *Ruminococcus*, *Streptococcus*, and *Veillonella*). Primary HCC samples were staged as previously described (Zhou et al., 2018). $^{**}p < 0.01$; $^{*}p < 0.05$.

the analyzed high-quality sequences (**Figure 2A**). In total, 54 genera were found to be significantly different among groups at the various primary HCC stages or the healthy controls based on the indicator value and the standard non-parametric Kruskal–Wallis test. Compared with healthy controls, *Actinomyces*, *Atopobium*, *Desulfococcus*, *Enterobacter*, *Paraprevotella*, *Planctomycetes*, *Prevotella*, *Veillonella* and many unidentified genera were enhanced in patients with stage I HCC. *Desulfococcus*, *Enterobacter*, *Lactococcus*, *Leptotrichia*, *Paraprevotella*, *Planctomycetes*, *Prevotella*, *Veillonella*, and many unidentified genera were enriched in patients with stage II HCC. *Actinomyces*, *Atopobium*, *Desulfococcus*, *Enterobacter*, *Haemophilus*, *Lactococcus*, *Leptotrichia*, *Neisseria*, *Oribacterium*, *Prevotella*, *Rothia*, *Selenomonas*, *Veillonella*, and many

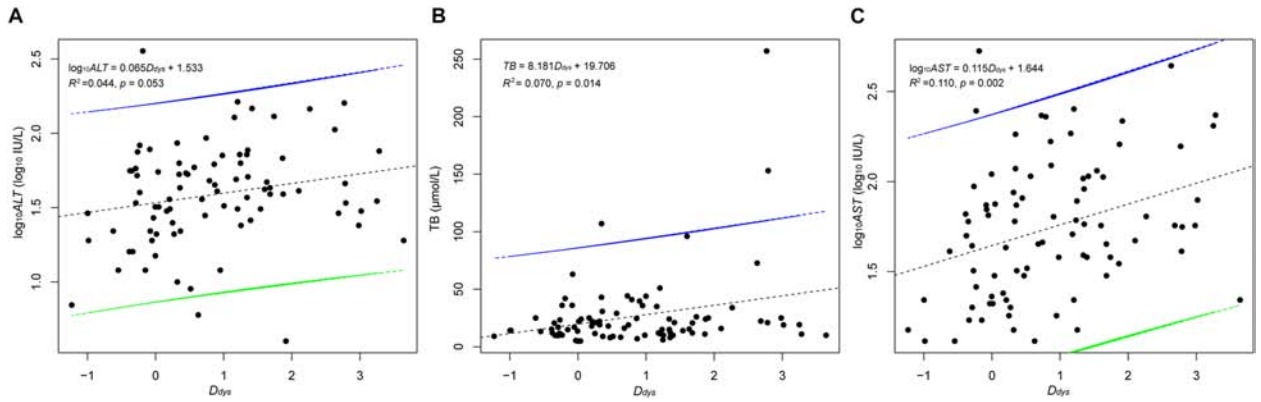

FIGURE 4 | Correlation between the D_{dys} and the ALT level **(A)**, the TB **(B)**, and the AST **(C)**. The D_{dys} was calculated based on seven probiotic bacterial genera (*Anaerostipes*, *Bifidobacterium*, *Coprococcus*, *Faecalibacterium*, *Lactobacillus*, *Oscillibacter*, and *Phascolarctobacterium*) and 13 harmful bacterial genera (*Akkermansia*, *Bacteroides*, *Clostridium*, *Dorea*, *Escherichia*, *Fusobacterium*, *Haemophilus*, *Helicobacter*, *Klebsiella*, *Prevotella*, *Ruminococcus*, *Streptococcus*, and *Veillonella*). The black dotted lines are the correlation lines. The intervals between the green and blue lines are the confidence intervals.

unidentified genera were multiplied in patients with stage III HCC (**Figure 2B** and **Supplementary Figure S2**). Further, *Desulfococcus*, *Enterobacter*, *Prevotella*, *Veillonella*, and many unidentified genera were increased in all stages of HCC. However, *Acidaminococcus*, *Cetobacterium*, *Coprobacillus*, *Pyramidobacter*, *Turicibacter*, and two unidentified genera were reduced in patients with stage I HCC; and *Anaerotruncus*, *Cetobacterium*, and an unidentified genus were decreased in patients with stage II HCC. Moreover, *Acidaminococcus*, *Anaerostipes*, *Anaerotruncus*, *Butyricimonas*, *Cetobacterium*, *Cloacibacillus*, *Coprobacillus*, *Holdemania*, *Methanobrevibacter*, *Odoribacter*, Pyramidobacter, Turicibacter, and four unidentified genera were reduced in patients with stage III HCC. *Cetobacterium* was reduced in all stages of primary HCC (**Figure 2B** and **Supplementary Figure S3**).

The ratio of abundance of Firmicutes to Bacteroidetes (Kruskal–Wallis test, $\chi^2 = 0.413$, $p = 0.938$; **Figure 3A**), autochthonous taxa to non-autochthonous taxa (Kruskal–Wallis test, $\chi^2 = 0.741$, $p = 0.864$; **Figure 3B**), and genus *Bifidobacterium* to the family Enterobacteriaceae (Kruskal–Wallis test, $\chi^2 = 2.942$, $p = 0.401$; **Figure 3C**) revealed no significant difference between primary HCCs at different stages and the healthy controls. However, this analysis was not comprehensive so this study created a more integrated index called degree of dysbiosis (D_{dys}) and analyzed the D_{dys} of the gut microbiota at each primary HCC stage and in healthy controls. Among the 20 common gut bacterial genera that were used to calculate the D_{dys}, one essentially probiotic bacterial genus (*Oscillibacter*) and two potentially harmful bacterial genera (*Akkermansia* and *Helicobacter*) were not detected in the present study. The D_{dys} significantly increased in patients with primary HCC compared with that in healthy controls. The increase in D_{dys} was continued, and a tendency of D_{dys} to increase emerged with the progression of primary HCC, although no significant difference was detected between patients with different stages of primary HCC (**Figure 3D**). In addition, although there was no significant correlation between the D_{dys} and the *ALT* level ($\log_{10}ALT = 0.065D_{dys} + 1.533$, $R^2 = 0.044$, $p = 0.053$; **Figure 4A**), the D_{dys} positively correlated with the total bilirubin concentration ($TB = 8.181D_{dys} + 19.706$, $R^2 = 0.070$, $p = 0.014$; **Figure 4B**) and AST level ($\log_{10}AST = 0.115D_{dys} + 1.644$, $R^2 = 0.110$, $p = 0.002$; **Figure 4C**), which are commonly used to indicate the liver function.

DISCUSSION

Accumulating evidence has supported the notion that persistent inflammation leads to HCC (Darnaud et al., 2013). Pro-inflammatory factors, such as lipopolysaccharide (LPS) and flagellin, activate the nuclear factor-κB pathway, produce pro-inflammatory cytokines [tumor necrosis factor-α, interleukin-6 (IL-6), and IL-1], and lead to liver inflammatory and oxidative damage (Darnaud et al., 2013). Dysbiosis of the gut microbiota increases LPS-producing bacteria and changes bile acid metabolism. Moreover, while controversial (Darnaud et al., 2013), dysbiosis is considered a promoter of liver inflammation which could ultimately lead to HCC (Yu et al., 2010; Yu and Schwabe, 2017; Ma et al., 2018). Therefore, dysbiosis has been extensively studied in order to characterize the gut microbiome in patients with HCC, or screen non-invasive biomarkers for primary HCC, and prevent or adjunctively treat primary HCC through gut microbiota (Ren et al., 2018).

Many indices are utilized to measure dysbiosis in patients with CLDs. Lu et al. (2011) reported that the *Bifidobacterium*/Enterobacteriaceae ratio may act as an indicator of the level of dysbiosis over the course of liver disease progression. Wong et al. (2013) reported that the abundance of Firmicutes reduced and those of Bacteroidetes increased in the fecal microbiota of patients with non-alcoholic steatohepatitis, which implied that the ratio of Firmicutes to Bacteroidetes could probably be used as an indicator of non-alcoholic steatohepatitis. In addition, the ratio of autochthonous to non-autochthonous taxa was calculated as the cirrhosis

dysbiosis ratio (Bajaj et al., 2014b). However, these indices did not apply to degree the dysbiosis experienced by patients with primary HCC in the present study (**Figures 3A–C**), and thus a new index was required. Thus, in this study, we introduced the D_{dys} index to be utilized as a tool to measure dysbiosis. Our results showed that the D_{dys} increased significantly in patients with primary HCC compared with that of the healthy controls. Additionally, the D_{dys} tended to increase as the HCC stage increased, suggesting that the D_{dys} may indicate the degree of dysbiosis in patients with primary HCC. The ratio of the abundance of *Bifidobacterium* to *Enterococcus* was proposed as a measure of pre-liver transplantation in gut dysbiosis (Grąt et al., 2015). However, more than four-fifths of the samples could not detect *Enterococcus* in the present study. Thus, we did not include this index in the present study.

The expansion of taxa from Proteobacteria, especially the family Enterobacteriaceae, was reported in many cases of dysbiosis in patients with different diseases (Shin et al., 2015; Grąt et al., 2016; Hegde et al., 2018). We also found that the relative abundance of Proteobacteria was enhanced in the present study (**Figure 1C**). In addition, many genera of Proteobacteria, such as *Enterobacter* and *Haemophilus*, were also increased in the fecal samples of patients with primary HCC (**Figure 2B**).

In the present study, the proliferated bacteria included into the calculation of the D_{dys} were commonly associated with inflammatory bowel disease (IBD) (Png et al., 2010; Shaw et al., 2016), irritable bowel syndrome (Bhattarai et al., 2017), liver tumor development and metastases (Ma et al., 2018; Ren et al., 2018), gastric cancer (Coker et al., 2018), and colorectal cancer (Aymeric et al., 2018; Oh, 2018; Shang and Liu, 2018), which are all associated with dysbiosis. Therefore, the D_{dys} index could potentially be used to indicated the degree of dysbiosis in patients with other diseases, such as IBD and colorectal cancer. However, further studies are needed to verify the applicability of this index in these diseases.

CONCLUSION

In conclusion, we introduced the D_{dys} index to measure dysbiosis and found that the D_{dys} was significantly increased in patients with primary HCC compared with that of the healthy controls. Additionally, the D_{dys} tended to increase with the development of primary HCC, although no significant difference was detected between patients with different stages of primary HCC. However, since the D_{dys} continued to increase in the bacterial genera that were closely correlated with dysbiosis in primary HCC, further studies are needed to verify the application of this index for use in other diseases.

DATA AVAILABILITY

The datasets generated for this study can be found in NCBI Sequence Read Archive database, SRP151835.

ETHICS STATEMENT

The study protocol was approved by the Medical Ethics Committee of Zhujiang Hospital, Southern Medical University (approval number: 2017-GDEK-002) and was performed in accordance with clinical ethics guidelines and the Declaration of Helsinki and Rules of Good Clinical Practice. Patients with HCC, as well as age-matched healthy controls, were recruited from five hospitals in Guangzhou, a large modern city in southern China. All patients and healthy controls provided informed consent for participation in the study. No specific medical intervention was conducted specifically for this study.

AUTHOR CONTRIBUTIONS

JN, RH, XX, HZ, KZ, and YG designed the research study. JN, RH, XX, YL, KZ, MG, XC, BH, MY, BP, QL, and PZ conducted the research. JN, RH, HZ, and PC collected and analyzed the data. JN, XX, and YG wrote the manuscript. All authors approved the final version of the manuscript.

FUNDING

This research was supported by the China Postdoctoral Science Foundation (No. 2017M612691) and the National Natural Science Foundation of China (No. 31500417). The funders had no role in the study design, data collection and interpretation, or the decision to submit the work for publication.

ACKNOWLEDGMENTS

We would like to thank Fenjia Xie from the First Affiliated Hospital of Guangzhou Medical University and Dawei Zhang from the Second Affiliated Hospital of Guangzhou Medical University for their help in sample collection. We would also like to thank Editage http://www.editage.cn for language editing.

SUPPLEMENTARY MATERIAL

The Supplementary Material for this article can be found online at: https://www.frontiersin.org/articles/10.3389/fmicb.2019.01458/full#supplementary-material

FIGURE S1 | Percentage bar diagram showing compositions of the dominant phyla (their relative abundances were more than 1% in at least one sample) in the gut microbiota of patients with different stages of primary HCC and healthy controls.

FIGURE S2 | Boxplots showing significantly enhanced taxa for the gut microbiota from patients at different stages of primary HCC compared with the healthy controls. Primary HCC samples were staged as previously described (Zhou et al., 2018). $^{***}p < 0.001$; $^{**}p < 0.01$; $^{*}p < 0.05$.

FIGURE S3 | Boxplots showing a significantly reduction in the taxa of the gut microbiota from patients at different stages of primary HCC compared with healthy controls. Primary HCC samples were staged as previously described (Zhou et al., 2018). $^{***}p < 0.001$; $^{**}p < 0.01$; $^{*}p < 0.05$.

REFERENCES

Anderson, M. J. (2001). A new method for non-parametric multivariate analysis of variance. *Austral. Ecol.* 26, 32–46. doi: 10.1111/j.1442-9993.2001.01070.pp.x

Aron-Wisnewsky, J., Gaborit, B., Dutour, A., and Clement, K. (2013). Gut microbiota and non-alcoholic fatty liver disease: new insights. *Clin. Microbiol. Infect.* 19, 338–348. doi: 10.1111/1469-0691.12140

Asnicar, F., Weingart, G., Tickle, T. L., Huttenhower, C., and Segata, N. (2015). Compact graphical representation of phylogenetic data and metadata with GraPhlAn. *PeerJ* 3:e1029. doi: 10.7717/peerj.1029

Aymeric, L., Donnadieu, F., Mulet, C., du Merle, L., Nigro, G., Saffarian, A., et al. (2018). Colorectal cancer specific conditions promote *Streptococcus gallolyticus* gut colonization. *Proc. Natl. Acad. Sci. U.S.A.* 115, E283–E291. doi: 10.1073/pnas.1715112115

Bajaj, J. S., Heuman, D. M., Hylemon, P. B., Sanyal, A. J., Puri, P., Sterling, R. K., et al. (2014a). Randomised clinical trial: *Lactobacillus* GG modulates gut microbiome, metabolome and endotoxemia in patients with cirrhosis. *Aliment. Pharm. Therap.* 39, 1113–1125. doi: 10.1111/apt.12695

Bajaj, J. S., Heuman, D. M., Hylemon, P. B., Sanyal, A. J., White, M. B., Monteith, P., et al. (2014b). Altered profile of human gut microbiome is associated with cirrhosis and its complications. *J. Hepatol.* 60, 940–947. doi: 10.1016/j.jhep.2013.12.019

Bhattarai, Y., Pedrogo, D. A. M., and Kashyap, P. C. (2017). Irritable bowel syndrome: a gut microbiota-related disorder? *Am. J. Physiol. Gastrointest. Liver Physiol.* 312, G52–G62. doi: 10.1152/ajpgi.00338.2016

Caporaso, J. G., Kuczynski, J., Stombaugh, J., Bittinger, K., Bushman, F. D., Costello, E. K., et al. (2010). QIIME allows analysis of high-throughput community sequencing data. *Nat. Methods* 7, 335–336. doi: 10.1038/nmeth.f.303

Chen, W., Zheng, R., Baade, P. D., Zhang, S., Zeng, H., Bray, F., et al. (2016). Cancer statistics in China, 2015. *CA Cancer J. Clin.* 66, 115–132. doi: 10.3322/caac.21338

Chen, Y., Yang, F., Lu, H., Wang, B., Chen, Y., Lei, D., et al. (2011). Characterization of fecal microbial communities in patients with liver cirrhosis. *Hepatology* 54, 562–572. doi: 10.1002/hep.24423

Coker, O. O., Dai, Z., Nie, Y., Zhao, G., Cao, L., Nakatsu, G., et al. (2018). Mucosal microbiome dysbiosis in gastric carcinogenesis. *Gut* 67, 1024–1032. doi: 10.1136/gutjnl-2017-314281

Darnaud, M., Faivre, J., and Moniaux, N. (2013). Targeting gut flora to prevent progression of hepatocellular carcinoma. *J. Hepatol.* 58, 385–387. doi: 10.1016/j.jhep.2012.08.019

Dixon, P. (2003). VEGAN, a package of R functions for community ecology. *J. Veg. Sci.* 14, 927–930. doi: 10.1111/j.1654-1103.2003.tb02228.x

Edgar, R. C. (2013). UPARSE: Highly accurate OTU sequences from microbial amplicon reads. *Nat. Methods* 10, 996–998. doi: 10.1038/NMETH.2604

Edgar, R. C., Haas, B. J., Clemente, J. C., Quince, C., and Knight, R. (2011). UCHIME improves sensitivity and speed of chimera detection. *Bioinformatics* 27, 2194–2200. doi: 10.1093/bioinformatics/btr381

El-Serag, H. B., and Kanwal, F. (2014). Epidemiology of hepatocellular carcinoma in the United States: where are we? where do we go? *Hepatology* 60, 1767–1775. doi: 10.1002/hep.27222

Fox, J. G., Feng, Y., Theve, E. J., Raczynski, A. R., Fiala, J. L. A., Doernte, A. L., et al. (2010). Gut microbes define liver cancer risk in mice exposed to chemical and viral transgenic hepatocarcinogens. *Gut* 59, 88–97. doi: 10.1136/gut.2009.183749

Gao, Z., Buo, B., Gao, R., Zhu, Q., and Qin, H. (2015). Microbiota dysbiosis is associated with colorectal cancer. *Front. Microbiol.* 6:20. doi: 10.3389/fmicb.2015.00020

Grąt, M., Hołówko, W., Wronka, K. M., Grąt, K., Lewandowski, Z., Kosińska, I., et al. (2015). The relevance of intestinal dysbiosis in liver transplant candidates. *Transpl. Infect. Dis.* 17, 174–184. doi: 10.1111/tid.12352

Grąt, M., Wronka, K. M., Krasnodêbski, M., Masior, Ł, Lewandowski, Z., Kosińska, I., et al. (2016). Profile of gut microbiota associated with the presence of hepatocellular cancer in patients with liver cirrhosis. *Transplant. Proc.* 48, 1686–1691. doi: 10.1016/j.transproceed.2016.01.077

Grice, E. A., and Segre, J. A. (2013). The human microbiome: our second genome. *Annu. Rev. Genomics Hum. Genet.* 13, 151–170. doi: 10.1146/annurev-genom-090711-163814

Hegde, S., Lin, Y.-M., Golovko, G., Khanipov, K., Cong, Y., Savidge, T., et al. (2018). Microbiota dysbiosis and its pathophysiological significance in bowel obstruction. *Sci. Rep.* 8:13044. doi: 10.1038/s41598-018-31033-0

Houghton, D., Stewart, C. J., Day, C. P., and Trenell, M. (2016). Gut microbiota and lifestyle interventions in NAFLD. *Int. J. Mol. Sci.* 17:447. doi: 10.3390/ijms17040447

Huang, R., Li, T., Ni, J., Bai, X., Gao, Y., Li, Y., et al. (2018). Different sex-based responses of gut microbiota during the development of hepatocellular carcinoma in liver-specific Tsc1-knockout mice. *Front. Microbiol.* 9:1008. doi: 10.3389/fmicb.2018.01008

Huang, Y., Fan, X.-G., Wang, Z.-M., Zhou, J.-H., Tian, X.-F., and Li, N. (2004). Identification of *helicobacter* species in human liver samples from patients with primary hepatocellular carcinoma. *J. Clin. Pathol.* 57, 1273–1277. doi: 10.1136/jcp.2004.018556

Kamada, N., Chen, G. Y., Inohara, N., and Núñez, G. (2013). Control of pathogens and pathobionts by the gut microbiota. *Nat. Immunol.* 14, 685–690. doi: 10.1038/ni.2608

Li, Z., Yu, E., Wang, G., Yu, D., Zhang, K., Gong, W., et al. (2018). Broad bean (*Vicia faba* L.) induces intestinal inflammation in grass carp (*Ctenopharyngodon idellus* C. et V) by increasing relative abundances of intestinal gram-negative and flagellated bacteria. *Front. Microbiol.* 9:1913. doi: 10.3389/fmicb.2018.01913

Lu, H., Wu, Z., Xu, W., Yang, J., Chen, Y., and Li, L. (2011). Intestinal microbiota was assessed in cirrhotic patients with hepatitis B virus infection. Intestinal microbiota of HBV cirrhotic patients. *Microb. Ecol.* 61, 693–703. doi: 10.1007/s00248-010-9801-8

Ma, C., Han, M., Heinrich, B., Fu, Q., Zhang, Q., Sandhu, M., et al. (2018). Gut microbiome-mediated bile acid metabolism regulates liver cancer via NKT cells. *Science* 876:eaan5931. doi: 10.1126/science.aan5931

Magoc, T., and Salzberg, S. L. (2011). FLASH: Fast length adjustment of short reads to improve genome assemblies. *Bioinformatics* 27, 2957–2963. doi: 10.1093/bioinformatics/btr507

Malaguarnera, M., Gargante, M. P., and Malaguarnera, G. (2010). *Bifidobacterium* combined with fructo-oligosaccharide versus lactulose in the treatment of patients with hepatic encephalopathy. *Eur. J. Gastroenterol. Hepatol.* 22, 199–206. doi: 10.1097/MEG.0b013e328330a8d3

McGeoch, M. A. (2007). "Insects and bioindication: theory and progress," in *Insect Conservation Biology*, eds A. J. A. Stewart, O. T. Lewis, and T. R. New (London: CABI Publishing), 144–174. doi: 10.1079/9781845932541.0144

Ni, J., Li, X., He, Z., and Xu, M. (2017). A novel method to determine the minimum number of sequences required for reliable microbial community analysis. *J. Microbiol. Methods* 139, 196–201. doi: 10.1016/j.mimet.2017.06.006

Oh, C. R. (2018). Correlation between dysbiosis of gut microbiota and human colorectal cancer. *Int. Res. J. Adv. Eng. Sci.* 3, 226–231.

Png, C. W., Lindén, S. K., Gilshenan, K. S., Zoetendal, E. G., McSweeney, C. S., Sly, L. I., et al. (2010). Mucolytic bacteira with increased prevalence in IBD mucosa augment *in vitro* utilization of mucin by other bacteria. *Am. J. Gastroenterol.* 105, 2420–2428. doi: 10.1038/ajg.2010.281

Quigley, E. M. M., Stanton, C., and Murphy, E. F. (2013). The gut microbiota and the liver. Pathophysiological and clinical implications. *J. Hepatol.* 58, 1020–1027. doi: 10.1016/j.jhep.2012.11.023

Ren, Z., Li, A., Jiang, J., Zhou, L., Yu, Z., Lu, H., et al. (2018). Gut microbiome analysis as a tool towards targeted non-invasive biomarkers for early hepatocellular carcinoma. *Gut* 68, 1014–1023. doi: 10.1136/gutjnl-2017-315084

Schnabl, B. (2013). Linking intestinal homeostasis and liver disease. *Curr. Opin. Gastroenterol.* 29, 264–270. doi: 10.1097/mog.0b013e32835ff948

Shang, F., and Liu, H. (2018). *Fusobacterium nucleatum* and colorectal cancer: a review. *World J. Gastrointest. Oncol.* 10, 71–81. doi: 10.4251/wjgo.v10.i3.71

Shaw, K. A., Bertha, M., Hofmekler, T., Chopra, P., Vatanen, T., Srivatsa, A., et al. (2016). Dysbiosis, inflammation, and response to treatment: a longitudinal study of pediatric subjects with newly diagnosed inflammatory bowel disease. *Genome Med.* 8:75. doi: 10.1186/s13073-016-0331-y

Shen, F., Zheng, R. D., Sun, X. Q., Ding, W. J., Wang, X. Y., and Fan, J. G. (2017). Gut microbiota dysbiosis in patients with non-alcoholic fatty liver disease. *Hepatobil. Pancreat. Dis. Int.* 16, 375–381. doi: 10.1016/S1499-3872(17)60019-5

Shin, N.-R., Whon, T. W., and Bae, J.-W. (2015). *Proteobacteria*: microbial signature of dysbiosis in gut microbiota. *Trends Biotechnol.* 33, 496–503. doi: 10.1016/j.tibtech.2015.06.011

Siegel, R. L., Miller, K. D., and Jemal, A. (2017). Cancer statistics, 2017. *CA Cancer J. Clin.* 67, 7–30. doi: 10.3322/caac.21387

Stecher, T., Normand, S., and Chamaillard, M. (2013). NOD2 prevents emergence of disease-predisposing microbiota. *Gut Microb.* 4, 353–356. doi: 10.4161/gmic.25275

Wang, Q., Garrity, G. M., Tiedje, J. M., and Cole, J. R. (2007). Naïve Bayesian classifier for rapid assignment of rRNA sequences into the new bacterial taxonomy. *Appl. Environ. Microbiol.* 73, 5261–5267. doi: 10.1128/aem.00062-07

Wong, V. W.-S., Tse, C.-H., Lam, T. T.-Y., Wong, G. L.-H., Chim, A. M.-L., Chu, W. C.-W., et al. (2013). Molecular characterization of the fecal microbiota in patients with nonalcoholic steatohepatitis – a longitudinal study. *PLoS One* 8:e62885. doi: 10.1371/journal.pone.0062885

Xiang, J., He, T., Wang, P., Xie, M., Xiang, J., and Ni, J. (2018). Opportunistic pathogens are abundant in the gut of cultured giant spiny frog (*Paa spinosa*). *Aquac. Res.* 49, 2033–2041. doi: 10.1111/are.13660

Xie, G., Wang, X., Liu, P., Wei, R., Chen, W., Rajani, C., et al. (2016). Distinctly altered gut microbiota in the progression of liver disease. *Oncotarget* 7, 19355–19366. doi: 10.18632/oncotarget.8466

Ye, S. L. (2009). Expert consensus on standardization of the management of primary liver cancer. *Chin. J. Hepatol.* 17, 403–410. doi: 10.3781/j.issn.1000-7431.2009.04.001

Yu, L. X., and Schwabe, R. F. (2017). The gut microbiome and liver cancer: mechanisms and clinical translation. *Nat. Rev. Gastroenterol. Hepatol.* 14, 527–539. doi: 10.1038/nrgastro.2017.72

Yu, L. X., Yan, H. X., Liu, Q., Yang, W., Wu, H. P., Dong, W., et al. (2010). Endotoxin accumulation prevents carcinogen-induced apoptosis and promotes liver tumorigenesis in rodents. *Hepatology* 52, 1322–1333. doi: 10.1002/hep.23845

Zhang, H.-L., Yu, L.-X., Yang, W., Tang, L., Lin, Y., Wu, H., et al. (2012). Profound impact of gut homeostasis on chemically-induced pro-tumorigenic inflammation and hepatocarcinogenesis in rats. *J. Hepatol.* 57, 803–812. doi: 10.1016/j.jhep.2012.06.011

Zhou, J., Sun, H.-C., Wang, Z., Cong, W.-M., Wang, J.-H., Zeng, M.-S., et al. (2018). Guidelines for diagnosis and treatment of primary liver cancer in China (2017 Edition). *Liver Cancer* 7, 235–260. doi: 10.1159/000488035

Zmora, N., Zilberman-Schapira, G., Suez, J., Mor, U., Dori-Bachash, M., Bashiardes, S., et al. (2018). Personalized gut mucosal colonization resistance to Empiric probiotics is associated with unique host and microbiome features. *Cell* 174, 1388–1405. doi: 10.1016/j.cell.2018.08.041

Conflict of Interest Statement: The authors declare that the research was conducted in the absence of any commercial or financial relationships that could be construed as a potential conflict of interest.

frontiers in Microbiology

ORIGINAL RESEARCH
published: 26 June 2019
doi: 10.3389/fmicb.2019.01439

Compositional and Functional Analysis of the Microbiome in Tissue and Saliva of Oral Squamous Cell Carcinoma

Zhen Zhang[1,2†], Junjie Yang[4,5,6†], Qiang Feng[7,8,9†], Bin Chen[3,5,6], Meihui Li[7,8,9], Cheng Liang[10], Mingyu Li[1,2], Zhihui Li[1,2], Qin Xu[1,2], Lei Zhang[3,5,6] and Wantao Chen[1,2*]*

[1] Department of Oral Maxillofacial Head and Neck Oncology, Ninth People's Hospital, Shanghai Jiao Tong University School of Medicine, Shanghai, China, [2] Shanghai Key Laboratory of Stomatology, Shanghai Research Institute of Stomatology, National Clinical Research Center of Stomatology, Shanghai, China, [3] Beijing Advanced Innovation Center for Big Data-Based Precision Medicine, Beihang University, Beijing, China, [4] College of Life Sciences, Qilu Normal University, Jinan, China, [5] Shandong Children's Microbiome Center, Qilu Children's Hospital of Shandong University, Jinan, China, [6] Qingdao Human Microbiome Center, The Affiliated Central Hospital of Qingdao University, Qingdao, China, [7] Shandong Provincial Key Laboratory of Oral Tissue Regeneration, School of Stomatology, Shandong University, Jinan, China, [8] Department of Human Microbiome, School of Stomatology, Shandong University, Jinan, China, [9] State Key Laboratory of Microbial Technology, Shandong University, Qingdao, China, [10] School of Information Science and Engineering, Shandong Normal University, Jinan, China

OPEN ACCESS

Edited by:
Nezar Al-hebshi, Temple University, United States

Reviewed by:
Renee Maxine Petri, University of Veterinary Medicine Vienna, Austria
Ranju Ralhan, Icahn School of Medicine at Mount Sinai, United States
Waleed Abu Al-Soud, Al Jouf University, Saudi Arabia

***Correspondence:**
Lei Zhang
microbiome@foxmail.com
Wantao Chen
chenwantao196323@sjtu.edu.cn

[†]These authors have contributed equally to this work

Specialty section:
This article was submitted to Systems Microbiology, a section of the journal Frontiers in Microbiology

Received: *11 February 2019*
Accepted: *07 June 2019*
Published: *26 June 2019*

Citation:
Zhang Z, Yang J, Feng Q, Chen B, Li M, Liang C, Li M, Li Z, Xu Q, Zhang L and Chen W (2019) Compositional and Functional Analysis of the Microbiome in Tissue and Saliva of Oral Squamous Cell Carcinoma. Front. Microbiol. 10:1439. doi: 10.3389/fmicb.2019.01439

Oral squamous cell carcinoma (OSCC) is affected by the interaction between oral pathogen and holobionts, or the combination of the host and its microbial communities. Studies have indicated the structure and feature of the microbiome in OSCC tissue and saliva, the relationships between microbiota and OSCC sites, stages remain unclear. In the present study, OSCC tissue (T), saliva (S) and mouthwash (W) samples were collected from the same subjects and carried out the microbiome study by 16S sequencing. The results showed the T group was significantly different from the S and W groups with the character of lower richness and diversity. Proteobacteria were most enriched in the T group at the phylum level, while Firmicutes were predominant in groups S and W. At the genus level, the predominant taxa of group T were *Acinetobacter* and *Fusobacterium*, and for group S and W, the predominant taxa were *Streptococcus* and *Prevotella*. The genera related to late stage tumors were *Acinetobacter* and *Fusobacterium*, suggesting microbiota may be implicated in OSCC developing. Both compositional and functional analyses indicated that microbes in tumor tissue were potential indicator for the initiation and development of OSCC.

Keywords: 16S rRNA gene, microbiota, OSCC, cross-sectional study, salivary and OSCC bacteriome

INTRODUCTION

As one of the largest habitats of microorganisms in human body, the oral cavity contains more than 1000 different kinds of microbes (Lamont et al., 2018). Within the oral cavity, the distinct habitats of hard and soft tissues contributed to the heterogeneous microbial communities which are formed depending on the oral anatomic location (Dewhirst et al., 2010). The dysbiosis of oral microenvironment was proved to be the cause of or closely related with a number of oral

diseases (Dewhirst et al., 2010; Ahn et al., 2012; Han and Wang, 2013; He et al., 2015),such as dental caries, periodontal disease, periapical and pulp diseases, and oral cancer (Takahashi and Nyvad, 2008; Zaura et al., 2009; Chen et al., 2010; Yost et al., 2015). Oral microorganisms and their metabolites also influence remote tissues and organs through the digestive tract and periodontal pocket ulceration (Pizzo et al., 2010), which were reported to associate with digestive system diseases (Warren et al., 2013), nervous system diseases (Riviere et al., 2002), cardiovascular diseases (Fåk et al., 2015), diabetes (Fardini et al., 2010), rheumatoid arthritis (Zhang et al., 2015), premature birth (Mendz et al., 2013) and were discovered in some malignant tumors (Meurman, 2010; Farrell et al., 2012). Therefore, the oral microecology is an important contributor of human health or diseases.

Oral cancer is one of the most prevalent cancers globally. More than 90% of oral cancer is squamous cell carcinoma (OSCC), which developed from the oral mucosa (Kademani, 2007). With surgery-based treatment, the 5-year survival rates of OSCC are only approximately 60.0%, which is greatly impact the patients' quality of life (Jemal et al., 2010). OSCCs could be induced by alcohol and tobacco consumption, residual root and rough artificial tooth stimulation, poor oral hygiene etc., which has become a clinical challenge due to the high prevalence, recurrent relapse, unpredictable metastasis, oral and maxillofacial damage (Hooper et al., 2007; Crozier and Sumer, 2010). During the process of oral carcinogenesis, the local microenvironment is altered and in the meantime the microbiota composition were changed (Rivera and Venegas, 2014). The oral pathogens and the metabolites induced including nitrosamine and acetaldehyde were reported to stimulate inflammation, promote the cellular proliferation and inhibit the cellular apoptosis (Hooper et al., 2009). The composition analysis of oral microbiota between OSCC patients and healthy volunteers showed the anaerobic bacteria and acid-resistant bacteria including *Porphyromonas gingivalis*, *Streptococcus mitis* and *Fusobacterium* were increased in OSCC tissues, while Firmicutes (mainly *Streptococcus*) and Actinobacteria (mainly *Rothia*) were significantly decreased (Hooper et al., 2006, 2007). In a comparison of healthy subjects, *Capnocytophaga gingivalis*, *Prevotella melaninogenica,* and *Streptococcus mitis* were increased in the saliva of OSCC patients (Smruti et al., 2012).

Oral microbiota are potential biomarkers for the development and prognosis of OSCC. The oral pathogens, *P. gingivalis* and *F. nucleatum*, are reported to facilitate cancer progression by establishing chronic inflammation and disrupt the local immune response by secreting virulence factors such as FimA and FadA adhesins (Whitmore and Lamont, 2014). The detection of *P. gingivalis* or *F. nucleatum* are promising indicators of a poor prognosis. Besides, the divergence and richness of saliva microbiota increase significantly in oral leukoplakia and OSCC (Hu et al., 2016). The overall shift of oral microbiota is another promising diagnostic index for OSCC. Bacteria related to resistance to chemotherapy or radiotherapy are therapeutic targets in the treatment of OSCC (Sonis, 2017). However, studies on the taxonomic characteristic of OSCC tissues and saliva samples are still inadequate.

To investigate the character of microbiota in different stages of OSCC and the relationship between OSCC tissue and saliva, we carried out the oral microbiome study on the resected tumor tissue, saliva samples. In the present study, 30 subjects were analyzed and compared based on 16S rRNA gene sequencing. Phylogenetic Investigation of Communities by Reconstruction of Unobserved States (PICRUSt) was applied to infer and compare the potential role of microbiota from different samples of OSCC.

MATERIALS AND METHODS

Ethics Statement

This study was approved by the Institutional Review Board of Ninth People's Hospital, Shanghai Jiao Tong University School of Medicine (ethical approval number: 2016144). All methods were performed according to relevant guidelines and protocols, including any relevant details. Written informed consent was obtained for each participant.

Sample Collection

Samples in this study were obtained from the sharing platform for the tissue sample and bioinformatics database of oral maxillofacial tumors[1]. 30 patients with different stages of cancer were enrolled without chemotherapy or radiotherapy. Oral cancer tissue samples were dissected from the site of the tumor during surgery, and the diameter of each sample was larger than 3 mm. Saliva and mouthwash liquid were collected pre surgery and before breakfast, a mouth rinse was performed twice with 20 ml of 0.9% saline to avoid contamination by cell debris, and the liquid from the second wash was collected into a 50 ml test tube. Saliva was collected into a 50 ml test tube after mouthwash (Corrêa et al., 2017). All samples were stored at −80°C within 20 min.

DNA Extraction

DNA extraction was performed with a TIANamp Micro DNA Kit (TIANGEN BIOTECH CO., LTD.), following the protocol from a previous study (Guan et al., 2016). A total of 10 ml saliva, 10 ml mouthwash, and 5 mg OSCC tissues were used for the bacterial DNA extraction. For saliva and mouthwash samples, the pallet was transferred to a 1.5 ml Eppendorf tube after centrifugation. Then, the tube was incubated at 56°C for 60 min with Buffer GA and proteinase K. The tube was incubated for another 10 min at 70°C with Buffer GB and carrier RNA stock solution. The entire lysate was transferred into Spin Column CR2 (with a 2 ml collection tube) after adding 200 μl of ethanol, and the contaminants were removed by centrifugation with 500 μl Buffer GD and 600 μl Buffer PW. The pure DNA was eluted with 50 μl Buffer TB and collected into a new 1.5 ml Eppendorf tube. The sample was stored at −20°C before 16S rRNA gene amplification. For tissue samples, all the specimens were treated at same time, they were incubated with Buffer GA and proteinase K for 60 min until fully resolved. The

[1]http://mdl.shsmu.edu.cn/OMNDB/page/home/home_en.jsp

following steps were the same as saliva and mouthwash DNA extraction procedures.

PCR and 16S rRNA Gene Sequencing

The amplification of a V1-V2 hypervariable region of the 16S rRNA gene was performed with universal primers 27F: 5′-AGAGTTTGATCMTGGCTCAG-3′ and 338R: 5′-GCTGCCTCCCGTAGGAGT-3′ which also contained Illumina adapter sequences. Barcodes were attached to the 5′ terminus of the forward primers to multiplex the samples during sequencing. The PCR was performed in a total volume of 25 μL with 20 ng of DNA sample and 25 pmol of each primer with 2 × Taq PCR MasterMix (Tiangen, Beijing, China). The reactions were initially denatured at 95°C for 10 min, 6 cycles of denaturation for 45 s at 92°C, 50°C annealing for 30 sec and 72°C extension for 1 min, followed by 20 cycles of denaturation for 45 s at 92°C, annealing for 30 s at 68°C and extension 30 s at 72°C, with a final elongation for 9 min at 72°C. The concentration and purity of PCR products were examined with a NanoDrop2000 spectrophotometer (Thermo Fisher Scientific Inc., Wilmington, MA, United States). Purification of PCR products was performed with VAHTSTM DNA Clean Beads (Vazyme Biotech) according to the manufacturer's instructions, and the purified PCR products were pooled afterward with equal nano mole. Sequencing of the 16S V1-V2 region of PCR products was performed by Illumina MiSeq platform (Illumina Incorporate, CA, United States).

Sequencing and Statistical Analysis

FLASH (Fast Length Adjustment of SHort reads) method described by Magoč and Salzberg is a software tool to find the correct overlap between paired-end reads and extend the reads by stitching them together (Magoč and Salzberg, 2011), it was adopted for the joining and quality filtering of 16S rRNA gene paired-end sequencing data set. The Quantitative Insights Into Microbial Ecology (QIIME, version 1.9.1) software suite was used for sequence analysis, following the QIIME tutorial[2]. The split_libraries_fastq.py command was then applied demultiplexing of Fastq sequence data. *De novo* models of Usearch61 were applied for the removal of chimeric sequences. Clusters of filtered sequences were referenced to the 2013 Green genes (13_5 release) ribosomal database's 97% reference dataset[3] with pick_open_reference_otus.py command. UCLUST was used to cluster unmatched sequences into *de novo* OTUs at 97% similarity. Taxonomic annotation of all OTUs was achieved by the RDP classifier from the reference data set of Green Genes. OTUs with relative abundance lower than 0.02% or present in less than 20% of samples were excluded. With the alpha diversity and rank abundance function from the QIIME pipeline, rarefaction curves and rank abundance curves were calculated from OTU tables using the alpha_rarefaction.py command. UPGMA clustering (Unweighted Pair Group Method with Arithmetic mean, also known as average linkage) was used to calculate the hierarchical clustering from population profiles with the prevalence and abundance of taxa based on the distance matrix of OTU abundance. By using the QIIME package, we obtained the results in a Newick formatted tree. Reads did not match with the amplicon sequence amplification were discarded to remove the contamination by host genomic DNA.

[2]http://qiime.org

[3]http://greengenes.secondgenome.com/

Statistical Analysis

The OTU table of raw counts was normalized to an OTU table of relative abundance values. Same types of taxa were agglomerated at the phylum, class, order, family and genus level. Non-parametric Wilcoxon test was used to compare the biodiversity between classified groups. The test about the alpha diversity of each groups adopt Kendall's Tau and Spearman's rank correlation coefficients. We used unweighted and weighted Unifrac distance of even OTU samples to perform Principal Coordinate Analyses (PCoA) and ANOSIM was used to analyze the difference among groups. LDA Effect Size (LEfSe) was performed to find out the differentially enriched taxa between groups. The functional prediction of microbiota was done with PICRUSt (Langille, Zaneveld et al., 2013). Only reads identified in closed reference picking (Greengenes 13_5 database) were used for the PICRUSt analysis, OTUs were picked at a 97% percent identity. The reference genome coverage of samples was also calculated using weighted Nearest Sequenced Taxon Index (NSTI) score with the -a option in the predict metagenomes.py script. The graphical representation of the results was performed by STAMP (Parks and Beiko, 2010).

RESULTS

A total of 4,606,312 raw reads were generated from OSCC tissue (T), saliva (S) and mouthwash (W) groups as shown in **Table 1**, data of four samples from the T group were excluded

TABLE 1 | Patient demographic data.

Variable	Total (*N* = 30)	Tissue (*n* = 26)	Saliva (*n* = 30)
Age, years			
Average (range)	58 (33–80)	60 (45–80)	58 (33–80)
Tumor stage			
I-II	25	22	25
III-IV	5	4	5
Tumor site			
Cheek	6	6	6
Gingiva	4	4	4
Oropharynx	7	6	7
Tongue	10	7	10
Others	3	3	3
TIcohol			
Yes	7	6	7
No	23	20	23
Tobacco			
Yes	8	7	8
No	22	19	22

Age, tobacco and alcohol consumption, and tumor information were provided in the form. The others option of tumor site included temple, mouth floor and maxillary.

due to insufficient reads. 2,507,184 clean reads were generated with an average of 29153.302 (std.dev. 932.637) for each subject, which covered 97.6% across samples on average. The percent of chimeras was 11.3%. As a result, 12 phyla, 40 families, 63 genera and 533 OTUs were annotated among the whole samples (also see **Supplementary Figures S1A,B** for information about class and order level).

As shown in **Figure 1**, the microecological composition of group S was similar to group W, but different from group T. T group enriched more Proteobacteria, which contributed to 52% of the taxonomic units, followed by Bacteroidetes (16%), Fusobacteria (12%), Firmicutes (12%) and Actinobacteria (2%) on phylum level (**Figure 1A**). However, Firmicutes was the most predominant phylum for groups S and W which accounting for 40% and 37% respectively, followed by Bacteroidetes (S: 27%, W: 26%), Proteobacteria (S: 15%, W: 21%), Fusobacteria (S: 10%, W: 7%) and Actinobacteria (S: 5%, W: 4%) (**Figure 1A**). At family level (**Supplementary Figure S1C**), *Enterobacteriaceae* (14%) and *Moraxellaceae* (12%) were higher abundant in group T, followed by *Fusobacteriaceae* (9%) and *Campylobacteraceae* (6%). For S and W groups, the top ranked taxa were *Prevotellaceae* (S: 18%, W: 14%), *Streptococcaceae* (S: 16%, W: 17%), *Veillonellaceae* (S: 9%, W:6%) and *Neisseriaceae* (S: 8%, W: 9%). At the genus level (**Figure 1B**), the most predominant taxa in group T were *Acinetobacter* (12%) and *Fusobacterium* (9%), followed by *Campylobacter* (6%) and *Prevotella* (6%). For groups S and W, genera *Streptococcus* (S: 16%, W:17%) and *Prevotella* (S:18%, W:14%) accounted for the majority of bacteria, which were only accounted for 2% and 6%, in group T.

Alpha and Beta Diversity Analysis on OSCC Tissue, Saliva and Mouthwash Groups

The alpha diversity of OSCC tissue, saliva and mouthwash groups was calculated at a maximum depth of 26,605 sequences per sample based on the Observed Species (**Figure 2A**), Chao1 index (**Figure 2B**), Shannon's index (**Figure 2C**) and Simpson index (**Figure 2D**). Results showed the alpha diversity in OSCC tissue was significantly lower than that in saliva and mouthwash while the taxonomic richness within-samples was more similar between groups S and W (**Figures 2A–D**). The beta diversity analysis by principal coordinates analysis (PCoA) was shown in **Figure 3**. The results showed that the phylogenetic distance significantly separated group T from group W and S in both the weighted (**Figure 3A**) and unweighted Unifrac (**Figure 3B**), the difference between the group W and S was not statistically significant. ANOSIM analysis showed that R equalled to 0.75 for weighted Unicfrac (p = 0.0001) when we compared T group with S and W groups. The above results showed group T was significantly different from group W and group S in terms of diversity within samples and similarity between samples.

A Venn diagram was used to identify the unique and common genera among all three groups (**Supplementary Figure S1D**). The results showed that at the genus level, taxa of group S were fully covered by group W, and 35 genera were shared by all three groups in total. There were 13 unique genera from group T, namely, *Deinococcus*, *Rubrobacter*, *Parabacteroides*, *Chryseobacterium*, *Sphingobacterium*, *Staphylococcus*, *Lachnospira*, *Faecalibacterium*, *Megamonas*, *Phascolarctobacterium*, *Burkholderia*, *Comamonas,* and *Serratia*. There were two unique genera in group W, *Schwartzia* and TG5 from Dethiosulfovibrionaceae.

Taxonomic Level Comparison of OSCC Tissue, Saliva and Mouthwash Groups

LDA Effect Size (LEfSe) is an algorithm to identify high-dimensional biomarkers from multiple groups. In this study, LEfSe analysis was used to identify the different composition of microbiota and to trace significant biomarkers (LDA > 2). As shown in **Figure 4**, the significant taxa at different levels were exhibited. The enriched taxa in OSCC tissue were aggregated under Proteobacteria, mainly in family *Campylobacteraceae*, *Enterobacteriaceae* and *Moraxellaceae*. At the genera level, the most enriched genus in OSCC was *Acinetobacter* followed by *Campylobacter*. The enriched taxa in saliva and mouthwash samples were from Firmicutes and Bacteroidetes, expect members of *Neisseriales*. *Prevotellaceae, Streptococcaceae, Veillonellaceae* were more abundant at family level. The genera *Prevotella* and *Streptococcus* were most enriched in saliva and mouthwash (**Supplementary Figure S2**).

Functional Prediction of Predominant Taxa of OSCC

We used Phylogenetic Investigation of Communities by Reconstruction of Unobserved States (PICRUSt) to infer the KEGG pathways between the microbiota of group T and groups S and W. A significant difference was found in the following KEGG pathways: the OSCC microbiome had a higher abundance in the p53 signaling pathway (**Figure 5A**, p = 4.31E-05) and LPS biosynthesis proteins (**Figure 5B**, p = 3.09E-09); the S and W groups were more enriched in the bacterial invasion of epithelial cells (**Figure 5C**, p = 4.89E-08) and bacterial toxins (**Figure 5D**, p < 1E-10).

Microbial Characteristics Analysis Among OSCC Stage and Location

In order to verify the relationship between microbial composition and OSCC in different parts, we first carried out microecological composition analysis. At the phylum level, the high abundance of Bacteroidetes and Fusobacteria was detected in tongue tumors, Firmicutes was enriched in gingiva sites and Proteobacteria was enriched in oropharynges (**Figure 6A**, correlation >0.6, p < 0.05). At the genus level, the most abundant taxa of each tumor site were *Prevotella* (tongue), *Acinetobacter* (oropharynx), *Pseudomonas* (gingiva) and *Fusobacterium* (cheek) (**Figure 7A**, correlation >0.8, p < 0.05). The results indicate that the bacteria associated with tumorigenesis may be different in different parts of OSCC.

We further analyzed the relationship between microbiota composition and different stages of OSCC. In the early tumor stage, the relative abundance of Bacteroidetes and Fusobacteria were significantly higher, while in the late tumor

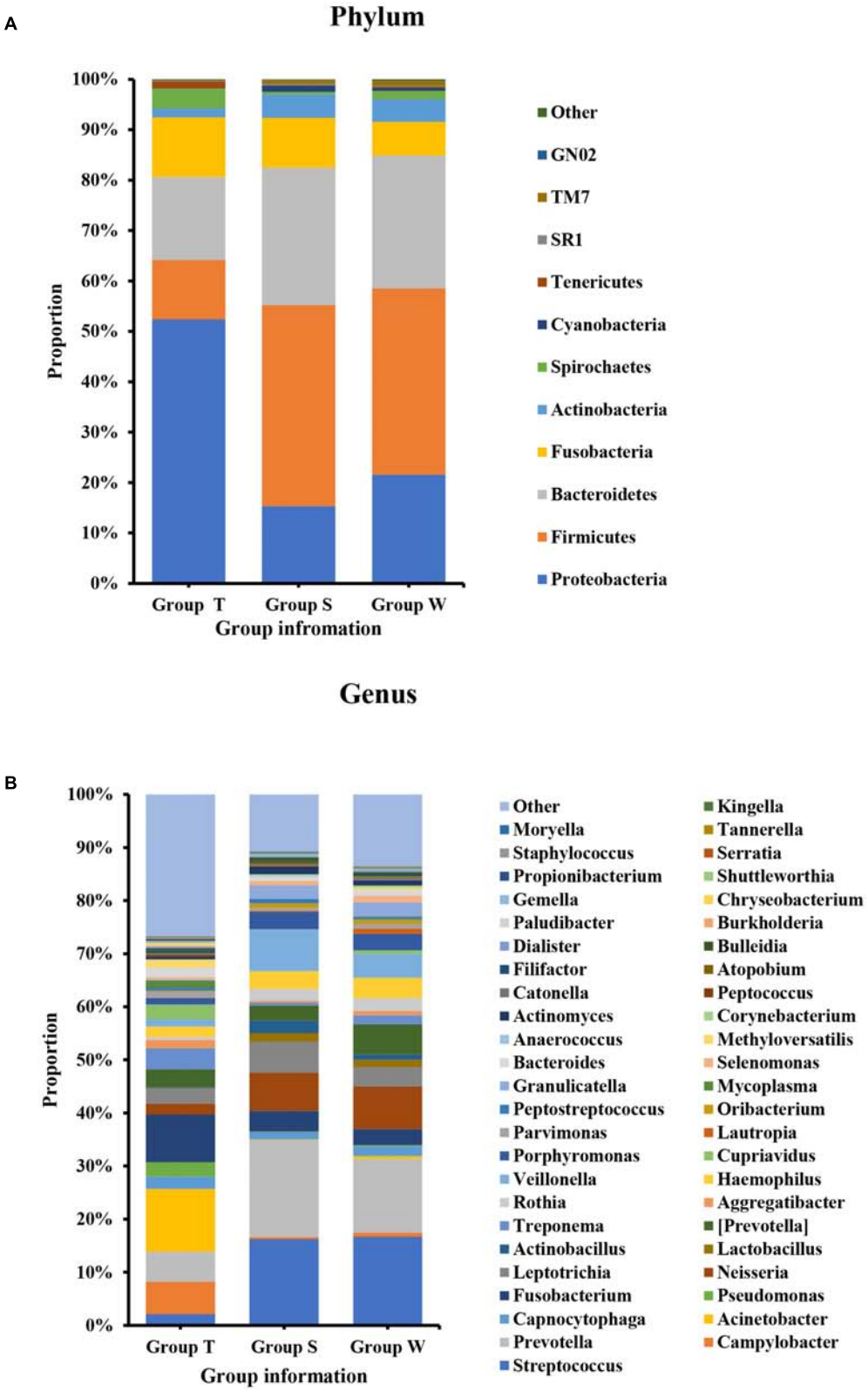

FIGURE 1 | Bacterial composition on phylum **(A)** and genus **(B)** levels by OTU analysis. S, saliva group; W, oral wash group; T, tumor tissue group. The leading phyla were Firmicutes, Bacteroidetes, Proteobacteria, Fusobacteria, and Actinobacteria. On the genus level, the predominant genera were *Prevotella, Streptococcus, Veillonella, Leptotrichia, Fusobacterium,* etc.

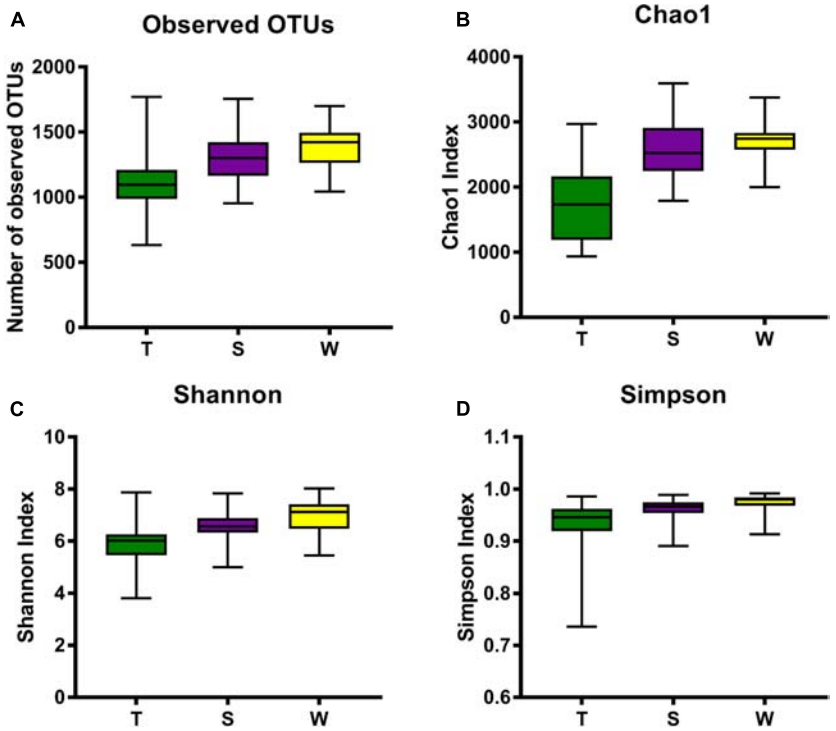

FIGURE 2 | Alpha diversity analysis against all three groups. Box plots of Observed OTUs **(A)**, Simpson index **(B)**, Shannon's index **(C)** and Chao 1 index **(D)** are shown. The indexes of groups S and W were higher than group T from the four plots, indicating that the S group and W group had higher alpha diversity than the T group.

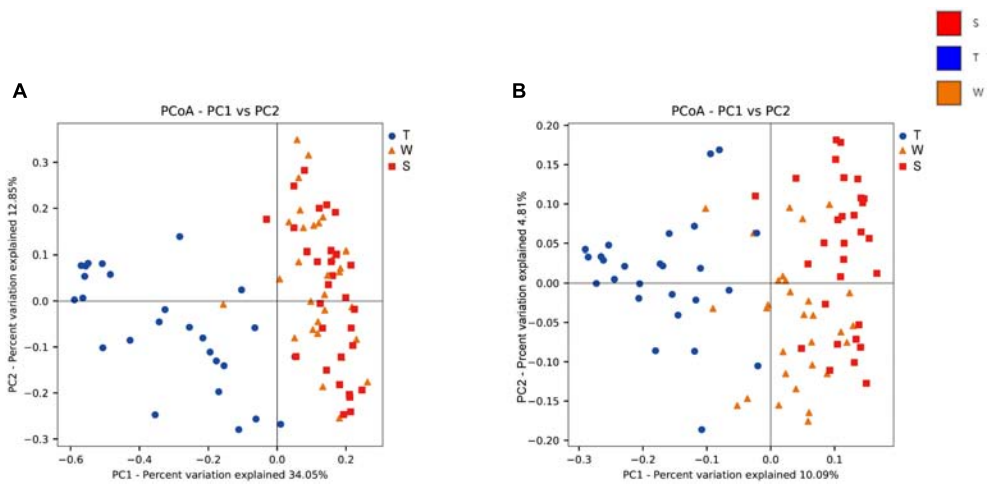

FIGURE 3 | Beta diversity analysis among groups. Weighted **(A)** and unweighted **(B)** PCoA plot with respect to the bacterial abundance and composition. In the weighted PCoA, PC1 explained 34.05% of the variation, and PC2 explained 12.85% of the variation. In the unweighted PCoA, PC1 accounted for 10.09% of the variation, and PC2 accounted for 4.81% of the variation.

stage, the significant enriched taxa were Firmicutes and Proteobacteria (**Figure 6B**, correlation >0.6, $p < 0.05$). At the genus level, the most enriched genera in the early OSCC stage were *Campylobacter* and *Prevotella*, while *Acinetobacter* and *Fusobacterium* were more enriched in the late OSCC stage (**Figure 7B**, correlation >0.8, $p < 0.05$). The shared taxa of different tumor sites (**Supplementary Figures S3A,B**) and tumor stages (**Supplementary Figures S3C,D**) were analysed, and no significantly enriched taxa were found. We performed the relative analysis of taxa against alcohol and smoking, but the relativeness of the taxa was all below 0.4 (**Supplementary Figure S4**).

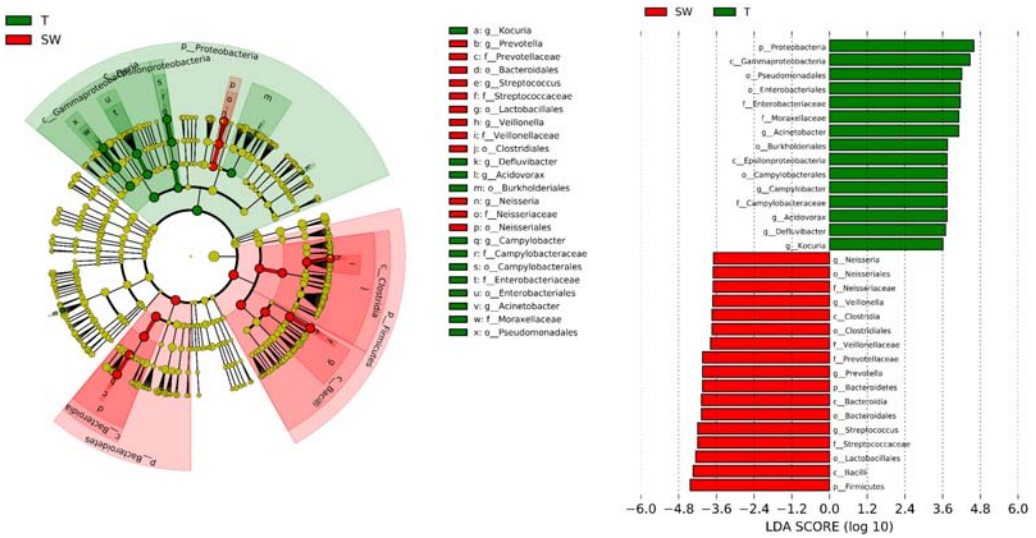

FIGURE 4 | Biomarker analysis. LEfSe analysis between OSCC tissue and saliva, biomarkers from the phylum level to genus level are indicated on the right.

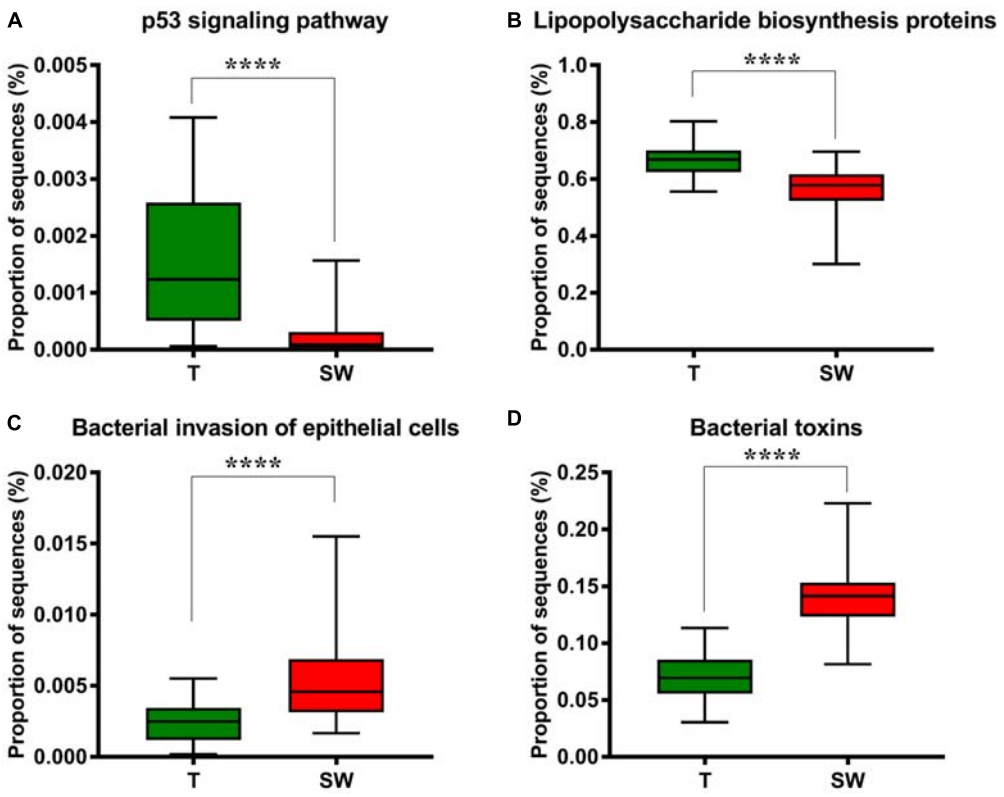

FIGURE 5 | Box plot showing the significantly different KEGG items between group T and groups S and W. Group T had a higher proportion of sequences in TP53 pathways **(A)** and lipopolysaccharide biosynthesis proteins **(B)**; Groups S and W had a higher proportion of sequences in bacterial invasion of epithelial cells **(C)** and bacterial toxins **(D)**.

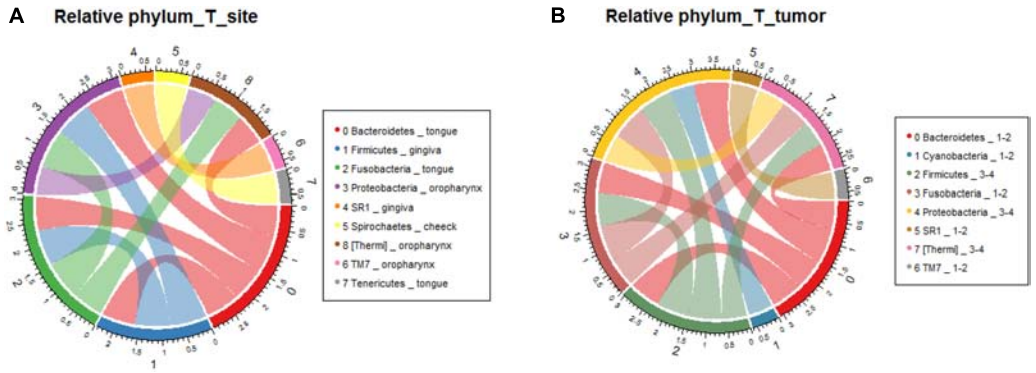

FIGURE 6 | Relative analysis of taxa against OSCC tumor sites. The correlations between the microbial profile and tumor sites were performed at the phylum level **(A)** and genus level **(B)**, respectively.

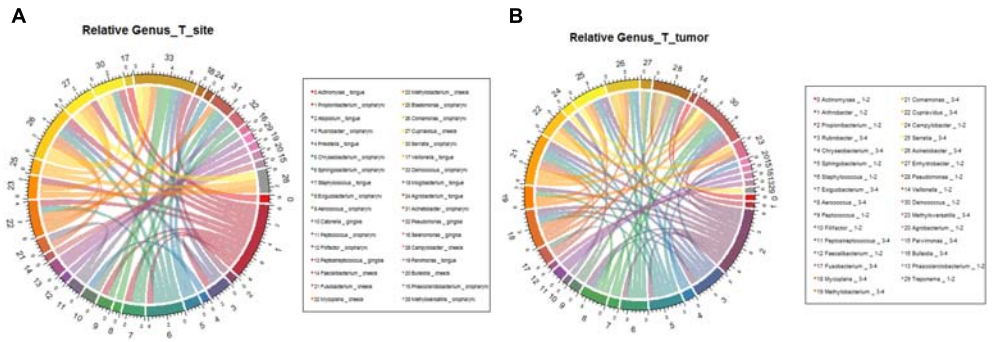

FIGURE 7 | Relative analysis of taxa against OSCC tumor stages. The correlations between the microbial profile and tumor stages were showed on phylum **(A)** and genus **(B)** levels.

DISCUSSION

Our study is a pilot report on the microbiota consistency and diversity in tumor tissues, saliva and oral wash samples from the same patient with OSCCs. In previous studies, some models of microbe infection and oral tumourigenesis have already been established. For instance, HPV is a cause of oral cancer through the Rb pathway (Hu et al., 2016). *Candida albicans* has been reported to have a higher prevalence in patients with OSCCs and leukoplakia. Infections by *P. gingivalis* and *F. nucleatum* have been proven to cause cancer through pathways of MMP9 and upregulation of cytokines such as TNF-α, IL-1β, and IL-6 (Herrero et al., 2003; Whitmore and Lamont, 2014; Jahanshahi and Shirani, 2015). However, the understanding of the relationship between the shift in oral microbiota and OSCC pathogenesis is still not fully established (Hu et al., 2016). Studies have been performed to analyze the microbial diversity between OSCC patients and healthy subjects using saliva or cancer tissue samples, but the relationship between microbiota in OSCC and oral cavity fluid was not clear.

The OSCC microbiota is spatially divided into two subgroups: the superficial and deep portions of the tumor tissue. The oral wash samples were included in this study as a supplement to the saliva and shed, during the sample collection, saliva was collected after rinse of the whole mouth, we supposed that mouthwash may have better contacts with tumor site, however, they showed similar properties to saliva microbiota (**Figures 1**, **3**). Thus, the saliva and mouthwash data were combined in the following analysis. Several studies have reported an increase in *Fusobacteria* in OSCC (Schmidt et al., 2014), which was consistent with the high level of *Fusobacteria* in our research, especially in the late tumor stage. The results showed that Proteobacteria was the most predominant phyla in OSCC tissue, and a previous study indicated that the relative abundance of Proteobacteria in oral cavity mucosa was less than 20% (Schmidt et al., 2014). The percentage of Firmicutes was lower in OSCC tissue than in the S and W groups. The relative abundance of *Proteobacteria* in group T was as high as 52% (**Figure 1A**), the richness was largely contributed by *Acinetobacter* and *Campylobacter*, but this was not observed in other studies. Since the Proteobacteria subgroups are mainly anaerobic and facultative anaerobic bacteria (Ringel et al., 2015), the inner tissue would be a suitable microenvironment for the colonization and growth of these bacteria. At the genera level, extremely low abundance of *Streptococcus* and *Rothia* were observed (**Figure 1B**), which was in agreement with previous research (Pushalkar et al., 2012). The high levels of *Fusobacterium*, *Acinetobacter* and *Campylobacter* were thought to be associated with local infection

and inflammation. The top 10 taxa that differentiate OSCC tissue from saliva were *p_Proteobacteria, c_Gammaproteobacteria, o_Pseudomonadales, o_Enterobacteriales, f_Moraxellaceae, g_Acinetobacter, o_Burkholderiales, c_Epsilonproteobacteria, o_Campylobacterales* and *g_Campylobacter* (**Figure 4**, ranked by LDA value from large to small). There is an immune suppression in a patient with advanced cancer, for instance, the accumulation of *Pseudomonadales* is related to several oral diseases, and *Enterobacteriales* and *Acinetobacter* are often observed in infections in the intestinal and urinary tract (Fouts et al., 2012; Peters et al., 2016); we speculated that the increase in these taxa in OSCC tissue was a signal of immune system depletion.

Our results indicated that there were unique genera in cancer tissue that were not detected from saliva or mouthwash (**Supplementary Figure S1D**). *Deinococcus* is known for its robust survival ability against ionizing radiation and oxidative stress. Species of the *Deinococcus* genus utilize their highly conserved helicase RecQ to precisely recover the genome from damage (Cox and Battista, 2005). Members of the *Rubrobacter* genus have similar antioxidant activities (Pavlopoulou et al., 2016). There were also genera found to be infectious, such as *Chryseobacterium*, *Sphingobacterium*, *Staphylococcus*, *Serratia,* and *Burkholderia*. For instance, in the *Chryseobacterium* genus, *C. meningosepticum* and *C. indologenes* are more commonly observed in human infections, and they usually cause meningitis and pneumonia, respectively, especially in patients with an impaired immune system (Nordmann and Poirel, 2002). On the other hand, we also noticed that all of these bacterial groups were typically involved in nosocomial infections, which were possibly attached during incision. Fecal bacteria such as *Parabacteroides*, *Lachnospira*, *Faecalibacterium*, *Megamonas,* and *Phascolarctobacterium* were also detected in the cancer tissue group, some of which were found to be more enriched in colon-rectal cancer (Kverka et al., 2011; Chen et al., 2012; Thomas et al., 2016; Zeng et al., 2016). The presence of these unusual taxa probably worsens the local inflammation of the OSCC inner micro environment.

To study the potential roles of microbiota in OSCC tissue and saliva sample, we performed a series of functional analyses (Wang and Ganly, 2014; Yang et al., 2018). By applying PICRUSt pathway analysis, we examined the capability of microbiota in epithelial cell invasion, bacterial toxin production, LPS synthesis protein and the p53 signaling pathway (**Figures 5A–D**). Overall, based on the proportion of sequences, group T had more sequences related to functions affecting the p53 signaling pathway and genes for LPS synthesis, while groups W and S were better at penetrating the epithelial cell and producing bacterial toxins. LPS may act as an effector molecule in shift oral epithelial cell to cancer (Gholizadeh et al., 2017). The p53 tumor suppressor gene is well known in oral cancer and mutated in 50% of oral cancer patients, the p53 signaling pathway is essential for regulation of cell cycle progression, differentiation, DNA repair and apoptosis (Sinevici and O'sullivan, 2016). In Greathouse's study (Greathouse et al., 2018), they established the microbiome-*TP53* gene interaction in human lung cancer tissue, and the higher abundance of certain taxa, including *Acidovorax*, were associated with *TP53* mutation in squamous cancer cells. Perera et al. (2018) suggested that compositional studies showed inconsistency among results, and functional predications were useful tools to examine the bacteriome in OSCC. In our study, the functional predication indicated that in OSCC tissues, the microbiota were more involved in LPS synthesis and escape of host cell cycle arrest, which were potential risk factors for OSCC, while in saliva, the microbiota functions were more enriched in penetrating cells and secreting toxins, which worsened the micro-environment. Considering that the functional analysis in 16S rRNA gene sequencing is based on bacteria at the genera level by targeting variable regions, which could not reflect the bacterial gene function and activity very precisely, metagenomic sequencing and co-culture with cell lines are needed in future studies (Wang et al., 2015).

CONCLUSION

In conclusion, this cross-sectional study illustrated the comparison between microbiota in OSCC and saliva samples collected from the same subjects. In OSCC tissue, the most abundant taxa were *Acinetobacter* and *Fusobacterium*, they were also found predominantly in the late stage of OSCC, their ability of causing infection and local inflammation were potential facilitator of OSCC progress. The microbiota composition in mouth wash samples were similar to saliva samples, but both of them were distinct from OSCC tissue. The PICRUSt pathway analysis suggested the role of OSCC and saliva microbiota, respectively. There were several limitations of this study: (1) Restricted by the resolution of the 16S technique, the similarity of OTUs was set to 97%, which was not accurate enough to differentiate members at the species level with limited functional information, and the amplification biases may lead to inaccuracy of the result; (2) In our study, we only included 30 subjects, which was still a small sample size. An enlarged group size will be needed in future validation studies. Strategies such as whole-genome shotgun sequencing and metabolomics will be used to achieve a more detailed analysis. Longitudinal research will be performed to study the relationship between oral microbiota shift and OSCC progress.

DATA AVAILABILITY

The datasets used and/or analyzed during the current study available from the corresponding author on reasonable request. Sequence files and metadata for all samples used in this study have been deposited in SRA (PRJNA528843).

AUTHOR CONTRIBUTIONS

WC and LZ designed the study. WC, QX, MiL, and ZhL collected all the saliva and tissue samples. ZZ, JY, BC, QF, and MeL performed the measurements and data analysis. ZZ, LZ, and

WC wrote the manuscript. All authors have read and critically revised the manuscript.

FUNDING

This work was supported by the National Key Research and Development Program of China No. 2016YFC0902700 (WC), the National Natural Science Foundation of China Nos. 81874126 and 91229103 (WC) and No. 31471202 (LZ), the Shanghai Science and Technology Commission No. 18DZ2291500 (WC), and the Taishan Scholars Program of Shandong Province No. tshw20120206 (LZ).

ACKNOWLEDGMENTS

We thank all members of the Ninth People's Hospital, Shanghai Jiao Tong University School of Medicine, Shanghai Research Institute of Stomatology, and Shanghai Key Laboratory of Stomatology for valuable suggestions and discussions of the experiment.

SUPPLEMENTARY MATERIAL

The Supplementary Material for this article can be found online at: https://www.frontiersin.org/articles/10.3389/fmicb.2019.01439/full#supplementary-material

FIGURE S1 | Compositional analysis of taxa at the class level **(A)**, order level **(B)** and family level **(C)**. **(D)** Venn diagram showing the number of shared and unique species of each group at the genus level.

FIGURE S2 | The most enriched genera in group T or S and W group.

FIGURE S3 | The shared taxa of different tumor sites **(A,B)** and tumor stages **(C,D)**.

FIGURE S4 | The relative analysis of taxa against smoking and drinking history of patients, the relation with OSCC tissue **(A)** and saliva **(B)** sample were showed. *Means between 0.05 and 0.1, **stands for less than 0.05.

REFERENCES

Ahn, J., Segers, S., and Hayes, R. B. (2012). Periodontal disease, *Porphyromonas gingivalis* serum antibody levels and orodigestive cancer mortality. *Carcinogenesis* 33, 1055–1058. doi: 10.1093/carcin/bgs112

Chen, T., Yu, W. H., Izard, J., Baranova, O. V., Lakshmanan, A., and Dewhirst, F. E. (2010). The human oral microbiome database: a web accessible resource for investigating oral microbe taxonomic and genomic information. *Database* 2010:baq013. doi: 10.1093/database/baq013

Chen, W., Liu, F., Ling, Z., Tong, X., and Xiang, C. (2012). Human intestinal lumen and mucosa-associated microbiota in patients with colorectal cancer. *PLoS One* 7:e39743. doi: 10.1371/journal.pone.0039743

Corrêa, J. D., Calderaro, D. C., Ferreira, G. A., Mendonça, S. M., Fernandes, G. R., Xiao, E., et al. (2017). Subgingival microbiota dysbiosis in systemic lupus erythematosus: association with periodontal status. *Microbiome* 5:34. doi: 10.1186/s40168-017-0252-z

Cox, M. M., and Battista, J. R. (2005). Deinococcus radiodurans |[mdash]| the consummate survivor. *Nat. Rev. Microbiol.* 3, 882–892. doi: 10.1038/nrmicro1264

Crozier, E., and Sumer, B. D. (2010). Head and neck cancer. *Med. Clin. North Am.* 94, 1031–1046.

Dewhirst, F. E., Chen, T., Izard, J., Paster, B. J., Tanner, A. C., and Yu, W. H. (2010). The human oral microbiome. *J. Bacteriol.* 192:5002. doi: 10.1128/JB.00542-10

Fåk, F., Tremaroli, V., Bergström, G., and Bäckhed, F. (2015). Oral microbiota in patients with atherosclerosis. *Atherosclerosis* 243:573. doi: 10.1016/j.atherosclerosis.2015.10.097

Fardini, Y., Chung, P., Dumm, R., Joshi, N., and Han, Y. W. (2010). Transmission of diverse oral bacteria to murine placenta: evidence for the oral microbiome as a potential source of intrauterine infection. *Infect. Immun.* 78:1789. doi: 10.1128/IAI.01395-09

Farrell, J. J., Zhang, L., Zhou, H., Chia, D., Elashoff, D., Akin, D., et al. (2012). Variations of oral microbiota are associated with pancreatic diseases including pancreatic cancer. *Gut* 61:582. doi: 10.1136/gutjnl-2011-300784

Fouts, D. E., Pieper, R., Szpakowski, S., Pohl, H., Knoblach, S., Suh, M. J., et al. (2012). Integrated next-generation sequencing of 16S rDNA and metaproteomics differentiate the healthy urine microbiome from asymptomatic bacteriuria in neuropathic bladder associated with spinal cord injury. *J. Transl. Med.* 10, 174. doi: 10.1186/1479-5876-10-174

Gholizadeh, P., Eslami, H., and Kafil, H. S. (2017). Carcinogenesis mechanisms of *Fusobacterium nucleatum*. *Biomed. Pharmacother.* 89, 918–925. doi: 10.1016/j.biopha.2017.02.102

Greathouse, K. L., White, J. R., Vargas, A. J., Bliskovsky, V. V., Beck, J. A., von Muhlinen, N., et al. (2018). Microbiome-TP53 gene interaction in human lung cancer. *bioRxiv*

Guan, H., Shen, A., Lv, X., Yang, X., Ren, H., Zhao, Y., et al. (2016). Detection of virus in CSF from the cases with meningoencephalitis by next-generation sequencing. *J. Neurovirol.* 22:240. doi: 10.1007/s13365-015-0390-7

Han, Y. W., and Wang, X. (2013). Mobile microbiome: oral bacteria in extra-oral infections and inflammation. *J. Dent. Res.* 92:485. doi: 10.1177/0022034513487559

He, J., Li, Y., Cao, Y., Xue, J., and Zhou, X. (2015). The oral microbiome diversity and its relation to human diseases. *Folia Microbiol.* 60, 69–80. doi: 10.1007/s12223-014-0342-2

Herrero, R., Castellsagué, X., Pawlita, M., Lissowska, J., Kee, F., Balaram, P., et al. (2003). Human papillomavirus and oral cancer: the international agency for research on cancer multicenter study. *J. Natl. Cancer Inst.* 95, 1772–1783. doi: 10.1093/jnci/djg107

Hooper, S. J., Crean, S. J., Fardy, M. J., Lewis, M. A., Spratt, D. A., Wade, W. G., et al. (2007). A molecular analysis of the bacteria present within oral squamous cell carcinoma. *J. Med. Microbiol.* 56, 1651–1659. doi: 10.1099/jmm.0.46918-0

Hooper, S. J., Crean, S. J., Lewis, M. A., Spratt, D. A., Wade, W. G., and Wilson, M. J. (2006). Viable bacteria present within oral squamous cell carcinoma tissue. *J. Clin. Microbiol.* 44, 1719–1725. doi: 10.1128/jcm.44.5.1719-1725.2006

Hooper, S. J., Wilson, M. J., and Crean, S. J. (2009). Exploring the link between microorganisms and oral cancer: a systematic review of the literature. *Head Neck* 31, 1228–1239. doi: 10.1002/hed.21140

Hu, X., Zhang, Q., Hua, H., and Chen, F. (2016). Changes in the salivary microbiota of oral leukoplakia and oral cancer. *Oral Oncol.* 56, e6–e8. doi: 10.1016/j.oraloncology.2016.03.007

Jahanshahi, G., and Shirani, S. (2015). Detection of *Candida albicans* in oral squamous cell carcinoma by fluorescence staining technique. *Dent. Res. J.* 12, 115–120.

Jemal, A., Siegel, R., Xu, J., and Ward, E. (2010). Cancer statistics. *CA Cancer J. Clin.* 60, 277–300. doi: 10.3322/caac.20073

Kademani, D. (2007). Oral cancer. *Mayo Clin. Proc.* 82, 878–887.

Kverka, M., Zakostelska, Z., Klimesova, K., Sokol, D., Hudcovic, T., Hrncir, T., et al. (2011). Oral administration of *Parabacteroides distasonis* antigens attenuates experimental murine colitis through modulation of immunity and microbiota composition. *Clin. Exp. Immunol.* 163, 250–259. doi: 10.1111/j.1365-2249.2010.04286.x

Lamont, R. J., Koo, H., and Hajishengallis, G. (2018). The oral microbiota: dynamic communities and host interactions. *Nat. Rev.Microbiol.* 16, 745–759. doi: 10.1038/s41579-018-0089-x

Langille, M. G. I, Zaneveld, J., Caporaso, J. G., McDonald, D., Knights, D., Reyes, J. A., et al. (2013). Predictive functional profiling of microbial communities using 16S rRNA marker gene sequences. *Nat. Biotechnol.* 31, 814–821. doi: 10.1038/nbt.2676

Magoč, T., and Salzberg, S. L. (2011). FLASH: fast length adjustment of short reads to improve genome assemblies. *Bioinformatics* 27, 2957–2963. doi: 10.1093/bioinformatics/btr507

Mendz, G. L., Kaakoush, N. O., and Quinlivan, J. A. (2013). Bacterial aetiological agents of intra-amniotic infections and preterm birth in pregnant women. *Front. Cell. Infect. Microbiol.* 3:58. doi: 10.3389/fcimb.2013.00058

Meurman, J. H. (2010). Oral microbiota and cancer. *J. Oral Microbiol.* 2:10.

Nordmann, P., and Poirel, L. (2002). Emerging carbapenemases in gram-negative aerobes. *Clin. Microbiol. Infect.* 8, 321–331. doi: 10.1046/j.1469-0691.2002.00401.x

Parks, D. H., and Beiko, R. G. (2010). Identifying biologically relevant differences between metagenomic communities. *Bioinformatics* 26, 715–721. doi: 10.1093/bioinformatics/btq041

Pavlopoulou, A., Savva, G. D., Louka, M., Bagos, P. G., Vorgias, C. E., Michalopoulos, I., et al. (2016). Unraveling the mechanisms of extreme radioresistance in prokaryotes: lessons from nature. *Mutat. Res. Rev. Mutat. Res.* 767, 92–107. doi: 10.1016/j.mrrev.2015.10.001

Perera, M., Al-Hebshi, N. N., Perera, I., Ipe, D., Ulett, G. C., Speicher, D. J., et al. (2018). Inflammatory bacteriome and oral squamous cell carcinoma. *J. Dent. Res.* 26, 725–732. doi: 10.1177/0022034518767118

Peters, B. A., Dominianni, C., Shapiro, J. A., Church, T. R., Wu, J., Miller, G., et al. (2016). The gut microbiota in conventional and serrated precursors of colorectal cancer. *Microbiome* 4:69. doi: 10.1186/s40168-016-0218-6

Pizzo, G., Guiglia, R., Lo Russo, L., and Campisi, G. (2010). Dentistry and internal medicine: from the focal infection theory to the periodontal medicine concept. *Eur. J. Intern. Med.* 21, 496–502. doi: 10.1016/j.ejim.2010.07.011

Pushalkar, S., Ji, X., Li, Y., Estilo, C., Yegnanarayana, R., Singh, B., et al. (2012). Comparison of oral microbiota in tumor and non-tumor tissues of patients with oral squamous cell carcinoma. *BMC Microbiol.* 12:144. doi: 10.1186/1471-2180-12-144

Ringel, Y., Maharshak, N., Ringel-Kulka, T., Wolber, E. A., Sartor, R. B., and Carroll, I. M. (2015). High throughput sequencing reveals distinct microbial populations within the mucosal and luminal niches in healthy individuals. *Gut Microbes* 6, 173–181. doi: 10.1080/19490976.2015.1044711

Rivera, C., and Venegas, B. (2014). Histological and molecular aspects of oral squamous cell carcinoma (Review). *Oncol. Lett.* 8, 7–11. doi: 10.3892/ol.2014.2103

Riviere, G. R., Riviere, K. H., and Smith, K. S. (2002). Molecular and immunological evidence of oral Treponema in the human brain and their association with Alzheimer's disease. *Oral Microbiol. Immunol.* 17:113. doi: 10.1046/j.0902-0055.2001.00100.x

Schmidt, B. L., Kuczynski, J., Bhattacharya, A., Huey, B., Corby, P. M., Queiroz, E. L., et al. (2014). Changes in abundance of oral microbiota associated with oral cancer. *PLoS One* 9:e98741. doi: 10.1371/journal.pone.0098741

Sinevici, N., and O'sullivan, J. (2016). Oral cancer: deregulated molecular events and their use as biomarkers. *Oral Oncol.* 61, 12–18. doi: 10.1016/j.oraloncology.2016.07.013

Smruti, P., Ji, X., Li, Y., Estilo, C., Yegnanarayana, R., Singh, B., et al. (2012). Comparison of oral microbiota in tumor and non-tumor tissues of patients with oral squamous cell carcinoma. *BMC Microbiol.* 12:144. doi: 10.1186/1471-2180-12-144

Sonis, S. T. (2017). The chicken or the egg? Changes in oral microbiota as cause or consequence of mucositis during radiation therapy. *Ebiomedicine* 18, 7–8. doi: 10.1016/j.ebiom.2017.03.017

Takahashi, N., and Nyvad, B. (2008). Caries ecology revisited: microbial dynamics and the caries process. *Caries Res.* 42, 409–418. doi: 10.1159/000159604

Thomas, A. M., Jesus, E. C., Lopes, A., Aguiar, S Jr., Begnami, M. D., Rocha, R. M., et al. (2016). Tissue-associated bacterial alterations in rectal carcinoma patients revealed by 16s rrna community profiling. *Front. Cell Infect. Microbiol.* 6:179. doi: 10.3389/fcimb.2016.00179

Wang, L., and Ganly, I. (2014). The oral microbiome and oral cancer. *Clin. Lab. Med.* 34, 711–719. doi: 10.1016/j.cll.2014.08.004

Wang, W., Jovel, J., Halloran, B., Wine, E., Patterson, J., Ford, G., et al. (2015). Metagenomic analysis of microbiome in colon tissue from subjects with inflammatory bowel diseases reveals interplay of viruses and bacteria. *Inflamm. Bowel Dis.* 21, 1419–1427. doi: 10.1097/MIB.0000000000000344

Warren, R. L., Freeman, D. J., Pleasance, S., Watson, P., Moore, R. A., Cochrane, K., et al. (2013). Co-occurrence of anaerobic bacteria in colorectal carcinomas. *Microbiome* 1:16. doi: 10.1186/2049-2618-1-16

Whitmore, S. E., and Lamont, R. J. (2014). Oral bacteria and cancer. *PLoS Pathog.* 10:e1003933. doi: 10.1371/journal.ppat.1003933

Yang, S. F., Huang, H. D., Fan, W. L., Jong, Y. J., Chen, M. K., Huang, C. N., et al. (2018). Compositional and functional variations of oral microbiota associated with the mutational changes in oral cancer. *Oral Oncol.* 77, 1–8. doi: 10.1016/j.oraloncology.2017.12.005

Yost, S., Duran-Pinedo, A. E., Teles, R., Krishnan, K., and Frias-Lopez, J. (2015). Erratum to: functional signatures of oral dysbiosis during periodontitis progression revealed by microbial metatranscriptome analysis. *Genome Med.* 7:27.

Zaura, E., Keijser, B. J., Huse, S. M., and Crielaard, W. (2009). Defining the healthy "core microbiome" of oral microbial communities. *BMC Microbiol.* 9:259. doi: 10.1186/1471-2180-9-259

Zeng, H., Ishaq, S. L., Zhao, F. Q., and Wright, A. G. (2016). Colonic inflammation accompanies an increase of β-catenin signaling and Lachnospiraceae/Streptococcaceae bacteria in the hind gut of high-fat diet-fed mice. *J. Nutr. Biochem.* 35:30. doi: 10.1016/j.jnutbio.2016.05.015

Zhang, X., Zhang, D., Jia, H., Feng, Q., Wang, D., Liang, D., et al. (2015). The oral and gut microbiomes are perturbed in rheumatoid arthritis and partly normalized after treatment. *Nat. Med.* 21:895. doi: 10.1038/nm.3914

Conflict of Interest Statement: The authors declare that the research was conducted in the absence of any commercial or financial relationships that could be construed as a potential conflict of interest.

frontiers in Microbiology

ORIGINAL RESEARCH
published: 02 August 2019
doi: 10.3389/fmicb.2019.01780

Characteristics of the Salivary Microbiota in Patients With Various Digestive Tract Cancers

*Shinya Kageyama[1], Toru Takeshita[1,2], Kenji Takeuchi[1], Mikari Asakawa[1], Rie Matsumi[1], Michiko Furuta[1], Yukie Shibata[1], Kiyoshi Nagai[3], Masahiko Ikebe[4], Masaru Morita[4], Muneyuki Masuda[5], Yasushi Toh[4], Yutaka Kiyohara[6], Toshiharu Ninomiya[7] and Yoshihisa Yamashita[1]**

[1] Section of Preventive and Public Health Dentistry, Division of Oral Health, Growth and Development, Faculty of Dental Science, Kyushu University, Fukuoka, Japan, [2] OBT Research Center, Faculty of Dental Science, Kyushu University, Fukuoka, Japan, [3] Department of Oral and Maxillofacial Surgery, National Hospital Organization Kyushu Cancer Center, Fukuoka, Japan, [4] Department of Gastroenterological Surgery, National Hospital Organization Kyushu Cancer Center, Fukuoka, Japan, [5] Department of Head and Neck Surgery, National Hospital Organization Kyushu Cancer Center, Fukuoka, Japan, [6] Hisayama Research Institute for Lifestyle Diseases, Fukuoka, Japan, [7] Department of Epidemiology and Public Health, Graduate School of Medical Sciences, Kyushu University, Fukuoka, Japan

The salivary microbiota is constantly swallowed and delivered to the digestive tract. These bacteria may be associated with gastrointestinal diseases. This case-control study examined the salivary microbiota in patients with digestive tract cancer (DTC) and evaluated their differential distribution based on the cancer sites. We collected saliva samples from 59 patients with cancer in any part of the digestive tract (tongue/pharynx, esophagus, stomach, and large intestine) and from 118 age- and sex-matched control subjects. There was no significant difference in periodontal status between DTC patients and control subjects ($P = 0.72$). We examined the bacterial diversity and composition in saliva by 16S ribosomal RNA gene sequencing. Salivary bacterial diversity in DTC patients was significantly higher than that in control subjects [number of operational taxonomic units (OTUs), $P = 0.02$; Shannon index, $P < 0.01$; Chao1, $P = 0.04$]. Eleven differentially abundant OTUs in DTC patients were identified using the linear discriminant analysis effect size (LEfSe) method. Based on the cancer sites, the diversity of salivary bacteria was especially higher in tongue/pharyngeal or esophageal cancer patients than in control subjects. Among the 11 differentially abundant OTUs in DTC patients, an OTU corresponding to *Porphyromonas gingivalis* was more abundant in the saliva of all groups of DTC patients compared to that in control subjects, and an OTU corresponding to *Corynebacterium* species was more abundant in all groups other than gastric cancer patients ($P < 0.01$). In addition, the relative abundances of OTUs corresponding to *Fusobacterium nucleatum*, *Streptococcus parasanguinis* II, and *Neisseria* species were significantly higher in tongue/pharyngeal cancer patients compared to their abundances in control subjects ($P < 0.01$). The relative abundance of an OTU corresponding to the *Neisseria* species was also significantly higher in gastric cancer patients and that of an OTU corresponding to *Actinomyces odontolyticus* was significantly higher in colorectal cancer patients ($P < 0.01$). These results suggest that the salivary microbiota might be associated with various digestive tract cancers.

Keywords: saliva, oral microbiota, digestive tract cancer, tongue cancer, pharyngeal cancer, esophageal cancer, gastric cancer, colorectal cancer

OPEN ACCESS

Edited by:
Nezar Al-hebshi,
Temple University, United States

Reviewed by:
Thuy Do,
University of Leeds, United Kingdom
Man Kit Cheung,
The Chinese University of Hong Kong, China

****Correspondence:***
Yoshihisa Yamashita
yoshi@dent.kyushu-u.ac.jp

Specialty section:
This article was submitted to Systems Microbiology, a section of the journal Frontiers in Microbiology

Received: *26 March 2019*
Accepted: *18 July 2019*
Published: *02 August 2019*

Citation:
Kageyama S, Takeshita T, Takeuchi K, Asakawa M, Matsumi R, Furuta M, Shibata Y, Nagai K, Ikebe M, Morita M, Masuda M, Toh Y, Kiyohara Y, Ninomiya T and Yamashita Y (2019) Characteristics of the Salivary Microbiota in Patients With Various Digestive Tract Cancers. Front. Microbiol. 10:1780. doi: 10.3389/fmicb.2019.01780

INTRODUCTION

The digestive tract comprises the oral cavity, pharynx, esophagus, stomach, and intestine. It has an indispensable role in the digestion and absorption of nutrients in the human body. Digestive tract cancer (DTC) is a malignant disease and is one of the most common cancers worldwide. In Japan, approximately 300,000 individuals are diagnosed with DTC annually (Hori et al., 2015). Among Japanese females, colorectal and gastric cancers are the first and fourth leading causes of cancer-related deaths, respectively, while among Japanese males they are the third and second leading causes, respectively (Ministry of Health, Labour and Welfare, 2018). Numerous epidemiological studies have demonstrated that smoking, alcohol intake, obesity, underweight, and low consumption of vegetables and fruits are lifestyle factors associated with DTC (Kabat et al., 1994; Bosetti et al., 2000; Engel et al., 2003; Huang et al., 2003; Ferrari et al., 2007; Freedman et al., 2007; Paskett et al., 2007; Botteri et al., 2008; Leung et al., 2008; Varela-Lema et al., 2010; Radoï et al., 2015; Shaukat et al., 2017). In addition, several studies have suggested the involvement of bacteria in several types of cancers, especially in organs continuously exposed to microbes, by the induction of chronic and persistent inflammation or the downregulation of host immunity (Allavena et al., 2008; Dalton-Griffin and Kellam, 2009; Tjalsma et al., 2012; Mima et al., 2015).

In the oral cavity, innumerable bacteria form a complex and stable bacterial community, which may play an important role in the oral and systemic diseases (Socransky et al., 1998; Pérez-Chaparro et al., 2014; Kholy et al., 2015; Mathews et al., 2016; Takeshita et al., 2016; Zaura et al., 2017; Asakawa et al., 2018; Kageyama et al., 2018). Considering that the oral microbiota is constantly swallowed along with saliva and delivered to the digestive tract, it is reasonable to consider that the oral microbiota is a possible risk factor for DTC, even in cancer sites that are distant from the oral cavity. In fact, *Fusobacterium nucleatum*, a periodontal disease pathogen, that usually inhabits the oral cavity is frequently detected and is abundant in colorectal carcinoma tissue (Mima et al., 2015; Nosho et al., 2016). Moreover, it is assumed that the causal link between oral microbiota and DTC differs by organs, because each digestive tract organ has a specific environment and an indigenous bacterial community. Evaluation of the characteristics of salivary microbiota in DTC patients according to the cancer sites may help in the elucidation of the microbial etiology of DTC, and aid in prediction or diagnosis of DTC.

Although previous studies have examined the association between the oral microbiota and DTC, interpretation of differences among these studies is not easy because the background of participants, such as race and food-related culture, differed in the studies (Peters et al., 2017; Zhao et al., 2017; Flemer et al., 2018; Yang et al., 2018). Additionally, although earlier studies suggested that several periodontal pathogens play a role in the development of DTC, no study has attempted to evaluate the relationship between oral microbiota and DTC accounting for the oral health condition, especially periodontal status, which is strongly related to bacterial diversity and composition in the oral cavity (Kageyama et al., 2017).

In this study, we examined the salivary microbiota collected from various DTC patients. We compared the bacterial diversity and composition in DTC patients with those from age- and sex-matched control subjects, using the 16S ribosomal RNA (16S rRNA) gene amplicon deep sequencing. Additionally, we accounted for the oral health condition of the subjects. The aim of this study was to compare the characteristics of the salivary microbiota in DTC patients and control subjects, and to evaluate their differential distribution by the cancer sites.

MATERIALS AND METHODS

Study Subjects

Study subjects in this study were patients with cancer who visited the National Kyushu Cancer Center, Fukuoka, Japan. We enrolled 71 Japanese patients at their first visit for preoperative oral care prior to cancer treatment from October 2015 to February 2017. We conducted a dental examination and collected saliva samples from these patients. Patients who used antibiotics within a month preceding sampling or who had already received cancer treatment were not recruited. After excluding 12 patients who had missing clinical data (n = 3) and whose cancer was not located in the digestive tract (n = 9), 59 patients were finally included in the analysis. For control subjects, we used saliva samples and clinical data of community-dwelling people who participated in the Hisayama study, a population-based prospective study performed in the town of Hisayama (a suburban rural area of Fukuoka city in southern Japan) (Hata et al., 2013). A part of the Hisayama study conducted in 2012 comprised dental examination and saliva sampling for residents ≥39 years of age. Of the 2,654 participants who received dental examination (56.4% of the total population in this age group), 2,111 underwent saliva sampling. We randomly sampled 118 age- and sex-matched control subjects (ratio 1:2, age difference within 1 year) from 1,913 participants after excluding those with missing periodontal examination data (n = 2), and self-reported medical history for cancer (n = 196). Written informed consent was obtained from all participants. The ethics committee of Kyushu University approved this study and the informed consent procedure (Approval Number 27–37).

Dental Examination and Sample Collection

The dental examination and sample collection in patients and control subjects were conducted according to a previously described protocol (Takeshita et al., 2016). In brief, the periodontal condition was evaluated by measuring the periodontal pocket depth (PPD) and by bleeding on probing (BOP) at two sites for all teeth (mesio- and mid-buccal sites) based on the NHANES III method. The oral hygiene status was assessed using the dental plaque score according to the Silness and Löe (1964) plaque index. Following the dental examination, the subjects chewed gum for 2 min; the stimulated saliva was collected in sterile plastic tubes. The samples were stored at −80°C until further analysis.

16S rRNA Gene Amplicon Sequencing of Saliva

DNA was extracted from each sample obtained from DTC patients using the bead-beating method (Yamanaka et al., 2012). The V1–V2 regions of 16S rRNA gene were amplified using the following primers: 8F (5′-AGA GTT TGA TYM TGG CTC AG-3′) with the Ion Torrent adapter A and the sample-specific 8-base index tag sequence, and 338R (5′-TGC TGC CTC CCG TAG GAG T-3′) with the Ion Torrent trP1 adapter sequence. PCR amplification, purification, and quantification of each PCR amplicon was performed as previously described (Takeshita et al., 2016). The purified PCR amplicons were pooled, and gel-purification was performed using Wizard SV Gel and PCR Clean-Up System (Promega, WI, United States). The DNA concentration was determined using a KAPA Library Quantification Kit (KAPA Biosystems, MA, United States) and the DNA was diluted for emulsion PCR. Emulsion PCR and enrichment of template-positive particles were performed using Ion PGM Hi-Q View OT2 Kit (Thermo Fisher Scientific, MA, United States) in the Ion One Touch 2 system (Thermo Fisher Scientific). The sequencing was performed on the Ion PGM (Thermo Fisher Scientific) using Ion PGM Hi-Q view Sequencing kit. DNA extraction from samples of control subjects, followed by PCR amplification, and purification were performed as described above. The purified PCR amplicons were pooled (up to 192 amplicons per pool) and sequencing was performed in 14 runs using Ion PGM Template OT2 400 Kit (Thermo Fisher Scientific) and Ion PGM Hi-Q Sequencing kit (Thermo Fisher Scientific).

Data Analysis and Taxonomy Assignment

We completed the quality filtering of raw sequence reads using a script written in R (version 3.5.1). The reads were excluded from the analysis when they exhibited $\leq$200 bases, had an average quality score $\leq$25, did not include the correct forward primer sequence, did not include the correct reverse primer sequence (one mismatch was allowed), or had a homopolymer run $>$6 nucleotides. The quality-checked reads were demultiplexed by examining the 8-base tag sequence, and then forward and reverse primer sequences were trimmed. The quality-checked reads derived from 177 subjects of this study were extracted and used for further analysis. Operational taxonomic units (OTUs) were constructed by clustering quality-checked reads, excluding singleton reads, with a minimum pairwise identity of 97% using UPARSE (Edgar, 2013) as described previously (Takeshita et al., 2016). All quality-checked reads were mapped to each OTU with $\geq$97% identity using UPARSE (Takeshita et al., 2016). Chimeras were identified using ChimeraSlayer and removed from analysis (Haas et al., 2011). The taxonomy of representative sequences was determined using BLAST against 889 oral bacterial 16S rRNA gene sequences (HOMD 16S rRNA RefSeq version 14.51) in the Human Oral Microbiome Database (Chen et al., 2010). Nearest-neighbor species with $\geq$98.5% identity were selected as candidates for each representative OTU. The taxonomy of sequences without hits was further determined using an RDP classifier with a minimum support threshold of 80% (Wang et al., 2007). The number of OTUs were calculated following rarefaction to 5,000 reads per sample using the vegan package of R and were used as an index of bacterial diversity in this study. The sequence data have been deposited in DDBJ Sequence Read Archive under accession number DRA008522.

Statistical Analyses

We compared the clinical and bacterial characteristics of patients and control subjects. Continuous variables were compared using Mann–Whitney *U*-test, and nominal or ordinal variables were compared using Fisher's exact test. We also evaluated the characteristics of patients by their cancer site, and each characteristic was respectively compared to that of healthy control subjects using Mann–Whitney *U*-test and Fisher's exact test. The UniFrac metric was used to determine the dissimilarity between any pair of bacterial compositions (Lozupone and Knight, 2005). Principal-coordinate analysis (PCoA) was performed based on the weighted and unweighted UniFrac distances using the cmdscale function in the stats package of R. The dissimilarity between patients and control subjects was evaluated using the analysis of similarities (ANOSIM) with 999 permutations based on weighted and unweighted UniFrac distances. The detection of discriminant bacterial species was performed using the linear discriminant analysis effect size (LEfSe) method (Segata et al., 2011). The linear discriminant analysis score (LDA score) indicated the effect size of each OTU and we defined OTUs with an LDA score $>$3.0 as differentially abundant OTUs.

RESULTS

Characteristics of DTC Patients and Salivary Microbiota Sequence

We examined 59 DTC patients (42 men and 17 women, 38–84 years of age) and 118 age- and sex-matched control subjects. The detailed characteristics of DTC patients and control subjects are presented in **Table 1**. Body mass index (BMI) of DTC patients was significantly lower and the percentage of teeth with BOP was significantly higher than those in control subjects ($P < 0.01$). There were no statistical differences between DTC patients and control subjects in the other lifestyle habits and oral conditions. We analyzed a total of 177 stimulated saliva samples by 16S rRNA gene amplicon analysis, and finally obtained 2,566,571 high-quality reads (14,500 $\pm$ 5,654 reads per sample) to determine their bacterial diversity and composition.

Bacterial Diversity and Composition in DTC Patients and Control Subjects

We examined the bacterial diversity of saliva in DTC patients and control subjects to evaluate the overall salivary microbiota. The saliva of DTC patients exhibited significantly higher bacterial diversity than that of control subjects (number of OTUs, $P = 0.02$; Shannon index, $P < 0.01$; Chao1, $P = 0.04$) (**Figure 1**). We also evaluated the similarity of bacterial composition in saliva of patients and control subjects. **Figure 2** presents a PCoA plot based on the UniFrac distances and **Supplementary Figure S1**

TABLE 1 | The characteristics of digestive tract cancer patients and control subjects.

	Digestive tract cancer (n = 59)	Control subjects (n = 118)	P-value
Age, mean ± SD	66.4 ± 10.2	66.4 ± 10.3	0.985
Male, n (%)	42 (71.2)	84 (71.2)	1
BMI, mean ± SD	21.7 ± 3.1	23.5 ± 3.5	< 0.01
Current smoking, n (%)	14 (24.1)	21 (17.8)	0.323
Current drinking, n (%)	32 (56.1)	70 (59.3)	0.745
Number of teeth, mean ± SD	20.8 ± 9.3	23.3 ± 7.0	0.148
Number of decayed teeth, mean ± SD	1.1 ± 2.3	0.8 ± 1.5	0.502
PPD (mm), mean ± SD	1.9 ± 0.6	1.8 ± 0.6	0.715
Teeth with BOP (%), mean ± SD	31.8 ± 25.0	15.7 ± 19.3	< 0.01
Mean plaque index, mean ± SD	0.7 ± 0.8	0.7 ± 0.6	0.141

SD, standard deviation; BMI, body mass index; PPD, periodontal pocket depth; BOP, bleeding on probing. Significant differences were determined using the Mann–Whitney U-test and the Fisher's exact test. Fifteen individuals with ≤8 teeth were excluded in PPD, percentage of teeth with BOP, and mean plaque index.

presents bar plots of dominant genera. Although there was a significant difference between DTC patients and control subjects in the overall bacterial composition of saliva according to ANOSIM (weighted, P = 0.037; unweighted, P < 0.001), a distinct difference was not observed. We also identified discriminant OTUs in salivary microbiota of DTC patients and control subjects using the LEfSe approach to evaluate the detailed difference in bacterial composition of saliva. The analysis revealed 11 OTUs including OTUs corresponding to *Actinomyces odontolyticus* HOT-701 [Human Oral Taxon (HOT) numbers are unique identification numbers in HOMD], *Streptococcus parasanguinis* I HOT-721, and *Corynebacterium* species that were differentially abundant in DTC patients compared to control subjects (**Figure 3**). Conversely, OTUs corresponding to *Prevotella melaninogenica* HOT-469, *Porphyromonas pasteri* HOT-279, and *Streptococcus* species were differentially abundant in control subjects. These results revealed the presence of specific bacteria in the saliva of DTC patients and control subjects.

Characteristics of DTC Patients by the Cancer Sites

We compared the characteristics of each patient group based on their cancer sites to control subjects. The detailed characteristics of each patient group are shown in **Table 2**. The cancer in patients was located in the tongue/pharynx (n = 13), esophagus (n = 12), stomach (n = 10), and rectum/colon (n = 24). BMI of tongue/pharyngeal, esophageal, or gastric cancer patients were significantly lower than that of control subjects (P < 0.01), while there was no significant difference in BMI between colorectal cancer patients and control subjects. The proportion of current smokers in tongue/pharyngeal cancer patients was 58.3%, which was significantly higher than that in control subjects (P < 0.01). Concerning oral conditions, tongue/pharyngeal cancer patients demonstrated more decayed teeth, while gastric cancer patients demonstrated fewer decayed teeth compared to control subjects. Gingival inflammatory condition based on BOP in tongue/pharyngeal, esophageal, or colorectal cancer patients was more severe than in the control subjects and oral hygiene status based on plaque index was better in gastric or colorectal cancer patients. There was no difference in the periodontal condition (based on PPD) between the patient groups and control subjects.

Bacterial Diversity and Composition in DTC Patients by the Cancer Sites

We examined the bacterial diversity of salivary microbiota in each patient group. Saliva from tongue/pharyngeal and esophageal cancer patients demonstrated significantly higher

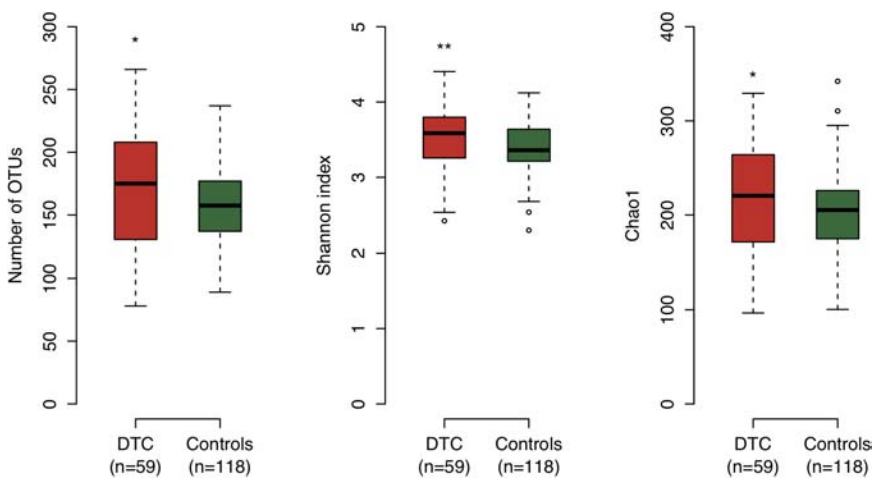

FIGURE 1 | Bacterial diversity of saliva in digestive tract cancer (DTC) patients and control subjects. Boxplots show the number of operational taxonomic units (OTUs), Shannon index, and Chao1 in patients and control subjects. Significant differences were determined using the Mann–Whitney U-test.
*P < 0.05 and **P < 0.01.

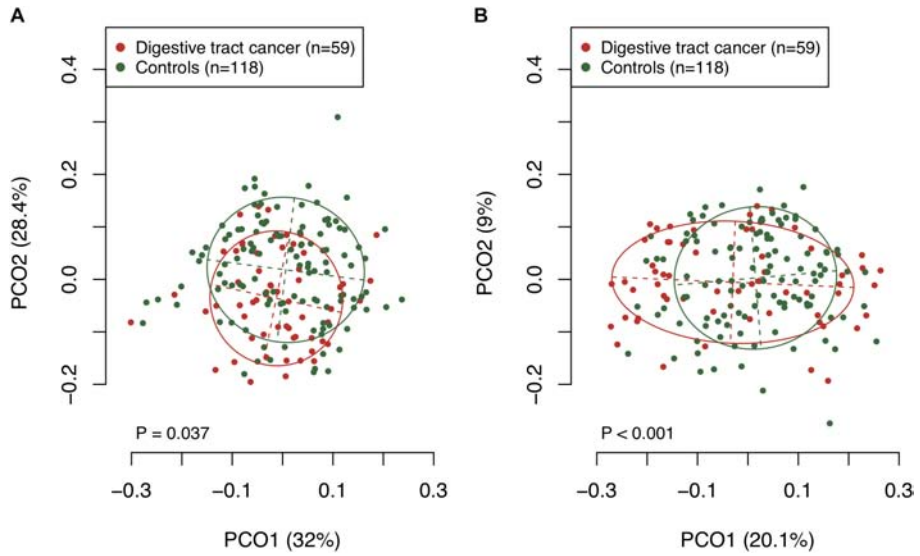

FIGURE 2 | Principal coordinate analysis based on **(A)** weighted and **(B)** unweighted UniFrac distances. The bacterial composition of patients and control subjects are depicted using different colors. These two components explained the 60.4% **(A)** and 29.1% **(B)** variances. The intersection of the broken lines indicates the center of gravity for each community type. The ellipse covers 67% of the samples belonging to each community type. The *P*-value was calculated by the analysis of similarities (ANOSIM).

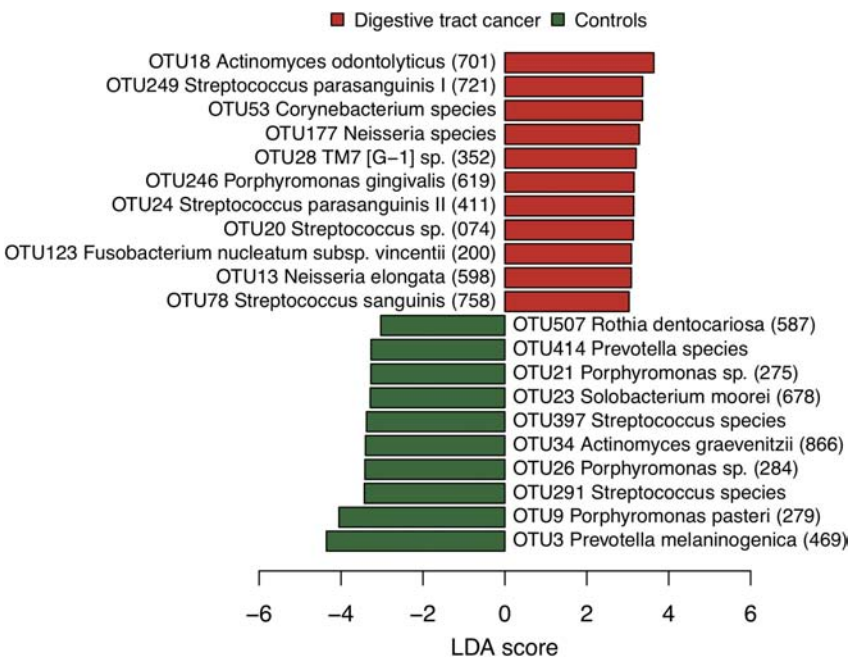

FIGURE 3 | Bacterial species corresponding to the differentially abundant operational taxonomic units (OTUs) between patients and control subjects. Bar plots show linear discriminant analysis (LDA) scores of each OTU. The LDA score indicates the effect size of each OTU and OTUs with an LDA score >3.0 are shown. The differentially abundant OTUs in patients and control subjects are depicted using different colors. Oral taxon identifications are in parentheses following bacterial names.

bacterial diversity compared to that of control subjects (number of OTUs, both $P < 0.01$; Shannon index, both $P = 0.02$; Chao1, $P < 0.01$ and $P = 0.02$, respectively) (**Figure 4**). In contrast, there was no significant difference in bacterial diversity between gastric and colorectal cancer patients and control subjects.

We also examined the relative abundance of the 11 differentially abundant OTUs in each patient group to identify the association between these OTUs and each DTC. The relative abundance of an OTU corresponding to *Porphyromonas gingivalis* HOT-619 was significantly higher in all groups

TABLE 2 | The characteristics of digestive tract cancer patients by the cancer sites.

	Tongue/pharyngeal (*n* = 13)	Esophageal (*n* = 12)	Gastric (*n* = 10)	Colorectal (*n* = 24)	Control subjects (*n* = 118)
Age, mean ± SD	62.5 ± 10.6	68.4 ± 7.8	70.5 ± 9.8	65.9 ± 10.9	66.4 ± 10.3
Male, n (%)	12 (92.3)	8 (66.7)	6 (60)	16 (66.7)	84 (71.2)
BMI, mean ± SD	20.5 ± 2.7**	20.8 ± 3.2**	20.8 ± 2.1**	23 ± 3.2	23.5 ± 3.5
Current smoking, n (%)	7 (58.3)**	3 (25)	1 (10)	3 (12.5)	21 (17.8)
Current drinking, n (%)	9 (75)	5 (45.5)	4 (40)	14 (58.3)	70 (59.3)
Number of teeth, mean ± SD	19.8 ± 9.9	19.2 ± 9.9	20.9 ± 9.5	22.1 ± 8.9	23.3 ± 7.0
Number of decayed teeth, mean ± SD	3.0 ± 3.8**	1.2 ± 2.0	0 ± 0*	0.5 ± 1.2	0.8 ± 1.5
PPD (mm), mean ± SD	1.8 ± 0.4	2.1 ± 0.6	1.7 ± 0.7	1.8 ± 0.7	1.8 ± 0.6
Teeth with BOP (%), mean ± SD	37.1 ± 25.5**	40.2 ± 27.3**	23.3 ± 27.2	28.3 ± 22.3**	15.7 ± 19.3
Mean plaque index, mean ± SD	1.1 ± 1.1	1.2 ± 0.9	0.3 ± 0.3*	0.4 ± 0.4*	0.7 ± 0.6

*SD, standard deviation; BMI, body mass index; PPD, periodontal pocket depth; BOP, bleeding on probing. Significant differences were respectively determined between each patient group and control subjects using the Mann–Whitney U-test and the Fisher's exact test. *P < 0.05 and **P < 0.01. Fifteen individuals with ≤8 teeth were excluded in PPD, percentage of teeth with BOP, and mean plaque index.*

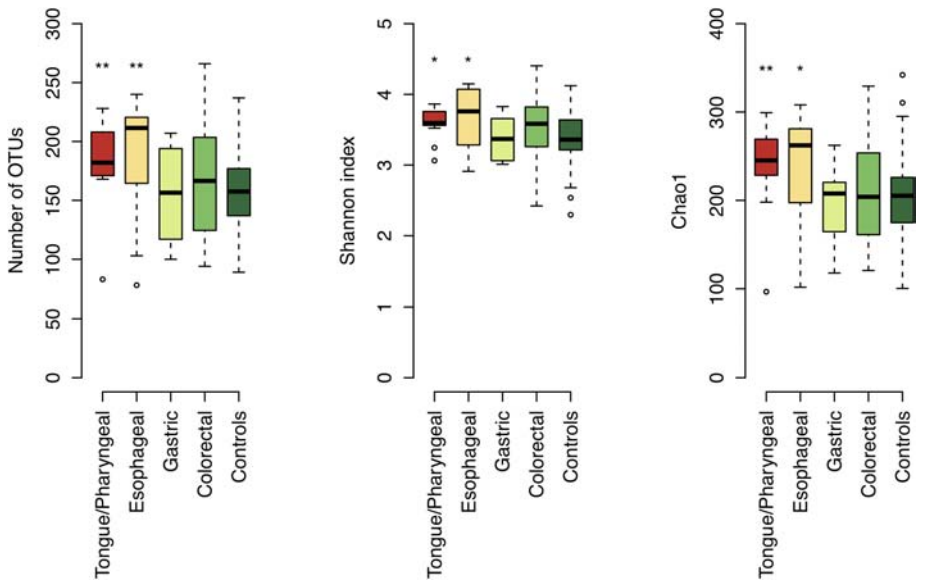

FIGURE 4 | Bacterial diversity of saliva in each patient group and control subjects. Boxplots show the number of operational taxonomic units (OTUs), Shannon index, and Chao1 in each patient group and control subjects. Significant differences are respectively, determined between each patient group and control subjects using the Mann–Whitney *U*-test. *$P < 0.05$ and **$P < 0.01$.

of DTC patients and that of an OTU corresponding to *Corynebacterium* species was significantly higher in all groups other than gastric cancer patients compared to that in control subjects ($P < 0.01$) (**Figure 5**). In tongue/pharyngeal cancer patients, OTUs corresponding to *F. nucleatum* HOT-200, *S. parasanguinis* II HOT-411, and *Neisseria* species were also more abundant ($P < 0.01$). The gastric cancer patients exhibited high relative abundance of an OTU corresponding to the *Neisseria* species and the colorectal cancer patients showed high relative abundance of an OTU corresponding to *A. odontolyticus* HOT-701 ($P < 0.01$). These results suggested that the associations between salivary microbiota and DTC differed depending on the cancer sites.

DISCUSSION

This case-control study of patients with various DTCs demonstrated an association of salivary microbiota with DTC. The salivary bacterial diversity was higher in DTC patients than that in control subjects. This result was consistent with other observed indices of bacterial diversity, such as Simpson index and phylogenetic diversity (**Supplementary Figure S2**). Particularly, tongue/pharyngeal and esophageal cancer patients demonstrated high bacterial diversity. In addition, several species-level OTUs characteristic of each DTC were identified using the LEfSe method. It was interesting that some of the OTUs were characteristic among several DTC

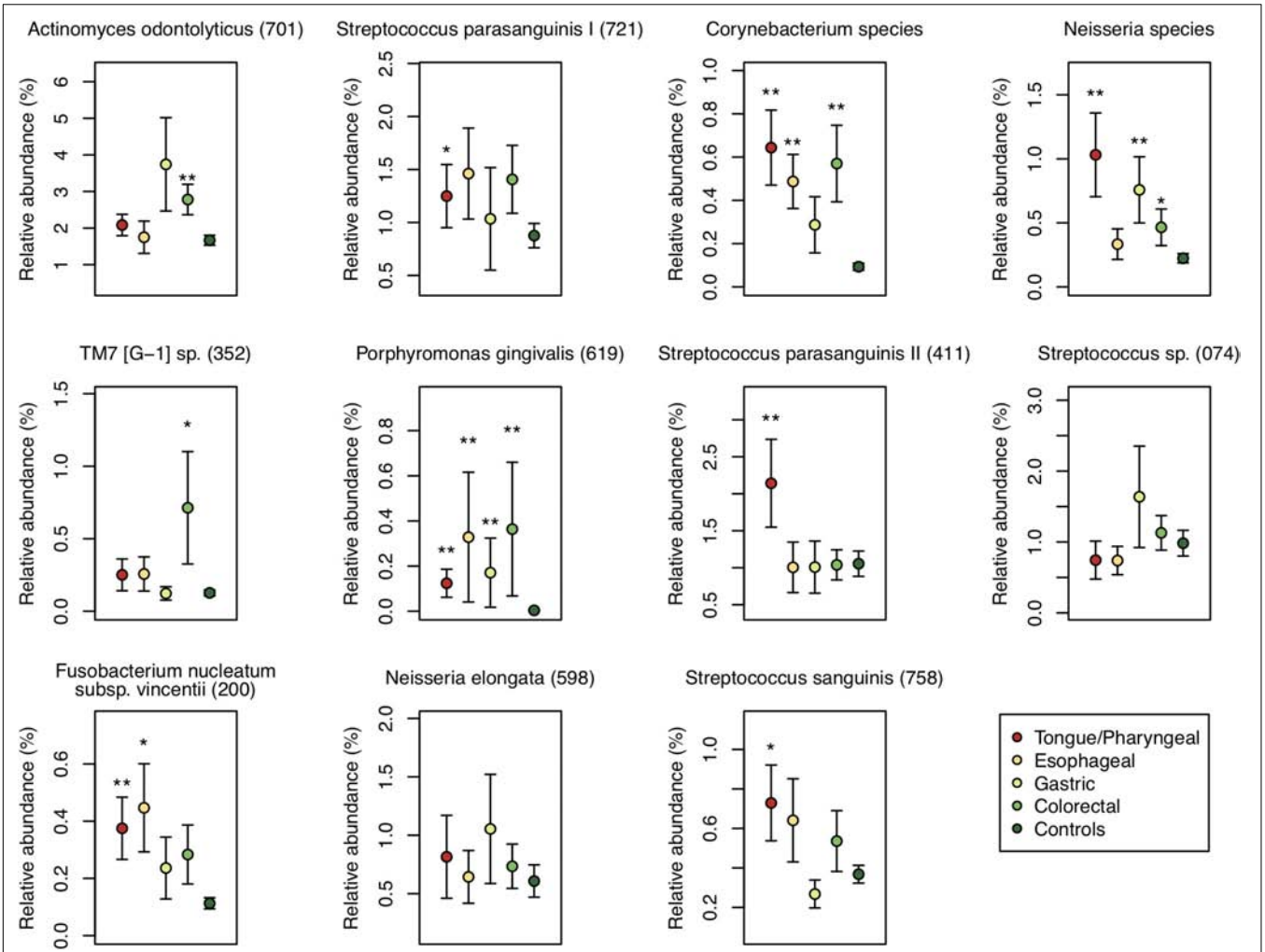

FIGURE 5 | Relative abundances of the 11 differentially abundant operational taxonomic units (OTUs) in each patient group and control subjects. Each plot shows average of the relative abundance of 11 differentially abundant OTUs of patients with digestive tract cancer in each patient group, and error bar shows standard error. Each group is depicted using different colors. Oral taxon identifications are in parentheses following bacterial names. Significant differences are respectively determined between each patient group and control subjects using the Mann–Whitney *U*-test. $^{*}P < 0.05$ and $^{**}P < 0.01$.

in common, even though distances from the oral cavity to each DTC varied.

We identified the 11 bacterial species that were characteristic of DTC patients using the LEfSe method. *P. gingivalis*, a periodontal pathogen included in these 11 species, plays a key role in the development of periodontitis by invasion of epithelial cells or by interfering with the host immunity (Hajishengallis and Lamont, 2014). In this study, the relative abundance of *P. gingivalis* was significantly higher in saliva of all groups of DTC patients than that of control subjects, even though there was no difference in PPD between any groups of DTC patients and control subjects, which has been frequently associated with the presence of *P. gingivalis*. The reason for the association between higher abundance of *P. gingivalis* in saliva and DTC is unknown. However, we cannot exclude the possibility that *P. gingivalis* affects DTC incidence through an unknown pathway. In addition, *F. nucleatum*, a periodontal pathogen, was also identified as a differentially abundant OTU in cancer patients and was more abundant in tongue/pharyngeal or esophageal cancer patients. The association between periodontal pathogens in the saliva and DTC should be explored to elucidate the etiology of DTC.

We found that an OTU corresponding to *Neisseria* species was more abundant in tongue/pharyngeal, gastric, or colorectal cancer patients. *Neisseria* species are capable of producing a high amount of acetaldehyde in a medium containing ethanol *in vitro* (Muto et al., 2000; Moritani et al., 2015). In addition, the acetaldehyde level in saliva was reported to be associated with the increased risk for developing upper DTC (Salaspuro, 2003). Therefore, *Neisseria* species might be associated with DTC due to the production of acetaldehyde in the oral cavity after alcohol consumption. However, our previous study suggested that their phenotypes *in vitro* do not necessarily reflect their behavior

in vivo because of interactions in the bacterial community (Yokoyama et al., 2018). To elucidate the acetaldehyde-mediated carcinogenesis, further comprehensive studies of these *Neisseria* species *in vitro* and *in vivo* are required.

In the present study, we conducted dental examinations for all participants and evaluated the oral health conditions, including PPD and BOP, which have seldom been evaluated in previous studies of the oral microbiota and DTC. While gingival inflammation (based on BOP) was significantly severe in tongue/pharyngeal, esophageal, or colorectal cancer patients, there was no statistical difference in PPD. This result suggests that the difference in the salivary microbiota between DTC patients and control subjects does not merely reflect subgingival bacteria shed from deep periodontal pockets with periodontitis. There may be a direct relationship between the salivary microbiota and DTC, and an indirect relationship via gingivitis. The elucidation of these etiologies would provide us with valuable information to understand the association between the oral microbiota and DTC. However, the sample size in this study was not large enough to confirm whether the differentially abundant OTUs are related to DTC independent of the gingival condition. Additionally, the small sample size did not allow us to evaluate the relationship between the oral microbiota and DTC accounting for the detailed cancer sites (e.g., gingiva, buccal mucosa, and tongue in the oral cavity or rectum and colon in the intestine) or cancer types (e.g., adenocarcinoma and squamous cell carcinoma). Further investigation with a larger sample size is needed to elucidate the relationship between the oral microbiota and DTC in detail.

We also performed LEfSe analysis between each cancer group and matched control subjects (**Supplementary Figure S3**). Although the sample size of each group was not large, several OTUs specific to each cancer group were detected including a subset of the 11 differentially abundant OTUs found in all DTC patients. It is particularly interesting that 5 of these 11 OTUs were detected by LEfSe analysis in colorectal cancer patients, even though colorectal cancers are physically most distant from the oral cavity, and its association with the salivary microbiota was likely to be masked by the other cancers. There might be a stronger association between the salivary microbiota and colorectal cancer than exists with the other cancers. More detailed analyses with larger sample sizes will be required to identify the respective associations of the salivary microbiota with each DTC.

CONCLUSION

In conclusion, the present case-control study demonstrated that the bacterial diversity and composition of saliva is associated with DTC. Understanding of these associations can help in establishing a novel concept for cancer prediction or diagnosis based on bacterial composition. The monitoring of salivary microbiota may help predict the development of DTC and assist with health maintenance.

DATA AVAILABILITY

The datasets generated for this study can be found in the DDBJ Sequence Read Archive under the accession number DRA008522.

ETHICS STATEMENT

This study was carried out in accordance with the recommendations of the ethics committee of Kyushu University with written informed consent from all subjects. All subjects gave written informed consent in accordance with the Declaration of Helsinki. The protocol was approved by the ethics committee of Kyushu University (approval number 27–37).

AUTHOR CONTRIBUTIONS

SK wrote the first draft of the manuscript. SK, TT, and YY edited the manuscript. TT, MF, and YS collected the clinical data and sample from control subjects. KN, MI, MMo, MMa, and YT collected the clinical data and samples from patients. MA and RM performed the molecular analysis. SK, TT, and KT performed the bioinformatics and statistical analysis. SK, TT, YY, KT, MI, MMo, MMa, and YT contributed to the conception and design of the study. YK and TN supervised the Hisayama study. All authors read and approved the submitted version of the manuscript.

FUNDING

This work was supported by the JSPS KAKENHI (Grant Numbers: JP15K15774, JP16H02692, JP16H05850, JP16H05557, and JP18H06296).

SUPPLEMENTARY MATERIAL

The Supplementary Material for this article can be found online at: https://www.frontiersin.org/articles/10.3389/fmicb.2019.01780/full#supplementary-material

FIGURE S1 | Mean relative abundances of bacterial genera in digestive tract cancer (DTC) patients and control subjects. Only 14 genera with a mean relative abundance of ≥1% in DTC patients or control subjects are shown. Error bars show standard error. Significant differences were determined using the Mann–Whitney *U*-test. $*P < 0.05$ and $**P < 0.01$.

FIGURE S2 | Simpson index and phylogenetic diversity of saliva in digestive tract cancer (DTC) patients, each patient group, and control subjects. Boxplots show these indices of bacterial diversity in DTC patients, each patient group, and control subjects. Phylogenetic diversity was calculated using the pd function in the picante package of R. Significant differences are determined between DTC patients and control subjects, or respectively determined between each patient group and control subjects using the Mann–Whitney *U*-test. $*P < 0.05$ and $**P < 0.01$.

FIGURE S3 | Bacterial species corresponding to the differentially abundant operational taxonomic units (OTUs) between each patient group and matched control subjects. Bar plots show linear discriminant analysis (LDA) scores of each OTU. The LDA score indicates the effect size of each OTU and OTUs with an LDA score >3.0 are shown. The differentially abundant OTUs in patients and control subjects are depicted using different colors. Oral taxon identifications are in parentheses following bacterial names.

REFERENCES

Allavena, P., Garlanda, C., Borrello, M. G., Sica, A., and Mantovani, A. (2008). Pathways connecting inflammation and cancer. *Curr. Opin. Genet. Dev.* 18, 3–10. doi: 10.1016/J.GDE.2008.01.003

Asakawa, M., Takeshita, T., Furuta, M., Kageyama, S., Takeuchi, K., Hata, J., et al. (2018). Tongue microbiota and oral health status in community-dwelling elderly adults. *mSphere* 3:e00332-18. doi: 10.1128/mSphere.00332-18

Bosetti, C., Negri, E., Franceschi, S., Conti, E., Levi, F., Tomei, F., et al. (2000). Risk factors for oral and pharyngeal cancer in women: a study from Italy and Switzerland. *Br. J. Cancer* 82, 204–207. doi: 10.1054/bjoc.1999.0900

Botteri, E., Iodice, S., Bagnardi, V., Raimondi, S., Lowenfels, A. B., and Maisonneuve, P. (2008). Smoking and colorectal cancer: a meta-analysis. *JAMA* 300, 2765–2778. doi: 10.1001/jama.2008.839

Chen, T., Yu, W. H., Izard, J., Baranova, O. V., Lakshmanan, A., and Dewhirst, F. E. (2010). The Human oral microbiome database: a web accessible resource for investigating oral microbe taxonomic and genomic information. *Database* 2010:baq013. doi: 10.1093/database/baq013

Dalton-Griffin, L., and Kellam, P. (2009). Infectious causes of cancer and their detection. *J. Biol.* 8:67. doi: 10.1186/jbiol168

Edgar, R. C. (2013). UPARSE: highly accurate OTU sequences from microbial amplicon reads. *Nat. Methods* 10, 996–998. doi: 10.1038/nmeth.2604

Engel, L. S., Chow, W. H., Vaughan, T. L., Gammon, M. D., Risch, H. A., Stanford, J. L., et al. (2003). Population attributable risks of esophageal and gastric cancers. *J. Natl. Cancer Inst.* 95, 1404–1413. doi: 10.1093/jnci/djg047

Ferrari, P., Jenab, M., Norat, T., Moskal, A., Slimani, N., Olsen, A., et al. (2007). Lifetime and baseline alcohol intake and risk of colon and rectal cancers in the European prospective investigation into cancer and nutrition (EPIC). *Int. J. Cancer* 121, 2065–2072. doi: 10.1002/ijc.22966

Flemer, B., Warren, R. D., Barrett, M. P., Cisek, K., Das, A., Jeffery, I. B., et al. (2018). The oral microbiota in colorectal cancer is distinctive and predictive. *Gut* 67, 1454–1463. doi: 10.1136/gutjnl-2017-314814

Freedman, N. D., Abnet, C. C., Leitzmann, M. F., Mouw, T., Subar, A. F., Hollenbeck, A. R., et al. (2007). A prospective study of tobacco, alcohol, and the risk of esophageal and gastric cancer subtypes. *Am. J. Epidemiol.* 165, 1424–1433. doi: 10.1093/aje/kwm051

Haas, B. J., Gevers, D., Earl, A. M., Feldgarden, M., Ward, D. V., Giannoukos, G., et al. (2011). Chimeric 16S rRNA sequence formation and detection in sanger and 454-pyrosequenced PCR amplicons. *Genome Res.* 21, 494–504. doi: 10.1101/gr.112730.110

Hajishengallis, G., and Lamont, R. J. (2014). Breaking bad: manipulation of the host response by *Porphyromonas gingivalis*. *Eur. J. Immunol.* 44, 328–338. doi: 10.1002/eji.201344202

Hata, J., Ninomiya, T., Hirakawa, Y., Nagata, M., Mukai, N., Gotoh, S., et al. (2013). Secular trends in cardiovascular disease and its risk factors in Japanese. *Circulation* 128, 1198–1205. doi: 10.1161/CIRCULATIONAHA.113.002424

Hori, M., Matsuda, T., Shibata, A., Katanoda, K., Sobue, T., and Nishimoto, H. (2015). Cancer incidence and incidence rates in Japan in 2009: a study of 32 population-based cancer registries for the Monitoring of Cancer Incidence in Japan (MCIJ) project. *Jpn. J. Clin. Oncol.* 45, 884–891. doi: 10.1093/jjco/hyv088

Huang, W. Y., Winn, D. M., Brown, L. M., Gridley, G., Bravo-Otero, E., Diehl, S. R., et al. (2003). Alcohol concentration and risk of oral cancer in puerto rico. *Am. J. Epidemiol.* 157, 881–887. doi: 10.1093/aje/kwg055

Kabat, G. C., Chang, C. J., and Wynder, E. L. (1994). The role of tobacco, alcohol use, and body mass index in oral and pharyngeal cancer. *Int. J. Epidemiol.* 23, 1137–1144. doi: 10.1093/ije/23.6.1137

Kageyama, S., Takeshita, T., Asakawa, M., Shibata, Y., Takeuchi, K., Yamanaka, W., et al. (2017). Relative abundance of total subgingival plaque-specific bacteria in salivary microbiota reflects the overall periodontal condition in patients with periodontitis. *PLoS One* 12:e0174782. doi: 10.1371/journal.pone.0174782

Kageyama, S., Takeshita, T., Furuta, M., Tomioka, M., Asakawa, M., Suma, S., et al. (2018). Relationships of variations in the tongue microbiota and pneumonia mortality in nursing home residents. *J. Gerontol. A Biol. Sci. Med. Sci.* 73, 1097–1102. doi: 10.1093/gerona/glx205

Kholy, K. E., Genco, R. J., and Van Dyke, T. E. (2015). Oral infections and cardiovascular disease. *Trends Endocrinol. Metab.* 26, 315–321. doi: 10.1016/J.TEM.2015.03.001

Leung, W. K., Wu, M. S., Kakugawa, Y., Kim, J. J., Yeoh, K. G., Goh, K. L., et al. (2008). Screening for gastric cancer in Asia: current evidence and practice. *Lancet Oncol.* 9, 279–287. doi: 10.1016/S1470-2045(08)70072-X

Lozupone, C., and Knight, R. (2005). UniFrac: a new phylogenetic method for comparing microbial communities. *Appl. Environ. Microbiol.* 71, 8228–8235. doi: 10.1128/AEM.71.12.8228-8235.2005

Mathews, M. J., Mathews, E. H., and Mathews, G. E. (2016). Oral health and coronary heart disease. *BMC Oral Health* 16:122. doi: 10.1186/s12903-016-0316-7

Mima, K., Sukawa, Y., Nishihara, R., Qian, Z. R., Yamauchi, M., Inamura, K., et al. (2015). *Fusobacterium nucleatum* and T Cells in colorectal carcinoma. *JAMA Oncol.* 1, 653–661. doi: 10.1001/jamaoncol.2015.1377

Ministry of Health, Labour and Welfare (2018). *Vital Statistics Japan*. Tokyo: Ministry of Health, Labour and Welfare.

Moritani, K., Takeshita, T., Shibata, Y., Ninomiya, T., Kiyohara, Y., and Yamashita, Y. (2015). Acetaldehyde production by major oral microbes. *Oral Dis.* 21, 748–754. doi: 10.1111/odi.12341

Muto, M., Hitomi, Y., Ohtsu, A., Shimada, H., Kashiwase, Y., Sasaki, H., et al. (2000). Acetaldehyde production by non-pathogenicNeisseria in human oral microflora: implications for carcinogenesis in upper aerodigestive tract. *Int. J. Cancer* 88, 342–350. doi: 10.1002/1097-0215(20001101)88:3<342::aid-ijc4>3.0.co;2-i

Nosho, K., Sukawa, Y., Adachi, Y., Ito, M., Mitsuhashi, K., Kurihara, H., et al. (2016). Association of *Fusobacterium nucleatum* with immunity and molecular alterations in colorectal cancer. *World J. Gastroenterol.* 22, 557–566. doi: 10.3748/wjg.v22.i2.557

Paskett, E. D., Reeves, K. W., Rohan, T. E., Allison, M. A., Williams, C. D., Messina, C. R., et al. (2007). Association between cigarette smoking and colorectal cancer in the women's health initiative. *J. Natl. Cancer Inst.* 99, 1729–1735. doi: 10.1093/jnci/djm176

Pérez-Chaparro, P. J., Gonçalves, C., Figueiredo, L. C., Faveri, M., Lobão, E., Tamashiro, N., et al. (2014). Newly identified pathogens associated with periodontitis: a systematic review. *J. Dent. Res.* 93, 846–858. doi: 10.1177/0022034514542468

Peters, B. A., Wu, J., Pei, Z., Yang, L., Purdue, M. P., Freedman, N. D., et al. (2017). Oral Microbiome composition reflects prospective risk for esophageal cancers. *Cancer Res* 77, 6777–6787. doi: 10.1158/0008-5472.CAN-17-1296

Radoï, L., Menvielle, G., Cyr, D., Lapôtre-Ledoux, B., Stücker, I., and Luce, D. (2015). Population attributable risks of oral cavity cancer to behavioral and medical risk factors in France: results of a large population-based case–control study, the ICARE study. *BMC Cancer* 15:827. doi: 10.1186/s12885-015-1841-5

Salaspuro, M. P. (2003). Acetaldehyde, microbes, and cancer of the digestive tract. *Crit. Rev. Clin. Lab. Sci.* 40, 183–208. doi: 10.1080/713609333

Segata, N., Izard, J., Waldron, L., Gevers, D., Miropolsky, L., Garrett, W. S. W., et al. (2011). Metagenomic biomarker discovery and explanation. *Genome Biol.* 12:R60. doi: 10.1186/gb-2011-12-6-r60

Shaukat, A., Dostal, A., Menk, J., and Church, T. R. (2017). BMI is a risk factor for colorectal cancer mortality. *Dig. Dis. Sci.* 62, 2511–2517. doi: 10.1007/s10620-017-4682-z

Silness, J., and Löe, H. (1964). Periodontal disease in pregnancy II. Correlation between oral hygiene and periodontal condition. *Acta Odontol. Scand.* 22, 121–135. doi: 10.3109/00016356408993968

Socransky, S. S., Haffajee, A. D., Cugini, M. A., Smith, C., and Kent, R. L. Jr. (1998). Microbial complexes in subgingival plaque. *J. Clin. Periodontol.* 25, 134–144. doi: 10.1111/j.1600-051x.1998.tb02419.x

Takeshita, T., Kageyama, S., Furuta, M., Tsuboi, H., Takeuchi, K., Shibata, Y., et al. (2016). Bacterial diversity in saliva and oral health-related conditions: the Hisayama study. *Sci. Rep.* 6:22164. doi: 10.1038/srep22164

Tjalsma, H., Boleij, A., Marchesi, J. R., and Dutilh, B. E. (2012). A bacterial driver–passenger model for colorectal cancer: beyond the usual suspects. *Nat. Rev. Microbiol.* 10, 575–582. doi: 10.1038/nrmicro2819

Varela-Lema, L., Ruano-Ravina, A., Juiz Crespo, M. A., and Barros-Dios, J. M. (2010). Tobacco consumption and oral and pharyngeal cancer in a Spanish male population. *Cancer Lett.* 288, 28–35. doi: 10.1016/J.CANLET.2009.06.015

Wang, Q., Garrity, G. M., Tiedje, J. M., and Cole, J. R. (2007). Naive bayesian classifier for rapid assignment of rRNA sequences into the new bacterial taxonomy. *Appl. Environ. Microbiol.* 73, 5261–5267. doi: 10.1128/AEM.00062-07

Yamanaka, W., Takeshita, T., Shibata, Y., Matsuo, K., Eshima, N., Yokoyama, T., et al. (2012). Compositional stability of a salivary microbiota against supragingival microbiota shift following periodontal therapy. *PLoS One* 7:e42806. doi: 10.1371/journal.pone.0042806

Yang, Y., Cai, Q., Shu, X. O., Steinwandel, M. D., Blot, W. J., Zheng, W., et al. (2018). Prospective study of oral microbiome and colorectal cancer risk in low-income and African American populations. *Int. J. Cancer* 144, 2381–2389. doi: 10.1002/ijc.31941

Yokoyama, S., Takeuchi, K., Shibata, Y., Kageyama, S., Matsumi, R., Takeshita, T., et al. (2018). Characterization of oral microbiota and acetaldehyde production. *J. Oral Microbiol.* 10:1492316. doi: 10.1080/20002297.2018.1492316

Zaura, E., Brandt, B. W., Prodan, A., Teixeira de Mattos, M. J., Imangaliyev, S., Kool, J., et al. (2017). On the ecosystemic network of saliva in healthy young adults. *ISME J.* 11, 1218–1231. doi: 10.1038/ismej.2016.199

Zhao, H., Chu, M., Huang, Z., Yang, X., Ran, S., Hu, B., et al. (2017). Variations in oral microbiota associated with oral cancer. *Sci. Rep.* 7, 1–10. doi: 10.1038/s41598-017-11779-9

Conflict of Interest Statement: The authors declare that the research was conducted in the absence of any commercial or financial relationships that could be construed as a potential conflict of interest.

frontiers in Microbiology

ORIGINAL RESEARCH
published: 18 September 2019
doi: 10.3389/fmicb.2019.02101

Chitooligosaccharides Prevents the Development of Colitis-Associated Colorectal Cancer by Modulating the Intestinal Microbiota and Mycobiota

Minna Wu[1,2], Jianmin Li[2,3], Yunying An[2], Puze Li[2], Wancheng Xiong[4], Jinsong Li[4], Dong Yan[2], Mingyong Wang[1] and Genshen Zhong[1]**

[1] Henan Key Laboratory of Immunology and Targeted Therapy, School of Laboratory Medicine, Xinxiang Medical University, Xinxiang, China, [2] School of Basic Medical Sciences, Xinxiang Medical University, Xinxiang, China, [3] Shaanxi Provincial Second People's Hospital, Xi'an, China, [4] The First Affiliated Hospital of Xinxiang Medical University, Xinxiang, China

OPEN ACCESS

Edited by:
Nezar Al-hebshi,
Temple University, United States

Reviewed by:
David L. Moyes,
King's College London,
United Kingdom
Shubha Priyamvada,
University of Illinois at Chicago,
United States

***Correspondence:**
Minna Wu
happy_minzi@163.com
Genshen Zhong
zhonggs@xxmu.edu.cn;
genshenzhong@163.com

Specialty section:
This article was submitted to Systems Microbiology, a section of the journal Frontiers in Microbiology

Received: 06 February 2019
Accepted: 26 August 2019
Published: 18 September 2019

Citation:
Wu M, Li J, An Y, Li P, Xiong W, Li J, Yan D, Wang M and Zhong G (2019) Chitooligosaccharides Prevents the Development of Colitis-Associated Colorectal Cancer by Modulating the Intestinal Microbiota and Mycobiota. Front. Microbiol. 10:2101. doi: 10.3389/fmicb.2019.02101

Gut microbes play a crucial role in the development of colorectal cancer. Chitooligosaccharides (COS), are oligomer that are depolymerized from chitosan and possess a wide range of biological activities. In this study, the effects of COS on colorectal cancer (CRC) development were evaluated using azoxymethane and dextran sulfate sodium (AOM/DSS) induced mouse model of CRC (CACM). In the COS-treated CRC group (CMCOS), COS protected mice from CRC by decreasing the disease activity index, tumor incidences and multiplicity, and the mRNA levels of COX-2, IL-6, TNF-α, IL-1β, IL-10, and IKK-β mRNA in colonic epithelial cells. The results of a cage-exchanged experiment, in which mice from the CACMe and CMCOSe treatments exchanged cages every day to interact with microbes, showed that gut microbes play an important role in preventing CAC by COS. The abundances of fecal bacteria (total bacteria, *Lactobacillus*, *Enterococcus*, *Fusobacterium nucleatum* and butyrate-producing bacteria) were detected by qPCR on the 0th, 1st, 3rd, 6th, 9th, and 10th weekends. Furthermore, microbiota and mycobiota were analyzed by high-throughput sequencing on an Illumina MiSeq PE300 system. COS protected mice from CRC by reversing the imbalance of bacteria and fungi, especially by reducing the abundance of *Escherichia–Shigella*, *Enterococcus*, and *Turicibacter*, and increasing the levels of *Akkermansia*, butyrate-producing bacteria and *Cladosporium*.

Keywords: chitooligosaccharides, colitis-associated colorectal cancer, microbiota, mycobiota, high-throughput sequencing

INTRODUCTION

Colorectal cancer (CRC) is the third most common cause of cancer death in the world (GLOBOCON, 2012), accounting for approximately 862,000 deaths in 2018 (∼8.98% of total cancer-related deaths, respectively) (World Health Organization, 2018, Fact sheet 297). In China, CRC is one of the 5 most commonly diagnosed cancers and has shown a significant upward trend in age-standardized incidence and mortality rates, accounting for 376,300 new cases and 191,000 deaths in 2015 (Chen et al., 2016). Various factors are considered to

be responsible for the development of CRC including inheritance (genetic alterations and family history) and environmental factors (diet, smoking, obesity, low physical activity, sex, ethnicity, etc.) (Dulal and Keku, 2014). Chronic inflammation is believed to promote carcinogenesis, and the risk for colon cancer increases with the duration and anatomic extent of colitis as well as the presence of other inflammatory disorders (Ullman and Itzkowitz, 2011; Brennan and Garrett, 2016). Interestingly, gut microbes can be influenced by these factors, and the involvement of gut microbes in colorectal carcinogenesis is becoming increasing clear due to their role in modulating host metabolism, barrier function, and innate and adaptive immunity (Dulal and Keku, 2014; Gagnière et al., 2016).

The human colon is well known to host a highly diverse and complex microbial community that includes bacteria, fungi, viruses and archaea. Many studies have implicated microbial dysbiosis, a pathological imbalance in the microbial community, in the etiology of CRC (Gagnière et al., 2016). Approximately 100 trillion bacteria of more than 1,000 heterogeneous species exist in colon (Human Microbiome Project Consortium, 2012). Some of which have been identified and are suspected to play a role in colorectal carcinogenesis, such as *Fusobacterium* spp., *Escherichia coli*, and *Bacteroides fragilis* (Arthur et al., 2012; Gur et al., 2015; Brennan and Garrett, 2016; Ramos and Hemann, 2017; Dejea et al., 2018). Bacteria also prevented the development of CRC by producing metabolites (e.g., acetate, propionate, and butyrate) (Louis et al., 2014). Due to their low levels in the gut (0.2%, 66 genera and 184 species), fungi are often ignored in studies of intestinal microbes. Recently, mycobiota have been linked with a number of diseases (e.g., colitis, antibiotic associated diarrhea, inflammatory bowel disease, and peptic ulcers) by interacting with microbiota, modulating immunity and producing mycotoxins (Iliev et al., 2012; Liguori et al., 2016; Li et al., 2017; Sokol et al., 2017). However, alteration of the gut mycobiota in CRC patients has rarely been reported. Luan et al. (2015) analyzed the fungal microbiota of biopsy samples from colorectal adenomas (some advanced cases can further develop into carcinoma) and adjacent tissues by sequencing and observed that fungal diversity was decreased in adenomas, while the size of adenomas and disease stage were closely related to changes in the mycobiota. Gao et al. (2017) observed fungal dysbiosis in colon polyps and CRC, including decreased fungal diversity in polyp patients, an increased Ascomycota/Basidiomycota ratio, and an increased proportion of the opportunistic fungi *Trichosporon* and *Malassezia*, which may favor the progression of CRC. Because of its effects on modulating immunity, producing mycotoxins and interacting with microbiota (Van Raay and Allen-Vercoe, 2017), the role of mycobiota in the development and prevention of CRC should be further investigated.

Chitooligosaccharides (COS) are oligomers that are depolymerized from chitosan. COS have been reported to possess a wide range of biological activities, such as antimicrobial, antioxidant, anti-inflammatory, anti-tumor, immunostimulatory, hypocholesterolemic activities (Liang et al., 2016; Qu and Han, 2016; Liagat and Eltem, 2018). COS have been used to inhibit the growth of various bacteria (e.g., *E. coli*, *Salmonella enteritidis*, and *Listeria monocytogenes*), fungi (e.g., *Trichophyton rubrum*) and virus (e.g., HIV-1) (Artan et al., 2010; Mei et al., 2015; Laokuldilok et al., 2017; Sánchez et al., 2017), and showed beneficial effects on probiotic bacteria together with inhibitory effects on intestinal pathogens (Nurhayati et al., 2016). The concentrations of SCFAs and the abundances of *Lactobacilli* and *Bifidobacteria* were significantly increased in the cecum of mice treated with COS (Pan et al., 2009). COS are also effective against various cancer cells *in vitro*, such as prostate, lung, hepatocellular, gastric and colon cancer cells (Park et al., 2011; Han et al., 2015, 2016; Ryu et al., 2017). However, the relationship between the anti-tumor activities of COS and its effects on bacteria *in vivo* remains unclear.

In this study, COS were administered intragastrically to AOM/DSS-induced CRC mice. The anti-tumor activity of COS toward CRC was evaluated by detecting tumor incidence and multiplicity, calculating the disease activity index (DAI), analyzing pathologic characteristics and quantifying the abundance of inflammation-associated factors/cytokines. The role of microbes in preventing the development of CRC was evaluated by exchanging the cages of CRC and COS-treated CRC mice. The dynamics of total bacteria, *Lactobacillus*, *Enterococcus*, *Fusobacterium nucleatum* and butyrate-producing bacteria were evaluated by quantitative PCR (qPCR). High-throughput sequencing was performed to reveal the structure of microbiota and mycobiota, and to determine the specific functional bacteria and fungi that contributed to the preventative effect of COS on CRC.

MATERIALS AND METHODS

Animals and Reagents

Eight-week-old male C57/BL6 mice (22-24 g) were purchased from Vital River Laboratory Animal Technology Co. Ltd. (Beijing, China). All animals were raised in sterilized cages under controlled conditions (i.e., temperature 23 $\pm$ 2°C, humidity 55 $\pm$ 5%, and 12 h light/dark cycles) and fed sterilized standard rodent chow food and sterilized water under specific pathogen-free conditions.

AOM was purchased from Sigma-Aldrich (St. Louis, MO, United States) and DSS was purchased from MP Biomedicals (molecular weight: 36−50 kDa, MP Biomedicals, Santa Ana, CA, United States) (Sinder et al., 2016). COS was purchased from Dalian Meilun Biotech Co., Ltd. (molecular weight: <3 kDa, Dalian, China). The QIAamp DNA Stool Mini Kits were purchased from Qiagen (HiCILen, Germany), and the Fecal Occulted Test Kits were purchased from Baso Diagnostics Inc. (Zhuhai, China). AOM was dissolved in normal saline to a final concentration of 0.5 mg/mL. DSS and COS were dissolved in sterile deionized water.

Experimental Procedures

Forty-eight eight-week-old male C57/BL6 mice were randomly and averagely divided into six treatments: the normal healthy

treatment (CK), COS control treatment (COS), AOM/DSS-induced colorectal cancer model mice (CACM), COS-treated CACM mice (CMCOS, 300 mg/kg COS in AOM/DSS-induced CRC), and the exchanged CACM (CACMe) and CMCOS (CMCOSe) groups. The number of replications in each treatment was 8. All mice in each treatment were fed a standard sterile rodent chow diet for 10 weeks. Sterile drinking water was provided to the mice in the CK and COS treatments. For the mice in the CACM, CMCOS, CACMe and CMCOSe treatments, CRC was induced using the AOM/DSS procedure, which was described in our previous study (Wu et al., 2016). The mice were injected intraperitoneally with a single dose (10 mg/kg) of AOM on the first day, and 1 week later, three experimental courses with DSS were performed. The mice were provided drinking water with 2% DSS for a week followed by sterile drinking water for 2 weeks in each course. In the COS, CMCOS and CMCOSe treatments, 300 mg/kg COS was administered intragastrically once a day and six times per week, starting from the first day of the study. The mice in CACMe and CMCOSe treatments were raised in individual cages, respectively. The mice from these two groups exchanged cages each other every day, and shared litters to interchange intestinal microbes.

Animal weights were evaluated and recorded at the end of each week. Disease activity index (DAI) curves were generated to evaluate disease progression, which was based on weight, hematochezia, and stool malformation. As described by Menghini et al. (2017), DAI were performed by an experimentalist blinded to the study. In detail, to obtain a total clinical DAI ranging from 0 (healthy) to 4 (maximal score for DSS-induced colitis), the average score of (a) body weight loss (i.e., 0, none; 1, 1–5%; 2, 5–10%; 3, 10–20%; and 4, >20%), (b) stool consistency (i.e., 0, normal; 2, loose stool; and 4, diarrhea), and (c) bloody stool (i.e., 0, negative; 2, fecal occult blood test positive; and 4, gross bleeding) was calculated for each experimental animal. The presence of blood in stools was tested with Fecal Occulted Test kits (Baso Diagnostics Inc., Zhuhai, China).

Fecal samples were collected at the end of the 0th (the day before the beginning of experiment), 1st, 3rd, 6th, 9th, and 10th weekends and stored at −80°C. All mice were sacrificed at the completion of the experiment at the end of the 10th week. Approximately 1-cm sections of colon were cut and immediately placed in 10% buffered formalin for fixation, and the rest of colons were subsequently dissociated, opened longitudinally, and rinsed with phosphate-buffered saline (pH 7.4). The number of tumors determined under a dissecting microscope. Then, the colon tissues were used to isolate epithelial cells as previously described (Tong et al., 2007). The isolated colonic epithelial cells were stored at −80°C for further study.

Histopathological Analysis

The fixed colon tissues were embedded in paraffin, sectioned at 3–4 μm and stained with hematoxylin and eosin (H&E). All processed sections were subsequently evaluated by a pathologist in a blinded fashion.

Analysis of Cytokines in Colonic Epithelial Cells by Quantitative RT-PCR

Total mRNA was extracted from colonic epithelial cells using TRIzol reagent (Takara, Dalian, China), as per manufacturer's instruction, and reverse transcription was conducted using a Reverse Transcription kit (Takara, Dalian, China). The quantity and quality of cDNA was evaluated by 1% (w/v) agarose gel electrophoresis in 0.5 mg/mL ethidium bromide and by Nano Drop 2000 ultraviolet spectrophotometry. RT-qPCR was performed to assess the fold changes in COX-2, IL-6, TNF-α, IL-1β and IL-10 expression using a Step One Plus System (ABI) and the $\Delta\Delta$Ct method (Bhatt et al., 2015).

Quantitation of Specific Bacteria by qPCR

Fecal bacterial DNA was extracted using a QIAamp DNA Stool Mini Kit (Qiagen, Hilden, Germany) according to the manufacturer's instructions. The abundances of total bacteria, *Lactobacillus*, *Enterococcus*, *F. nucleatum* and butyrate-producing bacteria were quantified by qPCR. Target gene copy numbers were determined by comparison to a standard curve and normalized to the total DNA. PCR reactions were performed using a Step One Plus System (ABI). The primer sequences and qPCR amplification protocol are shown in **Supplementary Table S1**.

High-Throughput Sequencing and Bioinformatics Analysis

Twenty-four fecal samples from the CK, COS, CACM, CMCOS, CACMe, and CMCOSe groups were randomly collected ($n = 4$) to perform high-throughput sequencing of the 16S and 18S rRNA. Genomic DNA was amplified with the bacterial 16S rRNA gene (V3-V5 region) primers 338F/806R and the 18S rRNA gene primers SSU0817/1196. Primers were linked to Illumina sequencing adapters, and the reverse primers contained a sample barcode. The PCR products were purified, and the concentrations were adjusted for sequencing on an Illumina MiSeq PE300 system (MajorBio Co., Ltd., Shanghai, China).

Raw read sequences were demultiplexed and quality-filtered using QIIME (version 1.8.0) (Caporaso et al., 2012) with the following criteria: (i) the 300-bp reads were truncated at any site receiving an average quality score of <20 over a 50-bp sliding window, discarding the truncated reads that were shorter than 50 bp; (ii) exact barcode matching, two nucleotide mismatches in primer matching, and reads containing ambiguous characters were removed; and (iii) only paired-end reads with overlap longer than 10 bp were assembled according to their overlap sequence. Reads that could not be assembled were discarded.

The UCHIME (Edgar et al., 2011) was used to cluster contigs and remove chimera. The optimized sequences were

clustered into operational taxonomic units (OTUs) with 97% similarity using UPARSE (version 7.1)[1] and aligned with SILVA database[2] using a confidence threshold of 70% (Amato et al., 2013). The data were analyzed on the free online platform of Majorbio I-Sanger Cloud Platform[3]. The alpha diversity analysis was performed using the QIIME 1.8.0 software (Caporaso et al., 2012). Statistical comparison of diversity indexes among different treatments were made by one-way analysis of variance (ANOVA) using the Statistical Package for the Social Sciences (SPSS, version 19.0, Chicago, IL, United States). An analysis of similarity (ANOSIM) was performed using the QIIME 1.8.0 software to determine whether AOM/DSS, COS and cage-exchanged had significantly different bacterial community compositions. Cluster dendrograms, bar plots, principal component analysis (PCA) and principal-coordinate analysis (PCoA), and heatmaps were created in the R software (version 3.7.0). To assess the effect size of each differentially abundant taxon, a metagenomic biomarker discovery approach was performed using LEfSe (linear discriminant analysis [LDA] coupled with effect size measurement)[4], which performed a non-parametric Wilcoxon sum-rank test followed by LDA analysis (Segata et al., 2011). The bacteria-fungi network was generated using the CoNet plugin (version 1.0b7) for Cytoscape (version 3.6.0) on the basis of non-parametric Spearman correlation coefficients, with a minimal cutoff threshold of 0.6 ($P < 0.01$, Bonferroni corrected) (Faust et al., 2012). Correlation data for dominant genera (relative abundance > 0. 1%) that were detected in microbiota and mycobiota are reported.

The raw data were deposited in the Sequence Read Archive (SRA) under the access numbers SRP143438 and SRP144668.

Statistical Analysis

SPSS (SPSS 19.0, Chicago, IL, United States) was used to perform data analysis, with the results expressed as the mean ± SD (i.e., standard deviation) for individual experiment. If multiple sets of variables were consistent with homogeneity of variance (Kruskal–Wallis H test), one-way analysis of variance (ANOVA) was used to compare multi-group variables. Statistical tests were two-sided, and a $P < 0.05$ was considered significant.

Ethics Statement

This study was carried out in accordance with the recommendations of the Institute Animal Care and Use Committee of Xinxiang Medical University, China. The experimental protocol for animal studies was reviewed and approved by the Institute Animal Care and Use Committee of Xinxiang Medical University, China.

[1]http://www.drive5.com/uparse/

[2]http://www.arb-silva.de/

[3]www.i-sanger.com

[4]http://huttenhower.sph.harvard.edu/galaxy/

RESULTS

COS Prevented CRC Development in C57/BL6 Mice

As shown in **Figure 1A**, the body weights of the COS group were similar to those of the CK group. Compared with the CK group, significant body weights loss was observed in AOM/DSS-induced CACM treatments (CACM and CACMe), and was effectively rescued by the COS treatment (CMCOS and CMCOSe). Interestingly, the body weight of the CACMe group, which exchanged microbiota with the CMCOSe group, was significantly higher than that of the CACM group, whereas the body weight of the CMCOSe group was obviously lower than that of the CMCOS group at the 10th weekend ($P < 0.05$) (**Supplementary Table S2**). DAI curves were developed to evaluate disease progression. The DAI scores were 0 in the CK and COS groups throughout the experimental period (**Figure 1B**). Three peaks corresponding to the three cycles of DSS administration (in drinking water) were observed in the other four groups. The DAI curves of the CACM and CACMe were similar, whereas those of the CMCOS and CMCOSe groups were similar. The COS treatment induced significant decrease of DAI score both in the CMCOS and CMCOSe groups. However, the DAI score in the CACMe was significantly lower than that observed in the CACM group ($P < 0.05$) (**Supplementary Table S3**).

The histopathological characteristics of tumor tissue samples from each group of mice were evaluated (**Supplementary Figure S1** and **Supplementary Table S4**). The tumor incidences in the CACM, CACMe, CMCOSe, CMCOS, COS, and CK groups were 100, 100, 87.5, 75.0, 0, and 0%, respectively. Tumor multiplicity (the number of tumors per centimeter colon) in the CACM, CACMe, CMCOSe, and CMCOS groups was 4.58 ± 0.38, 4.0 ± 0.45, 2.25 ± 0.52, and 1.58 ± 0.49, respectively (**Figure 1C**). Tumor multiplicities in the CACM and CACMe groups were significantly higher than that in CMCOSe and CMCOS groups ($P < 0.05$). The COS treatment significantly decreased the tumor incidence and multiplicity; however, the tumor multiplicity in the CMCOSe group was notably higher than that observed in the CMCOS group ($P < 0.05$).

To determine the association between the anti-cancer effects of COS, microbes and cytokine changes in colonic epithelial cells, the abundances of pro-inflammatory factors/cytokines that are often altered in colitis-associated CRC were quantified by RT-qPCR. As shown in **Figure 2**, the levels of COX-2, IL-1β, IL-6, IL-10 and TNF-α mRNA were significantly increased in the CACM and CACMe groups, whereas the COS treatment significantly reduced the mRNA levels of these genes. It is worth noting that the levels of COX-2 and IL-1β mRNA in the CMCOSe group were significantly higher than those observed in the CMCOS group.

Dynamic Changes of Specific Bacterial Taxa Based on qPCR

The dynamic changes in the total bacteria and some specific taxa (*Lactobacillus*, *Enterococcus*, *F. nucleatum* and butyrate-producing bacteria) were assessed by qPCR. As shown in

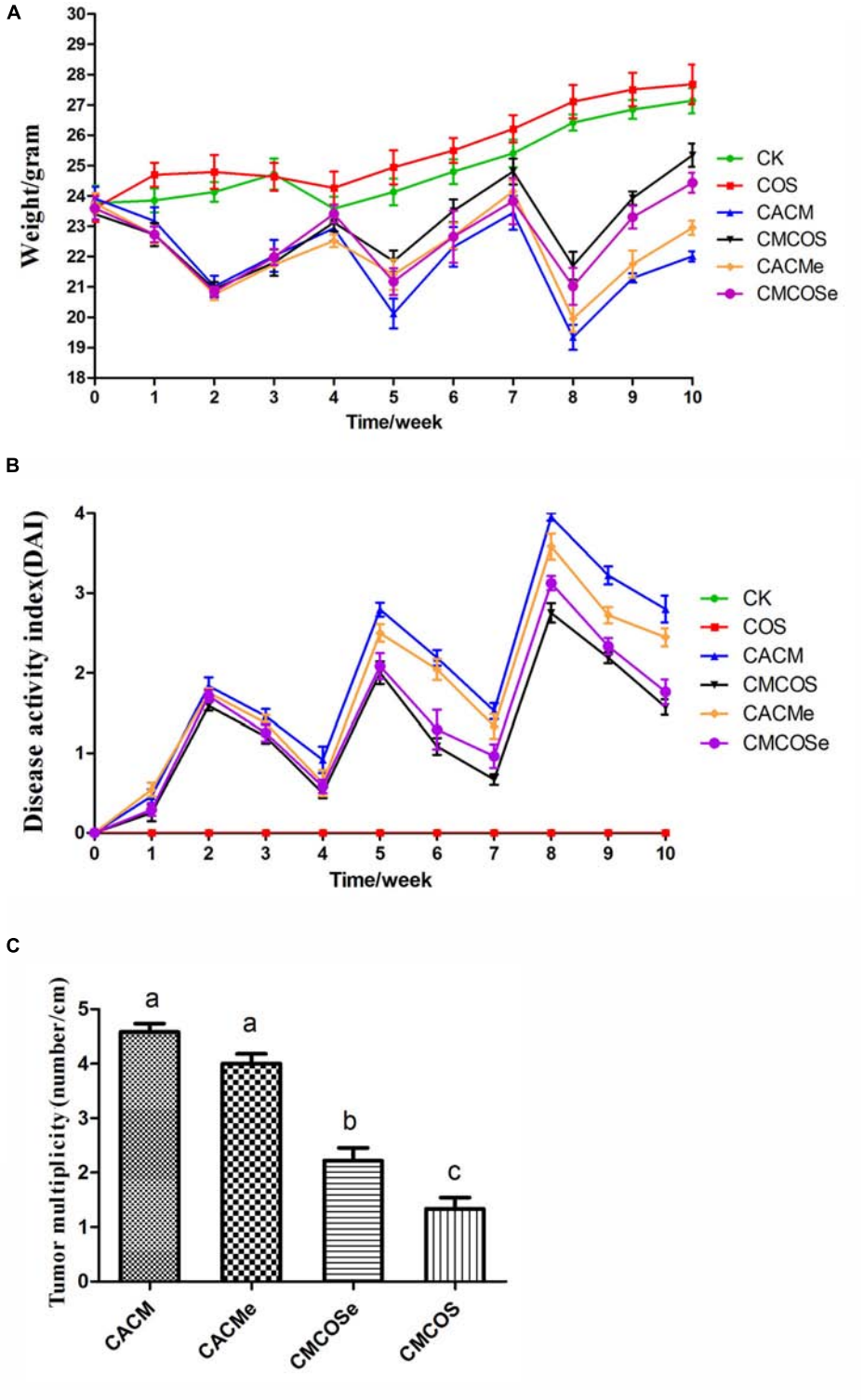

FIGURE 1 | COS protected mouse gastrointestinal tracts from AOM/DSS-induced CAC. **(A)** Changes in body weight. **(B)** DAI values based on weight loss, hematochezia, and diarrhea. **(C)** Tumor multiplicity (number of tumors per cm in colon). The results were presented as the mean ± standard deviation (SD); $n = 8$ for each treatment. Analysis of variance (ANOVA) was used, significant differences ($P < 0.05$) between treatments are indicated by the letters a, b, or c. CK, control treatment; COS, COS control treatment; CACM, AOM/DSS-induced colitis-associated CRC model mice; CMCOS, COS-treated CACM mice (300 mg/kg/d COS); CACMe, exchanged CACM treatment; CMCOSe, exchanged CMCOS treatment.

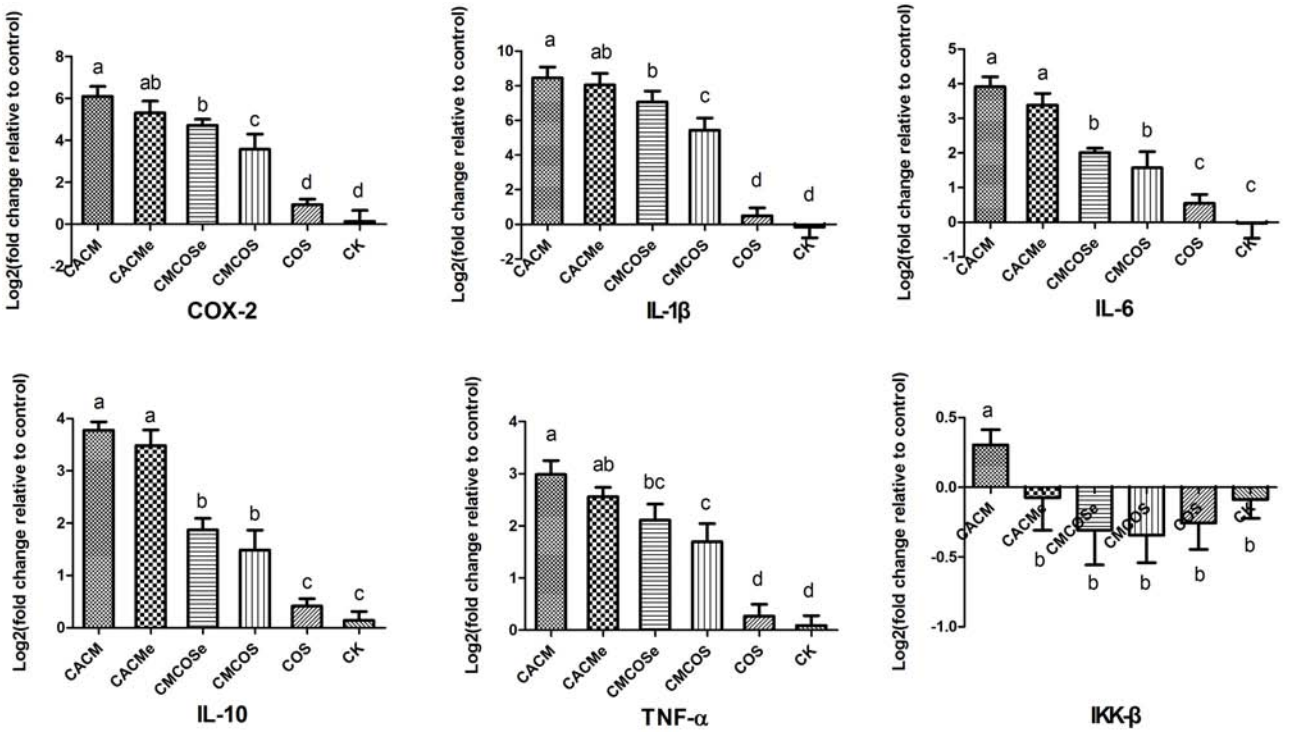

FIGURE 2 | COS inhibited cytokine expression in the CRC mouse at the 10th weekend. The results were presented as the mean ± standard deviation (SD); $n = 8$ for each treatment. Analysis of variance (ANOVA) was used, significant differences ($P < 0.05$) between treatments are indicated by the letters a, b, c, or d. CK, control treatment; COS, COS control treatment; CACM, AOM/DSS-induced colitis-associated CRC model mice; CMCOS, COS-treated CACM mice (300 mg/kg/d COS); CACMe, exchanged CACM treatment; CMCOSe, exchanged CMCOS treatment.

Supplementary Figure S2, total bacterial abundances were significantly lower in the CACM group than those observed in the CK and COS groups at the 6th, 9th, and 10th weekends and were significantly higher in the CMCOS group than in the CACM group at the 9th and 10th weekends. The treatment of COS significantly increased the total bacteria abundances at the 9th and 10th weekends in the AOM/DSS-induced CRC diseased mice, whereas there was no significant difference between the CMCOSe and CACMe groups.

After the 3rd weekend, significant differences in the abundance of *F. nucleatum* were observed between healthy mice (CK and COS) and CRC mice (**Supplementary Figure S3**). At the end of experiment (the 10th weekend), the abundance of *F. nucleatum* was significantly increased in the CACM and CACMe groups but was notably decreased in the COS-treated CACM mice (CMCOS). However, no significant difference was observed between the CMCOSe and CACM groups.

The abundances of the *Enterococcus* genus was significantly increased in the CACM and CACMe groups compared to those observed in the healthy control mice (CK and COS) after the 6th weekend (**Supplementary Figure S4**). The treatment of COS rescued the increase of *Enterococcus* in the AOM/DSS-induced CRC mice, which was present at significantly lower abundances in the CMCOS group than in the CACM group. However, at the 9th and 10th weekends, the abundance of *Enterococcus* in the CACM group significantly increased compared to that observed in the CACMe group. The abundance of *Enterococcus* also increased along with the development of CRC in the CACM, CACMe, and CMCOSe groups.

As shown in **Supplementary Figure S5**, the abundance of the *Lactobacillus* genus decreased at the 9th and 10th weekends in the healthy control mice (CK and COS) and in the COS-treated CRC mice (CMCOS and CMCOSe) and was significantly lower than those observed in the CRC mice (CACM and CACMe).

Butyrate-producing bacteria were sensitive to AOM, as this group of bacteria was significantly reduced at the 1st weekend in all groups given an intra-peritoneal injection of AOM (CACM, CACMe, CMCOS, and CMCOSe) (**Supplementary Figure S6**), with this trend lasted to the end of the experiment. On the 10th weekend, the quantity of butyrate-producing bacteria in the COS-treated CRC mice (CMCOS and CMCOSe) was significantly higher than that observed in the CACM mice (CACM and CACMe). However, the abundance of butyrate-producing bacteria was significantly lower in CMCOSe group than that in the CMCOS group.

Comparison of Bacterial Community Composition

From the 24 samples, 890,321 valid and trimmed sequences were obtained, with an average sequence length of 442 bp, with 460 OTUs obtained at 97% similarity level. The minimum

number of reads (30,008 reads) sub-sample was taken from each sample for subsequent analysis. As shown in **Table 1**, the observed Coverage values were approximately 1. The alpha diversity indexes, including Shannon, Chao, Ace, and Sob were significantly lower in the CACM and CMCOS than in the CK groups. Compared with the CACM and CACMe groups, the exchange of cages slightly increased alpha diversity, although a significant difference was not observed.

Based on the Bray–Curtis method, the hierarchical clustering with the taxonomic information at the OTU level showed that the bacterial communities in the CK and COS groups clustered into one branch, while all of the AOM/DSS treatment groups were classified into another cluster (**Figure 3A**). However, the CACM group clustered away from COS-treated CACM groups (CMCOS and CMCOSe) and the exchanged CACM group (CACMe). Similarity, principal co-ordinates analysis (PCoA) also revealed that the fecal bacterial community in the CACM group was different from those present in the other groups (**Figure 3B**). Samples from the CMCOS, CMCOSe, and CACMe groups were clustered together and were distinct from the healthy (CK and COS groups) and CACM groups. The cluster tree and PCoA indicated that the bacterial communities were separated based on AOM/DSS, COS and the exchange of cages.

The analysis of similarities (ANOSIM) at OTU (R = 0.8398, P = 0.001), species (R = 0.7789, P = 0.001), genus (R = 0.6866, P = 0.001), and family (R = 0.6706, P = 0.001) levels was conducted. As shown in **Supplementary Figure S7**, the inter-treatment differences were greater than the intra-treatment differences at the family, genus, species and OTU levels in all of the treatments. These results indicated that there were significant effects of AOM/DSS, COS and cage-exchanged on intestinal bacterial community composition.

To analyze the bacterial composition in detail, the percent of community abundance that exceeded 1% at the phylum, family, and genus levels are present in **Figure 4**. Based on the taxonomic results, Bacteroidetes and Firmicutes were the most predominant phyla, accounting for 28.89 ∼ 63.70% and 19.26 ∼ 40.71%, respectively (**Figure 4A**). Compared with the CK group, the percentages of Verrucomicrobia increased in the COS group (22.24 ± 11.60% *vs.* 0.65 ± 0.47%, $P < 0.05$), whereas Proteobacteria increased in the CACM groups (33.61 ± 9.01% *vs.* 0.82 ± 0.19%, $P < 0.05$) and Firmicutes decreased in CMCOSe group (19.26 ± 0.75% *vs.* 36.23 ± 12.87%, $P < 0.05$).

As shown in **Figure 4B**, 18 families that exceeded 1% of total bacteria in abundance were observed. Compared with the CK group, the COS treatment significantly increased the abundance (%) of Verrucomicrobiaceae (22.24 ± 6.60% *vs.* 0.65 ± 0.17%) and Erysipelotrichaceae (22.24 ± 5.60% *vs.* 0.65 ± 0.47%). In the CACM group, the percentages of Lachnospiraceae, Prevotellaceae and Ruminococcaceae significantly decreased

TABLE 1 | The alpha diversity indexes of microbiota at the 10th weekend determined by high-throughput sequencing.

Groups	Chao	Shannon	Sobs	Ace	Simpson	Coverage
CK	392.88 ± 6.30^{a}	4.09 ± 0.33^{a}	361 ± 12.96^{a}	392.35 ± 9.83^{a}	0.05 ± 0.03^{a}	1.00 ± 0.000276^{a}
COS	321.66 ± 25.49^{ab}	3.58 ± 0.30^{ab}	297 ± 25.47^{ab}	326.2 ± 23.52^{ab}	0.08 ± 0.04^{a}	1.00 ± 0.000291^{a}
CACM	228.22 ± 67.49^{c}	3.10 ± 0.46^{b}	198 ± 63.85^{c}	229.02 ± 69.77^{c}	0.11 ± 0.05^{a}	1.00 ± 0.000415^{a}
CMCOS	222.90 ± 49.96^{c}	3.03 ± 0.30^{b}	191.75 ± 41.71^{c}	223.32 ± 48.12^{c}	0.10 ± 0.02^{a}	1.00 ± 0.000253^{a}
CACMe	253.80 ± 36.95^{c}	3.10 ± 0.54^{b}	211.5 ± 41.00$_{bc}$	241.30 ± 34.83^{bc}	0.12 ± 0.07^{a}	1.00 ± 0.000247^{a}
CMCOSe	260.44 ± 25.93^{c}	3.31 ± 0.17^{ab}	216.75 ± 21.47^{bc}	257.29 ± 24.67^{bc}	0.07 ± 0.02^{a}	1.00 ± 0.000201^{a}

The results were presented as the mean ± standard deviation (SD); n = 4 for each treatment. Analysis of variance (ANOVA) was used, significant differences (P < 0.05) between treatments are indicated by the letters a, b, or c. CK, control group (P < 0.05); COS, COS-treated group; CACM, AOM/DSS-induced colitis-associated CRC model mice; CMCOS, COS-treated CACM mice (300 mg/kg COS), CACMe, exchanged CACM group; CMCOSe: exchanged CMCOS group.

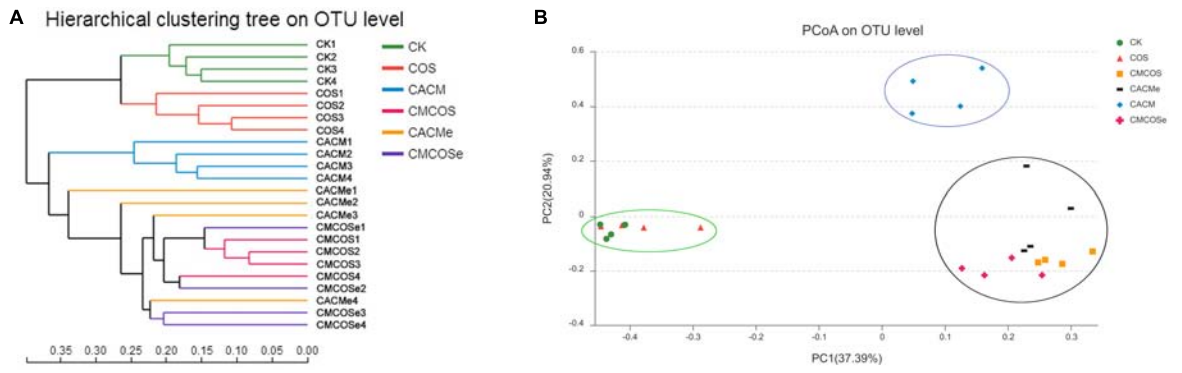

FIGURE 3 | Hierarchical clustering **(A)** and principal co-ordinates analysis (PCoA) of 16S rRNA gene sequences **(B)**. The statistics were performed based on Bray–Curtis distance, n = 4. PC1 and PC2 explained 37.39 and 20.94% of variation, respectively. CK, control treatment; COS, COS control treatment; CACM, AOM/DSS-induced colitis-associated CRC model mice; CMCOS, COS-treated CACM mice (300 mg/kg/d COS); CACMe, exchanged CACM treatment; CMCOSe, exchanged CMCOS treatment.

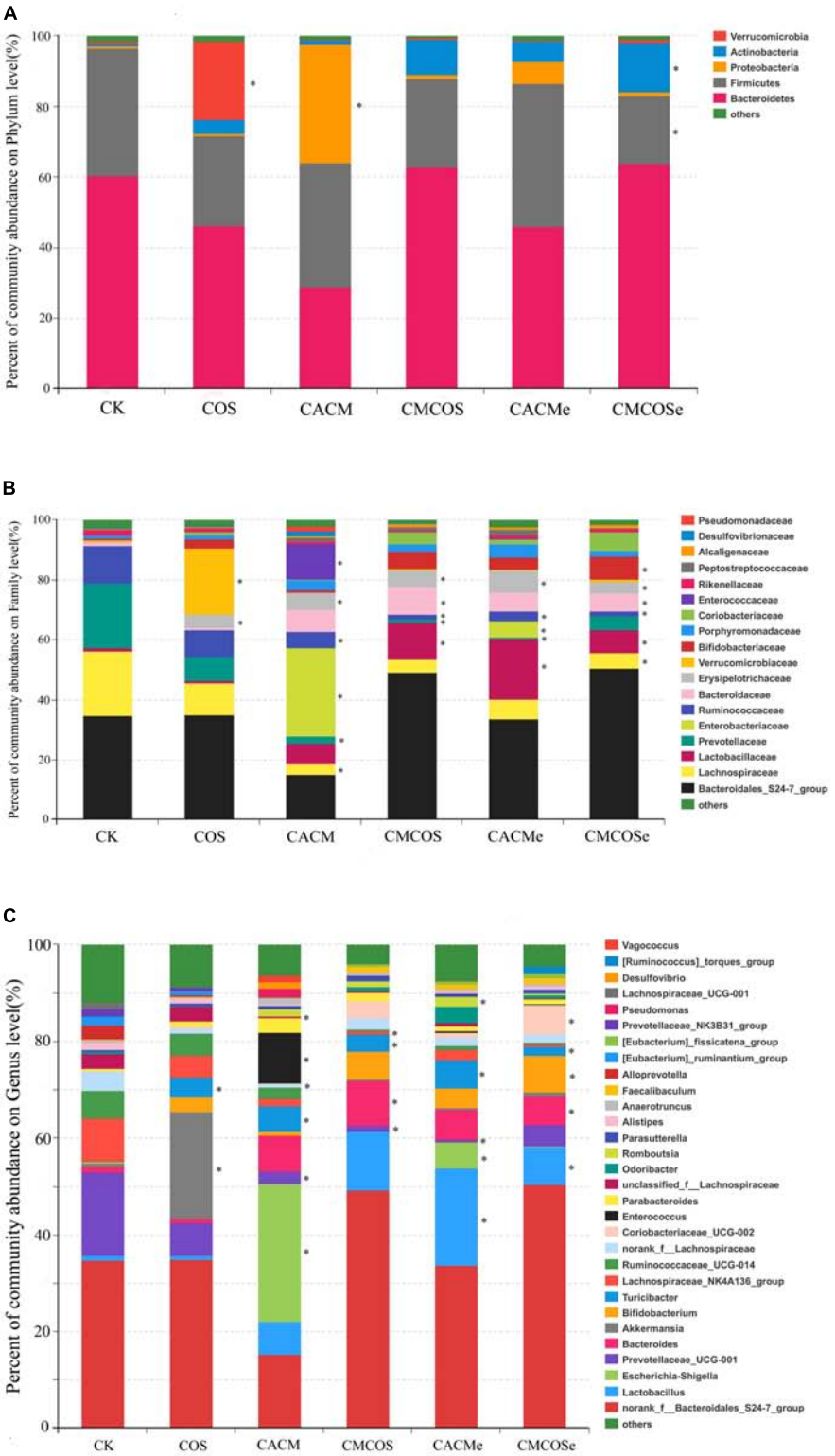

FIGURE 4 | Relative abundances at the phylum **(A)**, family **(B)**, and genus **(C)** levels for bacteria that exceeded 1% of the total. The results are presented as the mean ± standard deviation (SD); $n = 4$ for each treatment. *Analysis of variance (ANOVA) was used, significant differences between CK and treatments were indicated ($P < 0.05$). CK, control treatment; COS, COS control treatment; CACM, AOM/DSS-induced colitis-associated CRC model mice; CMCOS, COS-treated CACM mice (300 mg/kg/d COS); CACMe, exchanged CACM treatment; CMCOSe, exchanged CMCOS treatment.

(3.41 ± 1.75% *vs.* 21.62 ± 9.17%, 2.51 ± 1.07% *vs.* 21.56 ± 7.88%, 5.30 ± 2.86%, *vs.* 12.57 ± 4.21%, respectively), whereas those of Enterobacteriaceae, Erysipelotrichaceae, and Enterococcaceae notably increased (29.53 ± 7.05% *vs.* 0.005 ± 0.002%, 11.88 ± 7.50% *vs.* 0.003 ± 0.0009%, 5.74 ± 2.64% *vs.* 0.22 ± 0.09%, respectively). In the COS-treated CACM group, the increases of Enterobacteriaceae and Enterococcaceae were reversed, and no significant difference was observed between the CK and CMCOS groups with respect to Enterobacteriaceae and Enterococcaceae.

At the genus level, 30 genera that exceeded 1% of the total bacteria were observed (**Figure 4C**). Compared with the CK groups, the COS treatment significantly increased the percentage of *Akkermansia* (22.24 ± 11.60% *vs.* 0.65 ± 0.47%). In the CACM group, the percentages of *Escherichia–Shigella* (28.52 ± 7.06% *vs.* 0.0047 ± 0.0019%), *Enterococcus* (10.57 ± 3.70% *vs.* 0.0028 ± 0.0019%) and *Turicibacter* (5.32 ± 2.90% *vs.* 0.055 ± 0.021%) were significantly increased, whereas those of Prevotellaceae_UCG-001 (2.51 ± 1.07% *vs.* 17.21 ± 10.41%), norank_f_Lachnospiraceae (0.78 ± 0.39% *vs.* 3.95 ± 2.78%) and unclassified_f_Lachnospiraceae (0.44 ± 0.24% *vs.* 3.08 ± 0.89%) were notably decreased ($P < 0.05$). However, the COS-treated evidently reversed the increases of *Escherichia–Shigella* and *Enterococcus* that were induced by AOM and DSS. No significant difference was observed between the CK and CMCOS groups at with respect to *Escherichia–Shigella* and *Enterococcus*, while Prevotellaceae_UCG-001 (1.13 ± 0.76% *vs.* 17.21 ± 10.41%) and Lachnospiraceae_NK4A136_group (0.055 ± 0.021% *vs.* 3.53 ± 1.83%) decreased, *Turicibacter* (3.53 ± 1.83% *vs.* 0.055 ± 0.021%) and Bacteroides (8.84 ± 5.27% *vs.* 0.63 ± 0.26%) significantly increased ($P < 0.05$).

LaLEfSe analysis was subsequently performed from phylum to genus level to obtain a cladogram representation and the characteristic bacteria of the gut microbiota for the six treatments (**Figure 5**). Prevotellacea, Lachnospiraceae, and Ruminococcaceae were dominant in the CK group, whereas *Akkermansia* and Lachnospiraceae in the COS group, *Escherichia_Shigella* and *Enterococcus* in the CACM group, and *Bacteroides* in the CMCOS group. The exchange of cages induced shifts in the microbiota, with characteristic taxa of *Lactobacillus* and *Turicibacter* observed in the CACMe group, whereas Bacteroidales_S24-7_group and Coriobacteriaceae_UCG_002 were observed in the CMCOSe group.

Comparison of Fungal Community Composition

In total, 876,569 valid and trimmed sequences were obtained from all 24 samples ($n = 4$), with an average of 36,524 sequences per sample and an average length of 401 bp per sequence. All samples were subsampled at same sequence depth (30,452 reads). The total number of OTUs at the 97% similarity level was 117. According to the results of PCA and hcluster, two outliers from the CK and the COS groups were removed in the subsequent analyses, respectively.

The alpha diversity indexes of mycobiota are presented in **Table 2**. The Chao and Shannon indexes for the CACM group were significantly lower than that observed in the CK group, whereas the Simpson index for the CACM group was significantly higher than that observed in the CK, CMCOS, and CMCOSe groups. AOM and DSS significantly decreased the alpha diversity index values of mycobiota, while the COS treatment increased them. In addition, exchange of cages was less effective at promoting gut fungal diversity.

The PCA results showed that the samples from the CACM and CACMe groups clustered, while the samples from the other groups clustered together (**Supplementary Figure S8**). These indicated that the COS treatment reversed the shifts in the fungal communities induced by AOM/DSS. However, the effect of the exchange of cages on the mycobiota was limited.

Based on the taxonomic results, 7 phyla that exceed 1% in abundance were detected (**Supplementary Figure S9**). Ascomycota and Basidiomycota were the most predominant phyla, accounting for 70.59 ∼ 86.61% and 9.42 ∼ 26.30%, respectively. However, no significant difference was detected between any two groups at the phylum level. Twenty-nine families exceeding 1% in abundance are presented in **Supplementary Figure S9**, and Trichocomaceae was the most predominant family. No significant difference was observed between the CK and COS groups. Compared with the CK group, norank_o_Sporidiobolales and o_norank_c_Agaricomycetes significantly decreased in the CACM group (0 *vs.* 5.95 ± 1.42%; and 0.11 ± 0.07% *vs.* 4.84 ± 1.34%, respectively). In addition, Cystofilobasidiaceae decreased in the CMCOS group significantly (0.32 ± 0.14% *vs.*4.24 ± 0.75%) ($P < 0.05$). Due to the limitation of the fungal database, only 29 genera exceeding 1% in abundance were detected (**Supplementary Figure S9**). Unclassified_f_Trichocomaceae, unclassified_o_Hypocreales, *Boeremia* and *Cladosporium* were the most dominant genera. Between the CK and CACM groups, there were significant differences in norank_o_Sporidiobolales and o_norank_c_Agaricomycetes at the genus level ($P < 0.05$). Compared with the CK, *Mrakia* was significantly decreased in the CMCOS group (0.32 ± 0.14% *vs.*4.24 ± 0.75%) ($P < 0.05$).

LaLEfSe analysis from the phylum to species level was then performed to obtain a cladogram representation and the characteristic fungi of the gut mycobiota within the six groups. As shown in **Figure 6**, the greatest differences in taxa among the six groups were detected by LDA (score 3.0). In the CACM group, Trichocomaceae and Eurotiales were the characteristic fungi, while Sporidiobolales and *Pichia* in the CK group, *Cladosporium* and Microascaceae in the CMCOS group, and Oligohymenophorea in the CMCOSe group were the characteristic fungi.

The Correlation Between Gut Microbes and Environmental Factors

The correlation between intestinal microbes (the most abundant 50 genera or species) and environmental factors (DAI, tumor

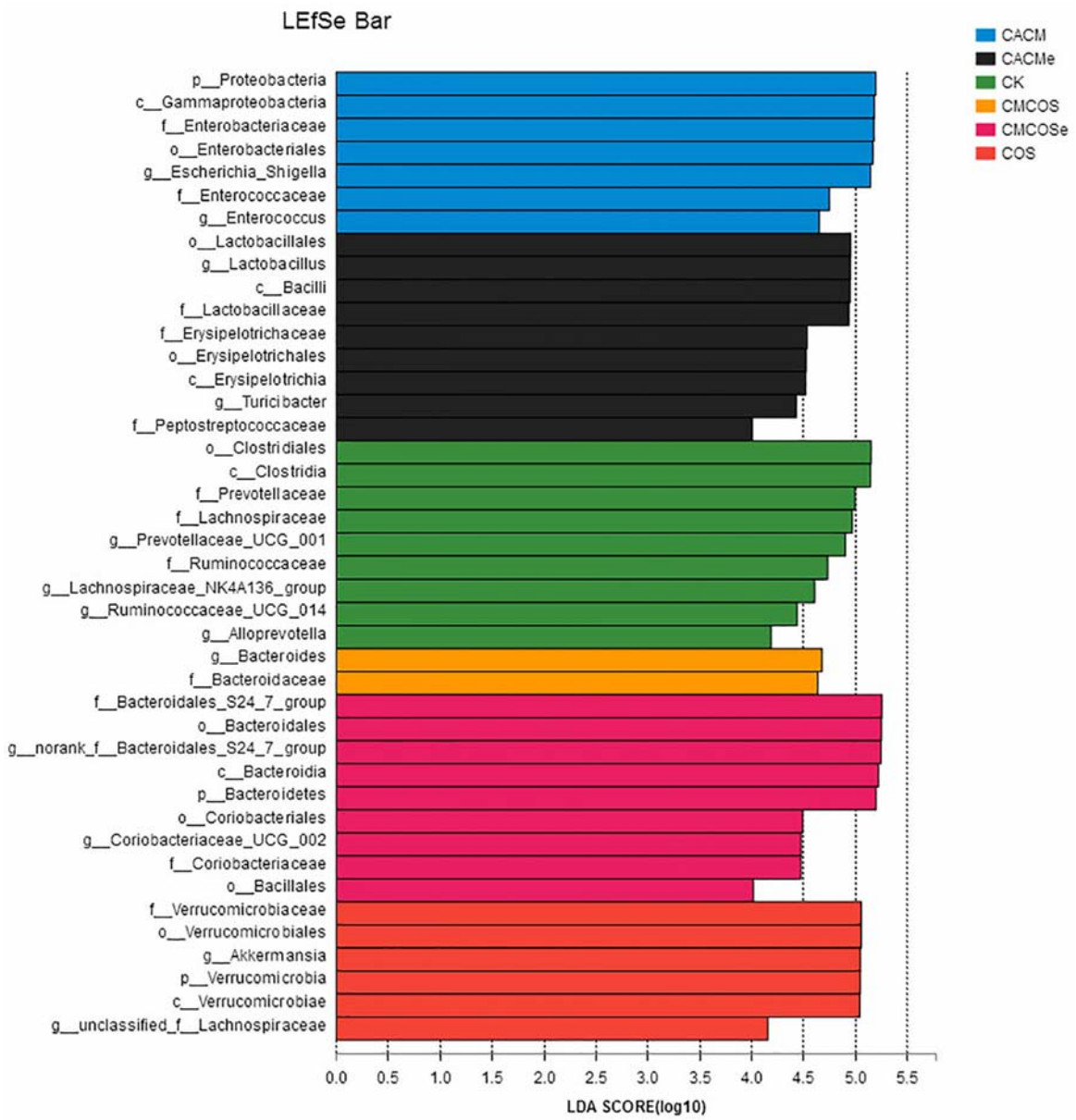

FIGURE 5 | Histogram of the LDA scores for differentially abundant bacteria among the six treatments. Non-parametric factorial Kruskal–Wallis (KW) sum-rank test was used. $n = 4$. CK, control treatment; COS, COS control treatment; CACM, AOM/DSS-induced colitis-associated CRC model mice; CMCOS, COS-treated CACM mice (300 mg/kg/d COS); CACMe, exchanged CACM treatment; CMCOSe: exchanged CMCOS treatment.

multiplicity and cytokines), were analyzed by Spearman correlation coefficient based on hierarchical clustering and heatmap analyses. At the genus level, some genera were strongly positively correlated with disease traits and cytokine mRNA abundances, such as *Escherichia–Shigella*, *Romboutsia*, *Pseudomonas*, *Vagococcus*, *Bacteroides*, *Enterococcus*, *Lactobacillus,* and *Turicibacter*. Some taxa were strongly negatively correlated with disease traits and cytokines, such as Lachnospiraceae_UCG-001, *Alloprevotella*, *Ruminantium* group, Prevotellaceae_NK3B31 group, *Akkermansia*, and *Alistipes* (**Figure 7**). Further analysis at the species level showed that most of highly correlated bacteria were unclassified species from the corresponding genera at the genus level. However, some detailed species also were obtained, with *Bacteroides uniformis*, *Bacteroides caccae*, *Lactobacillus johnsonii*, and *Vagococcus fluvialis* were strongly positively correlated with disease severity (**Supplementary Figure S10**).

The correlation analysis between mycobiota and the assayed factors of disease severity (DAI, tumor multiplicity and cytokines) showed that only several fungi were involved. At the genus level, unclassified Trichocomaceae was positively correlated, while *Claviceps* and norank of Sporidiobolales

TABLE 2 | The alpha diversity indexes of mycobiota at the 10th weekend determined by high-throughput sequencing.

Groups	Chao	Shannon	Simpson	Sobs	Ace	Coverage
CK	46.17 ± 9.65^{a}	2.59 ± 0.23^{a}	0.12 ± 0.04^{a}	36.33 ± 7.02^{a}	65.71 ± 41.86^{a}	1.00 ± 0.000153^{a}
COS	33.83 ± 7.91^{ab}	2.23 ± 0.32^{ab}	0.18 ± 0.06^{ab}	30.00 ± 2.65^{a}	43.18 ± 22.83^{a}	1.00 ± 0.000122^{a}
CACM	28.00 ± 4.08^{b}	1.78 ± 0.14^{b}	0.30 ± 0.01^{a}	26.75 ± 4.57^{a}	31.29 ± 5.61^{a}	1.00 ± 0.000054^{a}
CMCOS	35.75 ± 8.50^{ab}	2.51 ± 0.35^{a}	0.13 ± 0.04^{b}	35.50 ± 8.19^{a}	37.13 ± 9.90^{a}	1.00 ± 0.000065^{a}
CACMe	36.08 ± 6.04^{ab}	2.22 ± 0.17^{ab}	0.21 ± 0.07^{ab}	35.00 ± 4.97^{a}	36.15 ± 5.87^{a}	1.00 ± 0.000048^{a}
CMCOSe	40.56 ± 5.03^{ab}	2.37 ± 0.29^{a}	0.17 ± 0.08^{a}	38.25 ± 3.69^{a}	41.11 ± 4.74^{a}	1.00 ± 0.000082^{a}

The results were presented as the mean ± standard deviation (SD); n = 3 for the CK and COS groups, n = 4 for the CACM, CMCOS, CACMe, and CMCOSe groups. Analysis of variance (ANOVA) was used, significant differences ($P < 0.05$) between treatments are indicated by the letters a, b, or c. CK, control group; COS, COS-treated group; CACM, AOM/DSS-induced colitis-associated CRC model mice; CMCOS, COS-treated CACM mice (300 mg/kg COS); CACMe, exchanged CACM group; CMCOSe, exchanged CMCOS group.

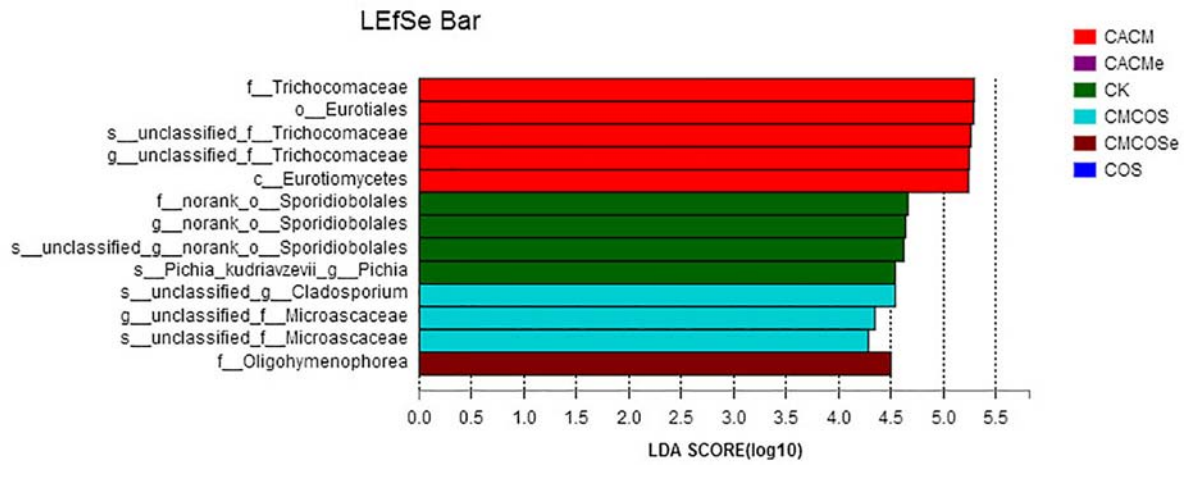

FIGURE 6 | Histogram of the LDA scores for differentially abundant fungi among the six treatments. Non-parametric factorial Kruskal–Wallis (KW) sum-rank test was used. *n* = 3 for the CK and COS groups, *n* = 4 for the CACM, CMCOS, CACMe, and CMCOSe groups. CK, control treatment; COS, COS control treatment; CACM, AOM/DSS-induced colitis-associated CRC model mice; CMCOS, COS-treated CACM mice (300 mg/kg/d COS); CACMe, exchanged CACM treatment; CMCOSe, exchanged CMCOS treatment.

were strongly negatively correlated with severely these factors (**Figure 8**). At the species level, *Pichia Kudriavzevii*, *Cladosporium herbarum* and unclassified Sporidiobolales were the most negatively correlated species, while unclassified Trichocomaceae and unclassified Basidiomycota were the most positively correlated species (**Supplementary Figure S11**).

The Co-association of Bacteria and Fungi

To study the possible interactions among microbiota and mycobiota, the dominant genera (relative abundance > 0.1%) were used to construct a network. Topological properties are always used in network analysis to describe the complex pattern of interrelationships. As shown in **Figure 9**, the network included 58 nodes and 201 edges. The average network distance between all pairs of nodes (average path length) was 2.97. The clustering coefficient (the degree to which they tend to cluster together) was 0.51. The heterogeneity value (the possibility of hubs) of this network was 0.792. The majority of the network generated was cooccurrent interactions (green lines), whereas the others exhibited mutual exclusions (red lines). *Alloprevotella* (19 edges), *Eubacterium ruminantium* (18 edges), Lachnospiraceae UCG001 (17 edges) and Prevotellaceae NK3B31 (17 edges) were the key genera of microbiota; and norank Agaricomycetes (5 edges) and unclassified Trichocomaceae (4 edges) were the key genera of mycobiota. However, few interactions were observed between bacteria and fungi.

DISCUSSION

Chitooligosaccharides are considered to be potential anticancer agents because of their anti-tumor activities. In this study, the treatment of COS notably decreased the DAI, the incidence and multiplicity of tumors in the CMCOS mice. These results indicated that COS suppress the development of CRC induced by AOM/DSS. In the COS-treated CRC mice, the levels of COX-2, IL-1β, IL-6, IL-10, and TNF-α mRNA decreased significantly ($P < 0.05$). These results are consistent with previous studies that showed the suppressive effects of gallate-COS on COX-2 mRNA transcription and TNF-α protein expression in A549 human lung epithelial cells (Vo et al., 2017) and NF-κB

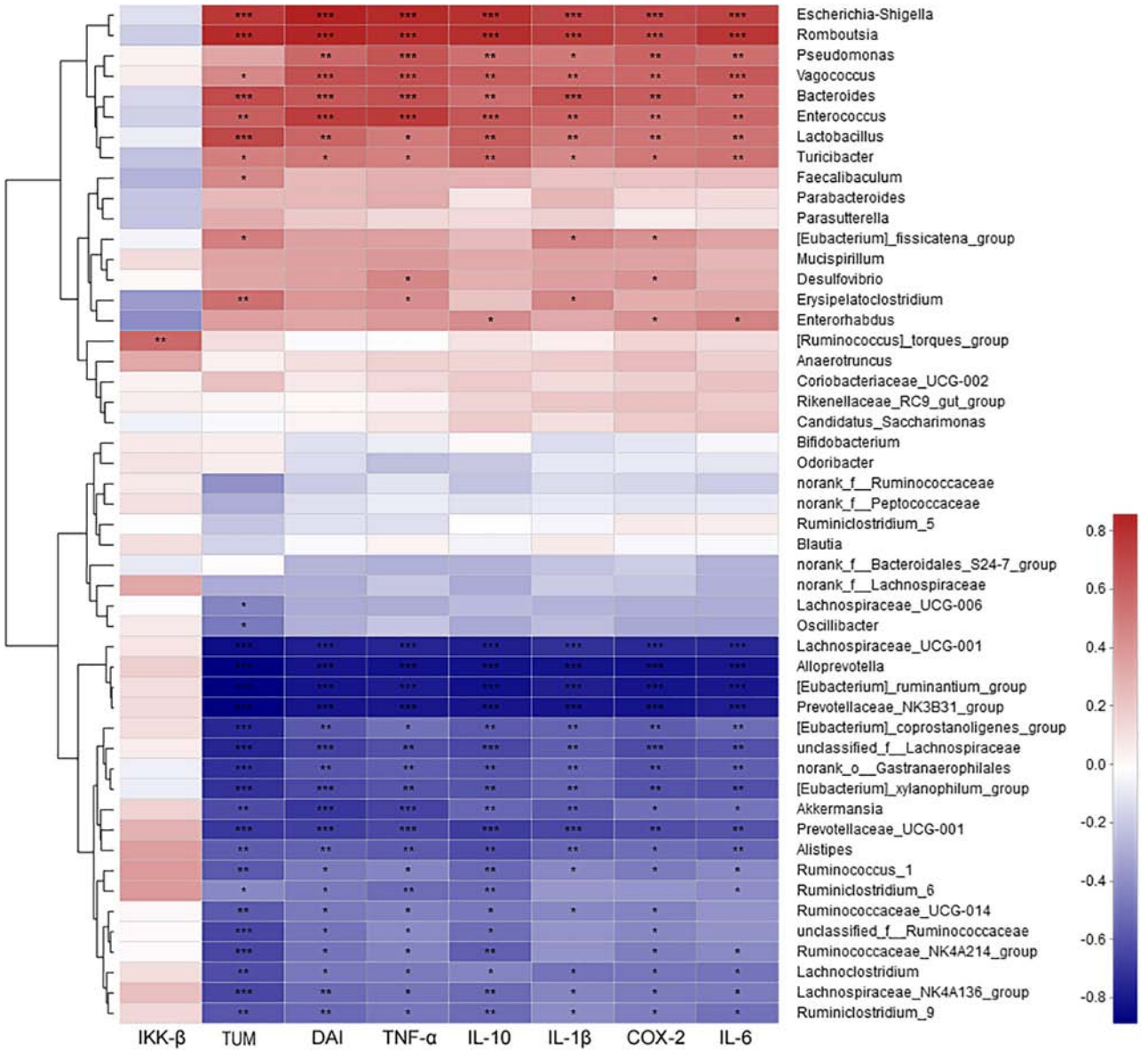

FIGURE 7 | The correlation between microbiota at genus level and environmental factors (DAI, tumor multiplicity and cytokines). The most abundant 50 genera in each sample were used to perform the hierarchical clustering and heatmap analyses based on Spearman correlation coefficient. $n = 4$. TUM, tumor multiplicity; DAI, disease activity index.

mediated inflammatory related protein expression in CRC mice (Mattaveewong et al., 2016).

Host genetic and environmental factors, such as (but not limited to) food, bedding, caging, and temperature shape the gut microbiota and account for their variability (Campbell et al., 2012; McCoy et al., 2017). However, litter and cohabitation had a detectable and measurable contribution in the variation of the gut microbial communities in the same mouse genetic background mouse, as mice housed in the same cage begin to share similar gut microbiota due to mixing by coprophagia (Benson et al., 2010; Campbell et al., 2012; Buffington et al., 2016). In this study, to protect the mice with more severe disease in the CACMe group than those in the CMCOSe, the cages of the mice were exchanged (shared litters) rather than cohousing. Strikingly, the DAI score, tumor multiplicity and IKK-β mRNA abundance were significantly decreased in the CACMe group compared to the CACM group, whereas the tumor multiplicity and the COX-2 and IL-1β mRNA abundance were significantly increased in the CMCOSe group compared to the CMCOS group. These results indicated that the cage-exchanged between the CACM and CMCOS mice effectively impacted the development of CRC. Compared with the independently caged CACM or CMCOS groups, the microbial community structure was shifted in the corresponding group with exchanged

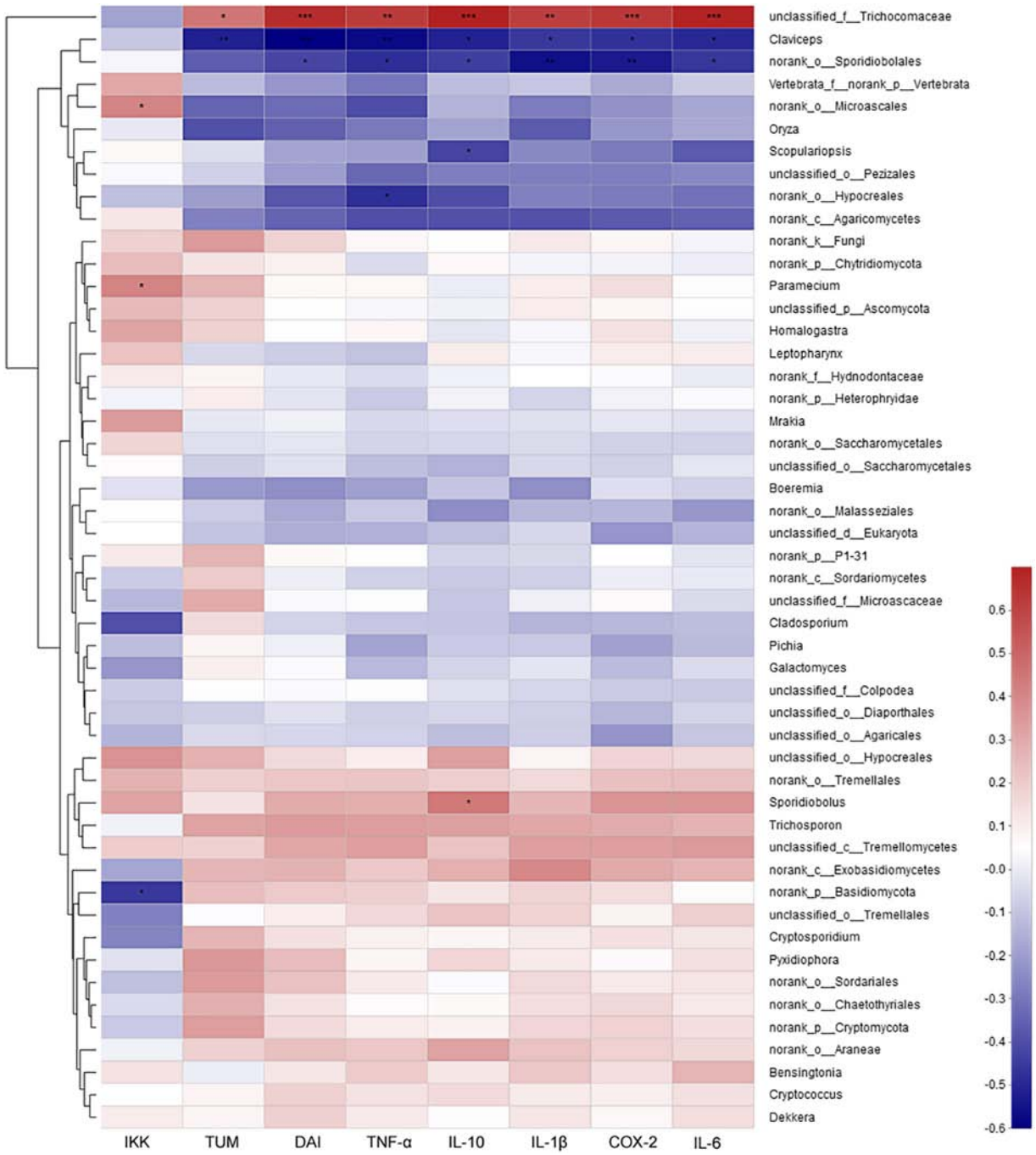

FIGURE 8 | The correlation between mycobiota at genus level and environmental factors (DAI, tumor multiplicity and cytokines). The most abundant 50 genera in each sample were used to perform the hierarchical clustering and heatmap analyses based on Spearman correlation coefficient. TUM, tumor multiplicity; DAI, disease activity index.

cages (CACMe or CMCOSe). At the end of the 9th and 10th weekends, compared with the CMCOS group, the abundance of *Enterococcus* and butyrate-producing bacteria in the CMCOSe group was significantly increased and decreased, respectively. The samples from the CACMe group clustered away from those of the CACM group but were close to those of the CMCOSe and CMCOS groups in the PCoA analysis of microbiota. The values of fungal diversity indexes (Chao, Simpson, and Shannon) in the CACM group were different from those in the CK group; however, the cage-exchanged reversed these alterations. Furthermore, LEfSe analysis showed that the characteristic bacteria and fungi shifted in the CACMe (compared to CACM)

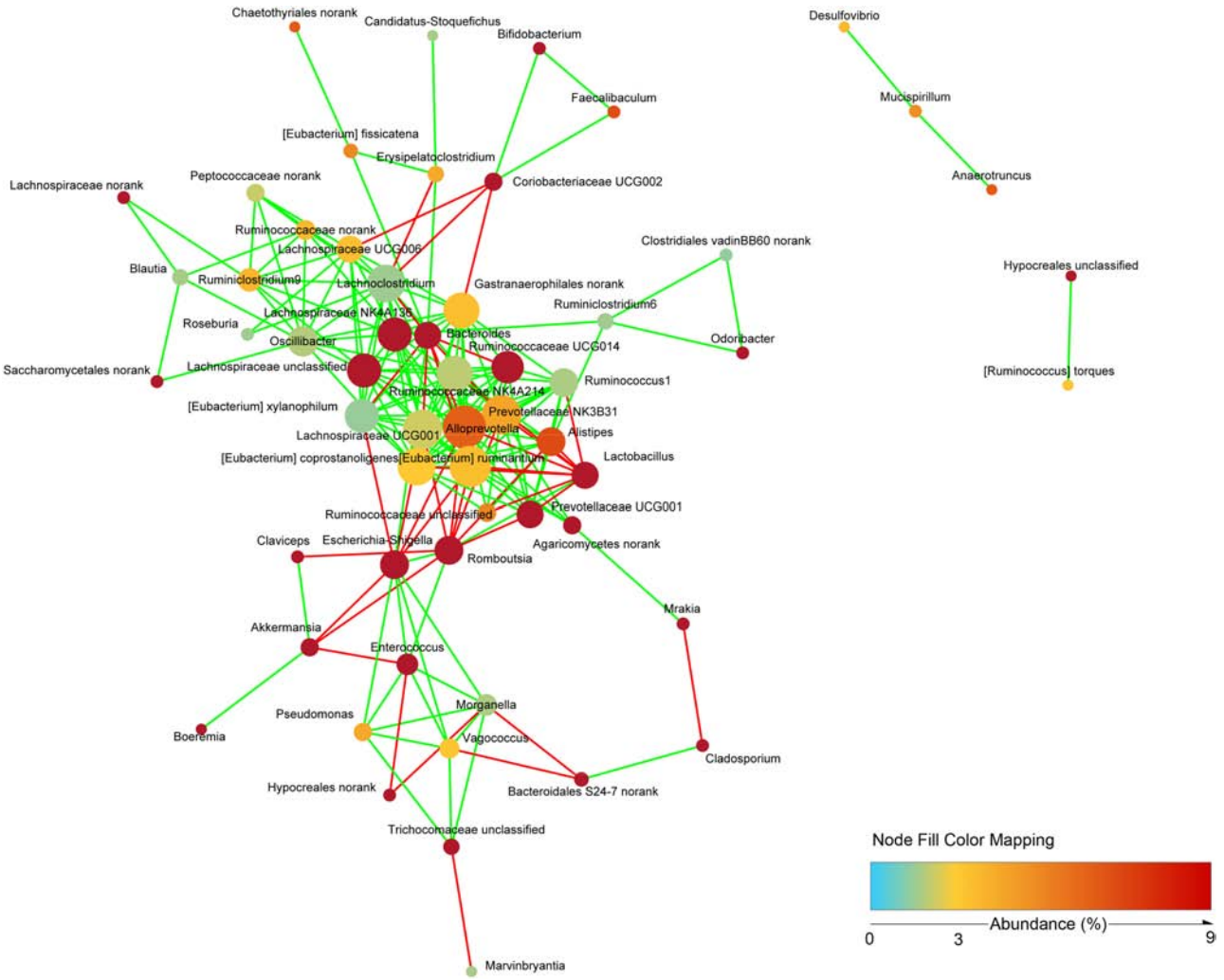

FIGURE 9 | Network analysis indicating interactions among dominant bacteria and fungi. The dominant bacterial and fungal genera that relative abundance >0.1% were used to generated network based on non-parametric Spearman correlation coefficients.

and CMCOSe (compared to CMCOS) groups. The correlation analysis between environmental factors and intestinal microbes also showed the high degree of correspondence with LEfSe. Thus, the daily exchange of cages effectively promoted the interchange of microbiota and mycobiota between the CACMe and CMCOSe groups, indicating that intestinal microbes (especially microbiota) play an important role in the development of CRC and the prevention of COS on CAC.

Consistent with previous studies, the imbalances of microbiota were observed in the AOM/DSS-induce CRC mice, including decreases in diversity, the reduction of total bacteria and butyrate-producing bacteria, the enrichment of *Enterococcus* and *Escherichia–Shigella*. However, in this study, the treatment of COS alleviated these imbalances and inhibited CRC development. Specific gut bacteria (*Fusobacterium nucleatum*, *Bacteroides fragilis*, *Enterococcus faecalis*, *Escherichia coli*, etc.) are well known to contribute to the development of CRC through a number of potential mechanisms, including promoting chronic inflammation, DNA damage and the production of bioactive carcinogenic metabolites (Keku et al., 2015). Short chain fatty acids (SCFAs) are generally considered to be beneficial metabolites in the human gut, and butyrate in particular is known to have anti-inflammatory effects through histone deacetylase inhibition and subsequent downregulation of proinflammatory cytokines (Chang et al., 2014). Prebiotics and traditional Chinese medicines reduce the risk of colitis and CRC development by influencing the microbiota. The result of a study by Higashimura et al. (2016) suggested that the oral intake of agaro-oligosaccharides prevents high-fat diet-induced gut dysbiosis, thereby inhibiting colon carcinogenesis. In another study, black raspberry anthocyanins played a central role in the chemoprevention of CRC by changing inflammation and the methylation status of the SFRP2 gene and modulating the composition of gut commensal microbiota (the abundance of *Desulfovibrio* sp. and *Enterococcus* spp. were decreased significantly, whereas probiotics such as *Eubacterium rectale*,

Faecalibacterium prausnitzii, and *Lactobacillus* were dramatically increased) (Chen et al., 2018). Huangqin decoction ameliorates DSS-induced colitis by altering of the gut microbiota (Yang et al., 2017). The results of our previous study also suggested that isoliquiritigenin protects mice from AOM/DSS-induced CRC by reducing the abundances of pathobionts (*Escherichia* and *Enterococcus*) and increasing those of probiotics, particularly butyrate-producing bacteria (*Butyricicoccus*, *Clostridium*, and *Ruminococcus*).

Of the genera altered by the AOM/DSS treatment, the genus *Turicibacter* is of particular interest. The intestinal *Turicibacter* population, which was previous shown to be a strong indicator of wild-type mice, exhibited low competitiveness and was unable to persist in the altered gut resulting from CD45 inactivation (Dimitriu et al., 2013). Zenewicz et al. (2013) also demonstrated a reduction in the abundance of *Turicibacter* in the GI of IL-22 deficiency mice. However, in this study, compared with the CK and COS groups, the abundance of *Turicibacter* significantly increased in all of the AOM/DSS-treated groups, including the CACM, CACMe, CMCOS and CMCOSe groups. An increased abundance of *Turicibacter* was also observed in our previous studied mice with AOM/DSS-induced CRC, where isoliquiritigenin treatment was shown to decrease the abundance of *Turicibacter* in CRC mice (Wu et al., 2016). Munyaka et al. (2016) investigated the fecal and colonic mucosa microbial composition and functional changes in mice treated with DSS and found that *Turicibacter* was positively correlated with the DSS-treated group but negatively correlated with the control group in the fecal and colonic samples. In light of these data, *Turicibacter* may simply be sensitive to DSS and increase in abundance during or after the development of colitis or CRC. Thus, the role of *Turicibacter* in CRC development needs to be further studied.

It is important to note that the abundance of *Akkermansia* was significantly higher in the COS group than in any other groups. Recently, the results of increasing numbers of studies have indicated that *Akkermansia muciniphila* is a component of the healthy gut microbiome and is a potential probiotic. *A. muciniphila* is positively correlated with a lean phenotype, reduced body weight gain, amelioration of metabolic responses and the restoration of gut barrier function by modulation of mucus layer thickness (Dao et al., 2016; Ottman et al., 2017). The Amuc_1100 protein, which was purified from the outer membrane of *A. muciniphila*, induced production of specific cytokines through activation of Toll-like receptor (TLR) 2 and TLR4, improved the gut barrier and partly recapitulates the beneficial effects of the bacterium (Ottman et al., 2017; Plovier et al., 2017). *Akkermansia* also has a positive role in inhibiting cancer development. The clinical responses of cancer patients to immune checkpoint inhibitors were closely correlated with the relative abundance of *A. muciniphila*, and oral supplementation with *A. muciniphila* after fecal microbiota transplantation with non-responder feces restored the efficacy of the PD-1 blockade in an interleukin-12-dependent manner by increasing the recruitment of $CCR9^{+}CXCR3^{+}CD4^{+}$ T lymphocytes into mouse tumor beds (Routy et al., 2018). HuR inhibition in APC ^{Min} mice, a model of FAP and colon cancer, decreased the number of small intestinal tumors, and increased the abundance of *Prevotella, Akkermansia*, and *Lachnospiraceae* (Lang et al., 2017). The dramatic increase of *Akkermansia* in the COS group in this study suggested that COS is a potential probiotic by stimulating the growth of *Akkermansia*. However, *Akkermansia* may be sensitive to AOM and/or DSS, because it was not enriched in all of the AOM/DSS-treated groups, including the CACM, CACMe, CMCOS, and CMCOSe treatments.

Of particular interest, the abundance of *Lactobacillus*, which is most known for its essential use in food fermentation and as a probiotic, was significantly higher in the CACM and CACMe groups than in the other groups. The qPCR revealed that the abundance of *Lactobacillus* was significantly enriched in the CACM and CACMe groups at the 6th, 9th, and 10th weekends, consistent with the results of the LEfSe analysis of sequences in which *Lactobacillus* was one of the characteristic genera in the CACMe group. Even though *Lactobacillus* is only a minor member of the human colonic microbiota, the proportion of this genus is frequently either positively or negatively correlated with human disease and chronic conditions (Heeney et al., 2018). Many studies suggested that *Lactobacillus* was beneficial to intestinal health, whereas those of other studies indicated that *Lactobacillus* was enriched during disease, such as Crohn's disease (Wang et al., 2014; Lewis et al., 2015), Type 2 diabetes (Karlsson et al., 2013), and head and neck squamous cell cancer (Guerrero-Preston et al., 2016). In this study, *L. johnsonii* was strongly positively correlated with the development of CRC. Although many studies reported that *L. johnsonii* was the most studied probiotic bacteria strain (Ashraf and Shah, 2014); Perez-Muñoz et al., 2014) found that spontaneous inflammation of the colons of core 1-derived *O*-glycans-deficient mice was associated with an increase of *L. johnsonii*. Thus, it is difficult to conclude whether *Lactobacillus* is a driver or just along for the ride in health and disease. Thus, the enrichment of *Lactobacillus* during the development of CRC in this study indicated that the role of *Lactobacillus* should be further investigated.

Little is known regarding the relationship between intestinal fungi and CRC. In this study, fungal diversity significantly decreased and fungal community composition notably shifted in the CACM group. These results are consistent with those of a previous study in which fecal samples were collected from 131 CRC patients and a distinct fungal dysbiosis and alteration of the fungal network was shown to potentially play important roles in polyp and CRC pathogenesis (Gao et al., 2017). In this study, treatment of COS recovered these changes in the CMCOS group. No significant difference was observed between the CK and CMCOS groups with respect to fungal diversity, and the samples from the CMCOS were clustered together with those from the CK group, and far away from those of the CACM group in the PCA analysis.

Interestingly, *Cladosporium* was a characteristic bacterial genus in the CMCOS group, and was one of the genera that strongly negatively correlated with tumor multiplicity, DAI and cytokine levels. Some *Cladosporium* metabolites have been reported to be effective at inhibiting the growth of human colon cancer cells. For instance, an isolated fungal taxol produced by *Cladosporium oxysporum* suppressed the growth of six

different human pathogenic bacteria and the cancer cell line HCT15 (Gokul Raj et al., 2015). In addition, cladosporols that were purified and characterized as secondary metabolites from *Cladosporium tenuissimum* inhibited the growth of various human colon cancers derived cell lines (HT-29, SW480, and CaCo-2) in a time- and concentration-dependent manner, especially toward HT-29 cells (Zurlo et al., 2013). Thus, the COS-induced enrichment of *Cladosporium* may be a potential factor that inhibited CRC development. However, due to the very limited reports of fungi in CRC and the even less-reported effect of cage-exchanged on modulating mycobiota described in this study, the role of fungi in CRC should be pursued in future studies.

Pichia kudriavzevii has been isolated from human fecal samples (Madeeha et al., 2016) and has shown expressed efficient probiotic properties (Srinivas et al., 2017). Metabolites secreted by *P. kudriavzevii* AS-12 demonstrated anticancer effects by inhibiting cell proliferation and inducing intrinsic and extrinsic apoptosis in colon cancer cells (Saber et al., 2017). In this study, *P. kudriavzevii* was strongly negatively correlated with tumor multiplicity, disease activity index and cytokines. Thus, *P. kudriavzevii* may play an important role in preventing the development of CRC, and further research on *P. kudriavzevii* and CRC needs to be performed.

Vagococcus fluvialis was previously isolated and characterized as probiotic strain exhibiting a protective effect against vibriosis in sea bass (Sorroza et al., 2012) and was also detected in the root canals and midgut of *Culex quinquefasciatus* mosquitoes (Schirrmeister et al., 2009; Chandel et al., 2015). Román et al. (2013, 2015) reported that *V. fluvialis* and its extracellular products had a clear immunomodulatory activity *in vitro* as well as the ability to induce cytokine production related to the immune response. In the present study, *V. fluvialis* was highly positively correlated with cytokines, tumor multiplicity and disease activity index. A relationship between *V. fluvialis* and cytokines was easily observed, as transcripts of cytokines (IL-1, TNF-α, COX-2, and IL-10) were highly up-regulated in sea bass after a 1-h of incubation with the probiotic strain *V. fluvialis* L-21. However, this was the first time that relationship between *V. fluvialis* and CRC has been observed. Due to the limitation knowledge of related references, the role of *V. fluvialis* in CRC should be further studied.

In summary, the results of this study provided the first evidence that microbiota contributed to the antitumor activity of COS toward CRC. These results were supported by different presentations of CRC incidence, tumor multiplicity, expression of cytokines, bacterial community diversity and composition between the intervention groups, especially between the separated and cage-exchanged groups (CACM *vs.* CACMe, and CMCOS *vs.* CMCOSe). Notably, these data also provided evidence that COS inhibited CRC development by enriching probiotics (*Akkermansia* and butyrate-producing bacteria) and decreasing pathobionts (*Escherichia_Shigella* and *Enterococcus*). Moreover, this study also revealed that mycobiota was altered during the CRC development process, and COS also effectively recovered the intestinal fungal community composition. Thus, COS may be a potential therapeutic for the prevention of CRC development, in part through regulating the gut microbiota and mycobiota.

AUTHOR CONTRIBUTIONS

MW and GZ conceived and designed the experiments. JiaL, YA, PL, WX, and MW performed the experiments and collected the data. MW, JiaL, JinL, and DY analyzed the data. MW and GZ wrote the manuscript.

FUNDING

This work was supported by the Key Scientific Research Projects for Higher Education of Henan Province (Grant Nos. 17A310022 and 15A320063), the Young Backbone Teachers Fellowship in Henan Province (2016GGJS-105), the Disciplinary group of Psychology and Neuroscience, Xinxiang Medical University (2016PN-KFKT-12), and the Natural Science Foundation of China (Grant No. 81872361).

SUPPLEMENTARY MATERIAL

The Supplementary Material for this article can be found online at: https://www.frontiersin.org/articles/10.3389/fmicb.2019.02101/full#supplementary-material

REFERENCES

Amato, K. R., Yeoman, C. J., Kent, A., Righini, N., Carbonero, F., Estrada, A., et al. (2013). Habitat degradation impacts black howler monkey (Alouatta pigra) gastrointestinal microbiomes. *ISME J.* 7, 1344–1353. doi: 10.1038/ismej.2013.16

Artan, M., Karadeniz, F., Karagozlu, M. Z., Kim, M. M., and Kim, S. K. (2010). Anti-HIV-1 activity of low molecular weight sulfated chitooligosaccharides. *Carbohyd. Res.* 345, 656–662. doi: 10.1016/j.carres.2009.12.017

Arthur, J. C., Perez-Chanona, E., Muhlauer, M., Tomkovich, S., Uronis, J. M., Fan, T. J., et al. (2012). Intestinal inflammation targets cancer-inducing activity of the microbiota. *Science* 338, 120–123. doi: 10.1126/science.1224820

Ashraf, R., and Shah, N. P. (2014). Immune system stimulation by probiotic microorganisms. *Crit. Rev. Food Sci. Nutr.* 54, 938–956. doi: 10.1080/10408398.2011.619671

Benson, A. K., Kelly, S. A., Legge, R., Ma, F., Low, S. J., Kim, J., et al. (2010). Individuality in gut microbiota composition is a complex polygenic trait shaped by multiple environmental and host genetic factors. *Proc. Natl. Acad. Sci. U.S.A.* 107, 18933–18938. doi: 10.1073/pnas.1007028107

Bhatt, R. S., Kothari, S. T., Gohil, D. J., D'Souza, M., and Chowdhary, A. S. (2015). Novel evidence of microglial immune response in impairment of dengue infection of CNS. *Immunobiology* 220, 1170–1176. doi: 10.1016/j.imbio.2015.06.002

Brennan, C. A., and Garrett, W. S. (2016). Gut microbiota, inflammation, and colorectal cancer. *Annu. Rev. Microbiol.* 70, 395–411.

Buffington, S. A., Prisco, G. V. D., Auchtung, T. A., Ajami, N. J., Petrosino, J. F., and Costa-Mattioli, M. (2016). Microbial reconstitution reverses maternal diet-induced social and synaptic deficits in offspring. *Cell* 165, 1762–1775. doi: 10.1016/j.cell.2016.06.001

Campbell, J. H., Foster, C. M., Vishnivetskaya, T., Campbell, A. G., Yang, Z. K., Wymore, A., et al. (2012). Host genetic and environmental effects on mouse intestinal microbiota. *ISME J.* 6, 2033–2044. doi: 10.1038/ismej.2012.54

Caporaso, J. G., Lauber, C. L., Walters, W. A., Berg-Lyons, D., Huntley, J., Fierer, N., et al. (2012). Ultra-high-throughput microbial community analysis on the Illumina HiSeq and MiSeq platforms. *ISME J.* 6, 1621–1624. doi: 10.1038/ismej.2012.8

Chandel, K., Parikh, R. Y., Mendki, M. J., Shouche, Y. S., and Veer, V. (2015). Isolation and characterization of *Vagococcus* sp from midgut of *Culex quinquefasciatus* (Say) mosquito. *J. Vector Borne Dis.* 52, 52–57.

Chang, P. V., Hao, L., Offermanns, S., and Medzhitov, R. (2014). The microbial metabolite butyrate regulates intestinal macrophage function *via* histone deacetylase inhibition. *Proc. Natl. Acad. Sci. U.S.A.* 111, 2247–2252. doi: 10.1073/pnas.1322269111

Chen, L., Jiang, B., Zhong, C., Guo, J., Zhang, L., Mu, T., et al. (2018). Chemoprevention of colorectal cancer by black raspberry anthocyanins involved the modulation of gut microbiota and SFRP2 demethylation. *Carcinogenesis* 39, 471–481. doi: 10.1093/carcin/bgy009

Chen, W., Zheng, R., Baade, P. D., Zhang, S., Zeng, H., Bray, F., et al. (2016). Cancer statistics in China, 2015. *CA Cancer J. Clin.* 66, 115–132. doi: 10.3322/caac.21338

Dao, M. C., Everard, A., Aron-Wisnewsky, J., Sokolovska, N., Prifti, E., Verger, E. O., et al. (2016). *Akkermansia muciniphila* and improved metabolic health during a dietary intervention in obesity: relationship with gut microbiome richness and ecology. *Gut* 65, 426–436. doi: 10.1136/gutjnl-2014-308778

Dejea, C. M., Fathi, P., Craig, J. M., Boleij, A., Taddese, R., Geis, A. L., et al. (2018). Patients with familial adenomatous polyposis harbor colonic biofilms containing tumorigenic bacteria. *Science* 359, 592–597. doi: 10.1126/science.aah3648

Dimitriu, P. A., Boyce, G., Samarakoon, A., Hartmann, M., Johnson, P., and Mohn, W. W. (2013). Temporal stability of the mouse gut microbiota in relation to innate and adaptive immunity. *Environ. Microbiol. Rep.* 5, 200–210. doi: 10.1111/j.1758-2229.2012.00393.x

Dulal, S., and Keku, T. O. (2014). Gut microbiome and colorectal adenomas. *Cancer J.* 20, 225–231. doi: 10.1097/ppo.0000000000000050

Edgar, R. C., Haas, B. J., Clemente, J. C., Quince, C., and Knight, R. (2011). UCHIME improves sensitivity and speed of chimera detection. *Bioinformatics* 27, 2194–2200. doi: 10.1093/bioinformatics/btr381

Faust, K., Sathirapongsasuti, J. F., Izard, J., Segata, N., Gevers, D., Raes, J., et al. (2012). Microbial co-occurrence relationships in the human microbiome. *PLoS Comput. Biol.* 8:e1002606. doi: 10.1371/journal.pcbi.1002606

Gagnière, J., Raisch, J., Veziant, J., Barnich, N., Bonnet, R., Buc, E., et al. (2016). Gut microbiota imbalance and colorectal cancer. *World J. Gastroenterol.* 22, 501–518. doi: 10.3748/wjg.v22.i2.501

Gao, R., Kong, C., Li, H., Huang, L., Qu, X., Qin, N., et al. (2017). Dysbiosis signature of mycobiota in colon polyp and colorectal cancer. *Eur. J. Clin. Microbiol. Infect. Dis.* 36, 2457–2468. doi: 10.1007/s10096-017-3085-6

GLOBOCON (2012). *Estimated Cancer Incidence, Mortality and Prevalence In*. Available at: http://globocan.iarc.fr (accessed May 1, 2014).

Gokul Raj, K., Manikandan, R., Arulvasu, C., and Pandi, M. (2015). Anti-proliferative effect of fungal taxol extracted from *Cladosporium oxysporum* against human pathogenic bacteria and human colon cancer cell line HCT 15. *Spectrochim. Acta A Mol. Biomol. Spectrosc.* 138, 667–674. doi: 10.1016/j.saa.2014.11.036

Guerrero-Preston, R., Godoy-Vitorino, F., Jedlicka, A., Rodríguez-Hilario, A., González, H., Bondy, J., et al. (2016). 16S rRNA amplicon sequencing identifies microbiota associated with oral cancer, human papillomavirus infection and surgical treatment. *Oncotarget* 7, 51320–51334. doi: 10.18632/oncotarget.9710

Gur, C., Ibrahim, Y., Isaacson, B., Yamin, R., Abed, J., Gamliel, M., et al. (2015). Binding of the Fap2 protein of *Fusobacterium nucleatum* to human inhibitory receptor TIGIT protects tumors from immune cell attack. *Immunity* 42, 344–355. doi: 10.1016/j.immuni.2015.01.010

Han, F., Yang, S., Lin, M., Chen, Y. Q., Yang, P., and Xu, J. M. (2016). Chitooligosaccharides promote radiosensitivity in colon cancer line SW480. *World J. Gastroenterol.* 22, 5193–5200. doi: 10.3748/wjg.v22.i22.5193

Han, F. S., Cui, B. H., You, X. F., Xing, Y. F., and Sun, X. W. (2015). Anti-proliferation and radiosensitization effects of chitooligosaccharides on human lung cancer line HepG2. *Asian Pac. J. Trop. Med.* 8, 757–761. doi: 10.1016/j.apjtm.2015.07.025

Heeney, D. D., Gareau, M. G., and Marco, M. L. (2018). Intestinal Lactobacillus in health and disease, a driver or just along for the ride? *Curr. Opin. Biotechnol.* 49, 140–147. doi: 10.1016/j.copbio.2017.08.004

Higashimura, Y., Naito, Y., Takagi, T., Uchiyama, K., Mizushima, K., Ushiroda, C., et al. (2016). Protective effect of agaro-oligosaccharides on gut dysbiosis and colon tumorigenesis in high-fat diet-fed mice. *Am. J. Physiol. Gastrointest. Liver Physiol.* 310, G367–G375. doi: 10.1152/ajpgi.00324.2015

Human Microbiome Project Consortium, (2012). Structure, function and diversity of the healthy human microbiome. *Nature* 486, 207–214. doi: 10.1038/nature11234

Iliev, I. D., Funari, V. A., Taylor, K. D., Nguyen, Q., Reyes, C. N., Strom, S. P., et al. (2012). Interactions between commensal fungi and the C-type lectin receptor Dectin-1 influence colitis. *Science* 336, 1314–1317. doi: 10.1126/science.1221789

Karlsson, F. H., Tremaroli, V., Nookaew, I., Bergström, G., Behre, C. J., Fagerberg, B., et al. (2013). Gut metagenome in European women with normal, impaired and diabetic glucose control. *Nature* 498, 99–103. doi: 10.1038/nature12198

Keku, T. O., Dulal, S., Deveaux, A., Jovov, B., and Han, X. (2015). The gastrointestinal microbiota and colorectal cancer. *Am. J. Physiol. Gastrointest. Liver Physiol.* 308, G351–G363. doi: 10.1152/ajpgi.00360.2012

Lang, M., Berry, D., Passecker, K., Mesteri, I., Bhuju, S., Ebner, F., et al. (2017). HuR small-molecule inhibitor elicits differential effects in adenomatosis polyposis and colorectal carcinogenesis. *Cancer Res.* 77, 2424–2438. doi: 10.1158/0008-5472.CAN-15-1726

Laokuldilok, T., Potivas, T., Kanha, N., Surawang, S., Seesuriyachan, P., Wangtueai, S., et al. (2017). Physicochemical, antioxidant, and antimicrobial properties of chitooligosaccharides produced using three different enzyme treatments. *Food Biosci.* 18, 28–33. doi: 10.1016/j.fbio.2017.03.004

Lewis, J. D., Chen, E. Z., Baldassano, R. N., Otley, A. R., Griffiths, A. M., Lee, D., et al. (2015). Inflammation, antibiotics, and diet as environmental stressors of the gut microbiome in pediatric Crohn's disease. *Cell Host Microbe* 18, 489–500. doi: 10.1016/j.chom.2015.09.008

Li, J., Chen, D., Yu, B., He, J., Zheng, P., Mao, X., et al. (2017). Fungi in gastrointestinal tracts of human and mice: from community to functions. *Microb. Ecol.* 75, 821–829. doi: 10.1007/s00248-017-1105-9

Liagat, F., and Eltem, R. (2018). Chitooligosaccharides and their biological activities: a comprehensive review. *Carbohydr. Polym.* 184, 243–259. doi: 10.1016/j.carbpol.2017.12.067

Liang, T. W., Chen, W. T., Lin, Z. H., Kuo, Y. H., Nguyen, A. D., Pan, P. S., et al. (2016). An amphiprotic novel chitosanase from *Bacillus mycoides* and its application in the production of chitooligomers with their antioxidant and anti-inflammatory evaluation. *Int. J. Mol. Sci.* 17:e1302. doi: 10.3390/ijms17081302

Liguori, G., Lamas, B., Richard, M. L., Brandi, G., da Costa, G., Hoffmann, T. W., et al. (2016). Fungal dysbiosis in mucosa-associated microbiota of Crohn's Disease Patients. *J. Crohns Colitis* 10, 296–305. doi: 10.1093/ecco-jcc/jjv209

Louis, P., Hold, G. L., and Flint, H. J. (2014). The gut microbiota, bacterial metabolites and colorectal cancer. *Nat. Rev. Microbiol.* 12, 661–672. doi: 10.1038/nrmicro3344

Luan, C., Miao, H., and Zhu, B. (2015). Gut mycobiota and adenomas. *Gut Microbes* 6, 331–333. doi: 10.1080/19490976.2015.1089380

Madeeha, I. R., Ikram, A., and Imran, M. (2016). A preliminary insight of correlation between human fecal microbial diversity and blood lipid profile. *Int. J. Food Sci. Nutr.* 67, 865–871. doi: 10.1080/09637486.2016.1201791

Mattaveewong, T., Wongkrasant, P., Chanchai, S., Pichyangkura, R., Chatsudthipong, V., Muanprasat, C., et al. (2016). Chitosan oligosaccharide suppresses tumor progression in a mouse model of colitis-associated colorectal cancer through AMPK activation and suppression of NF-κB and mTOR signaling. *Carbohydr. Polym.* 145, 30–36. doi: 10.1016/j.carbpol.2016.02.077

McCoy, K. D., Geuking, M. B., and Ronchi, F. (2017). Gut Microbiome standardization in control and experimental mice. *Curr. Protoc. Immunol.* 117, 23.1.1–23.1.13. doi: 10.1002/cpim.25

Mei, Y. X., Dai, X. Y., Yang, W., Xu, X. W., and Liang, Y. X. (2015). Antifungal activity of chitooligosaccharides against the dermatophyte *Trichophyton rubrum*. *Int. J. Biol. Macromol.* 77, 330–335. doi: 10.1016/j.ijbiomac.2015.03.042

Menghini, P., Di Martino, L., Lopetuso, L. R., Corridoni, D., Webster, J. C., Xin, W., et al. (2017). A novel model of colitis-associated cancer in SAMP1/YitFc mice with Crohn's disease-like ileitis. *PLoS One* 12:e0174121. doi: 10.1371/journal.pone.0174121

Munyaka, P. M., Rabbi, M. F., Khafipour, E., and Ghia, J. E. (2016). Acute dextran sulfate sodium (DSS)-induced colitis promotes gut microbial dysbiosis in mice. *J. Basic Microbiol.* 56, 986–998. doi: 10.1002/jobm.201500726

Nurhayati, Y., Manaf, A. A., Osman, H., Abdullah, A. B. C., and Tang, J. Y. H. (2016). Effect of chitosan oligosaccharides on the growth of bifidobacterium species. *Malaysian J. Appl. Sci.* 1, 13–23.

Ottman, N., Reunanen, J., Meijerink, M., Pietilä, T. E., Kainulainen, V., Klievink, J., et al. (2017). Pili-like proteins of *Akkermansia muciniphila* modulate host immune responses and gut barrier function. *PLoS One* 12:e0173004. doi: 10.1371/journal.pone.0173004

Pan, X. D., Chen, F. Q., Wu, T. X., Tang, H. G., and Zhao, Z. Y. (2009). Prebiotic oligosaccharides change the concentrations of short-chain fatty acids and the microbial population of mouse bowel. *J. Zhejiang Univ. Sci. B* 10, 258–263. doi: 10.1631/jzus.B0820261

Park, J. K., Chung, M. J., Choi, H. N., and Park, Y. I. (2011). Effects of the molecular weight and the degree of deacetylation of chitosan oligosaccharides on antitumor activity. *Int. J. Mol. Sci.* 12, 266–277. doi: 10.3390/ijms12010266

Perez-Muñoz, M. E., Bergstrom, K., Peng, V., Schmaltz, R., Jimenez-Cardona, R., Marsteller, N., et al. (2014). Discordance between changes in the gut microbiota and pathogenicity in a mouse model of spontaneous colitis. *Gut Microbes* 5, 286–295. doi: 10.4161/gmic.28622

Plovier, H., Everard, A., Druart, C., Depommier, C., Van Hul, M., Geurts, L., et al. (2017). A purified membrane protein from *Akkermansia muciniphila* or the pasteurized bacterium improves metabolism in obese and diabetic mice. *Nat. Med.* 23, 107–113. doi: 10.1038/nm.4236

Qu, D., and Han, J. (2016). Investigation of the antioxidant activity of chitooligosaccharides on mice with high-fat diet. *Rev. Bras. Zootec.* 45, 661–666. doi: 10.1590/s1806-92902016001100004

Ramos, A., and Hemann, M. T. (2017). Drugs, bugs, and cancer: *Fusobacterium nucleatum* promotes chemoresistance in colorectal cancer. *Cell* 170, 411–413. doi: 10.1016/j.cell.2017.07.018

Román, L., Acosta, F., Padilla, D., El Aamri, F., Bravo, J., Vega, B., et al. (2015). The in vitro immunomodulatory effect of extracellular products (E) of *Vagococcus fluvialis* L21 on European sea bass (*Dicentrarchus labrax*) leucocytes. *Fish Shellfish Immunol.* 42, 517–521. doi: 10.1016/j.fsi.2014.11.037

Román, L., Real, F., Padilla, D., El Aamri, F., Déniz, S., Grasso, V., et al. (2013). Cytokine expression in head-kidney leucocytes of European sea bass (*Dicentrarchus labrax* L.) after incubation with the probiotic *Vagococcus fluvialis* L-21. *Fish Shellfish Immunol.* 35, 1329–1332. doi: 10.1016/j.fsi.2013.07.036

Routy, B., Le Chatelier, E., Derosa, L., Duong, C. P. M., Alou, M. T., Daillère, R., et al. (2018). Gut microbiome influences efficacy of PD-1-based immunotherapy against epithelial tumors. *Science* 359, 91–97. doi: 10.1126/science.aan3706

Ryu, B., Kim, S. Y., Vo, T. S., Kim, W. S., Kim, D. G., and Kim, S. K. (2017). Characterization of the in vitro effects of gallic acid-grafted-chitooligosaccharides in the suppression of AGS human gastric cancer cell proliferation. *RSC Adv.* 7, 24561–24568. doi: 10.1039/c7ra02487h

Saber, A., Alipour, B., Faghfoori, Z., Mousavi Jam, A., and Yari Khosroushahi, A. (2017). Secretion metabolites of probiotic yeast, *Pichia kudriavzevii* AS-12, induces apoptosis pathways in human colorectal cancer cell lines. *Nutr. Res.* 41, 36–46. doi: 10.1016/j.nutres.2017.04.001

Sánchez, Á., Mengíbar, M., Rivera-Rodríguez, G., Moerchbacher, B., Acosta, N., and Heras, A. (2017). The effect of preparation processes on the physicochemical characteristics and antibacterial activity of chitooligosaccharides. *Carbohydr. Polym.* 157, 251–257. doi: 10.1016/j.carbpol.2016.09.055

Schirrmeister, J. F., Liebenow, A. L., Pelz, K., Wittmer, A., Serr, A., Hellwig, E., et al. (2009). New bacterial compositions in root-filled teeth with periradicular lesions. *J. Endod.* 35, 169–174. doi: 10.1016/j.joen.2008.10.024

Segata, N., Izard, J., Waldron, L., Gevers, D., Miropolsky, L., Garrett, W. S., et al. (2011). Metagenomic biomarker discovery and explanation. *Genome Biol.* 12:R60. doi: 10.1186/gb-2011-12-6-r60

Sinder, A. J., Bialkowska, A. B., Ghaleb, A. M., Yang, V. W., Obeid, L. M., and Hannun, Y. A. (2016). Murine model for colitis-associated cancer of the colon. *Methods Mol. Biol.* 1438, 245–254. doi: 10.1007/978-1-4939-3661-8_14

Sokol, H., Leducq, V., Aschard, H., Pham, H. P., Jegou, S., Landman, C., et al. (2017). Fungal microbiota dysbiosis in IBD. *Gut* 66, 1039–1048. doi: 10.1136/gutjnl-2015-310746

Sorroza, L., Padilla, D., Acosta, F., Román, L., Grasso, V., Vega, J., et al. (2012). Characterization of the probiotic strain *Vagococcus fluvialis* in the protection of European sea bass (*Dicentrarchus labrax*) against vibriosis by *Vibrio anguillarum*. *Vet. Microbiol.* 155, 369–373. doi: 10.1016/j.vetmic.2011.09.013

Srinivas, B., Rani, G. S., Kumar, B. K., Chandrasekhar, B., Krishna, K. V., Devi, T. A., et al. (2017). Evaluating the probiotic and therapeutic potentials of *Saccharomyces cerevisiae* strain (OBS2) isolated from fermented nectar of toddy palm. *AMB Express* 7:2. doi: 10.1186/s13568-016-0301-1

Tong, C., Yin, Z., Song, Z., Dockendorff, A., Huang, C., Mariadason, J., et al. (2007). c-Jun NH2-terminal kinase 1 plays a critical role in intestinal homeostasis and tumor suppression. *Am. J. Pathol.* 171, 297–303. doi: 10.2353/ajpath.2007.061036

Ullman, T. A., and Itzkowitz, S. H. (2011). Intestinal inflammation and cancer. *Gastroenterology* 140, 1807–1816.

Van Raay, T., and Allen-Vercoe, E. (2017). "Microbial interactions and interventions in colorectal cancer," in *Bugs As Drugs*, eds R. Britton and P. Cani (Washington, DC: ASM Press), 101–130.

Vo, T. S., Ngo, D. H., Ngo, D. N., Long, G. B., and Kim, S. K. (2017). The free radical scavenging and anti-inflammatory activities of gallate-chitooligosaccharides in human lung epithelial A549 cells. *Process Biochem.* 54, 188–194. doi: 10.1016/j.procbio.2017.01.001

Wang, W., Chen, L., Zhou, R., Wang, X., Song, L., Huang, S., et al. (2014). Increased proportions of *Bifidobacterium* and the *Lactobacillus* group and loss of butyrate-producing bacteria in inflammatory bowel disease. *J. Clin. Microbiol.* 52, 398–406. doi: 10.1128/JCM.01500-13

World Health Organization (2018). *Fact sheet 297*. Available at: http://www.who.int/mediacentre/factsheets/fs297/en/ (accessed September 12).

Wu, M., Wu, Y., Deng, B., Li, J., Cao, H., Qu, Y., et al. (2016). Isoliquiritigenin decreases the incidence of colitis-associated colorectal cancer by modulating the intestinal microbiota. *Oncotarget* 7, 85318–85331. doi: 10.18632/oncotarget.13347

Yang, Y., Chen, G., Yang, Q., Ye, J., Cai, X., Tsering, P., et al. (2017). Gut microbiota drives the attenuation of dextran sulphate sodium-induced colitis by Huangqin decoction. *Oncotarget* 8, 48863–48874. doi: 10.18632/oncotarget.16458

Zenewicz, L. A., Yin, X., Wang, G., Elinav, E., Hao, L., Zhao, L., et al. (2013). IL-22 deficiency alters colonic microbiota to be transmissible and colitogenic. *J. Immunol.* 190, 5306–5312. doi: 10.4049/jimmunol.1300016

Zurlo, D., Leone, C., Assante, G., Salzano, S., Renzone, G., Scaloni, A., et al. (2013). Cladosporol a stimulates G1-phase arrest of the cell cycle by up-regulation of p21(waf1/cip1) expression in human colon carcinoma HT-29 cells. *Mol. Carcinog.* 52, 1–17. doi: 10.1002/mc.20872

Conflict of Interest Statement: The authors declare that the research was conducted in the absence of any commercial or financial relationships that could be construed as a potential conflict of interest.

Advantages of publishing in Frontiers

OPEN ACCESS
Articles are free to read for greatest visibility and readership

FAST PUBLICATION
Around 90 days from submission to decision

HIGH QUALITY PEER-REVIEW
Rigorous, collaborative, and constructive peer-review

TRANSPARENT PEER-REVIEW
Editors and reviewers acknowledged by name on published articles

Frontiers
Avenue du Tribunal-Fédéral 34
1005 Lausanne | Switzerland

Visit us: www.frontiersin.org
Contact us: info@frontiersin.org | +41 21 510 17 00

REPRODUCIBILITY OF RESEARCH
Support open data and methods to enhance research reproducibility

DIGITAL PUBLISHING
Articles designed for optimal readership across devices

FOLLOW US
@frontiersin

IMPACT METRICS
Advanced article metrics track visibility across digital media

EXTENSIVE PROMOTION
Marketing and promotion of impactful research

LOOP RESEARCH NETWORK
Our network increases your article's readership